CHARLES UNIVERSITY

FACULTY OF MEDICINE IN PILSEN

DISSERTATION

CLINICOPATHOLOGICAL AND MOLECULAR BIOLOGIC CHARACTERISTICS OF SELECTED CUTANEOUS EPITHELIAL AND NONEPITHELIAL TUMORS

MD. LIUBOV KASTNEROVA

SUPERVISOR: Prof. MD. DMITRY KAZAKOV, CSc.

FIELD: PATHOLOGY

PILSEN 2019

INTRODUCTION

Skin tumors encompass a broad group of entities, with which a pathologist deals every day in his/her practice. Due to the complexity of the skin, the number of neoplasms that occur in this organ is likely the largest one compared to that seen in any other anatomic site, which portent potential diagnostic difficulties. The new WHO classification of skin tumors included listing a total of 250 entities divided into 6 chapters: 1) keratinocytic/epidermal tumors, 2) melanocytic tumors, 3) appendageal tumors, 4) tumors of hematopoietic and lymphoid origin, 5) soft tissue tumors and 6) inherited tumor syndromes associated with skin malignancies. (1) The classification of cutaneous neoplasms are based on their primary site of origin.

Some cutaneous neoplasms are commonly seen in routine practice and therefore easily recognized based on the typical histological features, whereas for the diagnosis of complex and rare tumors the clinical data, immunohistochemistry and molecular-genetic studies are often necessary.

Immunohistochemistry (IHC) is an important adjunct tool for the diagnosis of difficult neoplastic skin lesions, tumor staging, and, in some instances, for the identification of genetic variants of therapeutic significance. In addition to the many established and long-used IHC markers, due to rapid progress in our understanding of the genetic and epigenetic mechanisms of tumorigenesis, numerous new IHC markers have recently become available for application in the field of diagnostic dermatopathology. In some diagnostically difficult tumors, IHC can be decisive for the correct diagnosis, but in other neoplasms, the role of IHC is limited. IHC becomes a particularly powerful tool in the differential diagnosis of cutaneous lesions from the following categories: melanoma, epidermal tumors, cutaneous metastasis, soft tissue neoplasms, and hematologic malignancies.

Lately, various molecular techniques have also been integrated into the routine diagnostic process and currently play an important role in diagnostic dermatopathology, which is highlighted in the new WHO classification of skin tumors. (1) Molecular biologic assay such as comparative hybridization (CGH), fluorescence in situ hybridization (FISH), and next-generation sequencing (NGS) can aid in the differential diagnosis between malignant and benign melanocytic neoplasms and identify prognostic parameters in certain cases. Several significant and/or common gene mutations or gene fusions provided the basis for the classification of melanocytic neoplasms, along with the epidemiological, clinical, and pathological characteristics. Some genetics events are correlated with clinical behavior. In particular, homozygous deletion 9p21 and *TERT* promoter *(TERT-p)* mutations have been described as potential features suggesting an aggressive course of spitzoid lesions. (2), (3) Recently, mutually exclusive activating kinases fusions, involving *ALK, NTRK1, NTRK2, NTRK3, RET, MET, ROS1*, and *BRAF* have been found in a subset of spitzoid lesions. (4) Some of these genetic alterations have been correlated with specific morphological features.

In the dissertation thesis, the author underscores the application of IHC, and various molecular genetic techniques in cutaneous neoplasms, identification of new gene fusions and possible genotype-phenotype correlations. We used in our papers the broad spectrum of available molecular tests and cytogenetic analysis, including CGH, FISH, polymerase chain reaction (PCR)-based techniques, and NGS mutation analysis.

Due to the high numbers and complexity of cutaneous tumors, the author focuses on the clinicopathological and molecular biologic characteristics of selected cutaneous epithelial and nonepithelial tumors. The results have been published in a total of 20 articles in which the author of the dissertation listed as the first author and as a coauthor in 8 and 12 papers, respectively. All 20 articles have been published in American journals with impact factor. The dissertation is elaborated in the form of a summary/comments of the annotated publications. All publications are accompanied by a copy of the reprints (14 works) or by the submitted and accepted manuscripts with proof of acceptance (3 work) or epub ahead of print (3).

The first and the most substantial part of the doctoral thesis is focused on cutaneous epithelial tumors, including various adnexal neoplasms, such as lesions with apocrine and eccrine differentiation, follicular tumors, sebaceous neoplasms and lesions of anogenital mammary-like glands (AGMLG).

The second part covers selected nonepithelial cutaneous tumors, such as melanocytic tumors, lymphoproliferative disorders, and mesenchymal tumors.

DECLARATION

I declare that I have elaborated the dissertation independently and duly stated and quoted all used sources. The work was not used to obtain another or the same title. I agree with the permanent storage of the electronic version of my work in the database of the Charles University in Pilsen.

Pilsen, 17.7. 2019

SUMMARY

The doctoral thesis MD. Liubov Kastnerova (previous name Kyrpychova) is focused on the histomorphological and molecular biologic features of selected cutaneous epithelial and nonepithelial tumors and is structured as a commentary to the 20 articles published during four years, representing the completed scientific projects in the Ph.D. course. In eight papers, the author of the thesis is the first author, whereas she coauthored in the remaining 12 papers. The thesis is composed of the commented files of authors own publications and it is divided into cutaneous epithelial and nonepithelial tumors.

The first section, «Cutaneous epithelial tumors», includes 14 articles that are subdivided into two parts: adnexal tumors (9 articles) and lesions of anogenital mammary-like glands (5 articles).

Of the nine articles on adnexal tumors, there are 5 articles focused on various benign and malignant adnexal lesions with apocrine or eccrine differentiation. Novel findings in this part include the identification of hitherto unreported alterations of the *MYBL1* gene in adenoid cystic carcinoma of the skin and lack of deletion of the 1p36 locus in this neoplasm; the lack of a correlation between cellular composition and the presence *CRTC1-MAML2* fusions in hidradenoma, the absence of *CRTC3-MAML2* fusions in this tumor, and new histopathological features and novel *NFIX-PKN1* translocation in primary cutaneous secretory carcinoma. Also, we performed a complex study including the HPV analysis and *HRAS* and *BRAF V600* mutations in syringocystadenoma papilliferum located in the anogenital area, which has never been a subject of such investigation in this location.

One of two articles on follicular tumors is a clinicopathological, immunohistochemical, and molecular biological study of 22 cases of basal cell carcinoma with matrical differentiation. The novel findings included the description of an atypical matrical component in 2 cases and the mutation spectrum in these rare variants. The second article is based on IHC study of BAP1 expression in trichoblastomas, both solitary sporadic and multiple ones occurring in the setting of multiple familial trichoepithelioma (MFT)/Brooke-Spiegler syndrome (BSS).

Two articles are focused on sebaceous neoplasms. One is the largest series of sebaceous lesions with so-called organoid patterns, namely the rippled, labyrinthine/sinusoidal, carcinoid-like and petaloid patterns. We confirmed the previously suggested proposition that all these patterns represent a variation of a single morphological spectrum. We established no association with Muir–Torre syndrome and detected no missmatched repair (MMR) deficiency in most cases, the new data. The second study on periocular sebaceous carcinoma reports new features that may be used as a differential diagnostic clue, namely cells with squared-off nuclei and so-called "appliqué" pattern (peritumoral subnecrosis of peripherally located neoplastic cells).

The subsection on the lesions of anogenital mammary-like glands includes five articles, which add new data regarding their normal histology, provide the detailed immunohistochemical profile of AGMLG, and demonstrate molecular changes in lesions arising from AGMLG comparing these to breast homologs. The novel data also includes the depth of adnexal involvement by neoplastic cells in extramammary Paget disease (EMPD) a large series, which provides practical treatment implications.

The second part, «Cutaneous nonepithelial tumors», includes five articles which are divided between 3 subcategories: lymphoproliferative disorders, mesenchymal tumors, and melanocytic tumors.

One of the three articles in the subgroup of lymphoproliferative disorders represents the largest series of cutaneous Hodgkin disease in which we provide the first description of so-called mummified cells in this condition in the skin. These cells are known in lymph node disease but have been overlooked in skin biopsies judging from the previously published articles. Their presence can serve as a clue to the diagnosis. Included were also two case reports. The first on an extraordinary clinicopathological course of a recently described variant of lymphomatoid papulosis, type E. The second article is an extraordinary case report of cutaneous primary effusion lymphoma (PEL) with an unusual intravascular presentation, combined with Kaposi sarcoma (KS) involving the skin, lung and gastrointestinal tract harboring a *FAM175A* germline mutation.

In the subsection of melanocytic tumors, there are two articles. In the first paper, the author presents a detailed pathological study on spitzoid lesions with *ROS1* fusion and novel fusions of this gene. The study also includes the extensive genetic investigation of other genes, with some novel data. The second article is an extraordinary case report which describes a case of a polypoid atypical Spitz tumor a with a prominent fibrosclerotic stromal component, harboring a *CLIP2-BRAF* fusion, which has hitherto been not reported in melanocytic lesions.

As a representative entity of mesenchymal tumors, the authors describe a series of epithelioid fibrous histiocytomas in which new histopathological features and novel *ALK* gene fusions were found.

ABSTRAKT

Disertační práce MD. Liubov Kastnerové (dříve Kyrpychova) se zaměřuje na histomorfologické a molekulárně biologické vlastnosti vybraných kožních epiteliálních a neepiteliálních nádorů. Je strukturována jako komentář k 20 článkům publikovaným v průběhu čtyř let, které představují dokončené vědecké projekty v Ph.D. studiu. V osmi článcích je autorka první autor, ve zbývajících 12 pracích je spoluautorem. Doktorská dizertační práce je prezentovaná ve formě komentovaného souhrnu vlastních publikací a je rozdělena na kožní epiteliální a neepiteliální nádory.

První část, "Kožní epiteliální tumory", obsahuje 14 článků, které jsou členěny do dvou částí: adnexální tumory (9 článků) a léze z anogenitálních „mammary-like" žlázek (AGMLG) (5 článků).

Z devíti článků týkajících se adnexálních nádorů je jich 5 zaměřeno na různé benigní a maligní adnexální léze s apokrinní nebo ekrinní diferenciací. Nové poznatky v této části zahrnují identifikaci dosud nepopsaných změn genu *MYBL1* v adenoidně cystickém karcinomu kůže a absenci delece lokusu 1p36 v tomto nádoru. Dále prokazujeme chybění korelace mezi buněčným složením a přítomností fúzí *CRTC1-MAML2* v hidradenomu, absenci fúzí *CRTC3-MAML2* v tomto nádoru, a nové histopatologické znaky a translokace *NFIX-PKN1* v primárním kožním sekrečním karcinomu. Také jsme provedli první komplexní studii zahrnující analýzu HPV a prokázali jsme role *HRAS* a *BRAF V600* mutace v syringocystadenoma papilliferum nacházející se v anogenitální oblasti, která nikdy nebyla předmětem tohoto zkoumání v této lokalitě.

Jedním ze dvou článků o folikulárních nádorech je klinicko-patologická, imunohistochemická (IHC) a molekulárně biologická studie 22 případů bazocelulárního karcinomu s matrikální diferenciací. Nové poznatky zahrnovaly popis atypické matrikalní složky ve 2 případech a mutačního spektra v těchto vzácných variantách. Druhý článek je založen na IHC studii exprese *BAP1* v trichoblastomech a to jak solitárních, tak vícečetných, vyskytujících se v rámci mnohočetného familiárního trichoepiteliomu (MFT) / Brooke-Spieglerova syndromu (BSS).

Dva články jsou zaměřeny na sebaceozní nádory. Jedním z nich je největší série sebaceozních lézí s takzvanými organoidními rysy, jmenovitě s vlnitými, labyrintovými / sinusovými, karcinoidními a petaloidními vzory. Potvrdili jsme dříve navrhovanou hypotézu, že všechny tyto vzory představují variantu jednoho morfologického spektra. Nezjistili jsme žádnou souvislost se syndromem Muir – Torre a ve většině případů, s novými údaji, jsme nezjistili žádnou missmatched repair deficiency (MMR). Druhá studie o periokulárním sebaceozním karcinomu nachází nové rysy, které mohou být použity jako diferenciálně diagnostické vodítko, a to buňky s kvadratickým jádrem a tzv. „aplikaque" pattern (peritumorální subnekróza periferně lokalizovaných neoplastických buněk).

Podsekce o lézích anogenitálních prsních žláz obsahuje pět článků, které přidávají nová data týkající se jejich normální histologie, poskytují podrobný IHC profil AGMLG a demonstrují

molekulární změny v lézích vyplývajících z AGMLG ve srovnání s homology prsu. Nová data také zahrnují hloubku adnexálního postižení nádorovými buňkami při extramamární Pagetově chorobě (EMPD), což je velká série, která poskytuje praktické poznatky pro léčbu.

Druhá část, "Kožní neepiteliální nádory", zahrnuje pět článků, které jsou rozděleny do 3 podkategorií: lymfoproliferativní onemocnění, mesenchymální tumory a melanocytární tumory.

Jeden ze tří článků v podskupině lymfoproliferativních poruch představuje největší sérii kožních Hodgkinových nemocí, ve kterých poskytujeme prvopopis tzv. mummifikovaných buněk vyskytujících se v kůži u pacientů s tímto onemocněním. Z dříve publikovaných článků vyplývá, že tyto buňky jsou známy u onemocnění lymfatických uzlin, ale bývaly přehlédnuty v kožních biopsiích. Jejich přítomnost může sloužit jako vodítko k diagnóze. Zahrnuty byly také dvě kazuistiky. První z nich je mimořádný klinicko-patologický případ nedávno popsané varianty lymfomatoidní papulosy typu E. Druhým článkem je mimořádná kazuistika primárního kožního efuzního lymfomu (PEL) s neobvyklou intravaskulární prezentací v kombinaci s Kaposiho sarkomem (KS) postihujícím kůži, plíce a gastrointestinální trakt. V lézi jsme prokázali zárodečnou mutaci *FAM175A*.

V subsekci melanocytárních nádorů jsou představeny dva články. V první práci autorka předkládá podrobnou patologickou studii o spitzoidních lézích s fúzí *ROS1* a nových fúzích tohoto genu. Studie také zahrnuje rozsáhlé genetické vyšetření jiných genů, s některými novými daty. Druhý článek je mimořádnou kazuistikou, která popisuje případ polypoidního atypického Spitzova nádoru s prominentní fibrosklerotickou stromální složkou, která obsahuje fúzi *CLIP2-BRAF*, která nebyla dosud publikována u melanocytárních lézí.

Jako reprezentativní entitu mezenchymálních nádorů autoři popisují série epitelioidních fibrózních histiocytomů, ve kterých byly nalezeny nové histopatologické znaky a nové fúze genu *ALK*.

CONTENTS

LIST OF ABBREVIATIONS

ACC – adenoid cystic carcinoma

AGMLG - anogenital mammary-like glands

BCC – basal cell carcinoma

BSS – Brooke-Spiegler syndrome

CGH – comparative genetic hybridization

EBV – Epstein-Barr virus

EFH – epithelioid fibrous histiocytoma

EMPD - extramammary Paget disease

FISH – fluorescence in situ hybridization

IgH – immunoglobulin heavy chain

IHC – immunohistochemistry

KS – Kaposi sarcoma

LyP - lymphomatoid papulosis

MFT – multiple familiar trichoepitheliomas

MMR – mismatch repair

MTS - Muir-Torre syndrome

NGS – next generation sequencing

PCR – polymerase chain reaction

PEComa – perivascular epithelioid cell tumor

PEL - primary effusion lymphoma

RT-PCR – Reverse Transcriptase Polymerase Chain Reaction

SCAP – syringocystadenoma papilliferum

TCR – T-cell receptor

WHO – World Health organization

SUMMARY OF COMMENTED PUBLICATIONS

PART 1 - CUTANEOUS EPITHELIAL TUMORS

1.1 ADNEXAL TUMORS

This part includes nine articles resulting from studies on the histological, immunohistochemical and molecular-genetic features of various benign and malignant cutaneous adnexal tumors, including tumors with predominant apocrine and eccrine differentiation, lesions with predominant follicular differentiation and sebaceous tumors. In most of these papers, the author actively used the IHC technique and molecular-genetic analysis.

1.1.1 TUMORS WITH APOCRINE AND ECCRINE DIFFERENTIATION

This chapter includes five articles on various benign and malignant adnexal lesions with apocrine or eccrine differentiation; in four of them, the author of the thesis is the first author.

The first two papers are focused on primary cutaneous adenoid cystic carcinoma (ACC) of the skin is a rare malignant neoplasm histologically identical to homonymous tumors in other organs. (5), (6) There are three main growth patterns, presenting singly or more often in combination, recognized in this neoplasm, including cribriform, tubular, and solid formed by relatively bland basaloid cells. The typical histological features of ACC include pseudocysts containing abundant basophilic mucinous material and small true ductal lumina (ductal differentiation). (7), (8) Perineural and intraneural invasion is also a common feature. Cutaneous ACC, similar to their extracutaneous counterparts, have been found to harbor *MYB* gene activations, either through *MYB* chromosomal abnormalities or by the generation of the *MYB-NFIB* fusion. (9), (10) The translocation t(6;9) appears a tumor-type–specific, as it has been detected in ACC in different organs and anatomic structures, including salivary glands, lacrimal glands, breast, upper respiratory tract, ear, and Bartholin glands. (11), (12) In addition to the *MYB* gene, alterations in *MYBL1*, the gene closely related to *MYB*, have been reported in salivary gland ACC. (13), (14) The first article is titled «*A small subset of adenoid cystic carcinoma of the skin is associated with alterations of the MYBL1 gene similar to their extracutaneous counterparts*» shows the results of our study of 10 cases of cutaneous ACC for alterations in the *MYB, NFIB* and *MYBL1* genes, using FISH and PCR. In all cases, MYB immunostaining was also performed. Since we were not aware of any studies on cutaneous ACC studying alterations in *MYBL1*, our primary goal was to find out whether this gene is involved in cutaneous ACC. *MYB-NFIB* fusions were found in 4 cases in our series, whereas the break of *MYBL1* was found in 2 cases and in one of them, the *NFIB* break apart probe was positive, strongly indicating a *MYBL1-NFIB* fusion. In 2 cases, the *MYB* break apart test was positive, whereas no *MYB-NFIB* was detected, strongly suggesting another fusion partner. It is concluded that *MYBL1* alterations are detected in primary cutaneous ACC but are less common compared to *MYB* and *NFIB* alterations.

The second paper ,«*Lack of deletion of 1p36 in 8 cases of primary adenoid cystic carcinoma of the skin*», was published as a Letter to the Editor. It extended our previous study of

genetic alterations in cutaneous ACC by studying the deletion of the 1p36 locus that had been shown in salivary gland ACC to be associated with reduced overall survival, higher tumor stage, lower recurrence-free interval, and the absence of *MYBL1* break apart. (15) The author used the same 10 cases of primary cutaneous ACC for the detection of deletion of the 1p36 by FISH, which became available. None of these cases in our series, including two patients who died of metastatic disease, had a deletion of the 1p36. It was concluded that the deletion of this locus is not a feature of cutaneous ACC, but further studies on larger series are needed to confirm this assumption.

The main objectives of the next study that has resulted in the paper titled «*Cutaneous hidradenoma: a study of 21 neoplasms revealing neither correlation between the cellular composition and CRTC1-MAML2 fusions nor presence of CRTC3-MAML2 fusions*» were to find out whether there is a correlation between the particular cell type of hidradenoma (as claimed by some authors in a previous publication) and the presence of the *CRTC1-MAML2* and *CRTC3-MAML2* fusions. Hidradenoma is a benign adnexal neoplasm composed of several cell types, including polyhedral eosinophilic cells, clear cells, epidermoid cells, mucinous cells, oxyphilic cells, and various transitional cells. (16), (17), (8) The cellular composition occurs in variable proportions and in various combinations from case to case, and in some neoplasms, a particular cell type predominates. The neoplasm is usually solid and/or solid-cystic; less common is a markedly prevailing cystic component, multinodular sclerosing pattern or prominent glandular differentiation. Approximately 50% of hidradenomas harbor the t(11;19) translocation, which results in the fusion of the *CRTC1* gene with the *MAML2* gene. It has been claimed that t(11,19) translocation is associated with clear cell differentiation. (18) In mucoepidermoid carcinoma of the salivary gland, which is an analogue of cutaneous hidradenoma, apart from *CRTC1-MAML2* fusion, a subset of cases with *CRTC3-MAML2* fusions have been identified. (19) The objectives of our study were 1) to find out whether there is indeed a correlation between cellular composition and *CRTC1-MAML2* fusion and 2) to study *CRTC3-MAML2* fusions in this adnexal neoplasm. For each of the 21 hidradenomas, we analyzed the presence of a particular cell type (polyhedral eosinophilic, clear, mucinous, epidermoid (squamoid), and oncocytic (oxyphilic)) and the ratio of solid areas versus glandular areas, together with the connection to the epidermis. We found that t(11,19) translocation can be seen in cutaneous hidradenoma with various cytological compositions, and not only in clear cell predominant lesions. There are hidradenomas that manifest positive *MAML2* break apart probe but lack any demonstrable *CRTC1-MAML2* fusion, suggesting, among other things, a different fusion partner. No tumor in our series yielded *CRTC3-MAML2* fusion.

In the fourth paper «*Syringocystadenoma papilliferum (SCAP) of the anogenital area and buttocks: a report of 16 cases, including HPV analysis and HRAS and BRAF V600 mutation studies*» the author investigated the role of *HRAS* and *BRAF V600* mutations in the etiology and pathogenesis of SCAP in the anogenital area and buttock. SCAP is a benign adnexal tumor most commonly located on the head and neck area and often associated with nevus sebaceus. (20) Histopathologically, SCAP appears as an exo-endophytic, often crateriform lesion with a papillary

architecture formed by double-layered tubular structures composed of cuboidal to columnar luminal cells, often showing apocrine secretion surrounded by a peripheral layer of basal/myoepithelial cells. Various hyperplastic and metaplastic changes (mucinous metaplasia, squamous metaplasia, etc.) have been described in SCAP. (21) In its usual location, the HPV DNA and mutations in RAS/mitogen-activated protein kinase signaling pathway have been detected in SCAP. (22), (23) We studied 16 cases of SCAP in the anogenital area and buttock (a very rare and unusual location) and attempted to find out whether SCAP in these sites have different histopathological and molecular biological features. We revealed no significant difference between the morphology of anogenital SCAP and SCAP in other locations. Several tumors in our cohort demonstrated features resembling those seen in warts, but HPV DNA was not found in these lesions. On the contrary, we identified the DNA of HPV high-risk types in some tumors without HPV-related morphology. Our study confirms the role of *HRAS* and *BRAF V600* mutations in the pathogenesis of SCAP, including SCAP in the anogenital areas and buttock.

The fifth article of tumors with predominant apocrine and eccrine differentiation is a «*Secretory carcinoma of the skin: report of 6 cases, including a case with a novel NFIX-PKN1 translocation*» in which the author of the thesis is the first author. Primary cutaneous secretory carcinoma is a rare adnexal carcinoma that morphologically and immunohistochemically is identical to secretory carcinoma of the breast and salivary glands. (24) It is an indolent tumor mainly located in the axilla and often affecting young adults. Histologically, secretory carcinoma is composed of bland neoplastic cells arranged in microcystic, tubular, and solid growth patterns, with typical abundant bubbly secretion within the microcystic and tubular spaces. (25) Immunohistochemically, the neoplastic cells express S-100 protein, mammaglobin, STAT5, and GATA3. This tumor is associated with the presence of t (12;15) translocation, resulting in the *ETV6-NTRK3* gene fusion. (26), (27) Prior to our study, only 19 cases have been reported in the skin, mostly as isolated case reports. We described six new cases of primary cutaneous secretory carcinoma, including two cases with unusual microscopic features. One was with a focal mucinous component with small lakes of mucin containing small tumor nests or tubules of the neoplastic cells, whereas the second tumor featured a solid and papillary architecture, with only focal typical luminal secretions. All 6 cases have been studied for *ETV6-NTRK3* gene fusion. In 5 cases, t (12;15) translocation was detected, whereas in the remaining tumor a novel *NFIX-PKN1* gene fusion was found.

Small Subset of Adenoid Cystic Carcinoma of the Skin Is Associated With Alterations of the *MYBL1* Gene Similar to Their Extracutaneous Counterparts

Liubov Kyrpychova, MD,* Tomas Vanecek, PhD,*† Petr Grossmann, PhD,*† Petr Martinek, PhD,*†
Petr Steiner, MSc,*† Ladislav Hadravsky, MD, PhD,‡ Irena E. Belousova, MD, PhD,§
Ksenya V. Shelekhova, MD, PhD,¶‖ Marian Svajdler, MD, PhD,*† Pavol Dubinsky, PhD, MHA,**
Michal Michal, MD,*† and Dmitry V. Kazakov, MD, PhD*†

Abstract: Adenoid cystic carcinoma (ACC) of the skin is a rare malignant neoplasm histologically identical to homonymous tumors in other organs. Cutaneous ACC has been found to harbor *MYB* gene activations, either through *MYB* chromosomal abnormalities or by generation of the *MYB–NFIB* fusion. In salivary gland ACC, in addition to the *MYB* gene, alterations in *MYBL1*, the gene closely related to *MYB*, have been reported. We studied 10 cases of cutaneous ACC (6 women, 4 men; and age range 51–83 years) for alterations in the *MYB*, *NFIB*, and *MYBL1* genes, using FISH and PCR. *MYB* break-apart and *NFIB* break-apart tests were positive in 4 and 5 cases, respectively. *MYB–NFIB* fusions were found in 4 cases. The break of *MYBL1* was found in 2 cases, and in one of them, the *NFIB* break-apart probe was positive, strongly indicating a *MYBL1–NFIB* fusion. In 2 cases, the *MYB* break-apart test was positive, whereas no *MYB–NFIB* was detected, strongly suggesting another fusion partner. It is concluded that *MYBL1* alterations are detected in primary cutaneous ACC but are apparently less common compared with *MYB* and *NFIB* alterations.

Key Words: adenoid cystic carcinoma, skin, adnexal neoplasms, *MYB*, *MYBL1*, *NFIB*

(Am J Dermatopathol 2018;40:721–726)

INTRODUCTION

Adenoid cystic carcinoma (ACC) of the skin is a rare malignant neoplasm histologically identical to homonymous tumors in other organs, including salivary glands, respiratory tract, ear, lacrimal gland, ceruminous gland, Bartholin gland, and breast.[1–9] Approximately 60% of the studied cases of cutaneous ACC have been found to harbor *MYB* gene activations, either through *MYB* chromosomal abnormalities or by generation of the *MYB–NFIB* fusion.[10,11] In the latter case, a recurrent t(6;9) translocation fuses the myeloblastosis (*MYB*) proto-oncogene on chromosome 6q22-23 to the *NFIB* gene on chromosome 9p23-24.[12] The *MYB–NFIB* fusion oncogene activates transcription of genes involved in cell cycle control, DNA repair, and apoptosis. The translocation t(6;9) appears a tumor-type specific because it has been detected in ACC in different organs and anatomical structures, including salivary glands, lacrimal glands, breast, upper respiratory tract, ear, and Bartholin glands.[3,4,8,13,14] In addition to the *MYB* gene, alterations in *MYBL1*, the gene closely related to *MYB*, have been reported in salivary gland ACC.[15–17] Reciprocal *MYB* and *MYBL1* expression was consistently found in ACC.[16] Because we are not aware of any studies on cutaneous ACC studying alterations in *MYBL1*, our main goal was to find out whether this gene is involved in cutaneous ACC.

MATERIAL AND METHODS

Case Selection

Ten cases of cutaneous ACC with available paraffin blocks were randomly selected from our consultation files. The hematoxylin and eosin stained slides were reviewed together with the clinical information to confirm the diagnosis. Clinical data and follow-up information were obtained from the attending clinicians. In all cases, MYB immunostaining (clone EP769Y, diluation 1:100, ABCAM) was performed either at the time of the diagnosis or retrospectively.

Detection of *MYB–NFIB* Fusions and *MYBL1* Rearrangements by FISH

Four micrometre thick formalin-fixed paraffin-embedded (FFPE) sections were placed onto positively charged slides. Corresponding HE-stained slides were examined to determine the areas for cell counting. The unstained slides were routinely deparaffinized and incubated in the 1× Target Retrieval Solution Citrate pH 6

(Dako, Glostrup, Denmark) at 95°C/40 minutes and subsequently cooled for 20 minutes at room temperature in the same solution. The slides were washed in deionized water for 5 minutes and digested in a protease solution with Pepsin (0.5 mg/mL) (Sigma Aldrich, St. Louis, MO) in 0.01 M HCl at 37°C/25–60 minutes according to the sample conditions. The slides were then placed into deionized water for 5 minutes, dehydrated in a series of an ethanol solution (70%, 85%, 96% for 2 minutes each), and air-dried.

The *MYB–NFIB* fusions were detected by FISH using one commercial probe, ZytoLight SPEC *MYB* Dual Color Break-Apart Probe (ZytoVision GmbH, Bremerhaven, Germany) and custom-designed SureFish probes, namely a *NFIB* Break-Apart probe, a *MYB–NFIB* dual-fusion probe, and a *MYBL2* break-apart probe (Agilent Technologies, Santa Clara, CA). Chromosomal regions for the *NFIB* break-apart probe oligos are chr9:13740671-14140560 and chr9:14340306-14740560, for the *MYB–NFIB* fusion probe chr6:135271234-135771043 and chr9:13990266-14490285, and for the *MYBL1* probe chr8:67076230-67474559 and chr8:67526335-68426199.

For the SureFish designed probes, 0.5 μL of each probe (each color was delivered in a separated well), 0.5 μL of deionized water, and 3.5 μL of Locus Specific Identifier (LSI) buffer (Vysis/Abbott Molecular, Des Plaines, IL) were mixed before applying onto the specimen, whereas the *MYB* Dual Color Break-Apart Probe was factory premixed. An appropriate amount of the premixed probe was applied on the specimen, covered with a glass coverslip and sealed with rubber cement. The slides were incubated in the ThermoBrite instrument (StatSpin/Iris Sample Processing, Westwood, MA) with codenaturation at 85°C/8 minutes and hybridization at 37°C/16 hours. The rubber-cemented coverslip was then removed, and the slide was placed in a posthybridization wash solution (2× SSC/0.3% NP-40) at 72°C for 2 minutes. The slide was air-dried in the dark, counterstained with 4′, 6-diamidino-2-phenylindole (DAPI) (Vysis/Abbott Molecular), coverslipped, and immediately examined.

FISH Interpretation

The sections were examined with an Olympus BX51 fluorescence microscope (Olympus Corporation, Tokyo, Japan) using a 100× objective and filter sets triple band pass (DAPI/SpectrumGreen/SpectrumOrange), dual band pass (SpectrumGreen/SpectrumOrange), and single band pass (SpectrumGreen or SpectrumOrange). For each probe, 100 randomly selected nonoverlapping tumor cell nuclei were examined for the presence of yellow or green and orange fluorescent signals. Regarding break-apart probes, the yellow signals were considered negative, whereas the separate orange and green signals were considered positive. Conversely, for the

fusion probe, the yellow signals were considered positive, whereas the separate orange and green signals were considered negative. The cut off values were set to more than 10% and 20% of the nuclei (break-apart and fusion probes, respectively) with chromosomal breakpoint/fusion signals (mean + 3 SD in normal non-neoplastic control tissues).

Detection of *MYB–NFIB* Fusions by Reverse Transcipt Polymerase Chain Reaction RT-PCR

RNA from FFPE tissue samples was extracted using a QIASymphony RNA Kit (QIAGEN, Hilden, Germany) on the QIASymphony SP instrument (QIAGEN). RNA quantity and quality were measured using a Nanodrop 1000 Spectrophotometer (Thermo Scientific, Waltham, MA) and reverse transcribed using a Transcriptor First Strand cDNA Synthesis Kit (Roche, Basel, Switzerland) according to the manufacturer instructions. RNA integrity was determined by a control PCR comprising 2 μL of cDNA, 12.5 μL of HotStar Taq PCR Master Mix (QIAGEN), 10 pM of each primer, and distilled water up to 25 μL. The primers are showed in Table 1. The amplification program comprised 95°C/14 minutes, then 40 cycles of denaturation at 95°C/1 minute, annealing at 60°C/0.5 minutes, extension at 72°C/1 minute, and final extension at 72°C/7 minutes. Samples with RNA integrity below 133 bp were excluded from further analysis.

For the own fusion detection, 2 μL of cDNA was added to the reaction consisting of 12.5 μL of HotStar Taq PCR Master Mix (QIAGEN), 10 pM of each primer, and distilled water up to 25 μL. The amplification program comprises initial denaturation at 95°C/14 minutes, then 40 cycles of denaturation at 95°C/1 minute, annealing at 55°C/1 minute, and extension at 72°C/1.5 minutes. The program was finished by incubation at 72°C/7 minutes. The primers used for the PCR were described elsewhere.[18]

Successfully amplified PCR products of the *MYB–NFIB* fusion gene were purified, using a Montage PCR Centrifugal Filter Devices (Millipore, Billerica, MA). Then, the PCR products were both sides sequenced using a Big Dye Terminator Sequencing kit (Applied Biosystems, Carlsbad, CA), run on an automated genetic analyzer ABI Prism 3130xl (Applied Biosystems) at a constant voltage of 13.2 kV for 20 minutes and compared with the GenBank sequence.

RESULTS

Clinical Data

There were 6 female and 4 male patients, ranging in age at the diagnosis from 51 to 83 years (mean 68.5 years and median 67 years). Locations included the head (n = 4), thigh (n = 2), back (n = 2), and vulva (n = 2). All patients presented

TABLE 1. Primer Sequences With Respective Amplicon Lengths Used for RNA Integrity Testing

Primer Name	Amplicon Length, bp	Forward Primer Sequence	Reverse Primer Sequence
B2M	105	GAAAAAGATGAGTATGCCTG	ATCTTCAAACCTCCATGATG
B2M—133	133	CTCGCGCTACTCTCTCTTTCT	TGTCGGATTGATGAAACCCAG
PGK	247	CAGTTTGGAGCTCCTGGAAG	TGCAAATCCAGGGTGCAGTG

18

with a solitary neoplasm, varying in size from 5 to 50 mm in largest dimension (mean 18.6 mm). Two patients (case 7 and 9) presented with a recurrent tumor. In case 7, a small ACC had been removed at the same site 2 years earlier, whereas in case 9, the recurrence of vulvar ACC occurred 12 years after initial surgery. One patient (case 3) had been diagnosed with polycythemia 2 years before the occurrence of cutaneous ACC.

In 7 cases, the lesions were surgically removed, whereas in both patients with vulvar neoplasms, a vulvectomy with unilateral lymphadenectomy was performed, and in the remaining patient, surgery was combined with radiation therapy. Follow-up was available for 9 patients. In 7 patients, there was no evidence of disease at 6, 9, 37, 39, 40, 42, and 82 months. Two of them (cases 6, 10) later died, one of an unknown cause and the other patient because of an ovarian carcinoma. The patient (case 9) with the recurrent vulvar neoplasm developed pulmonary metastasis 1 year after the vulvectomy and then she was lost to follow-up. In the remaining patient (case 5), the tumor recurred within the scar 7 years after the initial diagnosis, and a year later, multiple pulmonary, rib, and liver metastases were detected; the patient died (Table 2).

Histopathologic and Immunohistochemical Features

In all but one case, there was a mixture of cribriform, tubular, and solid patterns forming variably shaped nodules in the dermis. In the remaining case, solid areas were lacking. The cribriform and tubular patterns dominated in 5 and 3 neoplasms, respectively, whereas in the remaining 2 cases, the solid pattern prevailed (>50% of the tumor volume). In all cases, both true small bilayered ducts and pseudocysts were recognized. The true ductal structures had small round lumina and were composed of inner epithelial cells with uniform round nuclei an outer layer of basal/myoepithelial cells. The pseudocystic structures were larger than the ducts and contained abundant basophilic mucinous material positive for Alcian blue at pH 2.5 and/or hyalinized PAS-positive eosinophilic material. The solid areas were composed of small basaloid cells with hyperchromatic, slightly angulated nucleus, and scant cytoplasm. Mitotic activity was low. Perineural invasion was seen in 4 cases. The stroma varied from hyalinized and paucicellular to focally fibrotic and myxoid. Of the 10 tumors studied, 5 neoplasms exhibited immunopositivity for MYB (>50% cells) (Fig. 1).

FISH Findings

MYB break-apart and *NFIB* break-apart tests were positive in 4 and 5 cases, respectively (Figs. 2 and 3). *MYB–NFIB* fusions were found in 4 cases (Fig. 4). The break of *MYBL1* was found in 2 cases, and in one of them, the *NFIB* break-apart probe was positive, strongly indicating a *MYBL1–NFIB* fusion (Fig. 5). In 2 cases, the *MYB* break-apart test was

TABLE 2. Main Clinicopathologic and Molecular Biologic Features

Case N	Sex/Age	Location/Size	Predominant Pattern/Perineural Invasion	IHC (MYB)	*MYB* ba	*NFIB* ba
1	F/58	Scalp	Cribriform/no	−	Neg	+
2	M/65	Thigh	Tubular/no	−	Neg	+
3	F/83	Scalp	Tubular/yes	+	Neg	Neg
4	M/51	Back	Cribriform/no	+	+	Neg
5	M/74	Shin	Solid/no	+	NA	NA
6	F/78	Head	Cribriform/yes	−	Neg	+
7	M/62	Face	Cribriform/no	−	Neg	Neg
8	F/69	Vulva	Tubular/yes	+	+	+
9	F/65	Vulva	Cribriform/yes	−	+	+
10	F/80	Sacral	Solid/no	+	+	Neg

Case N	*MYB–NFIB* Fusion	*MYBL1*	*MYB–NFIB* RT-PCR	Treatment	Follow-up
1	+	Neg	NA	Excision	Lost to follow-up
2	Neg	+	Neg	Excision	NED at 37 mo
3	Neg	Neg	NA	Excision	NED at 39 mo
4	Neg	Neg	Neg	Excision	NED at 40 mo
5	NA	Neg	Neg	Excision	Local recurrence in 87 mo, then pulmonary, liver and rib metastases 13 mo later and DOD
6	+	Neg	Neg	Excision	DUC at 82 mo
7	Neg	+	Neg	Excision	NED at 9 mo
8	+	Neg	+	Vulvectomy with lymphadenectomy	NED at 6 mo
9	+	Neg	Neg	Vulvectomy with lymphadenectomy	Pulmonary metastases in 1 y, then lost to follow-up
10	Neg	Neg	Neg	Excision + RT (51GY)	NED at 42 mo, then DUC 2 y later

DOD, death of disease; DUC, death of unknown or unrelated course; NA, not analyzable; NED, no evidence of disease; RT, radiation therapy.
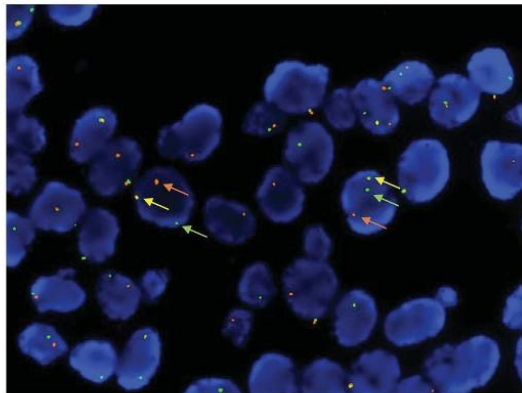
19
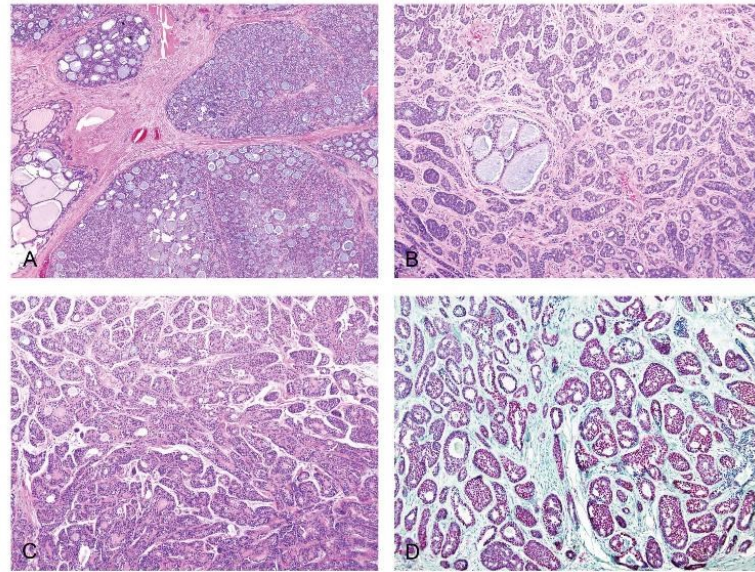
FIGURE 1. Adenoid cystic carcinoma of the skin with a predominant cribriform (A), tubular (B), and solid (C) patterns. Positive immunohistochemical staining for MYB protein (D).

positive, whereas no *MYB–NFIB* was detected, strongly suggesting another fusion partner. In case 3, all 4 FISH tests were negative, and in the remaining case, both *MYB* and *NFIB* break-apart samples were nonanalyzable, as were samples for *MYB–NFIB* fusions.

RT-PCR Findings

Of the 8 cases analyzed, *MYB–NFIB* fusions were detected in one neoplasm.

DISCUSSION

MYB is one of the earliest identified proto-oncogenes discovered as a cellular homologue of the viral oncogene (v-MYB) carried by 2 different avian leukemia retroviruses and plays a vital functional role in the establishment of definitive hematopoiesis. The MYB protein is a founding member of c-MYB transcription factor family that also encompasses MYBL1 (AMYB) and MYBL2 (BMYB) proteins. MYB plays a key role in the control of cell proliferation, survival,

FIGURE 2. Interphase FISH analysis using break-apart probe ZytoLight SPEC *MYB* dual color break-apart probe (6q23.3). Positive nuclei contains separate (split) orange and (or) green signals indicating a rearrangement (break) of one copy of the *MYB* gene region and also one orange-yellow-green fusion signal representing one normal (intact) copy of the homolog *MYB* locus.
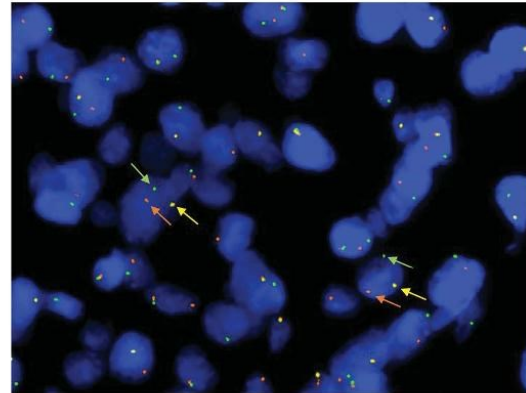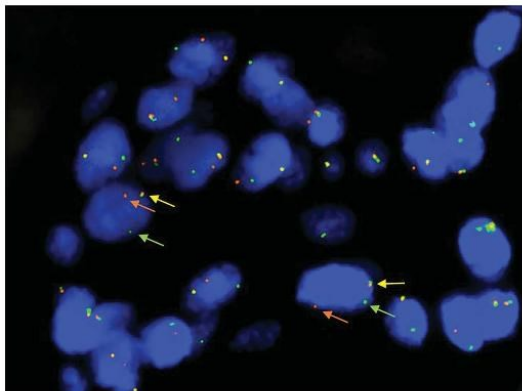

FIGURE 3. Interphase FISH analysis using custom-designed SureFISH *NFIB* break-apart probe (9p22.3). Positive nuclei contains separate (split) orange and (or) green signals indicating a rearrangement (break) of one copy of the *NFIB* gene region and also one orange-yellow-green fusion signal representing one normal (intact) copy of the homolog *NFIB* locus.

20
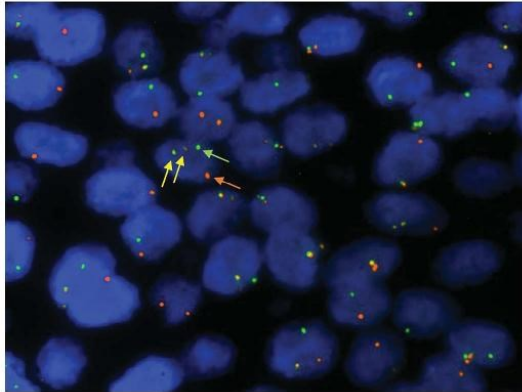
FIGURE 4. Interphase FISH analysis using custom-designed SureFISH *MYB–NFIB* dual fusion probe. Positive nuclei shows orange-yellow-green fusion signals representing reciprocal translocation t(6;9) (q22-23; p23-24) and also separate orange and green signals showing the normal homolog.

differentiation, and angiogenesis.[19,20] MYB expression has been found a potent driver of some animal and human neoplasms. In humans, *MYB* overexpression is detected in most myeloid and acute lymphoid leukemia.[19,20] Recent evidence showed that *MYB* alterations are common in ACC, as are changes involving *NFIB*.[1–7] *NFIB*, located on chromosome 9, is one of the 4 genes comprising the Nuclear Factor One family of transcription factors (*NFIA*, *NFIB*, *NFIC*, and *NFIX*). *NFIB* is essential for the development of various organ system, including salivary glands.[21] Involvement of *MYB* and/or *NFIB* in ACC in a variety of organs has been well documented, often as *MYB–NFIB* fusions.[1–7]

FIGURE 5. Interphase FISH analysis using custom–designed SureFISH *MYBL1* (8q13.1) break-apart probe positive nuclei contains separate (split) orange and (or) green signals indicating a rearrangement (break) of one copy of the *MYBL1* gene region and also one orange-yellow-green fusion signal representing one normal (intact) copy of the *MYBL1* locus.

Apart from *MYB–NFIB* gene fusions, alterations involving *MYBL1* have recently been identified in a subset of salivary gland ACC. Mitani et al described a novel *MYBL1–NFIB* gene fusion as a result of t(8;9) translocation and multiple rearrangements in the *MYBL1* gene in 35% of ACC (12 cases) negative for the t(6;9). All *MYBL1* alterations involved deletion of the C-terminal negative regulatory domain and were associated with high *MYBL1* expression. The authors also found reciprocal *MYB* and *MYBL1* expression. In addition, the authors identified 2 t(8;9) negative cases that were characterized by *MYBL1–YTHDF3* fusions. In addition, there were 2 cases negative for t(8;9) and showing no fusion of *MYBL1* but exhibiting *MYBL1* truncation. Lastly, in one case, a *MYBL1–RAD51B* fusion was found.[16] A case showing a similar fusion of *MYBL1* to an intron of the *RAD51B* gene on chromosome 14q23-q24.2, leading to antisense transcription of part of the *RAD51B* intron was found by Brayer et al.[17] The authors showed that the A-MYB protein is truncated, but no part of the *RAD51B* protein is included in the predicted fusion protein[17] Among 33 of ACC, Drier et al[7] found a case with *MYB* translocation to the *TGFBR3* locus. Among 33 cases of salivary gland ACC studied by Fujii et al,[15] *MYBL1–NFIB* fusions were seen in 2 cases, and in one case, the fusion partner for *MYBL1* remained unknown (labeled *MYBL1-X*), as it was unknown for 4 and 6 cases with *MYB* and *NFIB*, respectively (labeled *MYB-X* and *NFIB-X*). *MYBL1–NFIB* fusions were also detected by Rettig et al who additionally identified t(6;9) (q23.3; p22.3) fusions involving *MAP3K5-NFIB* 5. They also demonstrated that *NFIB* also recombined with 3 other genes on chromosome 6q, namely *RPS6KA2*, *MYO6*, and *RIMS1*. By contrast, *MYB* recombined with only one gene other than *NFIB*.[22]

In our series of cutaneous ACC, *MYB–NFIB* fusions were found in 4 cases. Remarkably, in 2 of these cases (cases 1 and 6), the *MYB* break-apart probe was negative. The discrepancies between break-apart and fusion probes in these cases be explained by several mechanisms including (1) an insertion of an *NFIB* gene segment immediately centromeric to the *MYB* gene outside the target region of the *MYB* break-apart probe, (2) breakpoints distal to the *MYB* gene (both reviewed in detail in Ref. 1), and (3) or by another yet undescribed mechanism. A similar pattern has been found in one of 9 vulvar ACC in a recent study.[8]

The break of *MYBL1* was found in our cohort in 2 cases (cases 2 and 7). In one of them (case 2), the *NFIB* break-apart probe was positive, strongly indicating a *MYBL1–NFIB* fusion, whereas in the second case (case 7), the fusion partner remained unknown.

In 2 cases (cases 4 and 10), the *MYB* break-apart test was positive, whereas no *MYB–NFIB* was detected, strongly suggesting another fusion partner. In one case (case 3), all 4 FISH tests were negative. In the remaining case (case 5), both *MYB* and *NFIB* break-apart samples were nonanalyzable, as were samples for *MYB–NFIB* fusions, whereas the remaining 2 investigations proved negative (Table 2).

Noteworthy is also the discrepancy between the results of FISH and RT-PCR for *MYB–NFIB* fusions. Of the 4 cases (cases 1, 6, 8, 9) where *MYB–NFIB* fusions were detected by FISH, only in one case was the fusion detected by RT-PCR.

Similar findings have previously been reported by North et al. In their series, *MYB–NFIB* fusion transcripts were identified in 2 of the 9 studied cases. All RT-PCR negative cases were immunohistochemically positive for MYB, and 4 showed various *MYB* rearrangements by FISH. The discrepancy can probably be explained by use of FFPE samples with degraded RNA and/or incapability of RT-PCR primes to detect all fusion transcript variants.

In our series, only 5 tumors manifested positivity for MYB (>50% cells), which is lower than previously reported. Among the 5 MYB-negative cases, there were 2 cases with *MYBL1* alterations, which is a likely explanation for the immunonegativity. For the remaining 3 cases, the immunonegative reaction for MYB oncoprotein is unclear. For comparison, in the series of North, 8 of the 9 cases stained for MYB were positive, but the authors used a different antibody.[10] It has recently been shown that MYB labeling by immunohistochemistry is more sensitive and more specific for mammary ACC than *MYB* labeling by FISH.[23] Obviously, this statement cannot be applied to primary ACC of the skin, nonetheless more studies are needed.

In conclusion, *MYBL1* alterations are detected in primary cutaneous ACC but are apparently less common compared with *MYB* and *NFIB* alterations. Our study suggests the occurrence of *MYBL1–NFIB* fusions but also the existence of another fusion partner in primary ACC of the skin.

REFERENCES

1. von Holstein SL, Fehr A, Persson M, et al. Adenoid cystic carcinoma of the lacrimal gland: MYB gene activation, genomic imbalances, and clinical characteristics. *Ophthalmology*. 2013;120:2130–2138.
2. Ho AS, Kannan K, Roy DM, et al. The mutational landscape of adenoid cystic carcinoma. *Nat Genet*. 2013;45:791–798.
3. Persson M, Andren Y, Mark J, et al. Recurrent fusion of MYB and NFIB transcription factor genes in carcinomas of the breast and head and neck. *Proc Natl Acad Sci U S A*. 2009;106:18740–18744.
4. West RB, Kong C, Clarke N, et al. MYB expression and translocation in adenoid cystic carcinomas and other salivary gland tumors with clinicopathologic correlation. *Am J Surg Pathol*. 2011;35:92–99.
5. D'Alfonso TM, Mosquera JM, MacDonald TY, et al. MYB-NFIB gene fusion in adenoid cystic carcinoma of the breast with special focus paid to the solid variant with basaloid features. *Hum Pathol*. 2014;45: 2270–2280.
6. Martelotto LG, De Filippo MR, Ng CK, et al. Genomic landscape of adenoid cystic carcinoma of the breast. *J Pathol*. 2015;237:179–189.
7. Drier Y, Cotton MJ, Williamson KE, et al. An oncogenic MYB feedback loop drives alternate cell fates in adenoid cystic carcinoma. *Nat Genet*. 2016;48:265–272.
8. Xing D, Bakhsh S, Melnyk N, et al. Frequent NFIB-associated gene rearrangement in adenoid cystic carcinoma of the vulva. *Int J Gynecol Pathol*. 2017;36:289–293.
9. Ramakrishnan R, Chaudhry IH, Ramdial P, et al. Primary cutaneous adenoid cystic carcinoma: a clinicopathologic and immunohistochemical study of 27 cases. *Am J Surg Pathol*. 2013;37:1603–1611.
10. North JP, McCalmont TH, Fehr A, et al. Detection of MYB alterations and other immunohistochemical markers in primary cutaneous adenoid cystic carcinoma. *Am J Surg Pathol*. 2015;39:1347–1356.
11. Prieto-Granada CN, Zhang L, Antonescu CR, et al. Primary cutaneous adenoid cystic carcinoma with MYB aberrations: report of three cases and comprehensive review of the literature. *J Cutan Pathol*. 2017;44: 201–209.
12. Brill LB II, Kanner WA, Fehr A, et al. Analysis of MYB expression and MYB-NFIB gene fusions in adenoid cystic carcinoma and other salivary neoplasms. *Mod Pathol*. 2011;24:1169–1176.
13. Chen TY, Keeney MG, Chintakuntlawar AV, et al. Adenoid cystic carcinoma of the lacrimal gland is frequently characterized by MYB rearrangement. *Eye (Lond)*. 2017;31:720–725.
14. Di Palma S, Fehr A, Danford M, et al. Primary sinonasal adenoid cystic carcinoma presenting with skin metastases–genomic profile and expression of the MYB-NFIB fusion biomarker. *Histopathology*. 2014;64:453–455.
15. Fujii K, Murase T, Beppu S, et al. MYB, MYBL1, MYBL2, and NFIB gene alterations and MYC overexpression in salivary gland adenoid cystic carcinoma. *Histopathology*. 2017;71:823–834.
16. Mitani Y, Liu B, Rao PH, et al. Novel MYBL1 gene rearrangements with recurrent MYBL1-NFIB fusions in salivary adenoid cystic carcinomas lacking t(6;9) translocations. *Clin Cancer Res*. 2016;22:725–733.
17. Brayer KJ, Frerich CA, Kang H, et al. Recurrent fusions in MYB and MYBL1 define a common, transcription factor-driven oncogenic pathway in salivary gland adenoid cystic carcinoma. *Cancer Discov*. 2016;6: 176–187.
18. Fehr A, Kovacs A, Loning T, et al. The MYB-NFIB gene fusion-a novel genetic link between adenoid cystic carcinoma and dermal cylindroma. *J Pathol*. 2011;224:322–327.
19. Ramsay RG, Gonda TJ. MYB function in normal and cancer cells. *Nat Rev Cancer*. 2008;8:523–534.
20. Drabsch Y, Robert RG, Gonda TJ. MYB suppresses differentiation and apoptosis of human breast cancer cells. *Breast Cancer Res*. 2010;12:R55.
21. Mellas RE, Kim H, Osinski J, et al. NFIB regulates embryonic development of submandibular glands. *J Dent Res*. 2015;94:312–319.
22. Rettig EM, Talbot CC Jr, Sausen M, et al. Whole-genome sequencing of salivary gland adenoid cystic carcinoma. *Cancer Prev Res (Phila)*. 2016; 9:265–274.
23. Poling JS, Yonescu R, Subhawong AP, et al. MYB labeling by immunohistochemistry is more sensitive and specific for breast adenoid cystic carcinoma than MYB labeling by FISH. *Am J Surg Pathol*. 2017;41: 973–979.

Lack of Deletion of 1p36 in 8 Cases of Primary Adenoid Cystic Carcinoma of the Skin

To the Editor:

In our previous study, we have demonstrated that primary cutaneous adenoid cystic carcinoma (ACC) manifests genetic changes similar to its salivary gland homologue, including alterations in the *MYB* and *MYBL1* genes.[1] Deletion of the 1p36 locus has been shown in salivary gland ACC (range of detection: 0%–44%),[2–4] in which this alteration has been found to be associated with reduced overall survival, higher tumor stage, lower recurrence-free interval, lower recurrence-free survival, solid histology, and the absence of *MYBL1* break.[4,5] As this technique has now become available for us, we investigated our previously published cohort of 10 patients with primary cutaneous ACC.[1] FISH for 1p36 was performed, as described elsewhere.[5] The analysis was successful in 8 of the 10 cutaneous neoplasms. All the cases, including 2 patients who died of metastatic disease, proved negative. It seems that the deletion of 1p36 is not a feature of cutaneous ACC, but further studies on larger series are needed to confirm this assumption.

Liubov Kyrpychova, MD*
Petr Šteiner, PhD†
Michal Michal, MD*†
Dmitry V. Kazakov, MD, PhD*†
*Šikl's Department of Pathology,
Medical Faculty in Pilsen,
Charles University in Prague,
Pilsen, Czech Republic
†Bioptical Laboratory,
Pilsen, Czech Republic

REFERENCES

1. Kyrpychova L, Vanecek T, Grossmann P, et al. Small subset of adenoid cystic carcinoma of the skin is associated with alterations of the MYBL1 gene similar to their extracutaneous counterparts. *Am J Dermatopathol.* 2018;40: 721–726.
2. Persson M, Andren Y, Moskaluk CA, et al. Clinically significant copy number alterations and complex rearrangements of MYB and NFIB in head and neck adenoid cystic carcinoma. *Genes Chromosomes Cancer.* 2012;51: 805–817.
3. Seethala RR, Cieply K, Barnes EL, et al. Progressive genetic alterations of adenoid cystic carcinoma with high-grade transformation. *Arch Pathol Lab Med.* 2011;135: 123–130.
4. Rao PH, Roberts D, Zhao YJ, et al. Deletion of 1p32-p36 is the most frequent genetic change and poor prognostic marker in adenoid cystic carcinoma of the salivary glands. *Clin Cancer Res.* 2008;14:5181–5187.
5. Steiner P, Andreasen S, Grossmann P, et al. Prognostic significance of 1p36 locus deletion in adenoid cystic carcinoma of the salivary glands. *Virchows Arch.* 2018;473:471–480.

Contents lists available at ScienceDirect

Annals of Diagnostic Pathology

Cutaneous hidradenoma: a study of 21 neoplasms revealing neither correlation between the cellular composition and *CRTC1-MAML2* fusions nor presence of *CRTC3-MAML2* fusions ☆,☆☆

Liubov Kyrpychova, MD [a], Denisa Kacerovska, MD, PhD [a,b], Tomas Vanecek, PhD [a,b], Petr Grossmann, PhD [a,b], Michal Michal, MD [a,b], Katrin Kerl, MD [c], Dmitry V. Kazakov, MD, PhD [a,c,*]

[a] Sikl's Department of Pathology, Medical Faculty in Pilsen, Charles University in Prague, Pilsen, Czech Republic
[b] Bioptical Laboratory, Pilsen, Czech Republic
[c] Dermatopathology Unit, Department of Dermatology, Zurich University Hospital, Zurich, Switzerland

A R T I C L E   I N F O

A B S T R A C T

Twenty-one hidradenomas from 20 patients (13 female, 7 male) ranging in age from 18 to 87 years (mean, 57.75 years; median, 60 years) were studied for *CRTC1-MAML2* and *CRTC3-MAML2* fusions to find out whether there is a correlation between the particular cell type (polyhedral eosinophilic, clear, mucinous, epidermoid, and oncocytic) and presence the above alterations. *CRTC1-MAML2* fusions were detected in 10 of the 21 neoplasms (47.6%). Fluorescence in situ hybridization for MAML2 break apart was analyzable in 13 specimens and in all these specimens was positive, including 4 tumors with no demonstrable *CRTC1-MAML2* fusion. In none of the cases was a *CRTC3-MAML2* fusion detected. No obvious correlation between the cellular composition and presence of t(11,19) translocation was found.

© 2016 Elsevier Inc. All rights reserved.

1. Introduction

Hidradenoma is a relatively common cutaneous adnexal neoplasm composed of several cell types, including polyhedral eosinophilic cells, clear cells, squamoid (epidermoid) cells, mucinous cells, oxyphilic (oncocytic) cells, and various transitional (intermediate) cells. These cell types occur in variable proportions and in various combinations from case to case, and in some tumors, a particular cell type predominates. The neoplasm is usually solid and/or solid cystic; less common is a markedly prevailing cystic component, multinodular sclerosing pattern, or prominent glandular differentiation [1–7]. Hidradenoma harbors the t(11;19) translocation which results in fusion of the mucoepidermoid carcinoma translocated 1 (*MECT1*) gene on chromosome 19p13 (synonyms: *TORC1*, *CRTC1*, *WAMTP1*) with the mastermind-like 2 (*MAML2*) gene on chromosome 11q21 [8]. This translocation is encountered in approximately 50% of cases and is said to be more common in cases with predominant clear cell differentiation [9]. Outside the skin, the translocation is often seen in mucoepidermoid

carcinoma (MEC) of salivary glands. In this salivary gland neoplasm, apart from *CRTC1-MAML2* fusion, a subset of cases with *CRTC3-MAML2* fusions has been identified [10]. The objectives of our study were (1) to find out whether there is indeed a correlation between cellular composition and *CRTC1-MAML2* fusion and (2) to study *CRTC3-MAML2* fusions in this adnexal neoplasm.

2. Materials and methods

2.1. Case inclusion/exclusion

Twenty cases of cutaneous hidradenoma were randomly selected from our files and were subjected to molecular biological studies for *CRTC3-MAML2* and *CRTC1-MAML2* fusions as indicated below. Three cases were excluded based on negative control amplifications, and new randomly selected 3 cases were added, with 1 patient having 2 neoplasms.

2.2. Light microscopic investigations

For each of the 21 tumors included, we analyzed the cellular composition of the tumor scoring the presence of a particular cell type (polyhedral eosinophilic, clear, mucinous, epidermoid [squamoid], and oncocytic [oxyphilic]) as follows: 0% (−), 1%-5% (+), 5%-25% (++), 25%-50% (+++), and >50% (++++). We also estimated the ratio of solid areas vs glandular areas and connection to the epidermis.

24

2.3. RNA extraction, RNA integrity, and reverse transcription

RNA from the formalin-fixed, paraffin-embedded tissue was extracted using the RecoverAll Total Nucleic Acid Isolation Kit (Ambion, Austin, TX). cDNA was synthesized by reverse transcription (RT) using the Transcriptor First Strand cDNA Synthesis Kit (RNA input 1 μg) (Roche Diagnostics, Mannheim, Germany). All procedures were performed according to the manufacturer's protocols.

Amplification of 105– and 133–base pair (bp) products of the [beta]-2-microglobulin gene and 247-bp product of the PGK gene was used to test the quality of the extracted RNA, as previously described [11–13]. A volume of 2 μL of cDNA was added to the polymerase chain reaction (PCR) mixture containing 12.5 μL of HotStar Taq PCR Master Mix (Qiagen, Hilden, Germany), 10 pmol of each primer (Table 1), and distilled water up to 25 μL. The amplification conditions for all control genes consisted of denaturation at 95°C for 14 minutes and then 40 cycles of denaturation at 95°C for 1 minute, annealing at 60°C for 1 minute, and extension at 72°C for 1 minute. The program was completed by incubation at 72°C for 7 minutes. Only those samples with at least 1 positive control amplification were further analyzed.

2.4. Detection of CRTC1-MAML2 and CRTC3-MAML2 fusion transcripts

Detection of CRTC1-MAML2 and CRTC3-MAML2 fusion transcripts was performed using nested RT-PCR with primers published elsewhere [10,14] (Table 1). A volume of 2 μL of cDNA was added to the PCR mixture containing 12.5 μL of HotStar Taq PCR Master Mix (Qiagen, Hilden, Germany), 10 pmol of each outer primer complementary to CRTC1-MAML2 or CRTC3-MAML2 fusion transcripts, and distilled water up to 25 μL. The amplification conditions comprised denaturation at 95°C for 14 minutes and then 35 cycles of denaturation at 95°C for 30 seconds, annealing at 55°C for 30 seconds, and extension at 72°C for 30 seconds. Each PCR product from the first run was diluted with distilled water at a ratio 1:50. A volume of 1 μL of the diluted product was added to a second run of the PCR, with the same reagents as in the first run except for the inner primers. The amplification conditions of the second round consisted of denaturation at 95°C for 14 minutes and then 35 cycles of denaturation at 95°C for 30 seconds, annealing at 60°C for 30 seconds, and extension at 72°C for 30 seconds. The program was finished by incubation at 72°C for 7 minutes. Successfully amplified RT-PCR products of the CRTC1-MAML2 or CRTC3-MAML2 fusion were purified with magnetic beads using the Agencourt AMPure Kit (Agencourt Bioscience Corporation, A Beckman Coulter Company, Beverly, MA), both sides sequenced using the Big Dye Terminator Sequencing Kit (Applied Biosystems, Foster City, CA) and purified with magnetic beads using the Agencourt CleanSEQ Kit (Agencourt Bioscience Corporation, Foster City, CA), all according to the manufacturer's instructions. Samples were then run on an automated sequencer ABI Prism 3130 × I (Applied Biosystems, Foster City, CA) at a constant voltage of 13.2 kV for 20 minutes and compared with the GenBank sequences.

2.5. Detection of MAML2 break by fluorescence in situ hybridization

Before performing fluorescence in situ hybridization (FISH), hematoxylin and eosin–stained slides were examined to determine the areas for cell counting. Then, a 4-μm-thick formalin-fixed, paraffin-embedded section was placed onto a positively charged slide. The unstained slide was routinely deparaffinized and incubated in the 1× Target Retrieval Solution Citrate pH 6 (Dako, Glostrup, Denmark) for 40 minutes at 95°C, subsequently cooled for 20 minutes at room temperature in the same solution, and washed in deionized water for 5 minutes. The slide was digested in protease solution with pepsin (0.5 mg/mL) (Sigma Aldrich, St Louis, MO) in 0.01 mol/L HCl at 37°C for 15 minutes. The slide was then rinsed in deionized water for 5 minutes, dehydrated in a series of ethanol solutions (70%, 85%, 96% for 2 minutes each), and air dried. An appropriate amount of factory premixed probe ZytoLight SPEC MAML2 Dual Color Break Apart Probe (11q21) (ZytoVision GmbH, Bremerhaven, Germany) was applied on the specimens, covered with a glass cover slip, and sealed with rubber cement. The slide was incubated in the ThermoBrite instrument (StatSpin/Iris Sample Processing, Westwood, MA) with codenaturation parameters of 85°C for 8 minutes and hybridization parameters of 37°C for 16 hours. The rubber-cemented cover slip was then removed, and the slide was placed in posthybridization wash solution (2 × SSC/ 0.3% NP-40) at 72°C for 2 minutes. The slides were air dried in the dark, counterstained with DAPI II (Vysis/Abbott Laboratories, Abbott Park, IL), covered with slip, and immediately examined under an Olympus BX51 fluorescence microscope using a ×100 objective and filter sets Triple Band Pass (DAPI/Spectrum Green/Spectrum Orange), Dual Band Pass (FITC/Texas Red), and Single Band Pass (Spectrum Green or Spectrum Orange). One hundred randomly selected nonoverlapping tumor cell nuclei were examined for the presence of yellow (normal) or green and red (chromosomal break point) fluorescent signals. The sample was considered positive if >10% of nuclei showed break point signal.

3. Results

3.1. Clinical data

There were 13 women and 7 men, ranging in age from 18 to 87 years (mean, 57.75 years; median, 60 years). All but 1 patient presented with solitary lesions; 1 woman had 2 tumors. Locations included the head and neck area (n = 8), extremities (n = 8), and trunk (n = 4). In 1 case, the location was unknown. The sized of the lesions varied from 2 to 30 mm (mean, 11.1 mm; median, 9 mm) (Table 2).

3.2. Histopathological findings

All neoplasms manifested a multinodular architecture and were composed of different cell types. A marked predominance of 1 cell type (++++) was seen in only 1 case in which a majority (90%) of cells were clear cells (Fig. 1). In 4 other lesions, there was predominance of polyhedral eosinophilic cells (40%-45%) over other cell types (Fig. 2). In the remaining lesions, there was no predominance of particular cell type, and most displayed 3-4 cell types, with 2 neoplasms composed of all 6 cell variants (Figs. 3 and 4). Mucinous cells and oxyphilic cells were the least common cell types, usually seen only focally. Focal glandular differentiation was always present but usually represented a minor moiety; a glandular component dominated over the solid areas only in 1 case (Fig. 5). In many cases, apocrine secretion was readily apparent in the glandular areas (Fig. 6). The epidermis was present in 17 specimens, and the tumor manifested connection to the epidermis in 7 cases (Fig. 7).

Table 1
Primers for nested PCR

Name of primer	Sequence 5'-3'
b2-mikroglob.F	GAAAAAGATGAGTATGCCTG
b2-mikroglob.R	ATCTTCAAACCTCCATGATG
B2M-133F	CTCGCGCTACTCTCTCTTTCT
B2M-133R	TGTCGGATTCGATGAAACCCAG
pgk-F	CAGTTTGGAGCTCCTGGAAG
pgk-R	TGCAAATCCAGGGTGCAGTG
CRTC1A (outer)	TCGCGCTGCACAATCAGAAG
CRTC1B (inner)	GAGGTCATGAAGGACCTGAG
CRTC3A (outer)	TCGCGCTGCACACGCAGAGA
CRTC3B (inner)	CAGAGACAGGCCGAGGAGAC
MAML2A (outer)	GGTCGCTTGCTGTTGGCAGG
MAML2B (inner)	TTGCTGTTGGCAGGAGATAG

Table 2
Main clinicopathological and molecular biological data

Case	Sex/age	Clinical data	Location	Size, mm	Architecture (S:G)	EC	ClC	PEC	SqC	OxC	TrC	MuC	t(11;19) CRTC1/MAML2	t(11;15) CRTC3/MAML2	Control genes 105/133/247 bp	MAML2 BA FISH
Case 1	F/66	Solitary nodule	Forearm	25	S > G	−	−	+	+	+	++	−	−	−	+/+/−	+
Case 2	F/38	Histiocytoma?	Lower leg	8	S > G	−	++++	+	−	−	+	−	−	−	+/+/+	+
Case 3	F/51	Cystic nodule, 6-y duration	Chest wall	25	S > G	−	++	+	+	−	++	+	+	−	+/+/+	NA
Case 4	F/50	Nodule, 2-y duration	Abdomen	15	S > G	−	+	+++	++	−	++	+	−	−	+/−/−	NA
Case 5	F/49	Solitary nodule	Unknown	9	S > G	−	++	+++	+	−	++	+	−	−	+/−/−	+
Case 6	M/60	Lipoma	Forehead	6	S ≈ G	NA	+	+++	−	+	++	−	−	−	+/+/−	NA
Case 7	M/76	Fibroadenoma	Chest wall	8	S > G	−	++	+	++	+	+	−	−	−	+/+/+	NA
Case 8	F/55	Verucca	Scapula	7	S > G	−	+	++	−	−	++	+	−	−	+/+/+	NA
Case 9	M/87	Solitary nodule	Shin	30	S > G	+	+	+	++	+	+	+	+	−	+/+/+	+
Case 10	F/39	Nodule	Finger	14	S > G	NA	+	+++	−	−	+	−	−	−	+/−/−	NA
Case 11	F/68	Histiocytoma, several years' duration	Tibia	10	G > S	−	++	+	−	−	+	−	−	−	+/+/+	NA
Case 12	F/74	Pyogenic granuloma?	Shin	6	S > G	+	+	−	+	−	+	−	−	+	+/+/−	+
Case 13	M/60	Nevus?	Forehead	8	S > G	+	+	+	+	−	+	−	+	−	+/+/+	+
Case 14	F/43	Atheroma?	Eyelid	2	S > G	−		+		−	++	−	−	−	+/+/−	NA
Case 15	F/64	Nodule	Shin	6	S > G	+	+	+	+	−	+	−	+	−	+/+/+	+
Case 16	M/18	Atheroma?	Neck	6	S > G	NA	++	+	−	−	+	−	+	−	+/+/+	+
Case 17	F/65	Solitary nodule	Scalp	9	S ≈ G	−	+	+	−	−	+	+	+	−	+/+/+	+
Case 18	M/52	Granuloma	Thigh	9	S > G	+	+	+	+	−	+	−	+	−	+/+/+	+
Case 19	M/66	Basal cell carcinoma	Scalp	11	S ≈ G	+	−	++	+	+	++	−	+	−	+/+/+	+
Case 20	F/73	A. Fibroma	A. Scalp	12	S > G	NA	+	+	+	+	+	+	+	−	A. +/+/+	A. +
		B. Verrucous nevus	B. Scalp	8	S > G	+	++	−	−	−	++	−	+	−	B. +/+/+	B. +

S, solid areas; G, glandular areas; NA, not accessible/not analyzable; ClC, clear cells; PEC, polyhedral eosinophilic cells; SqC, squamoid (epidermoid) cells; OxC, oxyphylic (oncocytic) cells; TrC, transitional cells; MuC, mucinous cells; BA, break apart.
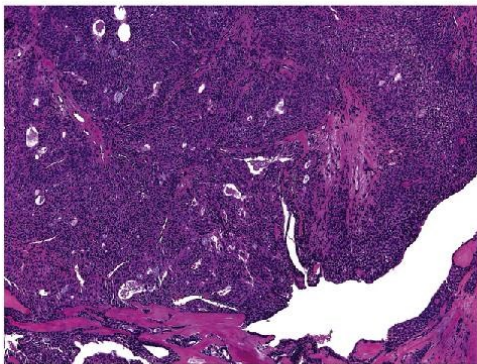
26
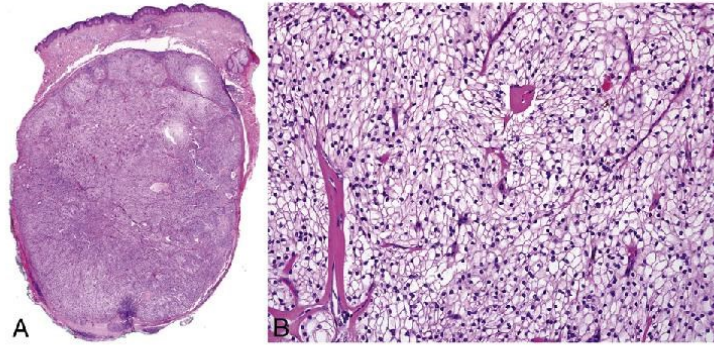
Fig. 1. Case 2. Hidradenoma with marked predominance of clear cells constituting about 90% of the neoplasm (A, B). No *CRTC1-MAML2* fusion was detected in this lesion, whereas FISH for *MAML2* break apart was positive.

3.3. Molecular biological findings

CRTC1-MAML2 fusions were detected in 10 of the 21 neoplasms (47.6%) (Fig. 8). FISH for *MAML2* break apart was analyzable in 13 specimens and in all these specimens was positive, including 4 tumors with no demonstrable *CRTC1-MAML2* fusion (Fig. 9). In none of the cases was a *CRTC3-MAML2* fusion detected.

4. Discussion

Our study revealed no obvious correlation between the cellular composition and presence of t(11,19) translocation. The latter was found even in lesions with very few clear cells. (Earlier, using different methodology, we observed presence of the above translocation even in cases of hidradenoma completely lacking clear cells [our unpublished observations].) However, some findings from the current study merit a short comment. All 5 lesions in which a particular cell type dominated over other cell types (1 neoplasm with clear cells [++++] and 4 tumors with polyhedral eosinophilic cells [+++]) lacked a detectable *CRTC1-MAML2* fusion. The latter was found in all but 1 tumor connected to the epidermis. One patient presented with 2 neoplasms that manifested different cellular composition, and both tumors harbored *CRTC1-MAML2* fusion. There were 4 samples with positive *MAML2* break-apart probe, yet no *CRTC1-MAML2* fusion was detected. This can be explained by suboptimal quality of RNA, low RNA expression,

different exon joining of the same genes, or a different fusion partner of *MAML2*. The *MAML2* break-apart probe proved positive in all analyzable specimens.

CRTC1 (*MECT1*) is a transducer of the cyclic AMP–responsive element-binding protein and a member of the highly conserved CREB coactivator. *MAML2* is a member of the mastermind-like gene family and encodes a nuclear protein that coactivates the Notch receptor path-
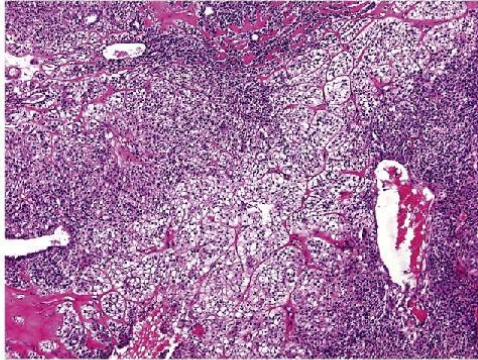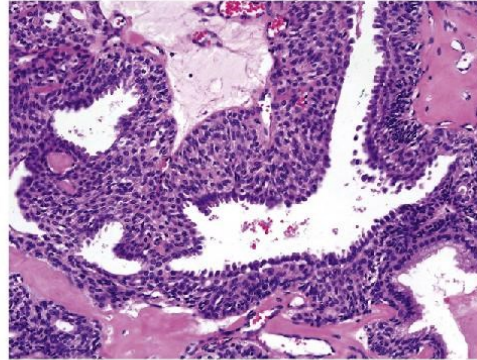

Fig. 2. Case 5. Hidradenoma with numerous polyhedral eosinophilic cells. Squamoid, transitional, and mucinous cells can also be recognized. No *CRTC1-MAML2* fusion was detected in this lesion, whereas FISH for *MAML2* break apart was positive.
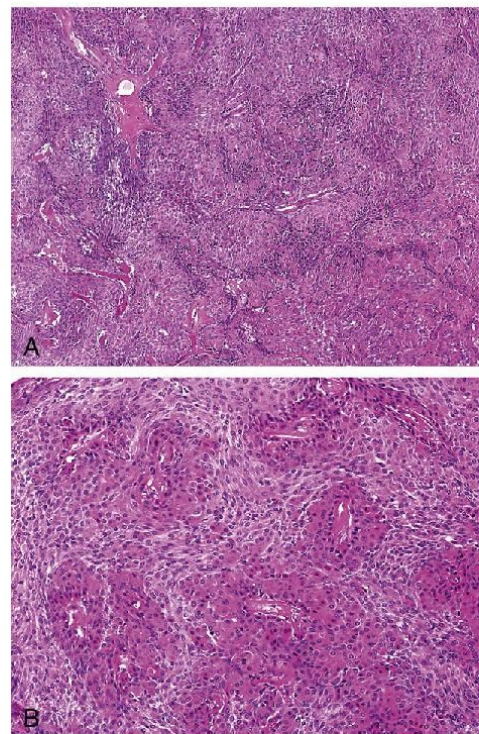
Fig. 3. Case 1. Hidradenoma without marked predominance of a particular cell type composed of polyhedral eosinophilic cells, squamoid cells, oxyphilic cells, and transitional elements. No *CRTC1-MAML2* fusion was detected in this lesion, whereas FISH for *MAML2* break apart was positive.

Fig. 4. Case 3. Hidradenoma without marked predominance of a particular cell type composed of clear cells, polyhedral eosinophilic cells, and transitional cells. Occasional squamoid and mucinous cells were detected in the lesion (not shown). *CRTC1-MAML2* fusion was detected in this lesion.

ways. The MAML2 protein forms a complex with the Notch intracellular domain and CSL transcription family members to activate the Notch downstream target genes (*HES1* and *HES5*). The fusion protein


A

B
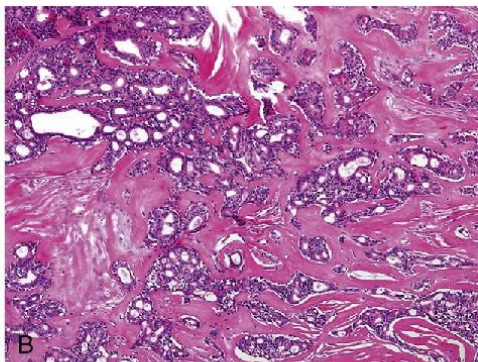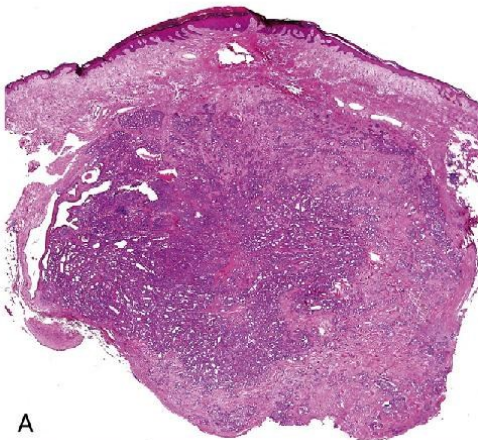
Fig. 5. Case 11. Hidradenoma in which a glandular component dominates over solid areas (A, B). No *CRTC1-MAML2* fusion was detected in this tumor.

Fig. 6. Case 17. Apocrine secretion in the glandular component. *CRTC1-MAML2* fusion was detected in this lesion.

influences expression of cAMP/CREB (*FLT1*) and Notch (*HES1* and *HES5*) target genes which associated with epithelial tumorigenesis [15]. Apart from cutaneous hidradenoma, the t(11;19) translocation has been detected in cutaneous hidradenocarcinoma and mammary hidradenoma, but the most common tumor harboring this alteration in MEC arises both in salivary glands and in other organs [16–22]. With respect to salivary gland MEC, this translocation was found in conventional neoplasm as well as unusual variants, including clear cell predominant and oncocytic tumors, and Warthin-like variant [23–26]. It has been found that MEC cases positive for *CRTC1-MAML2* have a better prognosis compared with fusion-negative lesions [27–30]. Apart from MEC, *CRTC1-MAML2* fusions were detected in other lesions. [9,31,32]; *CRTC1* rearrangements in the absence of t(11;19) has been found in a series of alleged primary cutaneous mucoepidermoid carcinoma, but judging from the microscopic illustrations and description of the neoplasms, some are likely to represent hidradenoma or hidradenocarcinoma [33].

Aside from *CRTC1*, there are 2 other *CRTC1*-related human genes, namely, *CRTC2* at 1q21 and *CRTC3* at 15q26. Previous studies on salivary gland MEC revealed a subset of cases with a *CRTC3-MAML2* fusion [34]. The latter was found in patients who presented favorable clinicopathological features and an indolent clinical course. As no studies of this alteration in cutaneous hidradenoma were available, we tested our cases for this translocation, but all proved negative.

In conclusion, our study shows that t (11,19) can be found in cutaneous hidradenoma with various cytological compositions and
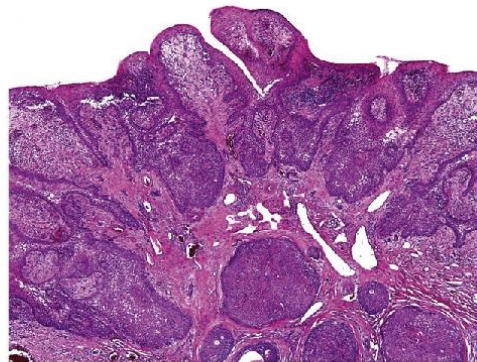
Fig. 7. Case 12. Connection of the hidradenoma to the overlying epidermis. *CRTC1-MAML2* fusion was not detected in this neoplasm; in all other lesions with epidermal connection, the fusion was identified.
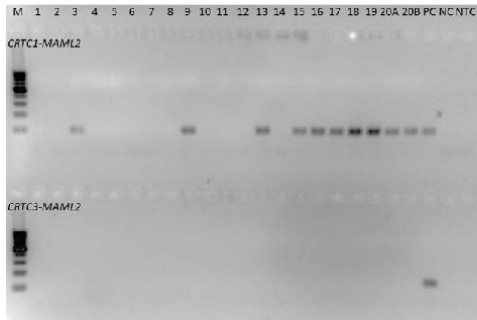
Fig. 8. Detection of *CRTC1-MAML2* and *CRTC3-MAML2* fusion transcripts by nested RT-PCR. 1-20, numbers of cases (A, B; 2 different tumors from the same patient); PC, positive control; NC, negative control; NTC, nontemplate control. Cases 3, 9, 13, and 15-20 are positive for *CRTC1-MAML2* fusion transcript. No *CRTC3-MAML2* fusions are identified.
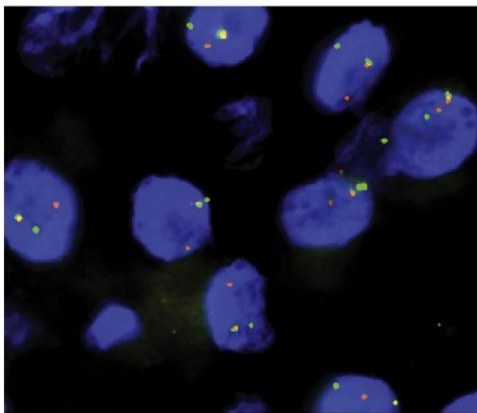
Fig. 9. FISH analysis using a break-apart rearrangement probe (ZytoLight SPEC MAML2 Dual Color Break Apart Probe [11q21]). Nuclei with 1 fusion (yellow), 1 orange, and 1 green (split) signal pattern indicative of a rearrangement of 1 copy of the *MAML2* gene region.

not only in clear cell–predominant lesions. There are hidradenomas that manifest positive *MAML2* break-apart probe but lack any demonstrable *CRTC1-MAML2* fusion, suggesting, among other things, a different fusion partner. No tumor in our series yielded *CRTC3-MAML2* fusion.

References

[1] Johnson Jr BL, Helwig EB. Eccrine acrospiroma. A clinicopathologic study. Cancer 1969;23:641–57.

[2] Requena L, Kiryu H, Ackerman AB. Neoplasms with apocrine differentiation. Philadelphia: Lippincott-Raven; 1998.

[3] Kazakov DV, Michal M, Kacerovska D, McKee PH. Cutaneous adnexal tumors. LWW; 2012 814.

[4] Roth MJ, Stern JB, Hijazi Y, Haupt HM, Kumar A. Oncocytic nodular hidradenoma. Am J Dermatopathol 1996;18:314–6.

[5] Angulo J, Jaqueti G, Kutzner H, Requena L. Squamous cell apocrine hidradenoma. J Cutan Pathol 2007;34:801–3.

[6] Stefanato CM, Ferrara G, Chaudhry IH, Guevara Pineda C, Waschkowski G, Rose C, et al. Clear cell nodular hidradenoma involving the lymphatic system: a tumor of uncertain malignant potential or a novel example of "metastasizing" benign tumor? Am J Surg Pathol 2012;36:1835–40.

[7] Goh SG, Carr R, Dayrit JF, Calonje E. Mucinous hidradenoma: a report of three cases. J Cutan Pathol 2007;34:497–502.

[8] Behboudi A, Winnes M, Gorunova L, van den Oord JJ, Mertens F, Enlund F, et al. Clear cell hidradenoma of the skin—a third tumor type with a t(11;19)-associated TORC1-MAML2 gene fusion. Genes Chromosomes Cancer 2005;43:202–5.

[9] Winnes M, Mölne L, Suurküla M, Andrén Y, Persson F, Enlund F, et al. Frequent fusion of the CRTC1 and MAML2 genes in clear cell variants of cutaneous hidradenomas. Genes Chromosomes Cancer 2007;46:559–63.

[10] Nakayama T, Miyabe S, Okabe M, Sakuma H, Ijichi K, Hasegawa Y, et al. Clinicopathological significance of the CRTC3-MAML2 fusion transcript in mucoepidermoid carcinoma. Mod Pathol 2009;22:1575–81.

[11] Gaffney R, Chakerian A, O'Connell JX, Mathers J, Garner K, Joste N, et al. Novel fluorescent ligase detection reaction and flow cytometric analysis of SYT-SSX fusions in synovial sarcoma. J Mol Diagn 2003;5:127–35.

[12] Dalal S, Berry AM, Cullinane CJ, Mangham DC, Grimer R, Lewis IJ, et al. Vascular endothelial growth factor: a therapeutic target for tumors of the Ewing's sarcoma family. Clin Cancer Res 2005;11:2364–78.

[13] Antonescu CR, Kawai A, Leung DH, Lonardo F, Woodruff JM, Healey JH, et al. Strong association of SYT-SSX fusion type and morphologic epithelial differentiation in synovial sarcoma. Diagn Mol Pathol 2000;9:1–8.

[14] Skálová A, Vanecek T, Simpson RH, Vazmitsel MA, Majewska H, Mukensnabl P, et al. CRTC1-MAML2 and CRTC3-MAML2 fusions were not detected in metaplastic Warthin tumor and metaplastic pleomorphic adenoma of salivary glands. Am J Surg Pathol 2013;37:1743–50.

[15] Tonon G, Modi S, Wu L, Kubo A, Coxon AB, Komiya T, et al. T(11;19)(q21;p13) translocation in mucoepidermoid carcinoma creates a novel fusion product that disrupts a notch signaling pathway. Nat Genet 2003;33:208–13.

[16] Kazakov DV, Ivan D, Kutzner H, Spagnolo DV, Grossmann P, Vanecek T, et al. Cutaneous hidradenocarcinoma: a clinicopathological, immunohistochemical, and molecular biologic study of 14 cases, including Her2/neu gene expression/amplification, TP53 gene mutation analysis, and t(11;19) translocation. Am J Dermatopathol 2009;31:236–47.

[17] Kazakov DV, Vanecek T, Belousova IE, Mukensnabl P, Kollertova D, Michal M. Skintype hidradenoma of the breast parenchyma with t(11;19) translocation: hidradenoma of the breast. Am J Dermatopathol 2007;29:457–61.

[18] Kazakov DV, Spagnolo DV, Kacerovska D, Rychly B, Michal M. Cutaneous type adnexal tumors outside the skin. Am J Dermatopathol 2011;33:303–15.

[19] Von Holstein SL, Fehr A, Heegaard S, Therkildsen MH, Stenman G. CRTC1-MAML2 gene fusion in mucoepidermoid carcinoma of the lacrimal gland. Oncol Rep 2012; 27:1413–6.

[20] Roden AC, García JJ, Wehrs RN, Colby TV, Khoor A, Leslie KO, et al. Histopathologic, immunophenotypic and cytogenetic features of pulmonary mucoepidermoid carcinoma. Mod Pathol 2014;27:1479–88.

[21] Bell D, Lewis C, El-Naggar AK, Weber RS. Primary intraosseous mucoepidermoid carcinoma of the jaw: reappraisal of the MD Anderson Cancer Center experience. Head Neck 2016;38:E1312–7.

[22] Camelo-Piragua SI, Habib C, Kanumuri P, Lago CE, Mason HS, Otis CN. Mucoepidermoid carcinoma of the breast shares cytogenetic abnormality with mucoepidermoid carcinoma of the salivary gland: a case report with molecular analysis and review of the literature. Hum Pathol 2009;40:887–92.

[23] Tajima S, Namiki I, Koda K. A clear cell variant of mucoepidermoid carcinoma harboring CRTC1-MAML2 fusion gene found in buccal mucosa: report of a case showing a large clear cell component and lacking typical epidermoid cells and intermediate cells. Med Mol Morphol 2015 [in press].

[24] Ishibashi K, Ito Y, Masaki A, Fuji K, Beppu S, Sakakibara T, et al. Warthin-like mucoepidermoid carcinoma: a combined study of fluorescence in situ hybridization and whole-slide imaging. Am J Surg Pathol 2015;39:1479–87.

[25] Fujimaki M, Fukumura Y, Saito T, Mitani K, Uchida S, Yokoyama J, et al. Oncocytic mucoepidermoid carcinoma of the parotid gland with CRTC1-MAML2 fusion transcript: report of a case with review of literature. Hum Pathol 2011;42:2052–5.

[26] El-Naggar AK. Clear cell hidradenoma of the skin—a third tumor type with a t(11;19)-associated TORC1-MAML2 gene fusion: genes chromosomes cancer. 2005;43:202–205. Adv Anat Pathol 2006;13:80–2.

[27] Okumura Y, Miyabe S, Nakayama T, Fujiyoshi Y, Hattori H, Shimozato K, et al. Impact of CRTC1/3-MAML2 fusions on histological classification and prognosis of mucoepidermoid carcinoma. Histopathology 2011;59:90–7.

[28] Bell D, Holsinger CF, El-Naggar AK. CRTC1/MAML2 fusion transcript in central mucoepidermoid carcinoma of mandible—diagnostic and histogenetic implications. Ann Diagn Pathol 2010;14:396–401.

[29] Seethala RR, Dacic S, Cieply K, Kelly LM, Nikiforova MN. A reappraisal of the MECT1/MAML2 translocation in salivary mucoepidermoid carcinomas. Am J Surg Pathol 2010;34:1106–21.

[30] Okabe M, Miyabe S, Nagatsuka H, Terada A, Hanai N, Yokoi M, et al. MECT1-MAML2 fusion transcript defines a favorable subset of mucoepidermoid carcinoma. Clin Cancer Res 2006;12:3902–7.

[31] Fehr A, Röser K, Belge G, Löning T, Bullerdiek J. A closer look at Warthin tumors and the t(11;19). Cancer Genet Cytogenet 2008;180:135–9.

[32] Bell D, Luna MA, Weber RS, Kaye FJ, El-Naggar AK. CRTC1/MAML2 fusion transcript in Warthin's tumor and mucoepidermoid carcinoma: evidence for a common genetic association. Genes Chromosomes Cancer 2008;47:309–14.

[33] Lennerz JK, Perry A, Dehner LP, Pfeifer JD, Lind AC, et al. CRTC1 rearrangements in the absence of t(11;19) in primary cutaneous mucoepidermoid carcinoma. Br J Dermatol 2009;161:925–9.

[34] Fehr A, Röser K, Heidorn K, Hallas C, Löning T, Bullerdiek J. A new type of MAML2 fusion in mucoepidermoid carcinoma. Genes Chromosomes Cancer 2008;47: 203–6.

Syringocystadenoma Papilliferum of the Anogenital Area and Buttocks: A Report of 16 Cases, Including Human Papillomavirus Analysis and *HRAS* and *BRAF V600* Mutation Studies

Anastasia M. Konstantinova, MD, PhD,†‡ Liubov Kyrpychova, MD,§ Jana Nemcova, MSc, PhD,§¶ Monica Sedivcova, MSc,¶ Michele Bisceglia, MD,‖ Heinz Kutzner, MD,** Michal Zamecnik, MD,†† Eva Sehnalkova, MD,‡‡ Michal Pavlovsky, MD,§§ Kamila Zateckova, MD,¶¶ Sergej Shvernik, MD,‖‖ Zuzana Spurkova, MD,‖‖ Michal Michal, MD,§¶ Katrin Kerl, MD,*** and Dmitry V. Kazakov, MD, PhD§¶****

Abstract: Syringocystadenoma papilliferum (SCAP) is a benign tumor most commonly located on the head and neck area often associated with nevus sebaceus. In its usual location, the human papillomavirus (HPV) DNA and mutations in the RAS/mitogen-activated protein kinase signaling pathway have been detected in SCAP. We studied 16 cases of SCAP in the anogenital areas and buttock where this neoplasm is rare and attempted to find out whether SCAP in these sites have different histopathological and molecular biological features. It seems that there is no significant difference between the morphology of anogenital SCAP and SCAP in other locations. Several tumors in our cohort demonstrated features resembling those seen in warts, but HPV DNA was not found in these lesions. On the contrary, we identified DNA of HPV high-risk types in some tumors without HPV-related morphology. Our study confirms the role of *HRAS* and *BRAF V600* mutations in the pathogenesis of SCAP, including SCAP in the anogenital areas and buttock.

Key Words: adnexal tumors, syringocystadenoma papilliferum

From the *Department of Pathology, Clinical Research and Practical Center for Specialized Oncological Care, Saint-Petersburg, Russia; †Department of Pathology, Medical Faculty, Saint-Petersburg State University, Saint Petersburg, Russia; ‡Department of Pathology, Saint-Petersburg Medico-Social Institute, Saint Petersburg, Russia; §Sikl's Department of Pathology, Medical Faculty in Pilsen, Charles University in Prague, Pilsen, Czech Republic; ¶Bioptical Laboratory, Pilsen, Czech Republic; ‖Anatomic Pathology, School of Biomedical Sciences, Etromapmax Pole, Lesina (FG), Italy; **Dermatopathologische Gemeinschaftspraxis, Friedrichshafen, Germany; ††Agel Laboratory of Pathology, Novy Jicin, Czech Republic; ‡‡Department of Pathology, Silesian Hospital, Opava, Czech Republic; §§Department of Pathology, Regional Hospital Most, Czech Republic; ¶¶Department of Pathology, Regional Hospital Decin, Decin, Czech Republic; ‖‖Department of Pathology, Bulovlka Hospital, Prague, Czech Republic; and ***Department of Dermatology, University Hospital Zurich, Zurich, Switzerland.

Correspondence: Dmitry V. Kazakov, MD, PhD, Sikl's Department of Pathology, Charles University Medical Faculty Hospital, Alej Svobody 80, 304 60 Pilsen, Czech Republic (e-mail: kazakov@medima.cz).

INTRODUCTION

Syringocystadenoma papilliferum (SCAP) is a rare benign adnexal neoplasm occurring either sporadically or as a secondary tumor in nevus sebaceus of Jadassohn. The commonest affected site is the head and neck area.[1] The trunk and extremities are occasionally involved, whereas lesions involving the groin, buttock, and anogenital SCAP have rarely been reported.[2,3] Histopathologically, SCAP appears exo-endophytic, often crateriform lesion with a papillary architecture formed by double-layered tubular structures composed of cuboidal to columnar luminal cells, often showing apocrine secretion surrounded by a peripheral layer of basal/myoepithelial cells. Various hyperplastic and metaplastic changes (mucinous metaplasia and squamous metaplasia) and also malignant transformation have been described in SCAP.[4–8] The pathogenesis of SCAP remains unclear, although both in sporadic cases and lesions arising in nevus sebaceus the human papillomavirus (HPV) DNA[2,9] and mutations in the RAS/mitogen-activated protein kinase signaling pathway have been detected.[10,11] The above histopathological and molecular changes have been found in SCAP in its usual location in the head and neck area. Our aim was to study SCAP in the anogenital area and buttock to find out whether the lesions in these sites have different features.

MATERIAL AND METHODS

Case Inclusion/Exclusion

A search in the consultation and routine institutional files of the authors between 1993 and 2017 yielded 243 cases of SCAP, of which 15 lesions involved the anogenital area (penis, mons pubis, vulva, and perianal area) and buttock. One case has recently been seen in routine practice. Hematoxylin–eosin–stained slides were reviewed to confirm the diagnosis, specifically to exclude cases of hidradenoma papilliferum with connection to the epidermis and plasma cell–rich infiltrate imitating SCAP as previously reported.[12–14] The

TABLE 1. Sequences of *HRAS* Primers

Sequences of *HRAS* Primers (5′- 3′)	Name of Primer
CACAAGGGAGGCTGCTGAC	*HRAS*-exon 4 reverse
CTGATCCCATCCCTCCTTTC	*HRAS*-exon 4 forward
GGGTCCCTGGCTAGCTGT	*HRAS*-exon 3 reverse
CTCTCGCTTTCCACCTCTCA	*HRAS*-exon 3 forward
CAGCCTCACGGGGTTCAC	*HRAS*-exon 2 reverse
CCCACGGAAGGTCCTGAG	*HRAS*-exon 2 forward
CCTATCCTGGCTGTGTCCTG	*HRAS*-exon 1 reverse
CAGGAGACCCTGTAGGAGGA	*HRAS*-exon 1 forward

histopathological findings were correlated with the clinical data to confirm the location and appropriate clinicopathological context.

Light Microscopic Studies

The number of tissue blocks available for review varied from 1 to 3. The following histopathological features were assessed: exophytic, verrucous and cystic alterations, different types of epithelial cell metaplasia, basal cell hyperplasia, and hyperplasia of luminal cells resulting in a cribriform appearance.

All cases were also examined for the presence of HPV-related features, using the criteria of Meisels for HPV infection (perinuclear halos surrounding hyperchromatic, enlarged angulated nuclei located in the superficial zones of the epidermis). In addition, we looked for granular layer disruption (abrupt alteration in the size, number, form, and density of keratohyaline granules) and percentage of koilocytosis in the spinous layer.[9,15] Any other unusual features, if present, were also recorded.

Twelve cases with available paraffin blocks/unstained slides were studied immunohistochemically for p16 expression (R19-D; Ventana; RTU), using the Ventana Benchmark XT automated stainer (Ventana Medical System Inc, Tucson, AZ), according to the manufacturer's protocol. Diffuse nuclear and cytoplasmic staining was classified as positive p16 staining. No positive cells and weak and focal positivity in some cells were classified as p16-negative staining.

Molecular Genetic Studies

Thirteen lesions were subjected for molecular-genetic studies, including HPV polymerase chain reaction (PCR) and *HRAS* mutations. Twelve cases were analyzed for the presence of the *BRAF V600* mutation.

For molecular-genetic studies, genomic DNA was isolated from formalin-fixed, paraffin-embedded tissue using QIAsymphony DNA Mini Kit (Qiagen, Hilden, Germany) according to manufacturer's protocol on QIAsymphony SP device (Qiagen). Special precautions were taken to prevent HPV DNA microcontamination. The quality of isolated DNA was checked by PCR that amplifies set of control genes.[16]

TABLE 2. Summary of Clinicopathological and Genetic Findings in the Cohort

| N	Sex/Age	Location	Histology*	IHC P16	HPV—Types	*HRAS* Whole Gene†/*HRAS* HS‡	*BRAF V600*
1	F/?	Vulva	3, 4, 5, and deposits of mucin in the epithelium	Neg	Neg	Neg/NA	ND
2	F/23	Perianal	2 and 5	Neg	HPV16+	NA/neg	+
3	F/42	Vulva	1, 2, and 5	Neg	Neg (NA)	NA/neg	+
4	F/95	Vulva and labium majus	3, 4, 5, 6, and 7	ND	ND	ND	ND
5	F/81	Vulva and labium majus	1 and foamy macrophages in the stroma	Neg (patchy sq)	Neg (NA)	NA/neg	+
6	F/78	Vulva	7 and 8	Neg	Neg (NA)	NA/neg	+
7	M/60	Perianal	1, 5, and 8	ND	HPV16+	NA/NA	NA
8	F/59	Perianal	5 and desmoplasia	Neg	Neg	c.182A > G, p.Gln61Arg/NA	Neg
9	F/44	Perianal	2 and 7	ND	ND	ND	ND
10	F/65	Right buttock	5 and 9	Neg	Neg	Neg/NA	+
11	M/33	Right buttock	1 and 7	Neg (patchy sq)	Neg	NA/neg	+
12	F/28	Left buttock	3 and 5	Neg	HPV68§	NA/neg	Neg
13	M/18	Buttock	3, 4, 7, and 8	Neg (patchy sq)	Neg (NA)	NA/neg	+
14	F/34	Buttock	1 and 8	ND	ND	ND	ND
15	M/54	Buttock	—	Neg	Neg	Neg/NA	Neg
16	M/79	Buttock	3	Neg	Neg	Neg	+

*1—exophytic; 2—cystic; 3—verrucous; 4—HPV-related morphology; 5—squamous metaplasia; 6—clear cell metaplasia; 7—cribriform structures; 8—basal cell hyperplasia.
†Sequencing analysis whole coding sequence of *HRAS* gene, including exon–intron junction.
‡Codons 12, 13, and 61.
§A very low quality of DNA, we cannot exclude the risk of false negativity for other HPV types.
F, female; M, male; NA, not available; ND, not done; neg (NA), no HPV virus found in the examined sample; however, the quality and quantity of DNA were very low, and therefore, we cannot exclude the risk of false negative finding; patchy sq, patchy staining of the squamous component.

31
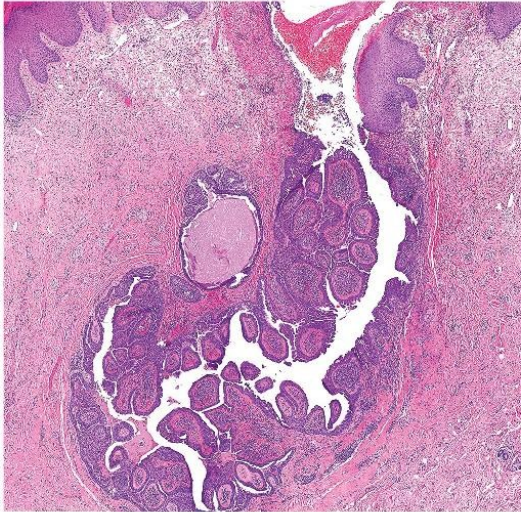
FIGURE 1. SCAP. The tumor has a papillary architecture with a transition from glandular epithelium to the keratinizing squamous epithelium at the skin surface.

The HPV DNA detection was performed using multiple PCR primers from the L1, E1, and E6–E7 regions of the HPV genome as previously described.[17] In brief, primers CPSGB and GP5+/GP6+ targeting the E1 and L1 regions of the HPV genome were used for a wide-range detection of high-risk (HR) and low-risk HPV types, and type-specific PCR detection of E6–E7 region of 6 most prevalent HR-HPV types, namely types 16, 18, 31, 33, 35, and 45, was used to increase sensitivity of HPV detection and to avoid negative finding due to the possible process of HPV integration into the human genome. Furthermore, an RHA kit HPV SPF10-LiPA25, version 1 (Bio-medical Products, Rijswijk, the Netherlands), was run to reveal possible multiple HPV types.

HRAS mutation detection was performed in compliance with the DNA quality of the analyzed DNA. Studied were cases in which more than 300 amplifiable base pairs of DNA were available. The analysis of 4 exons of the *HRAS* gene was performed by PCR using primers listed in Table 1. In cases

with a lower DNA quality, only hot spot mutation analysis of exons 2 and 3 of *HRAS* was performed according to the article by Roivainen et al.[18] Amplified products were sequenced on ABI Prism 3130xl (Applied Biosystems, Foster City, CA). DNA sequences were compared with the reference sequence by the online program BLAST.

The analysis of mutations in the *BRAF* gene (codon 600) was performed using the real-time PCR method by commercial kit cobas 4800 *BRAF V600* Mutation Test (Roche, Pleasanton, CA) according to the manufacturer instructions.
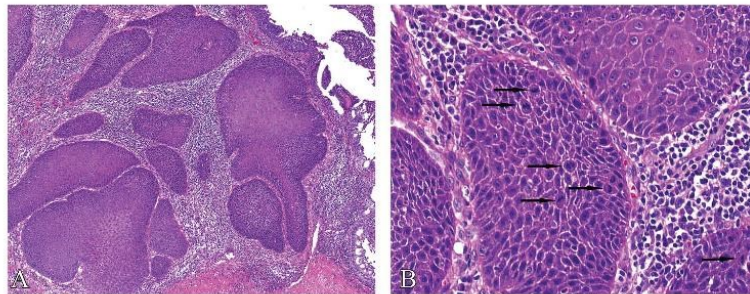
RESULTS

Clinical Data

There were 11 women and 5 men, whose ages at the time of diagnosis ranged from 18 to 95 years (median 54 years; mean 52.9 years). In one case, the age of patient remained unknown. In all cases, the lesions were a solitary tumor. Most neoplasms involved the buttock (43.8%) and the vulva (31.3%); less frequent site was the perianal area (25%) (Table 2). No features suggesting nevus sebaceus (linear arrangement and congenital lesions) were mentioned in the patients' charts.

Histopathological Features

All tumors had a papillary architecture with a transition from the glandular epithelium to the keratinizing squamous epithelium at the skin surface (Fig. 1). A dense plasma cell stromal infiltrate presented at the squamocolumnar junction. The glandular component was lined by a luminal layer of epithelial cuboidal to columnar cells surrounded by a layer of basal/myoepithelial cells. Prominent cystic change of the lesion identified in 3 (18.8%) cases. Five lesions (31.3%) were markedly exophytic with an arboreal growth pattern of the glandular elements. Three examples (cases 1, 4, and 13) (18.8%) demonstrated features resembling those seen in warts including acanthosis, papillomatosis, and HPV-associated changes (Figs. 2A, B).

The most common type of epithelial metaplasia was squamous (7 lesions; 43.8%). In one case, there was slight atypia in the squamous epithelium that focally showed rather basaloid cells that along with plentiful mitotic figures occasioned a resemblance to undifferentiated vulvar intra-epithelial neoplasia (Figs. 3A, B). One lesion exhibited focal

FIGURE 2. Squamous metaplasia with atypia in SCAP (A). Note slight atypia in the squamous epithelium, basaloid cells, and mitotic figures (arrows) (B).
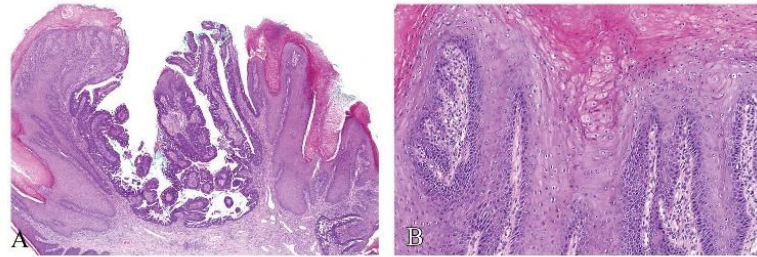
FIGURE 3. Wart-like changes in SCAP, including acanthosis, papillomatosis (A), and HPV-associated changes (B).

clear cell change of the luminal epithelial cells. The hyperplasia of luminal cells, which results in the formation of cribriform structures, was observed in 5 cases (31.3%) (Fig. 4). Four (25%) SCAP showed focal hyperplasia of basal/myoepithelial cells. In one case, mucin deposit was found in the basal part of the squamous epithelium.

Immunohistochemical Data

Among 12 lesions immunohistochemically available for p16 expression, all were scored as p16-negative (3 cases demonstrated a patchy staining of the squamous component) (Table 2).

Molecular Genetic Findings

DNA of HPV HR types was identified by PCR in 3 (23.1%) of the 13 analyzed cases, including HPV16 (2 cases) and HPV68 (1 case) (Table 2).

All but one case were negative for *HRAS* mutations. A missense mutation p.Gln61Arg in the proto-oncogene *HRAS* was identified in 1 lesion (7.7%) (Table 2).

BRAF V600 was detected in 8 of 12 cases (66.7%) (Table 2).
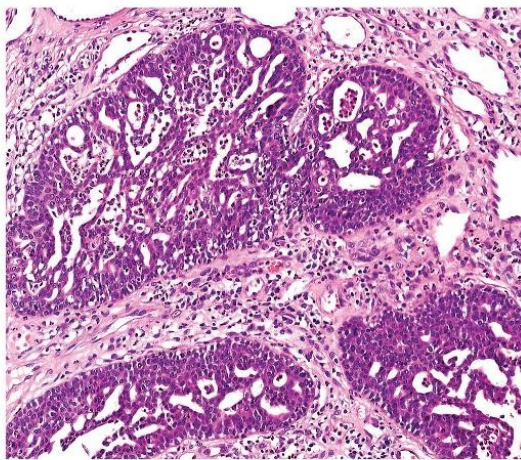
FIGURE 4. Hyperplasia of luminal cells resulting in cribriform appearance.

DISCUSSION

We have described 16 cases of SCAP in the anogenital areas and buttock. Albeit we have not studied a control group of SCAP in its usual location, it seems that there is no significant difference between the morphology of anogenital SCAP and SCAP in other locations. Such histological variations as epithelial metaplasia, cystic alteration, and hyperplastic changes with the formation of cribriform structures have been described in SCAP involved the head and neck, trunk and extremities.[1]

In addition, some SCAP in its usual location and neoplasms affected the anogenital area and buttock have viral wart-like changes presenting as verrucous tumors. Among 18 cases of SCAP with such a morphology described in the literature, the most common location was the cheek (16.7%), scalp (16.7%), and lower extremity (16.7%) followed by the buttock (11.1%), neck (11.1%), vulva (5.5%), sacral area (5.5%), back (5.5%), areola (5.5%), and eyelid (5.5%).[2,19–25]

The cause of such contiguous verrucous proliferations in SCAP is unclear. Some authors have suggested a possible role of HPV infection. Skelton et al[2] reported the presence of HPV 6/11 in the verrucous SCAP of the buttock identified by in situ hybridization. Carlson et al[9] detected HPV 16 type in 1 case and HPV 38 type in a second case of 4 SCAP associated with nevus sebaceus. In our cohort, we failed to identify HPV by p16 immunostaining in all analyzed cases. However, DNA of HPV HR types was identified by PCR in 3 (23.1%) of the 13 analyzed cases, including HPV 16 type (2 cases) and HPV 68 type (1 case). None of these cases demonstrated clear-cut HPV-related cytomorphology (unequivocal koilocytes). However, we noticed features suggesting HPV infection (wart-like acanthosis and papillomatosis) in 3 (18.8%) cases.

BRAF V600E and *HRAS* mutations are most common molecular alterations found in sporadic SCAP.[11,26,27] Shen et al investigated 23 cases of sporadic SCAP with only one case located in the gluteal area. The detection rate of *HRAS* mutations in their study was 26.1% (6 cases), whereas *BRAF V600E* mutations were identified in 52.2% (12 cases), which included a neoplasm located in the gluteal area.[11] Levinsohn et al[27] studied 10 cases of sporadic SCAP and detected *HRAS* pG13R mutations and *BRAF V600E* mutation in 10% and 40% of lesions, respectively.

An immunohistochemical expression of *BRAF V600*E protein has been studied by Friedman et al in 11 cases of

33

sporadic SCAP. The positive staining was identified in 7 (63.6%) cases.[25]

The detection rate of *HRAS* mutation in our cohort was 7.7%, which is lower compared with the previously reported material (10%–26.1%), while the frequency of *BRAF* mutations (66.7%) was a little more than the published rates of 40%–63.6%.

In conclusion, we present a series of sporadic SCAP located in the buttock and anogenital area detailing a spectrum of morphological changes that may occur in these lesions. Several tumors demonstrated features resembling those seen in warts, but HPV DNA was not found in these lesions. On the contrary, we identified DNA of HPV HR types in some tumors without HPV-related morphology. Our study confirms the role of *HRAS* and *BRAF V600* mutations in the pathogenesis of SCAP, including SCAP in the anogenital areas and buttock.

REFERENCES

1. Mammino JJ, Vidmar DA. Syringocystadenoma papilliferum. *Int J Dermatol.* 1991;30:763–766.
2. Skelton HG III, Smith KJ, Young D, et al. Condyloma acuminatum associated with syringocystadenoma papilliferum. *Am J Dermatopathol.* 1994;16:628–630.
3. Steshenko O, Chandrasekaran N, Lawton F. Syringocysadenoma papilliferum of the vulva: a rarity in gynaecology. *BMJ Case Rep.* 2014:1–3.
4. Kazakov DV, Bisceglia M, Calonje E, et al. Tubular adenoma and syringocystadenoma papilliferum: a reappraisal of their relationship. An interobserver study of a series, by a panel of dermatopathologists. *Am J Dermatopathol.* 2007;29:256–263.
5. Vazmitel M, Michal M, Mukensnabl P, et al. Syringocystadenoma papilliferum with sebaceous differentiation in an intradermal tubular apocrine component. Report of a case. *Am J Dermatopathol.* 2008;30:51–53.
6. Kazakov DV, Requena L, Kutzner H, et al. Morphologic diversity of syringocystadenocarcinoma papilliferum based on a clinicopathologic study of 6 cases and review of the literature. *Am J Dermatopathol.* 2010;32:340–347.
7. Kazakov DV, Michal M, Kacerovska D, et al. *Cutaneous Adnexal Tumors.* Philadelphia, PA: Lippincott Williams & Wilkins; 2012.
8. Requena L, Sangüeza O. *Cutaneous Adnexal Neoplasms.* Cham, Switzerland: Springer International Publishing AG; 2018.
9. Carlson JA, Cribier B, Nuovo G, et al. Epidermodysplasia verruciformis-associated and genital-mucosal high-risk human papillomavirus DNA are prevalent in nevus sebaceus of Jadassohn. *J Am Acad Dermatol.* 2008;59:279–294.
10. Groesser L, Herschberger E, Ruetten A, et al. Postzygotic HRAS and KRAS mutations cause nevus sebaceus and Schimmelpenning syndrome. *Nat Genet.* 2012;44:783–787.
11. Shen AS, Peterhof E, Kind P, et al. Activating mutations in the RAS/mitogen-activated protein kinase signaling pathway in sporadic trichoblastoma and syringocystadenoma papilliferum. *Hum Pathol.* 2015;46:272–276.
12. Kazakov DV, Spagnolo DV, Kacerovska D, et al. Lesions of anogenital mammary-like glands: an update. *Adv Anat Pathol.* 2011;18:1–28.
13. Konstantinova AM, Michal M, Kacerovska D, et al. Hidradenoma papilliferum: a clinicopathologic study of 264 tumors from 261 patients, with emphasis on mammary-type alterations. *Am J Dermatopathol.* 2016;38:598–607.
14. Stewart CJ. Syringocystadenoma papilliferum-like lesion of the vulva. *Pathology.* 2008;40:638–639.
15. Meisels A, Fortin R, Roy M. Condylomatous lesions of the cervix. II. Cytologic, colposcopic and histopathologic study. *Acta Cytol.* 1977;21:379–390.
16. van Dongen JJ, Langerak AW, Bruggemann M, et al. Design and standardization of PCR primers and protocols for detection of clonal immunoglobulin and T-cell receptor gene recombinations in suspect lymphoproliferations: report of the BIOMED-2 concerted action BMH4-CT98-3936. *Leukemia.* 2003;17:2257–2317.
17. Skalova A, Kaspirkova J, Andrle P, et al. Human papillomaviruses are not involved in the etiopathogenesis of salivary gland tumors. *Cesk Patol.* 2013;49:72–75.
18. Roivainen A, Jalava J, Pirila L, et al. H-ras oncogene point mutations in arthritic synovium. *Arthritis Rheum.* 1997;40:1636–1643.
19. Monticciolo NL, Schmidt JD, Morgan MB. Verrucous carcinoma arising within syringocystadenoma papilliferum. *Ann Clin Lab Sci.* 2002;32:434–437.
20. Hsu PJ, Liu CH, Huang CJ. Mixed tubulopapillary hidradenoma and syringocystadenoma papilliferum occurring as a verrucous tumor. *J Cutan Pathol.* 2003;30:206–210.
21. Li A, Sanusi ID, Pena JR, et al. Syringocystadenoma papilliferum contiguous to a verrucous cyst. *J Cutan Pathol.* 2003;30:32–36.
22. Sardesai VR, Agarwal VM, Manwatkar PP, et al. Giant condyloma acuminata with syringocystadenoma papilliferum. *Indian J Dermatol Venereol Leprol.* 2009;75:330.
23. Nascimento BA, Carneiro CM, Carvalho AH, et al. Syringocystadenoma papilliferum in an unusual location. *An Bras Dermatol.* 2015;90:900–902.
24. Pewitt JD, Burns EK, Chan LS. Eruptive syringocystadenoma papilliferum, keratoacanthoma, and verruca vulgaris in a keratinocytic epidermal nevus on the leg. *Skinmed.* 2015;13:395–397.
25. Friedman BJ, Sahu J, Solomides CC, et al. Contiguous verrucous proliferations in syringocystadenoma papilliferum: a retrospective analysis with additional evaluation via mutation-specific BRAF V600E immunohistochemistry. *J Cutan Pathol.* 2018;45:212–216.
26. Watanabe Y, Shido K, Niihori T, et al. Somatic BRAF c.1799T>A p. V600E Mosaicism syndrome characterized by a linear syringocystadenoma papilliferum, anaplastic astrocytoma, and ocular abnormalities. *Am J Med Genet A.* 2016;170A:189–194.
27. Levinsohn JL, Sugarman JL, Bilguvar K, et al. Somatic V600E BRAF mutation in linear and sporadic syringocystadenoma papilliferum. *J Invest Dermatol.* 2015;135:2536–2538.

Secretory Carcinoma of the Skin

Report of 6 Cases, Including a Case With a Novel NFIX-PKN1 Translocation

Liubov Kastnerova, MD,*† Boštjan Luzar, MD, PhD,‡ Keisuke Goto, MD,§||¶#**
Viktor Grishakov MD,†† Zoran Gatalica, MD,‡‡ Jivko Kamarachev, MD,§§
Petr Martinek, PhD,*† Veronika Hájková, MSc,† Petr Grossmann, PhD,*†
Hiroshi Imai, MD, PhD,|||| Hideaki Fukui, MD,¶¶ Michal Michal, MD,*† and
Dmitry V. Kazakov, MD, PhD*†

Abstract: Secretory carcinoma of the skin is a rare adnexal carcinoma, which is morphologically and immunohistochemically identical to secretory carcinoma of the breast and is associated with the presence of t (12;15) translocation, resulting in the *ETV6-NTRK3* gene fusion. Nineteen cases of primary cutaneous secretory carcinoma have been previously published in the literature. In this study, we describe 6 new cases of secretory carcinoma of the skin. The study group consisted of 5 female patients and 1 male patient, ranging in age from 57 to 98 years (mean: 74.2, median: 74). Locations included the axilla (2), neck, eyelid, thigh, and nipple base, each one. Microscopically, all but 1 tumor were well circumscribed and nonencapsulated and exhibited characteristic abundant secretions within the microcystic and tubular spaces comprised by bland oval, round to cuboidal neoplastic cells. In addition, solid areas and focal pseudopapillae were seen, and, in 1 case, a focal mucinous component with small lakes of mucin containing small tumor nests or tubules of the neoplastic cells was present. The remaining neoplasm was mostly solid and papillary, with only few characteristic lumina containing secretions. Immunohistochemically, all cases expressed S-100 protein, mammaglobin, STAT5, GATA3,

and NTRK. *ETV6-NTRK3* gene fusion was detected in 5 cases, whereas, in the remaining tumor, a novel *NFIX-PKN1* gene fusion was found.

Key Words: secretory carcinoma, mammary analog secretory carcinoma, adnexal neoplasms, *ETV6-NTRK3*, *NFIX-PKN1*, fusion

Primary cutaneous secretory carcinoma is a rare adnexal carcinoma that is histopathologically identical to homologous neoplasms in the salivary gland and breast.[1–7] It was recognized in the skin in 2009.[8] Since then, 19 cases have been reported, mostly as isolated case reports, with only a small series of 6 cases.[2,8–19] In addition to the distinctive histopathologic appearances, cutaneous secretory carcinoma seems to be associated with the characteristic balanced t(12;15) (p13; q25) *ETV6-NTRK3* translocation, akin to their mammary and salivary gland counterparts.[2] Herein, we report a series of 6 new cases of secretory carcinoma of the skin, including new microscopic features and a novel *NFIX-PKN1* translocation.

MATERIAL AND METHODS

Case Selection

Six cases of secretory carcinoma of the skin were identified, prospectively or retrospectively, in the consultation and institutional databases of the authors (2009-2018). None of the cases was previously published. Follow-up information was provided by attending physicians.

Immunohistochemical Studies

Immunohistochemical staining was performed on 4-μm-thick sections, cut from formalin-fixed, paraffin-embedded tissue, using a Ventana BenchMark XT automated stainer (Ventana Medical Systems, Tucson, AZ), according to the manufacturer's protocol.

The following antibodies were used: S-100 protein (polyclonal; RTU; Ventana), STAT5 (E289, 1:500, AbCam), mammaglobin (clone 304-1A5; RTU; DakoCytomation),

From the *Sikl's Department of Pathology, Medical Faculty in Pilsen, Charles University in Prague; †Bioptical Laboratory, Pilsen, Czech Republic; ‡Institute of Pathology, Medical Faculty University of Ljubljana, Ljubljana, Slovenia; ††Department of Pathology, Moscow City Oncology Hospital №62, Moscow, Russia; ‡‡Department of Pathology, Caris Life Sciences, Phoenix, AZ; §Department of Pathology, Tokyo Metropolitan Cancer and Infectious Disease Center Komagome Hospital; ||Department of Pathology, Itabashi Central Clinical Laboratory, Tokyo; ¶Department of Diagnostic Pathology, Shizuoka Cancer Center Hospital, Nagaizumi; #Department of Diagnostic Pathology and Cytology, Osaka International Cancer Institute, Osaka; **Department of Dermatology, Hyogo Cancer Center, Akashi; ||||Pathology Division, Mie University Hospital, Tsu; ¶¶Department of Surgical Pathology, Hokkaido University Hospital, Sapporo, Japan; and §§Department of Dermatology, University Hospital Zurich, Zurich, Switzerland.

Correspondence: Dmitry V. Kazakov, MD, Sikl's Department of Pathology, Charles University Medical Faculty Hospital, Alej Svobody 80, Pilsen 304 60, Czech Republic (e-mail: kazakov@medima.cz).

NTRK (A7H6R, 1:25; Cell Signaling), GATA3 (clone L50-823; 1:200; BioCareMedical), CK7 (clone OV-TL 12/30; 1:200; DakoCytomation), TTF-1 (8G7G3/1, 1:100, Dako), p63 (clone 4A4; RTU; Ventana), and CD117 (polyclonal, 1:800, Dako). The panel varied between individual cases depending on the origin.

Molecular Genetic Studies and Fluorescence In Situ Hybridization

Detection of *ETV6-NTRK3* Fusion and *NFIX-PKN1* Fusion Transcript by Reverse Transcription Polymerase Chain Reaction

RNA was extracted using the RecoverAll Total Nucleic Acid Isolation Kit (Ambion, Austin, TX). cDNA was synthesized using the Transcriptor First Strand cDNA Synthesis Kit (RNA input 500 ng) (Roche Diagnostics). All procedures were performed according to the manufacturer's protocols. Amplification of a 105 bp product and a 133 bp product of the β2-microglobulin gene, and a 247 bp product of the *PGK* gene, was used to test the quality of the extracted RNA, as previously described.[20–22]

For polymerase chain reaction (PCR), 2 μL of cDNA was added to the reaction, which consisted of 12.5 μL of HotStar Taq PCR Master Mix (Qiagen, Hilden, Germany), 10 pmol of each primer, and distilled water up to 25 μL.[23,24] The amplification program comprised denaturation at 95°C for 14 minutes followed by 45 cycles of denaturation at 95°C for 1 minute; annealing at temperatures 60°C was carried out for 1 minute and extension at 72°C for 1 minute. The procedure was completed by incubation at 72°C for 7 minutes.

Successfully amplified PCR product was purified with magnetic particles using Agencourt AMPure (Agencourt Bioscience Corporation, A Beckman Coulter Company, Beverly, MA). The product was then bidirectionally sequenced using Big Dye Terminator Sequencing Kit (PE/Applied Biosystems, Foster City, CA) and purified with magnetic particles using Agencourt CleanSEQ (Agencourt Bioscience Corporation); all this was carried out according to the manufacturer's protocols and run on an automated sequencer ABI Prism 3130×l (Applied Biosystems) at a constant voltage of 13.2 kV for 11 minutes.

Detection of *ETV6* and *NTRK3* by Fluorescence In Situ Hybridization Method

Four-μm-thick FFPE sections were placed onto positively charged slides. Hematoxylin and eosin–stained slides were examined for determination of areas for cell counting. The unstained slides were routinely deparaffinized and incubated in the 1× Target Retrieval Solution Citrate pH 6 (Dako, Glostrup, Denmark) at 95°C/40 minutes and subsequently cooled for 20 minutes at room temperature in the same solution. The slides were washed in deionized water for 5 minutes, and they were digested in protease solution with Pepsin (0.5 mg/mL) (Sigma Aldrich, St Louis, MO) in 0.01 M HCl at 37°C/25 to 60 minutes, according to the sample conditions. The slides were then placed in deionized water for 5 minutes, dehydrated in a series of ethanol solution (70%, 85%, and 96% for 2 min each), and air-dried.

For the detection of *ETV6* rearrangement, a commercial probe, Vysis ETV6 Break Apart FISH Probe Kit (Vysis/Abbott Molecular, Illinois), was used. The ETV6 probe was mixed with water and LSI/WCP (Locus-Specific Identifier/Whole Chromosome Painting) hybridization buffer (Vysis/Abbott Molecular) in a 1:2:7 ratio, respectively. The probe for the detection of the rearrangement of the *NTRK3* gene region was mixed from custom-designed SureFISH probes (Agilent Technologies Inc., Santa Clara, CA). Chromosomal regions for *NTRK3* break-apart probe oligos are chr15:87501469-88501628 and chr15:88701444-89700343. The probe mixture was prepared from corresponding probes (each color was delivered in a separated well), deionized water, and LSI Buffer (Vysis/Abbott Molecular) in a 1:1:1:7 ratio, respectively. An appropriate amount of mixed probe was applied on specimens, covered with a glass coverslip, and sealed with rubber cement. The slides were incubated in the ThermoBrite instrument (StatSpin/Iris Sample Processing, Westwood, MA) with co-denaturation at 85°C/8 minutes and hybridization at 37°C/16 hours. The rubber-cemented coverslip was then removed, and the slide was placed in the post-hybridization wash solution (2×SSC/0.3% NP-40) at 72°C/2 minutes. The slide was air-dried in the dark, counterstained with 4′, 6′-diamidino-2-phenylindole (DAPI; Vysis/Abbott Molecular), coverslipped, and immediately examined.

The sections were examined with an Olympus BX51 fluorescence microscope (Olympus Corporation, Tokyo, Japan) using a ×100 objective and the filter sets Triple Band Pass (DAPI/SpectrumGreen/SpectrumOrange), Dual Band Pass (SpectrumGreen/SpectrumOrange), and Single Band Pass (SpectrumGreen or SpectrumOrange).

For each probe, 100 randomly selected nonoverlapping tumor cell nuclei were examined for the presence of yellow or green and orange fluorescent signals. Yellow signals were considered negative, and separate orange and green signals were considered as positive. Cutoff values were set to >10% of nuclei with chromosomal breakpoint signals (mean, +3 SD in normal non-neoplastic control tissues).

Detection of *ETV6-NTRK3* and *NFIX-PKN1* Fusion Transcripts by Next-generation Sequencing

For next-generation sequencing (NGS) studies, 2 to 3 FFPE sections (10 μm thick) were macrodissected to isolate tumor-rich regions. The samples were extracted for total nucleic acid using Agencourt FormaPure Kit (Beckman Coulter, Brea, CA), following the corresponding protocol with overnight digestion and an additional 80°C incubation, as described in the modification of the protocol by ArcherDX (ArcherDX Inc., Boulder, CO).

Total nucleic acid was quantified using the Qubit Broad Range RNA Assay Kit (Thermo Fisher Scientific) and 2 μL of sample.

RNA Integrity Assessment and Library Preparation for NGS

Unless otherwise indicated, 250 ng of FFPE RNA was used as input for NGS library construction. To assess RNA quality, the PreSeq RNA QC Assay using iTaq Universal SYBR Green Supermix (Biorad, Hercules, CA)

was performed on all samples during library preparation to generate a measure of the integrity of RNA (in the form of a cycle threshold [Ct] value). Library preparation and RNA QC were performed following the Archer Fusion Plex Protocol for Illumina (ArcherDX Inc.). The Archer FusionPlex Solid Tumor Kit (covering 53 genes) was used. Final libraries were diluted 1:100,000 and quantified in a 10 µL reaction following the Library Quantification for Illumina Libraries protocol and assuming a 200 bp fragment length (KAPA, Wilmington, MA). The concentration of final libraries was around 200 nM. Threshold representing the minimum molar concentration for which sequencing can be robustly performed was set at 50 nM.

NGS Sequencing and Analysis

Libraries were sequenced on a NextSeq. 500 sequencer (Illumina, San Diego, CA). They were diluted to 4 nM, and equal amounts of up to 30 libraries were pooled per run. The optimal number of raw reads per sample was set to 3,000,000. Library pools were diluted to 1.8 pM library stock spiked with 20% PhiX and loaded in the NextSeq MID cartridge. Analysis of sequencing results was performed using the Archer Analysis software (v5.1.7; ArcherDX Inc.). Fusion parameters were set to a minimum of 5 valid fusion reads with a minimum of 3 unique start sites within the valid fusion reads.

RESULTS

Clinical Features

There were 5 female patients and 1 male patient, with ages ranging at diagnosis from 57 to 98 (mean: 74.2, median: 74). Location included axilla (n = 2), neck (n = 1), eyelid (n = 1), thigh (n = 1), and nipple base (n = 1). All skin tumors occurred as solitary nodules (Fig. 1). The patient with the lesion involving the nipple was a 75-year-old woman, who noticed uncomfortable rash to her right breast, above the nipple, for 2 months, with nipple protrusion. Her mammograms and breast ultrasound were negative at that time but magnetic

FIGURE 1. Case 4. A 15×10 mm slowly growing (8 mo) painless nodule on the lower eyelid.

TABLE 1. Summary of the Main Features

| Case | Sex/Age (y) | Location/Clinical Diagnosis | Treatment/Follow-up | Histology Mitosis (mm²) | Size (mm)* | Immunohistochemistry | Molecular-genetic Study | | | |
							Fusion	FISH ba	RT-PCR	NGS
1	F/75	Axilla/tumor	Excision. Reexcision within a month, then NED at 12 mo	Typical 4/mm²	7	S-100+, STAT5+, MGA+, NTRK+, GATA3+	ETV6-NTRK3	+	+	+
2	F/98	Axilla/tumor	Excision. NED at 2 mo, later lost to follow-up	Typical 1/mm²	6	S-100+, STAT5+, MGA+, NTRK+	ETV6-NTRK3	+	–	+
3	F/67	Neck/tumor	Excision/NED 32 mo	Typical 0/mm²	4	S-100+/–, STAT5+, MGA+, NTRK+, GATA3+	ETV6-NTRK3	ND	+	ND
4	M/73	Right lower eyelid/tumor	Excision/NED 6 mo	More solid, with true papillae and blastoid cells 2/mm²	14	S100+, MGA++, GATA3+, CD117+, TTF1-STAT5+/–, NTRK+	ETV6-NTRK3	+	ND	+
5	F/57	Left thigh/tumor	Excision/NED 14 mo	Mucinous component 4/mm²	7	S-100+, STAT5+, MGA+, CK7+, GATA3+/– p63+/–, CD117–	NFIX-PKN1	ND	+	+
6	F/75	Nipple base /rash	Right central partial mastectomy /mts to 1 of 15 axillary LN	Typical 0/mm²	6	S100+, STAT5+, MGA+, NTRK+	ETV6-NTRK3	+	ND	+

*Size is measured on the microscopic slides.
ba indicates break apart; FISH, fluorescence in situ hybridization; LN, lymph nodes; MGA, mammoglobin; ND, not done; NED, not evidence of disease.

37

resonance imaging was suspicious for malignancy in a right axillary lymph node, which was biopsied and turned positive for metastatic adenocarcinoma of a probable breast origin, with the following phenotype ER−, PR−, HER2-neu−, Ki-67 − 5%. A punch biopsy of the right nipple lesion was performed, and the diagnosis of secretory carcinoma was established on the basis of detection of *ETV6-NTRK3* fusion. Subsequent PET/CT revealed a hypermetabolic spot in the area of the seventh left rib. The patient had a history of a sixth left rib fracture about a year ago that was said to be due to a fall. There was a question whether the PET activity was due to the previous trauma or represented a metastatic disease. Finally, right central partial mastectomy was performed. No tumor in the breast parenchyma was found. In the other 5 cases, all neoplasms were surgically excised, with a conventional elliptical excision. In one case, reexcision was performed. None of these patients had evidence of disease (follow-up ranged from 2 to 32 mo) (Table 1).

Histopathologic Features

Of the 6 lesions, 5 manifested typical features with characteristic abundant intraluminal secretions within closely packed microcystic and tubular spaces comprised of bland oval, round to cuboidal neoplastic cells. In addition, solid areas and focal pseudopapillae were seen. When assessable, most tumors were relatively well circumscribed, nonencapsulated, and confined to the dermis (Fig. 2).

In one case (case 5), there was a focal mucinous component which was less regular and extended focally into the subcutis. It was composed of small lakes of mucin-containing tubules of the neoplastic cells or small tumor nests. Mucinous lacunae were often seen at the periphery of the intact tubules that gradually disappeared. Rare tubules contained a preserved peripheral basal/myoepithelial cell layer, likely representing an in situ lesion or preexisting eccrine/apocrine duct (Fig. 3). Another lesion containing an in situ component was the tumor from the nipple.

The lesion from the eyelid (case 4) was mostly solid and papillary, showing both micropapillae and true papillae with a fibrous core; characteristic lumina containing secretions were less conspicuous in comparison with the other 5 neoplasms. There also were variably sized lumina (some markedly distended) with apocrine or colloid-like secretion. Focally, the cells in this neoplasm assumed hobnail appearances, and there were areas with larger "blastoid" cells, but no high-grade atypia was evident (Fig. 4).

In no case was ulceration of the epidermis, perineural invasion, and lymphovascular involvement found. In neither axillary cases was there any evidence of residua of mammary tissue. The mitotic rate ranged from 0 to 4 mm^2. The lymph node metastasis from the nipple lesion (case 6) was not available for histopathologic review.

Immunohistochemical Findings

Neoplastic cells were positive for S-100 protein, mammaglobin, STAT5, GATA3, and NTRK. The neoplasm with a mucinous component (case5) manifested some differences between the mucinous and conventional parts, namely S-100 protein was weak and focal in the main bulk of the tumor with the conventional appearance,
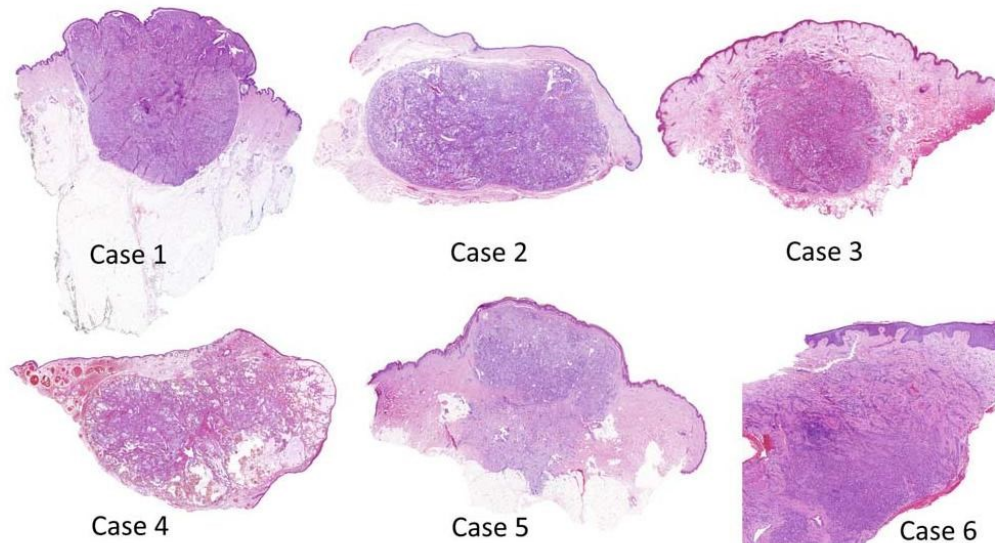
FIGURE 2. Whole-mount sections of 6 cases, 4 of which are well circumscribed. Case 4 shows a focal invasion into the subcutis, and the tumor on the nipple (case 6) has irregular outlines.

38
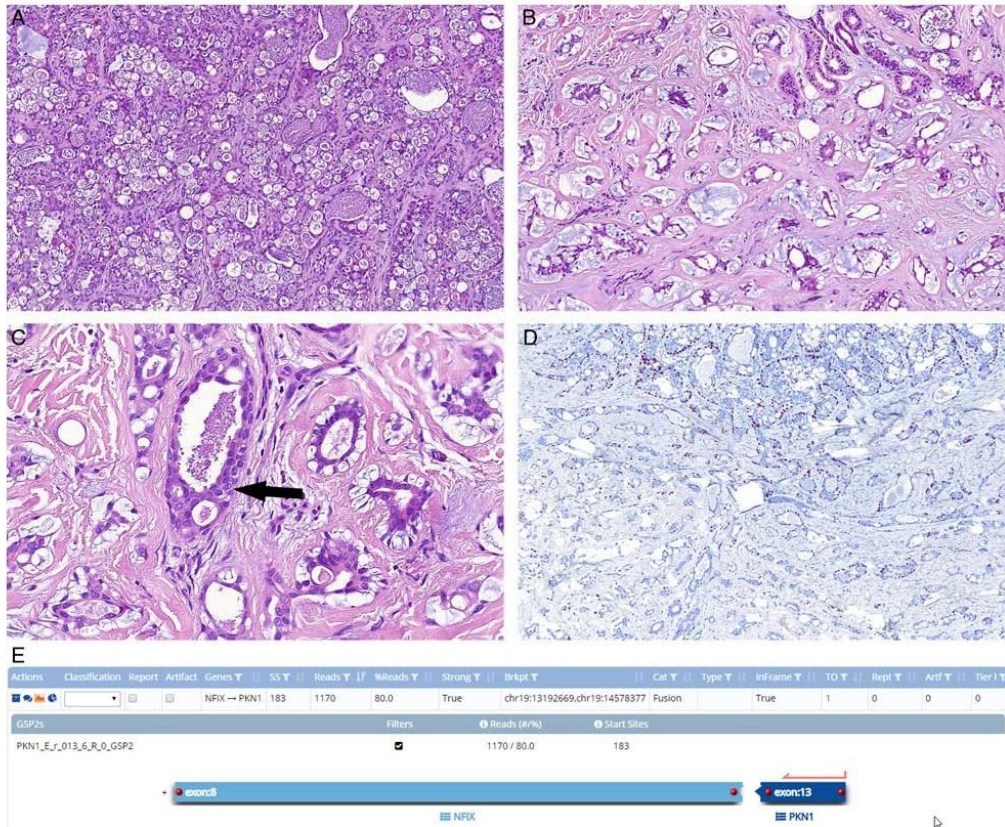
FIGURE 3. Secretory carcinoma with a novel *NFIX-PKN1* fusion (case 5). The typical appearance of closely packed microcysts and tubules lined by bland cells with characteristic abundant bubbly secretion (A). The mucinous component with small lakes of mucin, spilling into the surrounding dermis containing partly preserved or destroyed tubules. Note lacunae of the mucus located at the periphery of relatively intact tubules (B). The duct containing incipient secretions and intact peripheral basal/myoepithelial cell layer, likely representing preexisting apocrine/eccrine duct (an in situ lesion) (C, arrow). Positivity of p63 for the abluminal cells in the upper part of the tumor and loss of p63 expression in the mucinous areas (D). Screenshot from the Archer Analysis software, depicting the details of the detected *NFIX-PKN1* fusion: SS—the number of unique start sites supporting the event. Reads—the number of unique reads supporting the event. %Reads—the percent of reads supporting the event. Strong—True/False value indicating whether the Fusion has passed all Strong Evidence filters. Brkpt—True/False value indicating whether the Fusion has passed all Strong Evidence filters. InFrame—True/False/Unknown value indicating whether the event is predicted to be in-frame, and thus a functional transcript (E).

whereas diffuse positivity was seen in the mucinous moiety. There was also the loss of p63 in the mucinous areas compared with the conventional parts. The panel for each individual case is listed in Table 1.

Gene Fusions

In 5 cases, *ETV6-NTRK3* translocation was detected, whereas, in the remaining case, a novel in-frame *NFIX-PKN1*, with breakpoints located in exon 8 of the *NFIX* gene and exon 13 of the *PKN1* gene, was found. The fusions were detected in 5 cases by NGS and confirmed by either

break-apart fluorescence in situ hybridization (FISH) or reverse transcription polymerase chain reaction (RT-PCR) in 4 and 3 cases, respectively. In one case, only RT-PCR was used to detect the translocation (Table 1). In case of the *NFIX-PKN1* fusion, it was impossible to use FISH break-apart probes for validation, inasmuch as the genes are located too close to one another.

DISCUSSION

Our series extends the histopathologic spectrum of secretory carcinoma of the skin and the spectrum of its
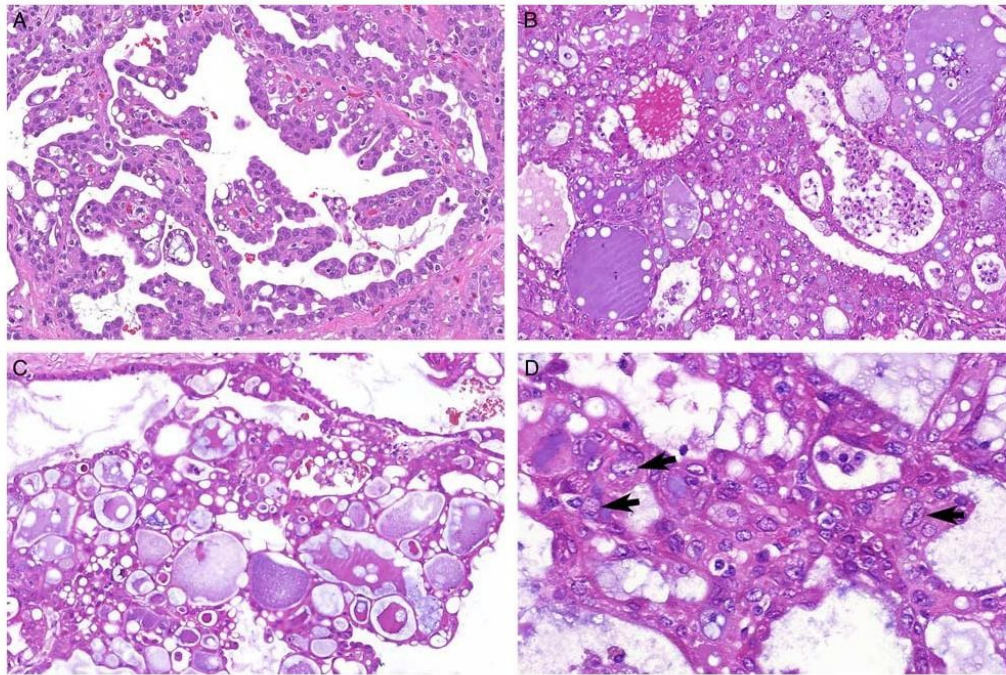
FIGURE 4. Secretory carcinoma of the eyelid (case 4). Numerous micropapillary structures and true papillae with a fibrous core within cystic spaces (A). The colloid-like (moth eaten) spaces with abundant secretion (B) and microcystic area containing abundant eosinophilic secretion (C). Atypical neoplastic cells with large nuclei (2 to 3 times larger than a majority of tumor cells) and pronounced nucleoli (D, arrows).

genetic alterations. Although most cases had typical histopathologic appearances, 2 cases are worthy of a short comment. In one case (case 5), in addition to conventional areas, there was a minor mucinous component, which has not been reported in skin lesions, to the best of our knowledge. However, a similar salivary gland tumor was included in the series of Skalova et al[25] (Fig. 2A). Notably, this mucinous component had slightly different immunophenotype from that in the main bulk of the lesion with respect to S-100 protein and p63 expression. Moreover, there were structures with an intact basal/myoepithelial cell layer but typical secretions, likely representing an in situ lesion in a preexisting duct. A similar feature has been documented in the paper by Huang et al.[15]

The tumor on the eyelid was unusual in that it had relatively few areas with typical closely packed lumina filled with secretions. The tumor instead was mainly composed of solid, papillary, and pseudopapillary areas with focal apocrine or colloid-like secretion. Similar lesions have been, however, reported both in the skin and salivary glands.[7,13] It is known that in some organs, for example, the thyroid glands, *ETV6-NTRK3* translocation was found in lesions that have different morphology from secretory carcinoma.[26,27] Because of colloid-like secretion, this case was stained for TTF1 but

proved negative. The patient did not have any evidence of a primary of the thyroid gland on a clinical work-up. Furthermore, the cells in this case in some areas were larger and had a blastoid appearance; however, we think this feature does not qualify for high-grade transformation, an event that has also been reported in extracutaneous secretory carcinomas.[23,24]

A purist can argue against considering the case with the nipple tumor as primary cutaneous. We, however, included this case on the basis of the fact that the lesion was superficial, confined to the nipple, and no breast parenchymal involvement was identified on a thorough work-up and, later, microscopically, following the mastectomy. It is known that some tumors typically occurring on the nipple, such as nipple adenoma, syringomatous adenoma, nodular mucinosis, and nipple pseudolymphoma, are covered by both dermatopathology and mammary pathology. Moreover, of interest is that this patient and another patient with a tumor in the axilla are the oldest individuals with secretory carcinoma ever reported (75 and 98 y, respectively).

In all but 1 case, *ETV6-NTRK3* translocation was found. In the remaining case, an *NFIX-PKN1* fusion was detected. The latter has been previously described in neither cutaneous secretory carcinoma nor in extracutaneous homonymous tumors. In fact, this fusion has not been reported at all, to the best of our knowledge. Nuclear factor I, X-type (*NFIX*) gene is

40

located on 19p13 and codes for a ubiquitous 47-kD dimeric DNA-binding protein, belonging to a family of transcription factors. Pathogenic variants of *NFIX* have also been reported as causative of Marshall-Smith Syndrome and Malan syndrome (Sotos syndrome 2).[28,29] The Protein kinase-1 (PKN1) gene is also located on 19p13 and codes for protein belonging to the protein kinase C superfamily that is activated by the Rho family of small G proteins and may mediate the Rho-dependent signaling pathway. Mutations in *PKN1* gene were described in rhabdomyosarcoma.[30]

Apart from the *ETV6-NTRK3* translocation, other gene fusions reported in secretory carcinoma in different organs include *ETV6-RET*, *ETV6-MET*, and dual fusion *ETV6-NTRK3* and *ETV6-MAML3*.[7,31,32] Cases of secretory carcinoma of the salivary gland with *NCOA4-RET* and *TRIM27-RET* gene fusions have subsequently been reclassified as intraductal carcinomas.[31,33]

In conclusion, we have described 6 new cases of secretory carcinoma involving the skin. Adding this series to the previously published 19 cases, it can be summarized that cutaneous secretory carcinoma mainly occurs in female individuals (female 16, male 9). The ages of the patients ranged from 13 to 98 years (mean: 51.8, median: 51.5). The most common location is the axilla (n = 10) followed by the neck (n = 3), and lip (n = 3). The tumors seem to follow an indolent course, without recurrence and metastasis. *ETV6-NTRK3* translocation has been identified in 22 of the 25 studied cases, and 1 case had a heterozygous deletion of *ETV6* in 25% of cells.[11] We extend the spectrum of translocations by reporting a novel *NFIX-PKN1* translocation and broaden the histopathologic spectrum by adding a case with a mucinous component.

REFERENCES

1. Skalova A, Vanecek T, Sima R, et al. Mammary analogue secretory carcinoma of salivary glands, containing the ETV6-NTRK3 fusion gene: a hitherto undescribed salivary gland tumor entity. *Am J Surg Pathol*. 2010;34:599–608.
2. Bishop JA, Taube JM, Su A, et al. Secretory carcinoma of the skin harboring ETV6 gene fusions: a cutaneous analogue to secretory carcinomas of the breast and salivary glands. *Am J Surg Pathol*. 2017;41:62–66.
3. Rosen PP, Cranor ML. Secretory carcinoma of the breast. *Arch Pathol Lab Med*. 1991;115:141–144.
4. Rosen PP. *Rosen's Breast Pathology*, 3rd ed. Philadelphia, PA: Lippincot Williams and Wilkins; 2008.
5. Kazakov DV, Michal M, Kacerovska D, et al. *Cutaneous Adnexal Tumors*. Philadelphia: Lippincot Williams and Wilkins; 2012:814.
6. Majewska H, Skalova A, Stodulski D, et al. Mammary analogue secretory carcinoma of salivary glands: a new entity associated with ETV6 gene rearrangement. *Virchows Arch*. 2015;466:245–254.
7. Skalova A, Vanecek T, Martinek P, et al. Molecular profiling of mammary analog secretory carcinoma revealed a subset of tumors harboring a novel ETV6-RET translocation: report of 10 cases. *Am J Surg Pathol*. 2018;42:234–246.
8. Brandt SM, Swistel AJ, Rosen PP. Secretory carcinoma in the axilla: probable origin from axillary skin appendage glands in a young girl. *Am J Surg Pathol*. 2009;33:950–953.
9. Amin SM, Beattie A, Ling X, et al. Primary cutaneous mammary analog secretory carcinoma with ETV6-NTRK3 translocation. *Am J Dermatopathol*. 2016;38:842–845.
10. Chang MD, Arthur AK, Garcia JJ, et al. ETV6 rearrangement in a case of mammary analogue secretory carcinoma of the skin. *J Cutan Pathol*. 2016;43:1045–1049.
11. Albus J, Batanian J, Wenig BM, et al. A unique case of a cutaneous lesion resembling mammary analog secretory carcinoma: a case report and review of the literature. *Am J Dermatopathol*. 2015;37:e41–e44.
12. Llamas-Velasco M, Mentzel T, Rutten A. Primary cutaneous secretory carcinoma: a previously overlooked low-grade sweat gland carcinoma. *J Cutan Pathol*. 2018;45:240–245.
13. Bao Y, Li J, Zhu Y. Mammary analog secretory carcinoma with ETV6 rearrangement arising in the conjunctiva and eyelid. *Am J Dermatopathol*. 2018;40:531–535.
14. Hindocha N, Wilson MH, Pring M, et al. Mammary analogue secretory carcinoma of the salivary glands: a diagnostic dilemma. *Br J Oral Maxillofac Surg*. 2017;55:290–292.
15. Huang S, Liu Y, Su J, et al. "Secretory" carcinoma of the skin mimicking secretory carcinoma of the breast: case report and literature review. *Am J Dermatopathol*. 2016;38:698–703.
16. Moore RF, Cuda JD. Secretory carcinoma of the skin: case report and review of the literature. *JAAD Case Rep*. 2017;3:559–562.
17. Kazakov DV, Hantschke M, Vanecek T, et al. Mammary-type secretory carcinoma of the skin. *Am J Surg Pathol*. 2010;34:1226–1227.
18. Hyrcza MD, Ng T, Crawford RI. Detection of the ETV6-NTRK3 translocation in cutaneous mammary-analogue secretory carcinoma. *Diagn Histopathol*. 2015;21:481–484.
19. Nguyen JK, Bridge JA, Joshi C, et al. Primary mammary analog secretory carcinoma (MASC) of the vulva with ETV6-NTRK3 fusion: a case report. *Int J Gynecol Pathol*. 2019;38:283–287.
20. Viswanatha DS, Foucar K, Berry BR, et al. Blastic mantle cell leukemia: an unusual presentation of blastic mantle cell lymphoma. *Mod Pathol*. 2000;13:825–833.
21. Gaffney R, Chakerian A, O'Connell JX, et al. Novel fluorescent ligase detection reaction and flow cytometric analysis of SYT-SSX fusions in synovial sarcoma. *J Mol Diagn*. 2003;5:127–135.
22. Antonescu CR, Kawai A, Leung DH, et al. Strong association of SYT-SSX fusion type and morphologic epithelial differentiation in synovial sarcoma. *Diagn Mol Pathol*. 2000;9:1–8.
23. Skalova A, Vanecek T, Majewska H, et al. Mammary analogue secretory carcinoma of salivary glands with high-grade transformation: report of 3 cases with the ETV6-NTRK3 gene fusion and analysis of TP53, beta-catenin, EGFR, and CCND1 genes. *Am J Surg Pathol*. 2014;38:23–33.
24. Xu B, Aryeequaye R, Wang L, et al. Sinonasal secretory carcinoma of salivary gland with high grade transformation: a case report of this under-recognized diagnostic entity with prognostic and therapeutic implications. *Head Neck Pathol*. 2018;12:274–278.
25. Skalova A, Gnepp DR, Lewis JS Jr, et al. Newly described entities in salivary gland pathology. *Am J Surg Pathol*. 2017;41:e33–e47.
26. Petersson F, Michal M, Kazakov DV, et al. A new hitherto unreported histopathologic manifestation of mammary analogue secretory carcinoma: "Masked MASC" associated with low-grade mucinous adenocarcinoma and low-grade in situ carcinoma components. *Appl Immunohistochem Mol Morphol*. 2016;24:e80–e85.
27. Dogan S, Wang L, Ptashkin RN, et al. Mammary analog secretory carcinoma of the thyroid gland: a primary thyroid adenocarcinoma harboring ETV6-NTRK3 fusion. *Mod Pathol*. 2016;29:985–995.
28. Aggarwal A, Nguyen J, Rivera-Davila M, et al. Marshall-Smith syndrome: novel pathogenic variant and previously unreported associations with precocious puberty and aortic root dilatation. *Eur J Med Genet*. 2017;60:391–394.
29. Martinez F, Marin-Reina P, Sanchis-Calvo A, et al. Novel mutations of NFIX gene causing Marshall-Smith syndrome or Sotos-like syndrome: one gene, two phenotypes. *Pediatr Res*. 2015;78:533–539.
30. Chen L, Shern JF, Wei JS, et al. Clonality and evolutionary history of rhabdomyosarcoma. *PLoS Genet*. 2015;11:e1005075.
31. Guilmette J, Dias-Santagata D, Nose V, et al. Novel gene fusions in secretory carcinoma of the salivary glands: enlarging the ETV6 family. *Hum Pathol*. 2019;83:50–58.
32. Rooper LM, Karantanos T, Ning Y, et al. Salivary secretory carcinoma with a novel ETV6-MET fusion: expanding the molecular spectrum of a recently described entity. *Am J Surg Pathol*. 2018;42:1121–1126.
33. Skalova A, Vanecek T, Uro-Coste E, et al. Molecular profiling of salivary gland intraductal carcinoma revealed a subset of tumors

1.1.2 TUMORS WITH FOLLICULAR DIFFERENTIATION

The diagnosis of follicular neoplasms requires the recognition of the types of differentiation toward a particular component of a hair follicle. The first paper in this part titled «*Basal cell carcinoma with matrical differentiation: clinicopathological, immunohistochemical and molecular biological study of 22 cases*» describes a very rare phenomenon (matrical differentiation) in a common neoplasm (basal cell carcinoma). Only 30 cases of basal cell carcinoma (BCC) with matrical differentiation have been previously documented, mainly as isolated case reports. (28), (29) The author studied a large series of this neoplasm, including cases with an atypical matrical component, a hitherto unreported feature. (28), (29) In a majority of the thus far reported cases, matrical differentiation was recognized by the presence of either shadow cells or nuclear expression of β-catenin in basaloid matrical cells. (30) Only several previously published cases of BCC with matrical differentiation have been studied by molecular genetic for mutations in the *CTNNB1* gene (*β-catenin* gene). (31) In our article, we described in detail the specific morphological features of matrical differentiation, such as matrical/supramatrical cells, shadow cells, bright red trichohyaline granules, and blue-grey corneocytes. Molecular genetic studies using Ion AmpliSeq Cancer Hotspot Panel v2 by massively parallel sequencing on Ion Torrent PGM were performed in 2 cases with an atypical matrical component (one was prior subjected to microdissection to sample the matrical and BCC areas separately) and revealed mutations in various genes. We concluded that matrical differentiation in BCC in most cases occur as multiple foci. Rare neoplasms manifest atypia in the matrical areas. IHC for BerEP4, EMA, and β-catenin can be helpful in limited biopsy specimens. BCC and matrical components appear to share some of the gene mutation spectra but have differences in others. This observation must be validated in a large series.

The second article, «*Sporadic trichoblastomas and those occurring in the setting of multiple familial trichoepithelioma/Brooke-Spiegler syndrome show no BAP1 loss*», was published as a Letter to the Editor. Mutations in *BAP1* have been demonstrated to increase susceptibility to the development of uveal and cutaneous melanomas, distinctive melanocytic nevi, mesothelioma, and some other neoplasms. (32) Few recent studies reported loss of BAP1 expression in familial cases of multiple BCC with a germline *BAP1* mutation, whereas sporadic BCC studied for control manifested no loss of BAP1. These findings prompted us to study BAP1 expression in sporadic and multiple trichoblastomas, occurring in the setting of multiple familial trichoepithelioma (MFT)/Brooke-Spiegler syndrome (BSS). (33), (34) A total of 35 neoplasms were studied (17 cribriform trichoblastomas came from 14 patients with MFT and one from BSS), but there was no single case with an immunohistochemical loss of BAP1 expression.

Basal Cell Carcinoma With Matrical Differentiation

Clinicopathologic, Immunohistochemical, and Molecular Biological Study of 22 Cases

Liubov Kyrpychova, MD,* Richard A. Carr, FRCP,† Petr Martinek, PhD,‡ Tomas Vanecek, PhD,*‡
Raul Perret, MD,§ Magdalena Chottová-Dvořáková, MD,‖ Michal Zamecnik, MD,¶
Ladislav Hadravsky, MD,* Michal Michal, MD,*‡ and Dmitry V. Kazakov, MD, PhD*‡

Abstract: Basal cell carcinoma (BCC) with matrical differentiation is a fairly rare neoplasm, with about 30 cases documented mainly as isolated case reports. We studied a series of this neoplasm, including cases with an atypical matrical component, a hitherto unreported feature. Lesions coded as BCC with matrical differentiation were reviewed; 22 cases were included. Immunohistochemical studies were performed using antibodies against BerEp4, β-catenin, and epithelial membrane antigen (EMA). Molecular genetic studies using Ion AmpliSeq Cancer Hotspot Panel v2 by massively parallel sequencing on Ion Torrent PGM were performed in 2 cases with an atypical matrical component (1 was previously subjected to microdissection to sample the matrical and BCC areas separately). There were 13 male and 9 female patients, ranging in age from 41 to 89 years. Microscopically, all lesions manifested at least 2 components, a BCC area (follicular germinative differentiation) and areas with matrical differentiation. A BCC component dominated in 14 cases, whereas a matrical component dominated in 4 cases. Matrical differentiation was recognized as matrical/supramatrical cells (n = 21), shadow cells (n = 21), bright red trichohyaline granules (n = 18), and blue-gray corneocytes (n = 18). In 2 cases, matrical areas manifested cytologic atypia, and a third case exhibited an infiltrative growth pattern, with the tumor metastasizing to a lymph node. BerEP4 labeled the follicular germinative cells, whereas it was markedly reduced or negative in matrical areas. The reverse pattern was seen with β-catenin. EMA was negative in BCC areas but stained a proportion of matrical/supramatrical cells. Genetic studies revealed mutations of the following genes: CTNNB1, KIT, CDKN2A,

TP53, SMAD4, ERBB4, and PTCH1, with some differences between the matrical and BCC components. It is concluded that matrical differentiation in BCC in most cases occurs as multiple foci. Rare neoplasms manifest atypia in the matrical areas. Immunohistochemical analysis for BerEP4, EMA, and β-catenin can be helpful in limited biopsy specimens. From a molecular biological prospective, BCC and matrical components appear to share some of the gene mutations but have differences in others, but this observation must be validated in a large series.

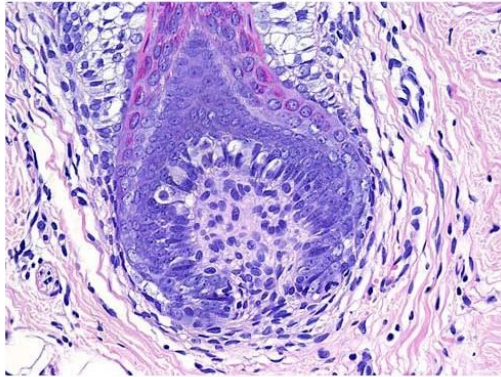**Key Words:** basal cell carcinoma, PTCH, CDKN2A, ERBB4, CTNNB1, matrical, pilomatrical carcinoma, β-catenin

(*Am J Surg Pathol* 2017;41:738–749)

Follicular matrix refers to a part of follicular bulb. Matrical cells are located at the base of the bulb and are visible in anagen follicles as mitotically active, crowded cells with round to oval, vesicular, basophilic nuclei and scanty cytoplasm. Matrical cells become larger, as they ascend, acquiring more distinct nucleoli, rounder nuclei, and more abundant cytoplasm (supramatrical cells). Complete maturation of matrical/supramatrical cells gives rise to hair and to the inner root sheath (IRS) (Fig. 1). Neoplasms with predominantly matrical differentiation, that is, pilomatricoma, melanocytic matricoma, and pilomatrical carcinoma, are mainly composed of cells that resemble matrical and supramatrical cells of a normal hair follicle bulb and, additionally, often display features of differentiation toward hair (shadow cells: polygonal eosinophilic anucleated cells) and the IRS (bright eosinophilic trichohyaline granules identical to those in the Huxley and Henle layers). In addition, characteristic blue-gray corneocytes typical for the IRS may be seen that recapitulate cornification in normal hair follicles.[1,2] Matrical differentiation can rarely be encountered in other adnexal tumors with follicular differentiation, including basal cell carcinoma (BCC). Approximately 30 cases of BCC with focal matrical differentiation have been described in the English literature, mostly as isolated case reports. In a majority of the reported cases, matrical differentiation was recognized by the presence of either shadow (ghost) cells or nuclear

FIGURE 1. A bulb of an anagen hair follicle overlying the follicular papilla. Matrical cells are located at the base of the bulb and have round to oval, vesicular, basophilic nuclei and scanty cytoplasm. As the cells ascend, they acquire more distinct nucleoli, rounder nuclei, and more abundant cytoplasm (supramatrical cells). Complete maturation of matrical/supramatrical cells gives rise to hair and to the IRS.

expression of β-catenin in basaloid matrical cells.[3–7] Few cases of BCC with matrical differentiation have been studied by molecular genetics for mutations in the *CTNNB1* gene (β-catenin gene).[8] Our objective was to study a large series of BCC with matrical differentiation, characterizing the latter in detail, including cases with an atypical matrical component, which is a hitherto unreported feature.

MATERIALS AND METHODS

Case Selection

Lesions coded as BCC with matrical differentiation/shadow cells were retrieved from our institutional, consultation, and personal archives and reviewed. Of the 27 cases found, 5 were excluded, with 2 representing large nodular trichoblastoma, 1 panfolliculoma, and 1 pilomatricoma; in 1 remaining case no matrical differentiation was present on available slides. Thus, 22 neoplasms were included in the study. Three cases were the subject of a previous investigation, focusing on mutations of the *CTNNB1* gene (β-catenin gene) in cutaneous adnexal neoplasms.[8]

Light Microscopic Studies

For each case the following features were documented: histopathologic type of BCC, the ratio of nonmatrical BCC to matrical component, distribution of the matrical component (unifocal vs. multifocal), and features of matrical differentiation (ie, matrical/supramatrical cells, shadow cells, blue-gray corneocytes, and trichohyaline granules).

Immunohistochemical Studies

In 12 cases, immunohistochemical (IHC) studies were performed using antibodies against BerEp4 (to label follicular germinative cells[9]) and β-catenin (to stain matrical cells). In addition, in some of these cases staining with epithelial membrane antigen (EMA), p53, CD10, CK20, and MIB1 was carried out.

Laser Capture Microdissection

One neoplasm in which there was an atypical matrical component was subjected to microdissection to study the gene profile in the BCC and the matrical component separately (vide infra). Formalin-fixed paraffin-embedded (FFPE) tissue sections were mounted on polyethylene terephthalate metal–framed slides, deparaffinized, and stained with hematoxylin and eosin. Areas of interest were selected and captured, using the MMI CellCut Plus instrument (MMI, Glattbrugg, Switzerland) following the manufacturer's recommended protocol.

Molecular Biology

DNA Extraction and Quality Control

DNA was extracted using the REPLI-g FFPE kit (for the microdissected case) and QIAsymphony DNA Mini Kit (for the second case) (Qiagen, Hilden, Germany) on automated extraction system (QIAsymphony SP, Qiagen) according to the manufacturer's supplementary protocol for FFPE samples (purification of genomic DNA from FFPE tissue using the QIAamp DNA FFPE Tissue Kit and deparaffinization solution). Concentration and purity of isolated DNA were measured using the NanoDrop ND-1000 (NanoDrop Technologies Inc., Wilmington, DE). DNA integrity was examined by amplification of control genes in multiplex polymerase chain reaction (PCR), producing fragments from 100 to 600 bp.[10]

Next-generation Sequencing

Two cases with an atypical matrical component (one microdissected and another as a whole sample) were investigated. Samples from both studied cases with DNA integrity ≥ 200 bp were selected for mutational analysis using Ion AmpliSeq Cancer Hotspot Panel v2 (Table 1) by massively parallel sequencing on Ion Torrent PGM (Life Technologies, part of Thermo Fisher Scientific, Waltham, MA). The extracted DNA (10 ng) was amplified, and adapters were ligated using the Ampliseq library preparation kit. Sequencing beads were templated and enriched using the Hi-Q Template OT2 200 Kit, and sequencing was performed on 318v2 chips using the Hi-Q Sequencing kit (Life Technologies) according to the manufacturer's protocols. Signal processing, mapping, and quality control were performed with Torrent Suite v.5.0 (Life Technologies). Sequence variants were called using Ion Reporter v5.2 using AmpliSeq CHPv2 single-sample workflow and default settings. Variants were subsequently filtered to include only exonic, nonsynonymous variants with an allele frequency higher

TABLE 1. Overview of the 50 Cancer Genes Included in the Ion Ampliseq Cancer Hotspot Panel

Gene	Exons	Gene	Exons	Gene	Exons
ABL1	4,5,6,7	*FGFR3*	7,9,14,16,18	*NOTCH1*	26,27,34
AKT1	3,6	*FLT3*	11,14,16,20	*NPM1*	11
ALK	23,25	*GNA11*	5	*NRAS*	2,3,4
APC	16	*GNAQ*	5	*PDGFRA*	12,14,15,18
ATM	8,9,12,17,26,34,35,36,39,50,54,55,56,59,61,63	*GNAS*	8,9	*PIK3CA*	2,5,7,8,10,14,19,21
BRAF	11,15	*HNF1A*	3,4	*PTEN*	1,3,5,6,7,8
CDH1	3,8,9	*HRAS*	2,3	*PTPN11*	3,13
CDKN2A	2	*IDH1*	4	*RB1*	4,6,10,11,14,17,18,20, 21,22
CSF1R	7,22	*IDH2*	4	*RET*	10,11,13,15,16
CTNNB1	3	*JAK2*	14	*SMAD4*	3,4,5,6,8,9,10,11,12
EGFR	3,7,15,18,19,20,21	*JAK3*	4,13,16	*SMARCB1*	2,4,5,9
ERBB2	19,20,21	*KDR*	6,7,11,19,21, 26,27,30	*SMO*	3,5,6,9,11
ERBB4	3,4,6,7,8,9,15,23	*KIT*	2,9,10,11,13, 14,15,17,18	*SRC*	14
EZH2	16	*KRAS*	2,3,4	*STK11*	1,4,4/5,6,8
FBXW7	5,8,9,10,11	*MET*	2,11,14,16,19	*TP53*	2,4,5,6,7,8,10
FGFR1	4,7	*MLH1*	12	*VHL*	1,2,3
FGFR2	7,9,12	*MPL*	10		

than 10%. All filtered variants were annotated using the HGVS nomenclature.

Sanger Sequencing of the PTCH1 Gene

Mutational analysis of coding exons of the *PTCH1* gene was performed using PCR and direct sequencing on whole FFPE material from 2 cases with an atypical matrical component. PCR was carried out under conditions and using primers as reported elsewhere.[11,12]

RESULTS

Clinical Features

Of the 22 patients, 13 were male and 9 were female, ranging in age at diagnosis from 41 to 89 years (mean 71; median 77 y). Locations included back (n = 3), upper limb (n = 3), lower limb (n = 3), ear/periauricular area (n = 3), scalp (n = 2), nose (n = 2), abdomen (n = 2), axilla (n = 1), and cheek (n = 1). In 2 cases, the location was unknown. The size of the lesion, clinical or gross, was indicated in 6 cases and ranged from 6 to 110 mm in largest dimension. The duration of the lesion, when indicated, ranged from 2 months to 8 years (Table 2). In most cases, the clinical differential diagnosis comprised a BCC versus squamous cell carcinoma, or the lesions were merely described as tumors or nodules, some of which were ulcerated. Three patients had previously histologically proven BCC, and 1 had a history of renal cell carcinoma removed 20 years earlier.

The follow-up information was available in 10 cases (range, 3 to 118 mo, mean 52 mo, median 43 mo). One patient had lymph node (LN) involvement (vide infra) at presentation but was alive with LN disease at 18 months; at that time, fine-needle aspiration confirmed LN disease, but the patient was not operated due to chronic obstructive pulmonary disease. Seven patients (including 2 with an atypical matrical component, vide infra) were alive without evidence of disease, and the remaining 2 patients died of other causes (metastatic colorectal carcinoma and unknown cause).

Histopathologic Features

By definition, all lesions manifested at least 2 components, typical BCC area (follicular germinative differentiation characterized by undifferentiated basaloid cells with areas of peripheral palisading, retraction, and interstitial mucin) and matrical differentiation. The

TABLE 2. Summary of the Main Clinicopathologic Features

Features	N (%)
Age (y)	
Range	41-89
Mean	71
Median	77
Sex	
Male	13 (59)
Female	9 (41)
Location	
Head and neck	8 (36.3)
Trunk	6 (27.3)
Limbs	6 (27.3)
Unknown	2 (9.1)
Size (mm)	
Range	6-110
Mean	48.5
Median	40
BCC:AMD ratio	
BCC > AMD	14 (63.6)
AMD > BCC	4 (18.2)
BCC ≈ AMD	4 (18.2)
AMD	
Multifocal	16 (72.7)
Unifocal	6 (27.3)
Volume of AMD (%)	
1-5	4 (18.2)
5-25	5 (22.7)
25-40	5 (22.7)
≈ 50	4 (18.2)
> 50	4 (18.2)
Matrical differentiation	
Matrical/supramatrical cells	21 (95.5)
Shadow cells	21 (95.5)
Red trichohyline granules	18 (81.8)
Blue-gray corneocytes	18 (81.8)

AMD indicates areas with matrical differentiation; BCC, basal cell carcinoma.

45

typical BCC component was predominant in 14 cases, the matrical component was predominant in 4 cases, and both were in approximately equal proportions in 4 cases. In all cases, BCC was of a nodular pattern, accompanied either by a superficial pattern (n = 4), conspicuous cystic change (n = 1), or a morpheiform/infiltrative pattern (n = 2). Focal squamoid differentiation/metaplasia and clear cell differentiation were noted in 2 and 1 lesions, respectively.

Matrical differentiation was recognized as matrical/supramatrical cells (n = 21), shadow cells (n = 21), bright red trichohyaline granules (n = 18), and blue-gray corneocytes (n = 18). Of the 22 lesions, 16 manifested >1 area of matrical differentiation, whereas 6 tumors were unifocal for matrical differentiation (Figs. 2, 3). Matrical cells usually manifested a higher mitotic rate compared with follicular germinative cells but were cytologically bland in all but 2 cases. In the latter 2 tumors, in addition to inconspicuous matrical/supramatrical cells, there was significant pleomorphism of the cells comprising the matrical component. In both cases, the matrical areas dominated (60% and 80%) over a BCC moiety. In 1 of these 2 lesions, in addition to BCC and matrical components, there was an area of actinic keratosis. In the second lesion, there were minor foci with follicular-type stroma closely resembling trichoblastoma, clear cell change in the BCC component, and focal ductal differentiation (probably entrapment of sweat gland) (Figs. 3, 4).

Intratumoral melanin (4 cases) and deposits of calcium (6 cases) were also noted. No prominence of intratumoral melanocytes was seen.

In one patient, a particularly large fungating lesion from the axilla comprised approximately equal proportions of BCC and matrical components and was characterized by deep subcutaneous extension resembling the lower aspect of large terminal hair follicles. The latter tumor had lymphovascular invasion and was associated with a histologically confirmed synchronous ipsilateral axillary LN deposit, with tumor in the efferent lymphatics, showing matrical differentiation (Fig. 5).

IHC Features

BerEP4 labeled basaloid BCC areas (follicular germinative cells) diffusely in all cases studied but was markedly reduced or negative in matrical areas. Nuclear staining for β-catenin was either negative or only focal and scattered in BCC areas in all cases studied. Nuclear expression of β-catenin was detected in the matrical cell component but was often heterogenous (compared with the pattern of diffuse nuclear staining seen in most pilomatrical neoplasms reported in the literature). EMA was negative in the basaloid areas of typical BCC but showed focal (up to 10%) staining of matrical/supramatrical cells in approximately 50% of cases. The proliferation index Ki-67 varied widely (10% to 90%), being usually similar in BCC and matrical areas but showing hot spots in areas of matrical differentiation in some cases. Staining for p53 revealed 3 cases that were considered positive (moderate/strong staining in >50%

of the tumor) and 4 wild type; no null cases (complete immunonegative reaction for p53) were encountered. CD10 staining performed in 8 cases demonstrated positivity in the epithelium in all cases (range, 10% to 60% of the tumor area) but was inconsistent and quite variable in the stroma (roughly less than epithelial staining in 4, relatively equal in 3, and relatively greater compared with epithelial staining in 1 case).

Molecular Genetic Findings

Three cases were studied for mutations of the *CTNNB1* gene (β-catenin gene), and 2 of these harbored mutations *S37F* in exon 3 of the gene, as reported elsewhere.[8] Next-generation sequencing (NGS) identified pathogenic mutations or mutations with uncertain impact on the function of the protein. These findings together with allele frequency are listed in Table 3. Sanger sequencing performed in both cases with an atypical matrical component revealed, in 1 of them (case 2), a *PTCH1* mutation (c.550C > T/p.Gln184Ter.) representing substitution of C by T in position 550 (COSMIC Mutation Id: COSM17598) resulting in a premature stop codon that leads to shortening of the gene product. *PTCH1* mutations were not found in the remaining case.

DISCUSSION

The current study shows that BCC can rarely manifest features of matrical differentiation as collections of matrical/supramatrical cells, shadow cell aggregations, bright red trichohyaline granules (IRS differentiation), and foci of blue-gray cornified masses (IRS cornification), and, in a majority of cases, all these features can be recognized at multiple foci within the neoplasm. In most cases, areas with matrical differentiation represent a minor component, but in a third of cases matrical areas are equal to the follicular germinative cell (BCC) component or even dominant. In nearly all cases, shadow cell cornification could be appreciated in the scanning view that prompted a closer inspection and recognition of the other components of matrical and IRS differentiation.

Shadow cells, believed to represent a flawed attempt to differentiation toward hair,[13] may be found in extracutaneous tumors including craniopharyngioma (central nervous system), calcifying epithelial odontogenic tumor and ameloblastoma (jaw), all of them bearing a resemblance to follicular tumors of the skin.[14] Ghost cells have also been described in some visceral lesions, including atypical endometrial hyperplasia, endometrioid adenocarcinoma, intestinal adenocarcinoma, urothelial carcinoma, small cell carcinoma of the gallbladder, and testicular teratoma. No other features of cutaneous-type follicular differentiation were seen in the latter group, and shadow cells were suggested to represent a nonspecific form of cell death.[15–24]

To our knowledge, no cases of BCC with matrical differentiation in which the matrical areas manifest architectural or cytologic atypia have been previously recorded. In our series, there were 2 cases in which cytologic atypia was prominent in the matrical component (along with cytologically bland areas), and a third case
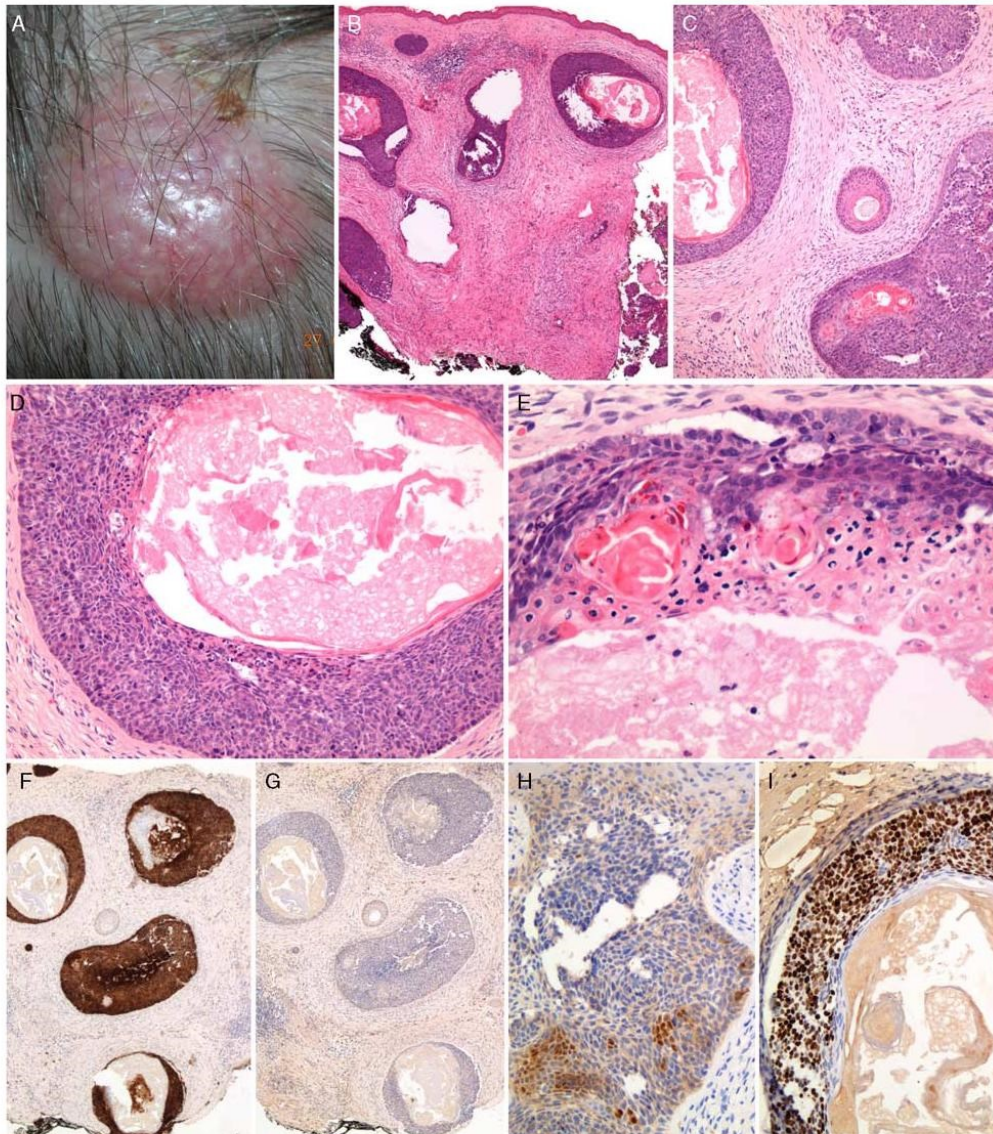
FIGURE 2. BCC with matrical differentiation. A, Telangiectactic nodule on the scalp 5×8 cm with crusting at the site of the punch biopsy. B, Basaloid lobules well separated by fibrotic stroma (H&E ×50). C, There are ghosted keratinocytes on the left and bright orange abrupt keratinization hinting at IRS differentiation (H&E ×100). D, Lobule with slight peripheral palisading, only focal retraction artifact, and central abrupt matrical keratinization (H&E ×200). E, Area of prominent trichohyaline granules and matrical keratinization (H&E ×400). F, Diffuse BerEP4 (×50), (G) negative EMA (×50), (H) focal nuclear β-catenin only (×200); all support a diagnosis of BCC. I, Exceedingly high proliferation fraction (Ki67 ×200). H&E indicates hematoxylin and eosin.

exhibited an infiltrative growth pattern, with the tumor metastasizing to an LN also manifesting matrical differentiation. In the latter lesion, matrical areas dominated, and therefore one can perhaps view this neoplasm as a composite lesion with malignant follicular germinative cells and malignant matrical differentiation. In a series of
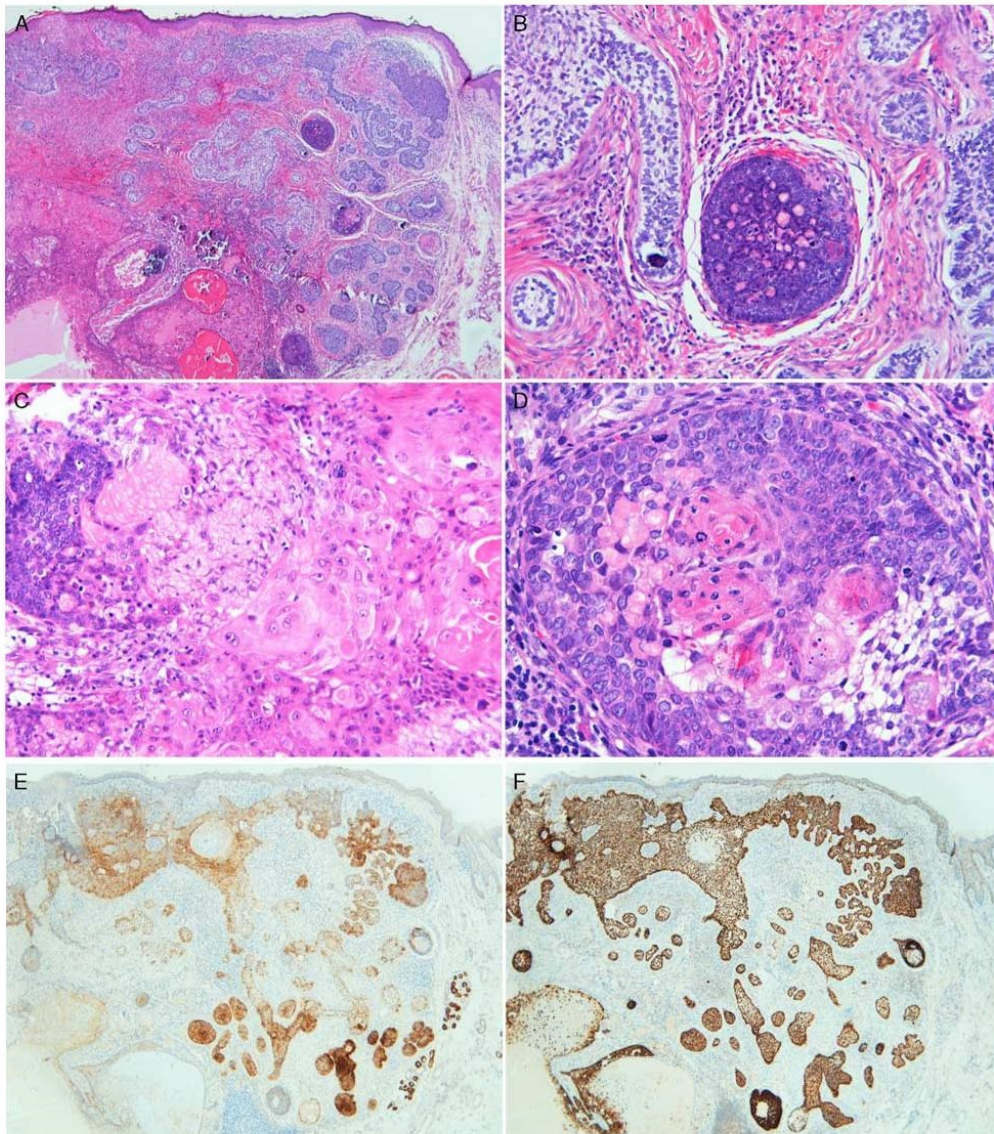
FIGURE 3. BCC with focal trichoblastoma-like areas and an atypical matrical component. A, Areas typical for BCC superficially and centrally blend with an area to the right that has a prominent stromal cuff around the basaloid islands and stromal clefts resembling trichoblastoma. In the lower right there are cystic matrical areas (H&E ×50). B, Close view of the trichoblastoma-like areas with specific follicular stroma and areas of slightly clear cell BCC with focal retraction and mucin (lower right, H&E ×100). C, Matrical areas with ghosted keratinocytes and atypical cells (H&E ×200). D, Basaloid matrical area with trichohyaline granules and individual ghosted keratinocytes (H&E ×200). E, BerEP4 is slightly reduced in clear cell areas of BCC and markedly reduced in cystic matrical areas (lower left, BerEP4, ×50). F, Diffuse strong p53 with reduced staining in the supramatrical and ghosted keratinocytes (bottom left, p53 ×50). H&E indicates hematoxylin and eosin.

48
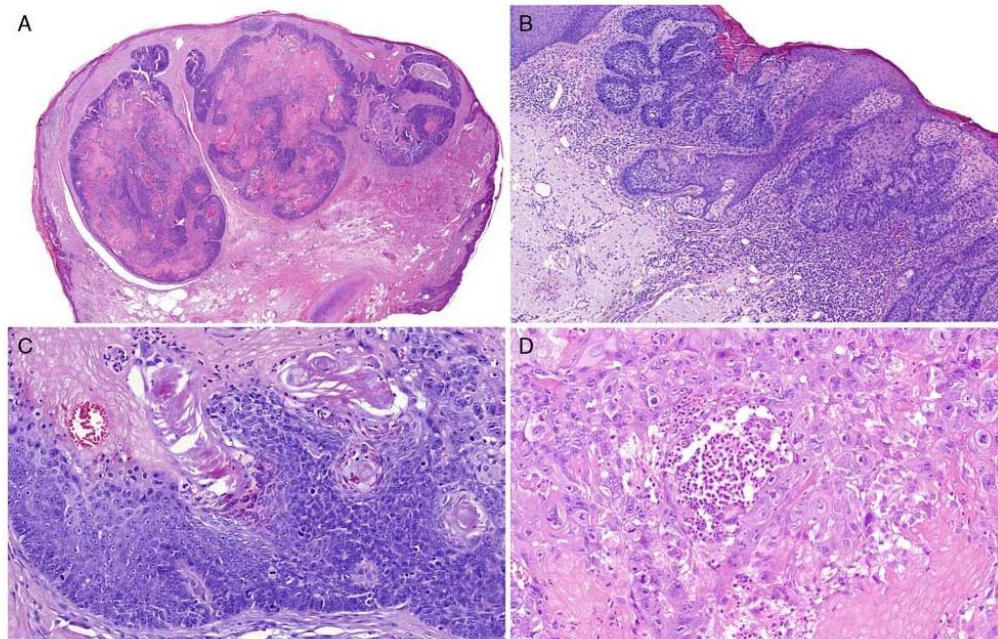
FIGURE 4. A, Neoplasm with a predominant matrical component over BCC areas. B, Basal cell carcinoma component. C, Uniform matrical cells, shadow cells, trichohyaline granules, and blue-gray corneocytes in areas without atypia. D, Cytologic pleomorphism in atypical matrical areas.

17 cases of metastatic BCC by Farmer and Helwig,[25] the authors identified 2 cases with bone marrow metastasis in which shadow cells were present within the metastatic deposits; however, no shadow cells were identified in the primary cutaneous lesions. Whether the atypical matrical component seen in the other 2 cases from our series represents a malignant matrical component and whether such lesions have a greater metastatic potential remains unsettled due to the short follow-up period. Given that cutaneous follicular tumors may show a great variability in the range of differentiation toward different parts of a normal hair follicle within a single neoplasm, it is not surprising that BCC, a tumor with predominant differentiation toward the follicular germinative epithelium, may occasionally exhibit matrical and IRS differentiation, and we suspect this feature is underrecognized.[26,27] Scarce infundibular structures, clear cell areas (likely outer root sheath differentiation[28–30]), and focal specific follicular stroma, occasioning a resemblance to trichoblastomas, may altogether be considered as signs of panfollicular differentiation. However, in a panfolliculoma, trichoblastomatous areas usually predominate.[13,31–33] A single case in our series showed focal ductal differentiation, which is seen in some adnexal tumors with multilineage differentiation and which can be explained by the folliculosebaceous-apocrine unit hypothesis.[26,34–61]

The WNT/β-catenin signaling pathway has been implicated in the pathogenesis of lesions with matrical differentiation. Mutations in the *CTNNB1* gene (β-catenin gene) have been found in both pilomatricomas and pilomatrical carcinomas.[8,62] This gene is located in the 3p22-p21.3 region, has 16 exons, spans 23.2 kb, and encodes for β-catenin, a 92 kDa protein, which apart from intercellular adhesion is involved in the WNT-signaling pathway.[63–65] The WNT/β-catenin/Tcf-Lef (lymphoid enhancer factor) pathway is activated in normal hair follicle matrix cells to induce differentiation toward the hair shaft. In an animal model, transgenic mice expressing an activated β-catenin localized to the nucleus developed skin tumors resembling pilomatricoma.[62,66–71] In addition to the 3 cases of BCC with matrical differentiation investigated previously, we found a missense pathogenic mutation in the atypical matrical component of 1 of the 2 investigated lesions, whereas BCC microdissected areas harbored no β-catenin mutation. Identical mutations in *TP53* were identified in the atypical matrical and BCC areas. Whereas mutations in the tumor-suppressor gene *TP53* have been reported in up to 50% of BCCs, no reports of mutations in this gene in pilomatricomas/ pilomatrical carcinomas exist, to the best of our knowledge.[72] Lazar et al[62] found immunohistochemically significant nuclear accumulation of p53 in 2 of 11

49
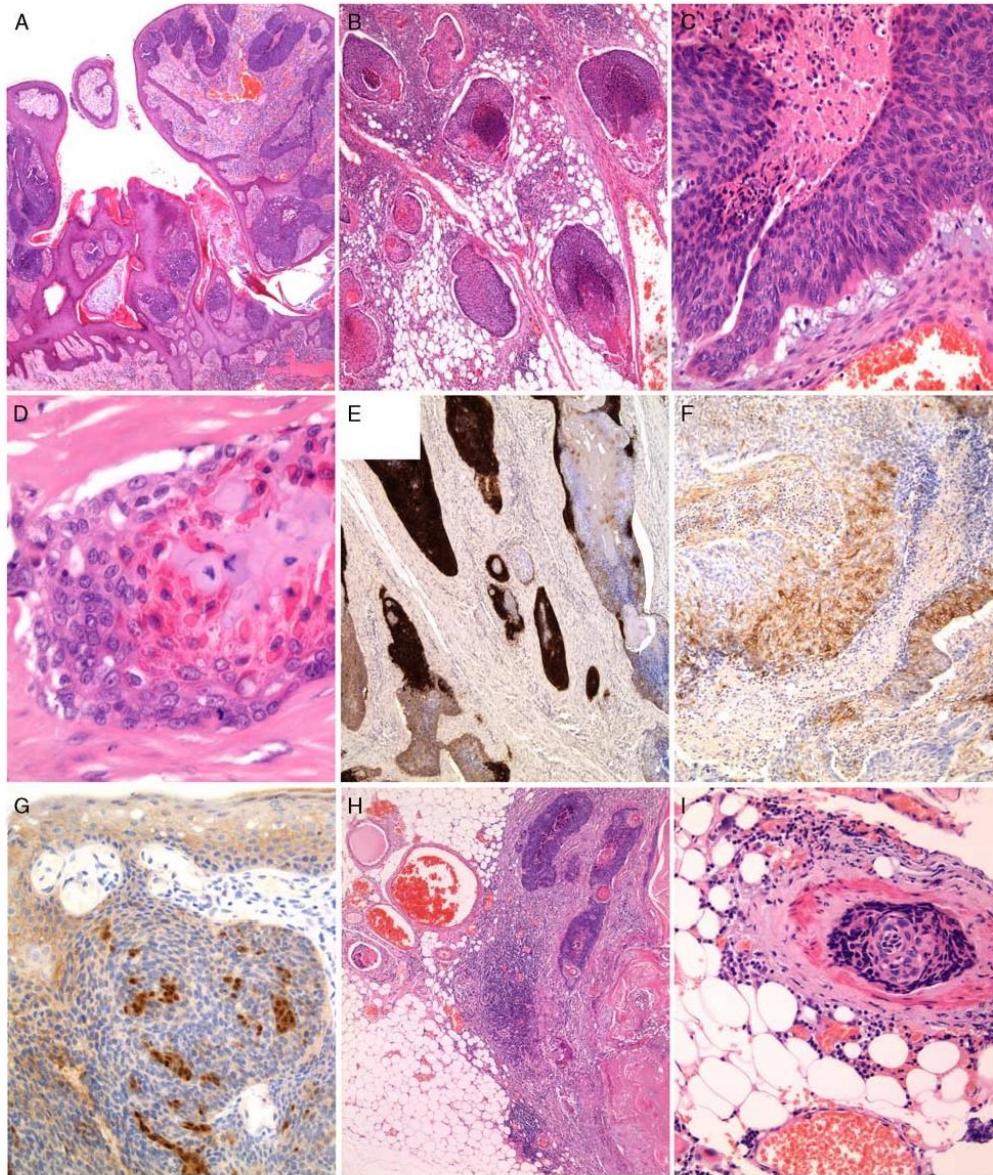
FIGURE 5. BCC with prominent IRS differentiation. A, Large partly polypoid basaloid tumor with surface connections (H&E ×20). B, Deep subcutaneous extensions resemble the deeper aspect of terminal hair follicles (H&E ×50). C, Typical BCC (H&E ×200). D, Prominent trichohyaline granules and blue-gray corneocytes widespread in deeper areas (H&E ×400). E, Strong BerEP4 in areas of BCC but markedly reduced in the areas of IRS and matrical differentiation (BerEP4, ×50). F, EMA was focally positive in areas of matrical/supramatrical differentiation only (EMA, ×100). G, Focal nuclear β-catenin only (β-catenin, ×200). H, Deposit of tumor in axillary LN with tumor in the adjacent vessel (H&E, ×50). I, Tumor in a muscular vessel adjacent to the LN deposit (H&E, ×200). H&E indicates hematoxylin and eosin.

50

TABLE 3. Molecular Genetic Features of 2 Tumors With an Atypical Matrical Component

Case	Gene	Function	Exon	Protein	Allele Frequency (%)	COSMIC—SIFT/PolyPhen Prediction or COSMIC Information
Case 1: Matrical area (microdissected)	CTNNB1	Missense	3	p.Asp32Asn	90	COSM5661—pathogenic
	KIT	Missense	2	p.Ser38Phe	70	ND—susp. benign
	CDKN2A	Missense	2	p.Met54Arg	80	ND—susp. pathogenic
	TP53	Missense	6	p.Val218Gly	61	COSM44198 pathogenic
	TP53	Missense	5	p.Pro152Ser	100	COSM43582 susp. pathogenic
Case 1 BCC area (microdissected)	CDKN2A	Missense	2	p.Met54Arg	88	ND—susp. pathogenic
	TP53	Missense	6	p.Val218Gly	58	COSM44198 pathogenic
	TP53	Missense	5	p.Pro152Ser	80	COSM43582 susp. Pathogenic
	SMAD4	Missense	5	p.Ile179Thr	88	ND—susp benign
	SMAD4	Missense	5	p.Ala190Glu	90	ND—susp pathogenic
	ERBB4	Missense	4	p.Pro170Ser	17	ND—susp benign
Case 2 BCC + matrical areas (whole lesion)	KIT	Missense	11	p.Pro577Ser	14	COSM1293—susp. pathogenic
	CDKN2A	Nonsense	2	p.Arg58Ter	30	ND—susp. pathogenic
	TP53	Missense	8	p.Gly279Trp	22	COSM43674—susp. pathogenic
	TP53	Missense	5	p.Pro152Leu	29	COSM45018—susp. pathogenic

In addition, both cases (as whole lesions) were studied by Sanger sequencing for mutations in the *PTCH1* gene, and a c.550C > T/p.Gln184Ter mutation was found in case 2.

ND indicates not described.

pilomatrical carcinomas, but no genetic studies for mutation in the *TP53* gene were performed. In addition, both components in our microdissected case had a missense mutation in the *CDKN2A* gene. This gene on chromosome 9p21 encodes 2 proteins, p16INK4a and p14ARF, which function as tumor suppressors by means of the retinoblastoma or p53 pathway. Alterations of *CDKN2A* have been reported in some cases of BCC, but no mutation of this gene in matrical neoplasms is known.[73–75] Lastly, the BCC component harbored mutations in *SMAD4* (encoding a member of the Smad family of signal transduction proteins, which are phosphorylated and activated by transmembrane serine–threonine receptor kinases in response to TGF-β signaling) and *ERBB4* (a member of the EGFR subfamily of receptor tyrosine kinases). Alterations in *SMAD4* have previously been reported in BCC.[76]

Sporadic BCCs often harbor somatic mutations in the sonic hedgehog pathway genes including *PTCH1*, *SMO*, *SUFU*, and *GLI1*, of which *PTCH1* is most commonly altered.[77–80] At least 1 *PTCH1* alteration (sequence mutations and loss of heterozygosity at 9q) has been reported in 82% of BCCs, with almost half the cases showing biallelic *PTCH1* inactivation.[72] A substantial proportion of mutations in *PTCH1* represent ultraviolet light (UV) signature point mutations C > T and CC > TT. Apart from the UV signature, mutations found at bipyrimidine sites suggest a UV-independent mechanism in BCC.[72,81–83] *PTCH1* is a tumor-suppressor gene located on chromosome 9q22.3-q31, consists of 23 coding exons, with 12 transmembrane regions, 2 extracellular loops, and a putative sterol-sensing domain. It encodes a 1447-amino-acid integral membrane protein, patched homolog 1 (PTCH), which functions as the receptor for the sonic hedgehog (SHH), and is also an inhibitor for Smoothened (SMO), another transmembrane protein.

Binding of PTCH and SHH abolishes the inhibition that PTCH exerts on SMO, activating the downstream transcription factor GLI-1 that enters the nucleus and transactivates genes related to cell proliferation (cyclin D1, WNT, and TGF-β-related signaling pathways).[72]

As the NGS panel we used did not contain the *PTCH1* gene, we performed Sanger sequencing of both cases with an atypical matrical component as whole lesions and found a *PTCH1* mutation in 1 of them. The mutation detected in our case (c.550C > T/p.Gln184Ter.) may be related to the UV signature. With respect to other genes in the sonic hedgehog pathway, the NGS panel covers *SMO*, but no mutation of the gene was identified.

The diagnosis of BCC with focal matrical differentiation should be straightforward, provided one is familiar with this phenomenon. For cases with atypia in the matrical component, pilomatrical carcinoma is the differential diagnostic consideration. The diagnosis of pilomatrical carcinoma requires the identification of unequivocal signs of matrical differentiation and malignant architectural (ulceration, asymmetry, irregular borders, a multinodular growth pattern, prominent necrosis en masse, lymphovascular involvement) and/or cytologic (marked pleomorphism to anaplasia) features.[84–92] In contrast to BCC with matrical differentiation, pilomatrical carcinoma does not contain a typical BCC component. Problems can be encountered in a limited biopsy specimen, and in these circumstances IHC can be helpful.[93] In 3 cases in our series with punch biopsies, IHC staining (for BerEP4, EMA, and β-catenin) concurred with the final excision. In our opinion, a relatively confident diagnosis could be suggested on these small biopsies with the caveat that complete excision is recommended in all cases due to variability of staining patterns. In addition, the scanning view of β-catenin may also give a false impression of widespread staining, and care must be taken to assess only moderate or strong nuclear expression.

51

In conclusion, we have presented the largest series of BCC with follicular matrical differentiation. The matrical/IRS component is often minor but occasionally predominates. Diffuse BerEp4 staining and lack of diffuse nuclear β-catenin can be used to confirm the diagnosis in small biopsies in which pilomatrical carcinoma may be a diagnostic consideration. We recommend running EMA in parallel, because it is consistently completely negative in the basaloid areas of typical BCC with the caveat that it may stain focally in matrical/supramatrical cells. Rare neoplasms manifest atypia in the matrical component, and more cases with follow-up information are needed to establish the course of these lesions. One tumor in our series has metastasized, but whether this can be attributed to the unusually large size remains speculative. Diffusely positive p53 (moderate or strong staining in >80% of nuclei) or possibly a null phenotype (not seen in our series) may be helpful for confirming a malignant lesion in some cases. Our limited molecular workup indicates some tumor heterogeneity, but BCC and matrical components may, at least partially, share genetic alterations; this observation must, however, be validated in a larger series.

REFERENCES

1. Ackerman A, Reddy VB, Soyer HP. *Neoplasms with follicular differentiation*, 2nd ed. New York, NY: Ardor Scribendi Publishers; 2001.
2. Kazakov DV, Michal M, Kacerovska D, et al. Cutaneous adnexal tumors. Philadelphia, PA: LWW; 2012:p814.
3. Ambrojo P, Aguilar A, Simon P, et al. Basal cell carcinoma with matrical differentiation. *Am J Dermatopathol*. 1992;14:293–297.
4. Aloi FG, Molinero A, Pippione M. Basal cell carcinoma with matrical differentiation. Matrical carcinoma. *Am J Dermatopathol*. 1988;10:509–513.
5. Del Sordo R, Cavaliere A, Sidoni A. Basal cell carcinoma with matrical differentiation: expression of beta-catenin [corrected] and osteopontin. *Am J Dermatopathol*. 2007;29:470–474.
6. Haskell HD, Haynes HA, McKee PH, et al. Basal cell carcinoma with matrical differentiation: a case study with analysis of beta-catenin. *J Cutan Pathol*. 2005;32:245–250.
7. Kwittken J. Shadow cell basal cell carcinoma with acantholysis. *Cutis*. 2002;69:57–60. 63-65.
8. Kazakov DV, Sima R, Vanecek T, et al. Mutations in exon 3 of the CTNNB1 gene (beta-catenin gene) in cutaneous adnexal tumors. *Am J Dermatopathol*. 2009;31:248–255.
9. Fan YS, Carr RA, Sanders DS, et al. Characteristic Ber-EP4 and EMA expression in sebaceoma is immunohistochemically distinct from basal cell carcinoma. *Histopathology*. 2007;51:80–86.
10. van Dongen JJ, Langerak AW, Bruggemann M, et al. Design and standardization of PCR primers and protocols for detection of clonal immunoglobulin and T-cell receptor gene recombinations in suspect lymphoproliferations: report of the BIOMED-2 Concerted Action BMH4-CT98-3936. *Leukemia*. 2003;17:2257–2317.
11. Kazakov DV, Grossmann P, Spagnolo DV, et al. Expression of p53 and TP53 mutational analysis in malignant neoplasms arising in preexisting spiradenoma, cylindroma, and spiradenocylindroma, sporadic or associated with Brooke-Spiegler syndrome. *Am J Dermatopathol*. 2010;32:215–221.
12. Kazakov DV, Ivan D, Kutzner H, et al. Cutaneous hidradenocarcinoma: a clinicopathological, immunohistochemical, and molecular biologic study of 14 cases, including Her2/neu gene expression/amplification, TP53 gene mutation analysis, and t(11;19) translocation. *Am J Dermatopathol*. 2009;31:236–247.
13. Ackerman BA, Reddy VB, Soyer PH. *Neoplasms with follicular differentiation*. New York: Ardor Scribendi, Ltd; 2001.
14. Kazakov DV, Spagnolo DV, Kacerovska D, et al. Cutaneous type adnexal tumors outside the skin. *Am J Dermatopathol*. 2011; 33:303–315.
15. Ishida T, Abe S, Miki Y, et al. Intraosseous pilomatricoma: a possible rare skeletal manifestation of Gardner syndrome. *Skeletal Radiol*. 2007;36:693–698.
16. Minkowitz G, Lee M, Minkowitz S. Pilomatricoma of the testicle. An ossifying testicular tumor with hair matrix differentiation. *Arch Pathol Lab Med*. 1995;119:96–99.
17. Ulbright TM, Srigley JR. Dermoid cyst of the testis: a study of five postpubertal cases, including a pilomatrixoma-like variant, with evidence supporting its separate classification from mature testicular teratoma. *Am J Surg Pathol*. 2001;25:788–793.
18. Zamecnik M, Michal M. Shadow cell differentiation in tumours of the colon and uterus. *Zentralbl Pathol*. 1995;140:421–426.
19. Zamecnik M, Michal M, Mukensnabl P. Shadow cells in extracutaneous locations. *Arch Pathol Lab Med*. 1996;120:426–428.
20. Zamecnik M, Michal M, Mukensnabl P. Pilomatrixoma-like visceral carcinomas. *Histopathology*. 1998;33:395.
21. Zamecnik M, Michal M, Mukensnabl P. Cell death in pilomatricoma. *J Cutan Pathol*. 2000;27:100.
22. Zamecnik M, Michal M, Mukensnabl P. Collagenous spherulosis versus shadow cell differentiation in endometrioid adenocarcinoma. *Histopathology*. 2000;36:470–471.
23. Zamecnik M, Mukensnabl P, Curik R, et al. Shadow cell differentiation in testicular teratomas. A report of two cases. *Cesk Patol*. 2005;41:102–106.
24. Zamecnik M, Bartos P, Kascak P. Shadow cell differentiation in endometrioid carcinomas of the uterus. Its frequent occurrence and beta-catenin expression. *Cesk Patol*. 2015;51:123–126.
25. Farmer ER, Helwig EB. Metastatic basal cell carcinoma: a clinicopathologic study of seventeen cases. *Cancer*. 1980;46:748–757.
26. Kazakov DV, Vanecek T, Nemcova J, et al. Spectrum of tumors with follicular differentiation in a patient with the clinical phenotype of multiple familial trichoepitheliomas: a clinicopathological and molecular biological study, including analysis of the CYLD and PTCH genes. *Am J Dermatopathol*. 2009;31:819–827.
27. Misago N, Satoh T, Miura Y, et al. Merkel cell-poor trichoblastoma with basal cell carcinoma-like foci. *Am J Dermatopathol*. 2007; 29:249–255.
28. Kazakov DV, Mentzel T, Erlandson RA, et al. Clear cell trichoblastoma: a clinicopathological and ultrastructural study of two cases. *Am J Dermatopathol*. 2006;28:197–201.
29. Misago N, Satoh T, Narisawa Y. Basal cell carcinoma with tricholemmal (at the lower portion) differentiation within seborrheic keratosis. *J Cutan Pathol*. 2003;30:196–201.
30. Tronnier M. Clear cell trichoblastoma in association with a nevus sebaceus. *Am J Dermatopathol*. 2001;23:143–145.
31. Schirren CG, Rutten A, Plewig G. Panfolliculoma. Clinical and immunohistochemical findings in 4 cases. *Hautarzt*. 1996;47: 610–615.
32. Gonzalez-Guerra E, Requena L, Kutzner H. Immunohistochemical study of calretinin in normal hair follicles and tumors with follicular differentiation. *Actas Dermosifiliogr*. 2008;99:456–463.
33. Kacerovska D, Michal M, Kazakov DV. Panfolliculoma with sebaceous differentiation—a case report. *Am J Dermatopathol*. 2012;34:e90–e93.
34. Requena L, Kiryu H, Ackerman AB. *Neoplasms with apocrine differentiation*. Philadelphia: Lippincott-Raven; 1998.
35. Requena L, Sanchez Yus E, Santa Cruz DJ. Apocrine type of cutaneous mixed tumor with follicular and sebaceous differentiation. *Am J Dermatopathol*. 1992;14:186–194.
36. Kazakov DV, Belousova IE, Bisceglia M, et al. Apocrine mixed tumor of the skin ("mixed tumor of the folliculosebaceous-apocrine complex"). Spectrum of differentiations and metaplastic changes in the epithelial, myoepithelial, and stromal components based on a

histopathologic study of 244 cases. *J Am Acad Dermatol*. 2007; 57:467–483.

37. Vazmitel M, Michal M, Mukensnabl P, et al. Syringocystadenoma papilliferum with sebaceous differentiation in an intradermal tubular apocrine component. Report of a case. *Am J Dermatopathol*. 2008;30:51–53.

38. Kazakov DV, Kacerovska D, Michal M. Microcystic adnexal carcinoma with multiple areas of follicular differentiation toward germinative cells and specific follicular stroma (trichoblastomatous areas). *Am J Dermatopathol*. 2011;33:e47–e49.

39. McCalmont TH. A call for logic in the classification of adnexal neoplasms. *Am J Dermatopathol*. 1996;18:103–109.

40. Kazakov DV, Kutzner H, Spagnolo DV, et al. Sebaceous differentiation in poroid neoplasms: report of 11 cases, including a case of metaplastic carcinoma associated with apocrine poroma (sarcomatoid apocrine porocarcinoma). *Am J Dermatopathol*. 2008;30:21–26.

41. Kazakov DV, Mukensnabl P, Michal M. An unusual hamartoma of the folliculosebaceous-apocrine unit: a case report. *J Cutan Pathol*. 2006;33:365–368.

42. Sanchez Yus E, Requena L, Simon P, et al. Complex adnexal tumor of the primary epithelial germ with distinct patterns of superficial epithelioma with sebaceous differentiation, immature trichoepithelioma, and apocrine adenocarcinoma. *Am J Dermatopathol*. 1992; 14:245–252.

43. Kazakov DV, Soukup R, Mukensnabl P, et al. Brooke-Spiegler syndrome: report of a case with combined lesions containing cylindromatous, spiradenomatous, trichoblastomatous, and sebaceous differentiation. *Am J Dermatopathol*. 2005;27:27–33.

44. Apisarnthanarax P, Bovenmyer DA, Mehregan AH. Combined adnexal tumor of the skin. *Arch Dermatol*. 1984;120:231–233.

45. Groben PA, Hitchcock MG, Leshin B, et al. Apocrine poroma: a distinctive case in a patient with nevoid basal cell carcinoma syndrome. *Am J Dermatopathol*. 1999;21:31–33.

46. Grosshans E, Hanau D. [The infundibular adenoma: a follicular poroma with sebaceous and apocrine differentiation (author's transl)]. *Ann Dermatol Venereol*. 1981;108:59–66.

47. Ikeya T. Multiple linear eccrine adenomas associated with multiple trichoepitheliomas. *J Dermatol*. 1987;4:48–53.

48. Hanau D, Grosshans E, Laplanche G. A complex poroma-like adnexal adenoma. *Am J Dermatopathol*. 1984;6:567–572.

49. Harvell JD, Kerschmann RL, LeBoit PE. Eccrine or apocrine poroma? Six poromas with divergent adnexal differentiation. *Am J Dermatopathol*. 1996;18:1–9.

50. Kamiya H, Oyama Z, Kitajima Y. "Apocrine" poroma: review of the literature and case report. *J Cutan Pathol*. 2001;28:101–104.

51. Okuda C, Ito M, Fujiwara H, et al. Sebaceous epithelioma with sweat gland differentiation. *Am J Dermatopathol*. 1995;17:523–528.

52. Pujol RM, LeBoit PE, Su WP. Microcystic adnexal carcinoma with extensive sebaceous differentiation. *Am J Dermatopathol*. 1997;19: 358–362.

53. Kazakov DV, Vanecek T, Zelger B, et al. Multiple (familial) trichoepitheliomas: a clinicopathological and molecular biological study, including CYLD and PTCH gene analysis, of a series of 16 patients. *Am J Dermatopathol*. 2011;33:251–265.

54. Kazakov DV, Vittay G, Michal M, et al. High-grade trichoblastic carcinosarcoma. *Am J Dermatopathol*. 2008;30:62–64.

55. Masuda T, Arata J. An epithelioma with hair follicle and apocrine differentiation. *J Dermatol*. 1987;14:81–84.

56. Muller-Hess S, Delacretaz J. [Trichoepithelioma with features of apocrine adenoma]. *Dermatologica*. 1973;146:170–176.

57. Misago N, Satoh T, Narisawa Y. Basal cell carcinoma with ductal and glandular differentiation: a clinicopathological and immunohistochemical study of 10 cases. *Eur J Dermatol*. 2004;14:383–387.

58. Kazakov DV, Kutzner H, Mukensnabl P, et al. Low-grade adnexal carcinoma of the skin with multidirectional (glandular, trichoblastomatous, spiradenocylindromatous) differentiation. *Am J Dermatopathol*. 2006;28:341–345.

59. LeBoit PE, Parslow TG, Choy SH. Hair matrix differentiation. Occurrence in lesions other than pilomatricoma. *Am J Dermatopathol*. 1987;9:399–405.

60. Lee NH, Lee SH, Ahn SK. Apocrine poroma with sebaceous differentiation. *Am J Dermatopathol*. 2000;22:261–263.

61. Kazakov DV, Mukensnabl P, Michal M. Tubular adenoma of the skin with follicular and sebaceous differentiation: a report of two cases. *Am J Dermatopathol*. 2006;28:142–146.

62. Lazar AJ, Calonje E, Grayson W, et al. Pilomatrix carcinomas contain mutations in CTNNB1, the gene encoding beta-catenin. *J Cutan Pathol*. 2005;32:148–157.

63. McCrea PD, Turck CW, Gumbiner B. A homolog of the armadillo protein in Drosophila (plakoglobin) associated with E-cadherin. *Science*. 1991;254:1359–1361.

64. Nollet F, Berx G, Molemans F, et al. Genomic organization of the human beta-catenin gene (CTNNB1). *Genomics*. 1996;32:413–424.

65. Kraus C, Liehr T, Hulsken J, et al. Localization of the human beta-catenin gene (CTNNB1) to 3p21: a region implicated in tumor development. *Genomics*. 1994;23:272–274.

66. Chan EF, Gat U, McNiff JM, et al. A common human skin tumour is caused by activating mutations in beta-catenin. *Nat Genet*. 1999;21:410–413.

67. Chan EF. Pilomatricomas contain activating mutations in beta-catenin. *J Am Acad Dermatol*. 2000;43:701–702.

68. Durand M, Moles JP. [Beta-catenin mutations in a common skin cancer: pilomatricoma]. *Bull Cancer*. 1999;86:725–726.

69. Moreno-Bueno G, Gamallo C, Perez-Gallego L, et al. beta-catenin expression in pilomatrixomas. Relationship with beta-catenin gene mutations and comparison with beta-catenin expression in normal hair follicles. *Br J Dermatol*. 2001;145:576–581.

70. Kajino Y, Yamaguchi A, Hashimoto N, et al. beta-Catenin gene mutation in human hair follicle-related tumors. *Pathol Int*. 2001; 51:543–548.

71. Ha SJ, Kim JS, Seo EJ, et al. Low frequency of beta-catenin gene mutations in pilomatricoma. *Acta Derm Venereol*. 2002;82:428–431.

72. Reifenberger J, Wolter M, Knobbe CB, et al. Somatic mutations in the PTCH, SMOH, SUFUH and TP53 genes in sporadic basal cell carcinoma. *Br J Dermatol*. 2005;152:43–51.

73. Kanellou P, Zaravinos A, Zioga M, et al. Deregulation of the tumour suppressor genes p14(ARF), p15(INK4b), p16(INK4a) and p53 in basal cell carcinoma. *Br J Dermatol*. 2009;160:1215–1221.

74. Stacey SN, Helgason H, Gudjonsson SA, et al. New basal cell carcinoma susceptibility loci. *Nat Commun*. 2015;6:6825–6834.

75. Harms PW, Fullen DR, Patel RM, et al. Cutaneous basal cell carcinosarcomas: evidence of clonality and recurrent chromosomal losses. *Hum Pathol*. 2015;46:690–697.

76. Shao Y, Zhang J, Zhang R, et al. Examination of Smad2 and Smad4 copy-number variations in skin cancers. *Clin Transl Oncol*. 2012; 14:138–142.

77. Wolter M, Reifenberger J, Sommer C, et al. Mutations in the human homologue of the Drosophila segment polarity gene patched (PTCH) in sporadic basal cell carcinomas of the skin and primitive neuroectodermal tumors of the central nervous system. *Cancer Res*. 1997;57:2581–2585.

78. Gailani MR, Stahle-Backdahl M, Leffell DJ, et al. The role of the human homologue of Drosophila patched in sporadic basal cell carcinomas. *Nat Genet*. 1996;14:78–81.

79. Nagano T, Bito T, Kallassy M, et al. Overexpression of the human homologue of Drosophila patched (PTCH) in skin tumours: specificity for basal cell carcinoma. *Br J Dermatol*. 1999;140:287–290.

80. Emmert S, Schon MP, Haenssle HA. Molecular biology of basal and squamous cell carcinomas. *Adv Exp Med Biol*. 2014;810:234–252.

81. Daya-Grosjean L, Couve-Privat S. Sonic hedgehog signaling in basal cell carcinomas. *Cancer Lett*. 2005;225:181–192.

82. Ratner D, Peacocke M, Zhang H, et al. UV-specific p53 and PTCH mutations in sporadic basal cell carcinoma of sun-exposed skin. *J Am Acad Dermatol*. 2001;44:293–297.

83. Saldanha G, Shaw JA, Fletcher A. Evidence that superficial basal cell carcinoma is monoclonal from analysis of the Ptch1 gene locus. *Br J Dermatol*. 2002;147:931–935.

84. Chen KT, Taylor DR Jr. Pilomatrix carcinoma. *J Surg Oncol*. 1986;33:112–114.

85. Green DE, Sanusi ID, Fowler MR. Pilomatrix carcinoma. *J Am Acad Dermatol*. 1987;17:264–270.

53

86. Hardisson D, Linares MD, Cuevas-Santos J, et al. Pilomatrix carcinoma: a clinicopathologic study of six cases and review of the literature. *Am J Dermatopathol*. 2001;23:394–401.
87. Lineaweaver WC, Wang TN, Leboit PL. Pilomatrix carcinoma. *J Surg Oncol*. 1988;37:171–174.
88. Lopansri S, Mihm MC Jr. Pilomatrix carcinoma or calcifying epitheliocarcinoma of Malherbe: a case report and review of literature. *Cancer*. 1980;45:2368–2373.
89. Wood MG, Parhizgar B, Beerman H. Malignant pilomatricoma. *Arch Dermatol*. 1984;120:770–773.
90. Zagarella SS, Kneale KL, Stern HS. Pilomatrix carcinoma of the scalp. *Australas J Dermatol*. 1992;33:39–42.
91. LeBoit PE, Burg G, Weedon D, et al. *World Health Organization Classification of Tumours Pathology and Genetics of Skin Tumours*. Lyon: IARC Press; 2006.
92. van der Walt JD, Rohlova B. Carcinomatous transformation in a pilomatrixoma. *Am J Dermatopathol*. 1984;6:63–69.
93. Sherley-Dale AC, Chachlani N, Sanders DS, et al. Trichoblastoma of the breast detected by screening mammography: a diagnostic pitfall. *Am J Surg Pathol*. 2010;34:748–754.

54

TABLE 3. Average Number of Sox10-Positive Cells Within Scar Tissue (Antibody 2 Results Only) Compared With Desmoplastic Melanoma

	Average No. Sox10+, Cells/mm²	95% Confidence Interval
Scar	44	±27
Desmoplastic Melanoma	1292	±905

This difference was statistically significant ($P < 0.001$).

in the numbers of positive cells seen; however, all cases which we assessed showed at least some positive cells. Indeed, in most cases, the number of cells could be sufficient to cause some level of diagnostic concern for an occult melanocytic proliferation, particularly in the context of the reports referenced above. The cause for the discrepancy between our findings and those reported by others is not clear. We considered that there may be differences associated with different antibodies; however, a comparison of 3 different commercially available products (including both polyclonal and monoclonal examples) revealed no difference in the staining pattern within scar tissue. One can only assume that there is a technical difference in the immunohistochemical methodology between the respective laboratories. In this regard, we note that both of the aforementioned studies used a different antibody to that used in this study.[7,8]

Delineating the exact nature of the Sox10-positive cells within the scar tissue was beyond the scope of this study; however, some inferences can be drawn from previous work. In particular, Trejo et al demonstrated the presence of spindled cells within scar tissue, a proportion of which expressed markers of early Schwann cell differentiation.[11] They propose that proliferation of such cells might form part of the normal wound-healing process. It seems reasonable to propose that at least a proportion of the Sox10-positive cells which we have observed may represent similar Schwann cell precursors.

Despite our finding that Sox10-positive cells can be identified within scar tissue, our anecdotal experience was that the magnitude of this staining was far less than that seen within bona fide desmoplastic melanoma. Indeed, the digital imaging analysis confirmed that there is a significantly greater number of cells showing Sox10 positivity with

desmoplastic melanomas than that in scars (Table 3, and compare Fig. 1F with Figs. 1B, D). Thus, we would argue that it remains a useful marker to detect residual desmoplastic melanomas in re-excision specimens, so long as the reporting pathologist is aware of the potential for smaller numbers of spindle cells to stain positively within otherwise benign scar tissue.

Nathan T. Harvey, FRCPA*†
Nathan J. Acott, BSc*
Benjamin A. Wood, FRCPA*†
*Department of Anatomical Pathology,
PathWest, QEII Medical Centre,
Perth, Western Australia
†School of Pathology and
Laboratory Medicine,
University of Western Australia,
Perth, Western Australia

REFERENCES
1. Wegner M. Secrets to a healthy Sox life: lessons for melanocytes. *Pigment Cell Res.* 2005; 18:74–85.
2. Mollaaghababa R, Pavan WJ. The importance of having your SOX on: role of SOX10 in the development of neural crest-derived melanocytes and glia. *Oncogene.* 2003;22:3024–3034.
3. Bondurand N, Kobetz A, Pingault V, et al. Expression of the SOX10 gene during human development. *FEBS Lett.* 1998;432:168–172.
4. Mohamed A, Gonzalez RS, Lawson D, et al. SOX10 expression in malignant melanoma, carcinoma, and normal tissues. *Appl Immunohistochem Mol Morphol.* 2013;21:506–510.
5. Tacha D, Qi W, Ra S, et al. A newly developed mouse monoclonal SOX10 antibody is a highly sensitive and specific marker for malignant melanoma, including spindle cell and desmoplastic melanomas. *Arch Pathol Lab Med.* 2015;139:530–536.
6. Wood BA. Desmoplastic melanoma: recent advances and persisting challenges. *Pathology.* 2013;45:453–463.
7. Plaza JA, Bonneau P, Prieto V, et al. Desmoplastic melanoma: an updated immunohisto-
chemical analysis of 40 cases with a proposal for an additional panel of stains for diagnosis. *J Cutan Pathol.* 2016;43:313–323.
8. Ramos-Herberth FI, Karamchandani J, Kim J, et al. SOX10 immunostaining distinguishes desmoplastic melanoma from excision scar. *J Cut Pathol.* 2010;37:944–952.
9. Harvey J, Thomas C, Wood B, et al. Practical issues concerning the implementation of Ki-67 proliferative index measurement in breast cancer reporting. *Pathology.* 2015;47:13–20.
10. Chorny JA, Barr RJ. S100-positive spindle cells in scars: a diagnostic pitfall in the re-excision of desmoplastic melanoma. *Am J Dermatopathol.* 2002;24:309–312.
11. Trejo O, Reed JA, Prieto VG. Atypical cells in human cutaneous re-excision scars for melanoma express p75NGFR, C56/N-CAM and GAP-43: evidence of early Schwann cell differentiation. *J Cut Pathol.* 2002;29:397–406.

Sporadic Trichoblastomas and Those Occurring in the Setting of Multiple Familial Trichoepithelioma/ Brooke–Spiegler Syndrome Show No BAP1 Loss

To the Editor

The BRCA1-associated protein 1 (*BAP1*) is a tumor suppressor gene located on chromosome region 3p21 coding a deubiquitinating enzyme that regulates key cellular pathways, including cell cycle, cellular differentiation, transcription, and DNA damage response. Mutations in *BAP1* have been demonstrated to increase susceptibility to the development of uveal and cutaneous melanomas, distinctive Spitz nevi, mesothelioma, and some other neoplasms.[1–4] Loss of BAP1 expression has recently been reported in familial cases of multiple basal cell carcinomas (BCCs) with a germline *BAP1* mutation, whereas sporadic BCC studied for control manifested no loss of BAP1.[5–7] Our aim was to study BAP1 expression in trichoblastomas, both
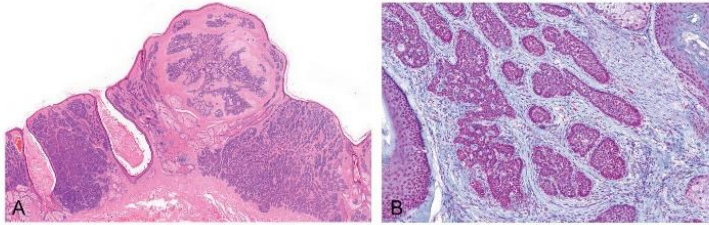
FIGURE 1. MFT. This patient developed BCC as discussed by Kazakov et al[8] (A). Nuclear BAP1 expression is retained in this case (B).

solitary sporadic and multiple ones, occurring in the setting of multiple familial trichoepithelioma (MFT)/Brooke–Spiegler syndrome (BSS).

A total of 35 neoplasms were studied. Of these, 17 cribriform trichoblastomas came from 14 patients with MFT and 1 from BSS. All lesions were located on the face. These syndromic patients included 10 women and 5 men, ranging in age at diagnosis from 11 to 65 years (mean 33 years). All patients have been a subject of 5 previous publications.[8–12] The 17 sporadic trichoblastomas (12 cribriform and 5 desmoplastic) were randomly selected from our files and came from 12 female and 5 male patients, ranging in age from 12 to 80 years (mean 48.7 years). All but one lesion were located on the face and scalp. The remaining tumor was on the shin.

Immunohistochemical (IHC) studies were conducted with an automated IHC system (Ventana BenchMark XT; Ventana Medical Systems Inc, Tucson, AZ) using an alkaline phosphatase method and a red chromogen, according to the manufacturer's instructions. The BAP1 antibody (clone C-4, 1:50 dilution; Santa Cruz Biotechnology Inc, Santa Cruz, CA) was used. In none of the 35 neoplasms was there loss of BAP1, including a case in which there was malignant transformation of trichoblastoma into BCC[8] (Fig. 1).

Various neoplasms from patients with a germline BAP1 mutation have been shown to exhibit loss of BAP1 immunohistochemically. In sporadic tumors in various organs, this is a rarely encountered phenomenon (<1%), with the exception for pleural mesothelioma which manifests loss of BAP1 expression in over 50% of cases.[13,14] Somatic BAP1 mutations and loss of BAP1 have also been found in peritoneal mesothelioma.[15] In some

tumors, such as clear cell renal carcinoma or intrahepatic cholangiocarcinoma, loss of nuclear BAP1 protein expression has been associated with a poor prognosis or higher grade.[16–18] With respect to the skin, a group of spitzoid melanocytic lesions with loss of BAP1 expression (and BAP1 mutations) occurring sporadically or as part of a familial cancer syndrome has been recognized. Three studies on familial cases of multiple BCC with a germline *BAP1* mutation showed loss of BAP1; by contrast, sporadic BCC retained nuclei expression of this protein. As BCC and trichoblastoma may be viewed as poles of a spectrum of follicular tumors, we studied both sporadic and multiple trichoblastomas associated with MFT/BSS, but there was no single case with loss of BAP1 expression. Because IHC for BAP1 correlates with biallelic BAP1 loss and has positive and negative predicative values of 100% and 98.6%, respectively,[19] no molecular genetic studies were conducted.

Liubov Kyrpychova, MD
Denisa Kacerovska, MD, PhD
Michal Michal, MD
Dmitry V. Kazakov, MD, PhD
Sikl's Department of Pathology, Medical Faculty in Pilsen, Charles University in Prague, Pilsen, Czech Republic

REFERENCES

1. Wiesner T, Obenauf AC, Murali R, et al. Germline mutations in BAP1 predispose to melanocytic tumors. *Nat Genet.* 2011;43:1018–1021.
2. Cigognetti M, Lonardi S, Fisogni S, et al. BAP1 (BRCA-associated protein 1) is a highly specific marker for differentiating mesothelioma from reactive mesothelial proliferations. *Mod Pathol.* 2015;28:1043–1057.
3. Joseph RW, Kapur P, Serie DJ, et al. Loss of BAP1 protein expression is an independent marker of poor prognosis in patients with low-risk clear cell renal cell carcinoma. *Cancer.* 2014;120:1059–1067.
4. Murali R, Wiesner T, Scolyer RA. Tumours associated with BAP1 mutations. *Pathology.* 2013;45:116–126.
5. Mochel MC, Piris A, Nose V, et al. Loss of BAP1 expression in basal cell carcinomas in patients with germline BAP1 mutations. *Am J Clin Pathol.* 2015;143:901–904.
6. de la Fouchardiere A, Cabaret O, Savin L, et al. Germline BAP1 mutations predispose also to multiple basal cell carcinomas. *Clin Genet.* 2015;88:273–277.
7. Wadt KA, Aoude LG, Johansson P, et al. A recurrent germline BAP1 mutation and extension of the BAP1 tumor predisposition spectrum to include basal cell carcinoma. *Clin Genet.* 2015;88:267–272.
8. Kazakov DV, Vanecek T, Nemcova J, et al. Spectrum of tumors with follicular differentiation in a patient with the clinical phenotype of multiple familial trichoepitheliomas: a clinicopathological and molecular biological study, including analysis of the CYLD and PTCH genes. *Am J Dermatopathol.* 2009;31:819–827.
9. Kazakov DV, Schaller J, Vanecek T, et al. Brooke-Spiegler syndrome: report of a case with a novel mutation in the CYLD gene and different types of somatic mutations in benign and malignant tumors. *J Cutan Pathol.* 2010;37:886–890.
10. Kazakov DV, Vanecek T, Zelger B, et al. Multiple (familial) trichoepitheliomas: a clinicopathological and molecular biological study, including CYLD and PTCH gene analysis, of a series of 16 patients. *Am J Dermatopathol.* 2011;33:251–265.
11. Vanecek T, Halbhuber Z, Kacerovska D, et al. Large germline deletions of the CYLD gene in patients with Brooke-Spiegler syndrome and multiple familial trichoepithelioma. *Am J Dermatopathol.* 2014;36:868–874.
12. Sima R, Vanecek T, Kacerovska D, et al. Brooke-Spiegler syndrome: report of 10 patients from 8 families with novel germline mutations: evidence of diverse somatic mutations in the same patient regardless of tumor type. *Diagn Mol Pathol.* 2010;19:83–91.
13. Andrici J, Jung J, Sheen A, et al. Loss of BAP1 expression is very rare in peritoneal and gynecologic serous adenocarcinomas and can be useful in the differential diagnosis with abdominal mesothelioma. *Hum Pathol.* 2016;51:9–15.
14. Andrici J, Parkhill TR, Jung J, et al. Loss of expression of BAP1 is very rare in non-small cell lung carcinoma. *Pathology.* 2016;48:336–340.
15. Alakus H, Yost SE, Woo B, et al. BAP1 mutation is a frequent somatic event in peritoneal malignant mesothelioma. *J Transl Med.* 2015;13:122.
16. Andrici J, Goeppert B, Sioson L, et al. Loss of BAP1 expression occurs frequently in intrahepatic cholangiocarcinoma. *Medicine (Baltimore).* 2016;95:e2491.
17. Pena-Llopis S, Vega-Rubin-de-Celis S, Liao A, et al. BAP1 loss defines a new class of renal cell carcinoma. *Nat Genet.* 2012;44:751–759.
18. Minardi D, Lucarini G, Milanese G, et al. Loss of nuclear BAP1 protein expression is a marker of poor prognosis in patients with clear cell renal cell carcinoma. *Urol Oncol.* 2016;34:e11.
19. Piris A, Mihm MC Jr, Hoang MP. BAP1 and BRAFV600E expression in benign and malignant melanocytic proliferations. *Hum Pathol.* 2015;46:239–245.

56

1.1.3 SEBACEOUS TUMORS

In this part, we describe morphological and immunohistochemical characteristics of a group of lesions with sebaceous differentiation. In the first paper titled « *Sebaceous neoplasms with rippled, labyrinthine/sinusoidal, petaloid and carcinoid-like patterns: a study of 56 cases validating their occurrence as a morphological spectrum and showing no significant association with Muir-Torre syndrome or DNA mismatch repair protein deficiency*», the author studied sebaceomas and sebaceous carcinomas with an organoid pattern (rippled, labyrinthine/sinusoidal, carcinoid-like and petaloid). Sebaceoma is a rare benign sebaceous neoplasm that usually presents as a solitary, flesh-colored papule located mainly on the head and neck. It manifests histologically as a well-circumscribed tumor located in the dermis and composed mostly of immature, small, basophilic sebocytes with a variable admixture of mature sebocytes and sebaceous ducts. (35) Sebaceous carcinoma is a malignant sebaceous tumor occurring periorbital and in extraocular sites. It is composed of mature and immature sebaceous cells and shows all the attributes of a malignant tumor. (36) Some sebaceomas and rare sebaceous carcinomas have previously been shown to manifest organoid growth patterns, including 1) carcinoid-like (cellular trabeculae, ribbons, rosettes and pseudorosettes resembling carcinoid tumors (low-grade neuroendocrine carcinoma) of other sites, 2) labyrinthine/sinusoidal (complex, tortuous, intricate arrangement of cells in closely packed cords and strands showing sinusoidal-like spaces of stroma between them), 3) rippled (cells arranged in palisades with the formation of parallel rows resembling the Verocay bodies in schwannoma), and 4) petaloid (floral arrangement of neoplastic cells). (37), (38), (39), (40) It has been suggested that the above patterns may represent merely a variation of a single histopathological spectrum. The objectives of this study were to validate this proposition by studying a large number of cases, determine if there are specific associations with clinical features and if they have any association with Muir-Torre syndrome (MTS). Fifty-three sebaceomas and three sebaceous carcinomas from 35 males and 18 females were studied, ranging in age from 22 to 89 years (mean, 63 years). All patients presented with a solitary nodule, located on the head and neck area. Of the 56 tumors, 23 manifested a single growth pattern (carcinoid-like pattern was most frequent in this category), 23 had a combination of 2 patterns and ten a combination of 3 patterns (the labyrinthine/sinusoidal pattern was predominant in the "polypatterned" lesions). Immunohistochemically, MMR protein deficiency was detected in 3 of the 22 cases studied, while 5 of the 33 patients with available follow-up had an internal malignancy. We demonstrate that sebaceous neoplasms with organoid patterns are mostly benign lesions (sebaceomas) occurring in the elderly and showing a male predilection, with a striking predilection for the head and neck. In most cases, more than one of the organoid patterns are present. These lesions do not appear to be associated with internal malignancy or MMR deficiency in the majority of cases.

In the second article titled *«Squared-off nuclei and "appliqué" pattern as a histopathological clue to periocular sebaceous carcinoma: a clinicopathological study of 50 neoplasms from 46 patients. »,* the author examined 50 periocular sebaceous carcinomas from 46 patients to determine the frequency of two histological features seen in this neoplasm, namely cells

with squared-off nuclei and so-called "appliqué" pattern (peritumoral subnecrosis of peripherally located neoplastic cells). These features have never been emphasized upon in the previously published material. Periocular sebaceous carcinoma is a rare malignant tumor, usually affecting the elderly, mostly located on the eyelid and usually shows an aggressive behavior locally and metastasizes into regional lymph nodes and distant organs. (41), (42) The histopathological diagnosis of periocular sebaceous carcinoma can be difficult in poorly differentiated cases showing few mature sebocytes. We identified additional features that may aid in the diagnosis of periocular sebaceous carcinoma. Cells with "squared off" nuclei were found in all cases, independent from the degree of sebaceous differentiation. The "appliqué" pattern was found in a third of the cases. We concluded that both features taken together can serve as a quite characteristic, simple diagnostic clue for periocular sebaceous carcinomas, especially in a limited biopsy specimen.

Sebaceous Neoplasms With Rippled, Labyrinthine/Sinusoidal, Petaloid, and Carcinoid-Like Patterns: A Study of 57 Cases Validating Their Occurrence as a Morphological Spectrum and Showing No Significant Association With Muir–Torre Syndrome or DNA Mismatch Repair Protein Deficiency

Katharina Wiedemeyer, MD,* Liubov Kyrpychova, MD,†‡ Özlem Tanas Işikci, MD,§
Dominic V. Spagnolo, MBBS, FRCPA,¶‖ Heinz Kutzner, MD,** Arno Rütten, MD,**
Maria T. Fernandez-Figueras, MD, PhD,†† Natalja Denisjuk, MD,‡‡ Saul Suster, MD,§§
Michal Pavlovsky, MD,¶¶ Fredrik Petersson, MD, PhD,‖‖‖ Michal Michal, MD,†‡ Joyce Lee, MD,***
Katrin Kerl, MD,††† and Dmitry V. Kazakov, MD, PhD††††

Abstract: Sebaceous neoplasms with an organoid pattern (rippled, labyrinthine/sinusoidal, carcinoid-like, and petaloid) are rare. Previous studies suggested that the above patterns likely represent variations along a morphological continuum. The objectives of this study were to (1) validate this proposition by studying a large number of cases, (2) determine whether there are specific associations with clinical features, (3) establish their frequency, and (4) determine whether they have any association with Muir–Torre syndrome. Fifty-seven sebaceous neoplasms (54 sebaceomas and 3 sebaceous carcinomas) with organoid growth patterns were studied. These occurred in 36 men and 18 women (sex unknown in 3), with ages at diagnosis ranging from 22 to 89 years (mean, 63 years). All patients presented with a solitary nodule (mean size, 11 mm) on the head and neck area. Of the 57 tumors, 24 manifested a single growth pattern, 23 had a combination of 2 patterns, and 10 a combination of 3 patterns, indicating that these patterns are part of a morphological continuum of changes. The carcinoid-like pattern was the most frequent in the "monopatterned" neoplasms (13 cases), whereas the labyrinthine/sinusoidal pattern comprised most of the "polypatterned" lesions, in which various combinations occurred. Immunohistochemically, mismatch repair protein deficiency was detected in 3 of the 22 cases studied, whereas 5 of the 33 patients with available follow-up had an internal malignancy/premalignancy. In conclusion, sebaceous neoplasms with organoid growth patterns are predominantly sebaceomas having a predilection for the scalp, occurring as solitary lesions in elderly patients (male to female ratio of 2:1). Such patterns are expected to be found in a quarter of sebaceomas. In most cases, more than one of the organoid patterns is present. These lesions do not appear to be associated with internal malignancy or mismatch repair deficiency in most cases. However, confirmation of the absence of any significant association with Muir–Torre syndrome syndrome will require genetic studies.

Key Words: adnexal neoplasm, ripple pattern, sebaceoma, mismatch repair protein, Muir–Torre syndrome

(*Am J Dermatopathol* 2018;40:479–485)

INTRODUCTION

Sebaceoma is a benign sebaceous neoplasm that usually presents as a solitary, flesh-colored papule located mainly on the head and neck. It manifests histologically as a well-circumscribed, usually multinodular tumor located in the dermis and composed mostly of immature, small, basophilic sebocytes with a variable admixture of mature sebocytes and sebaceous ducts.[1] Sebaceous carcinoma is a malignant sebaceous tumor occurring periorbitally and in extraocular sites. It is composed of mature and immature sebaceous cells and shows all the attributes of a malignant

neoplasm (infiltrative growth, atypical mitoses, pleomorphism, necrosis en masse, etc.).[2–4]

Some sebaceomas and rare sebaceous carcinomas have been shown to manifest organoid growth patterns, including (1) carcinoid-like (cellular trabeculae, ribbons, rosettes, and pseudorosettes resembling carcinoid tumors [low-grade neuroendocrine carcinoma] of other sites), (2) labyrinthine/sinusoidal (complex, tortuous, and intricate arrangement of cells in closely packed cords and strands [labyrinthine] showing wider [sinusoidal-like] spaces of stroma between them), (3) rippled (cells arranged in palisades with the formation of parallel rows resembling the Verocay bodies in schwannoma), and (4) petaloid (floral arrangement of neoplastic cells) (Fig. 1).[5–13] These unusual patterns are seen in a minority of sebaceous lesions and may lead to misinterpretation of the neoplasms as trichoblastoma, basal cell carcinoma, or spiradenoma/cylindroma by the unaware.

Based on our previous studies of sebaceous lesions exhibiting these organoid patterns, we have suggested that the above patterns likely represent variations along a morphological continuum.[14] The objectives of this study were to (1) validate this proposition by studying a large number of cases, (2) determine whether there are specific associations with clinical features including age, sex, and location, (3) establish their frequency, and (4) determine whether they have any association with Muir–Torre syndrome (MTS; OMIM 158320). MTS is a phenotypic variant of hereditary nonpolyposis colorectal cancer syndrome (HNPCC; Lynch syndrome) caused by dominantly inherited mutations in the DNA mismatch repair (MMR) genes and defined by the coincidence of at least 1 cutaneous sebaceous neoplasm and at least 1 internal malignancy.

MATERIALS AND METHODS

Case Selection

Hematoxylin and eosin–stained slides from approximately 400 sebaceous neoplasms (sebaceoma and sebaceous carcinoma) retrieved from our consultation, institutional, and personal files were reviewed. Lesions with organoid patterns occurring in association with nevus sebaceus of Jadassohn were excluded.[15] A total of 57 neoplasms with organoid patterns were included, 17 of which have been the subject of 3 previous studies.[14,16,17] To be included in the study, at least a third of the tumor bulk needed to show at least 1 of the organoid patterns, irrespective of whether there was additionally any cohesive cellular growth. Clinical information and follow-up were obtained from the original pathology reports, submitting pathologists, and consulting physicians, and we specifically sought any personal or family history of internal malignancy.

Light Microscopic Studies

For each case, particular patterns (rippled, labyrinthine/sinusoidal, carcinoid-like, and petaloid) alone or in combination were documented, and the dominant pattern was also recorded. Features that may be found in sebaceous lesions associated with MTS (marked cystic change due to holocrine secretion, intratumoral mucin deposits, keratoacanthoma-like architecture, conspicuous intratumoral and peritumoral lymphocytes, and intertumoral and intratumoral heterogeneity) were evaluated.[3] Other features such as apocrine or follicular differentiation were also assessed.

Immunohistochemical Studies

In 22 cases with available tissue blocks, immunohistochemistry was performed using monoclonal antibodies

FIGURE 1. Carcinoid-like pattern refers to the arrangement of neoplastic cells as trabeculae, ribbons, rosettes, and pseudorosettes closely that the growth patterns found in carcinoids. Note a single mature sebocytes with a vacuolated cytoplasm (arrow) (A). The labyrinthine/sinusoidal pattern refers to an intricate, complex, and tortuous arrangement of closely packed strands and cords of neoplastic cells (labyrinthine), showing focally wider, sinusoidal spaces of stroma between the neoplastic elements (sinusoidal) (B). The rippled pattern is characterized by the arrangement of the neoplastic cells in palisades with the formation of parallel rows resembling a ripple or the Verocay bodies of schwannoma (C). The petaloid pattern petaloid is characterized by the floral arrangement of neoplastic cells (D).
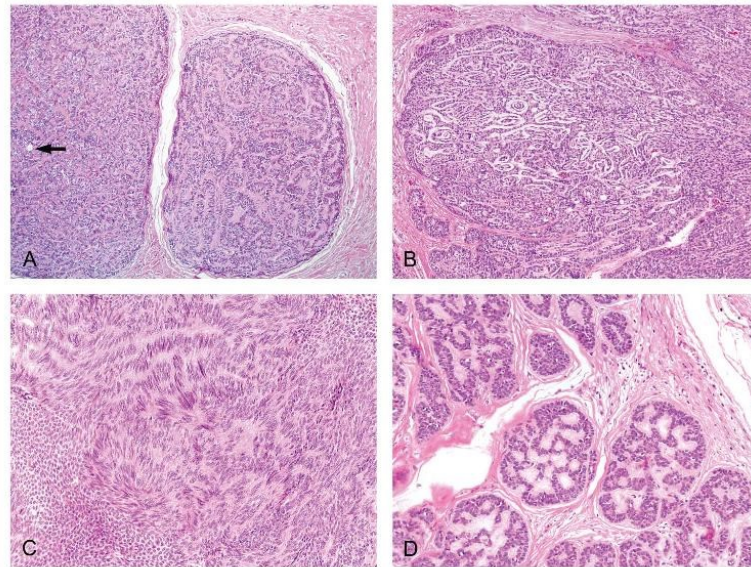
against DNA MMR proteins MSH2 (clone G219-1129, CELL MARQUE, Rocklin, CA), MSH6 (clone 44, Ventana, Tucson, AZ), MLH1 (clone G168-728, CELL MARQUE, Rocklin, CA), and PMS2 (clone EPR 3947, CELL MARQUE, Rocklin, CA). MMR deficiency was defined as a loss or marked reduction of 1 or more of the MMR proteins. Prospectively, in a subset of cases, staining for epithelial membrane antigen or adipophilin was performed to visualize mature sebocytes.

RESULTS

Clinical Data

There were 36 men and 18 women (sex unknown in 3), with ages ranging at diagnosis from 22 to 89 years (mean, 63 years). Clinically, all patients presented with a solitary nodule located on the head and neck areas, including the scalp (n = 37), nose (n = 6), cheek (n = 3), external ear (n = 1), external auditory canal (n = 1), forehead (n = 1), neck and head, and not specified (n = 2). The exact location was unknown in 5 cases. Tumor size ranged from 3 to 27 mm (mean, 11 mm) (Fig. 2). The clinical diagnoses included "nodule," lipoma, fibroma, dermatofibroma, and fibrous papule. Duration was specified in only 7 cases and ranged from 6 months to 3 years.

Family and personal medical histories and follow-up (range 6–329 months, mean 94 months) were obtained for 33 patients, of whom 28 had no evidence internal neoplasia. The 5 remaining patients had internal malignancy or premalignancy raising the possibility of MTS. These included (1) a 49-year-old woman with a history of 3 moderately dysplastic tubulovillous adenomas and a synchronous rectosigmoid adenocarcinoma which involved the bladder and vagina; (2) a 67-year-old man with a well-differentiated colorectal adenocarcinoma with lymph node metastasis 7 years later; (3) a 68-year old woman with a 9-year history of invasive ductal carcinoma of the breast with "fibrosarcomatous areas"; (4) a 41-year-old man who developed a low-grade urothelial carcinoma of the urinary bladder 3 years after a diagnosis of

FIGURE 2. Sebaceoma. The patient is a 31-year-old Chinese man with a skin colored nodule with overlying telangiectasia measuring 1.4 × 1.2 cm over his left temporal region for 2–3 years.

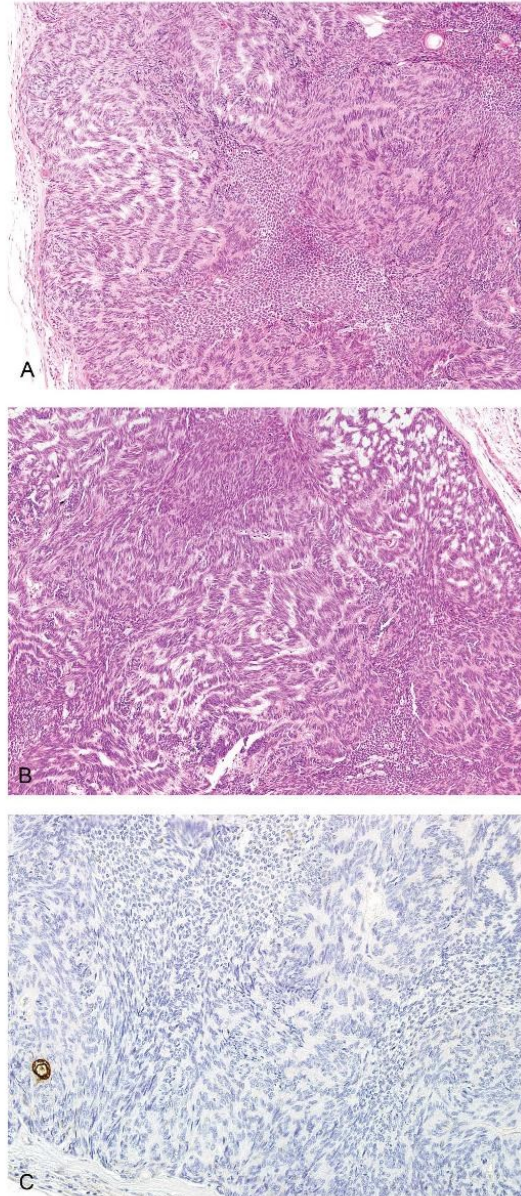sebaceoma; and (5) and a 81-year-old man with 2 moderately dysplastic colonic tubular adenomas.

One patient additionally gave a history of a cutaneous squamous cell carcinoma on the thigh. All sebaceous neoplasms were surgically removed. In only 1 patient did a 2 cm sebaceoma recur at the same location on the scalp after 82 months. Local recurrence after 6 years was also seen in a patient with a sebaceous carcinoma, as previously reported by us.[14]

Histopathological Findings

Of the 57 neoplasms, 54 were classified as sebaceoma and 3 as low-grade sebaceous carcinoma (cases 1–3 in reference 14). All sebaceomas were well circumscribed and composed of multiple, variably sized nodules with smooth borders enveloped by compressed fibrous tissue. Monomorphic basaloid cells with scanty cytoplasm (immature sebocytes) predominated, admixed with mature sebocytes having vacuolated cytoplasm, and scalloped nuclei. Of the 57 tumors, 24 manifested a single organoid growth pattern, 23 a combination of 2 patterns, and the remaining 10 a combination of 3 patterns. The carcinoid-like pattern was the most common in the "monopatterned" neoplasms (13 cases), followed by the labyrinthine/sinusoidal pattern (7 cases), and the rippled pattern (4 cases). No case displayed an entirely petaloid pattern.

Of the 23 lesions with 2 patterns, the combination of labyrinthine/sinusoidal and carcinoid-like patterns was the most common (13 cases). A combination of labyrinthine/sinusoidal, rippled, and carcinoid-like patterns was the most commonly seen (6 cases) in lesions with 3 patterns (Table 1). No lesion showed a combination of all 4 patterns (Figs. 2–5).

With respect to the predominant pattern in "polypatterned" lesions, the labyrinthine/sinusoidal dominated in 18/33 cases, followed by the carcinoid-like (7/33) and rippled patterns (6/33).

By definition, the above patterns comprised the major part of the tumor in each case; however, minor areas with cohesive growth of immature sebocytes were often seen.

None of the lesions revealed features that are often encountered in MTS-associated tumors, such as cystic alterations due to excessive holocrine secretion, keratoacanthoma-like architecture, numerous intratumoral and peritumoral lymphocytes, and prominent intratumoral heterogeneity. Focal inconspicuous cystic change and scarce intratumoral and peritumoral lymphocytes were seen in 3 cases each. These features were even absent in tumors from patients with a history internal malignancy or whose sebaceous neoplasms were MMR deficient.

Infundibulocystic structures were recognized in 10 sebaceomas and were accompanied by marked squamous metaplasia in 6, as reported elsewhere.[17] Four tumors showed focal apocrine glandular differentiation in the form of simple round or elongated tubules (scattered or grouped) lined by a row of cuboidal to columnar cells having eosinophilic cytoplasm. Focally, a peripheral layer of small cells resembling basal/myoepithelial cells of normal eccrine and apocrine glands could be discerned around some glands. In 1 case, this layer appeared hyperplastic, with 2 or more rows of cells that could even form small islands. These changes, reminiscent of

TABLE 1. Main Clinicopathological Data

	Frequency
Clinical data	
Gender distribution	
Male	36
Female	18
Unknown	3
Age, yrs	
Range	22–89
Mean	63
Median	67
Size, mm	
Range	3–27
Mean	11
Median	10
Location	
Scalp	37
Nose	6
Cheek	3
Other parts of head/neck area	6
Unknown	5
Association with internal malignancy	5 of 33 with follow-up
Histopathological data	
Sebaceoma versus carcinoma	54:3
"Monopatterned" lesions	24 of 57
Carcinoid-like only	13
Labyrinthine/sinusoidal only	7
Rippled only	4
Petaloid only	0
Two pattern combination	23 of 57
Labyrinthine/sinusoidal + carcinoid-like	13
Labyrinthine/sinusoidal + rippled	6
Labyrinthine/sinusoidal + petaloid	2
Carcinoid-like + petaloid	1
Carcinoid-like + rippled	1
Three pattern combination	10 of 57
Labyrinthine/sinusoidal + carcinoid-like + rippled	6
Labyrinthine/sinusoidal + carcinoid-like + petaloid	4
Predominant pattern in 33 "polypatterned" lesions	
Labyrinthine/sinusoidal	18
Carcinoid-like	7
Rippled	6
Petaloid	2
MMR protein deficiency	3 of 22 studied

FIGURE 3. Sebaceoma with a predominant rippled pattern (A) and with focal areas corresponding to the labyrinthine/sinusoidal area (B). The mature sebocytes stained for epithelial membrane antigen (EMA) (C).

basal cell hyperplasia in the prostate, we have reported previously.[16]

Immunohistochemical Findings

Of the 22 tumors studied, 2 sebaceomas showed reduced MSH6 expression but neither patient had any
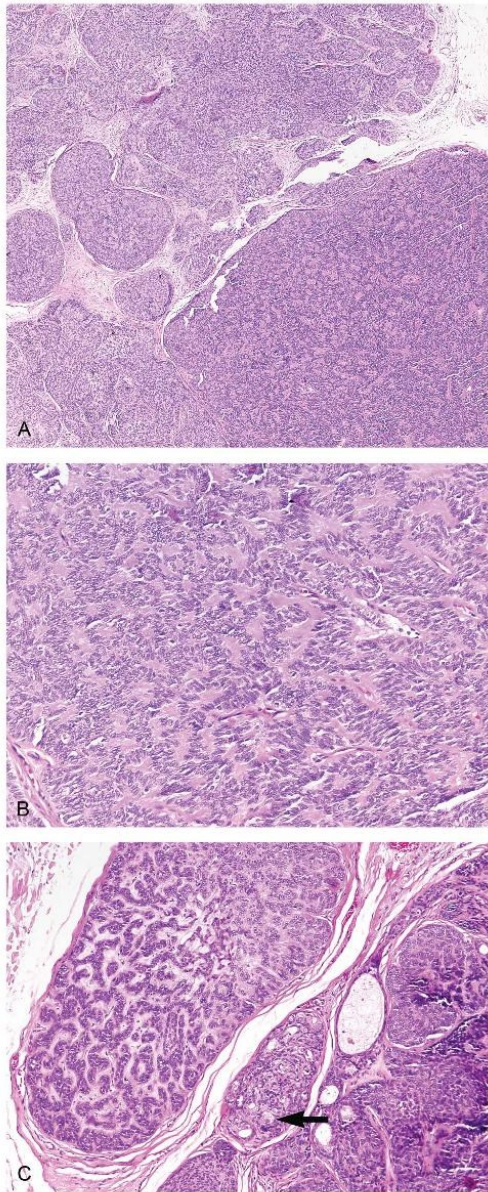
FIGURE 4. Carcinoid-like pattern with conspicuous pseudorosettes (A), which on close inspection are formed by spindled cells that additionally focally are arranged in a parallel row like that seen in the rippled pattern (B). There are also areas with labyrinthine/sinusoidal arrangement of the neoplastic cells with recognizable matures sebocytes (arrow) in the adjacent areas (C).

clinical manifestations or history to suggest MTS. In 1 neoplasm, there was reduced expression of MLH1 and PMS2; this tumor occurred in the patient with a history of 2 moderately dysplastic colonic tubular adenomas (see above). No MMR protein deficiency was detected in the remaining 19 neoplasms.

DISCUSSION

Our study shows that sebaceous neoplasms with organoid patterns are mostly benign lesions (sebaceomas) that have a striking predilection for the head and neck, preferentially involving the scalp, occurring in the elderly and showing a male predilection (2:1). These clinical data are in line with the largest (at that time) series of rippled pattern sebaceoma (21 cases) by Ansai and Kimura who found the same gender/anatomic distribution and a similar frequency (approximately 26%) of organoid patterns in sebaceoma.[8]

A majority of the lesions manifested a combination of 2 or 3 organoid patterns, supporting the idea that all these patterns are part of a morphological continuum of changes. A combination of several patterns can be recognized in the illustrations accompanying previously published articles, even those describing "monopatterned" lesions. For example, in Figure 1 in the study of Ansai and Kimura[8] illustrating a rippled sebaceoma, 1 can clearly recognize rosettes and pseudorosettes (carcinoid-like pattern) and a hint of labyrinthine/sinusoidal patterns. Nuances of pattern interpretation are not unexpected between observers. Identical patterns have been described as zebra-like, reticulated, organoid, and retiform by others.[18,19]

Any association of sebaceous neoplasms with organoid patterns and MTS has not always been specifically examined in previously published material, although it seems that the syndromic association has so far not been reported. Of the 33 patients with available follow-up and medical history, 5 (15%) have been known to have malignant or premalignant lesions, which meets the clinical definition of MTS. In 1, the tumor proved to be MMR protein deficient on immunohistochemistry. The main limitation in our study was, however, that peripheral blood was not available; hence, analysis of gemline mutations of MMR genes could not be performed to confirm MTS. The lesions did not reveal any of the typical histological features seen in sebaceous tumors occurring in the setting of MTS (ie, cystic changes, keratoacanthoma-like architecture, mucin deposits, etc.). Further investigations into any possible syndromic association utilizing molecular biological studies are warranted, albeit, at present, one can safely conclude that in most cases, a sebaceous neoplasm with organoid patterns is not predictive of MTS.

The difficulty of making the distinction between benign and malignant sebaceous neoplasms in some instances has been stressed by several authors.[20–22] An overwhelming majority of cases in our series were sebaceomas, 2 lesions were low-grade sebaceous carcinomas, and in a further case, the distinction between benign sebaceoma and sebaceous carcinoma was difficult. In this last case, although the architecture was benign, and the tumor was well circumscribed composed mainly of regular small basaloid cells without
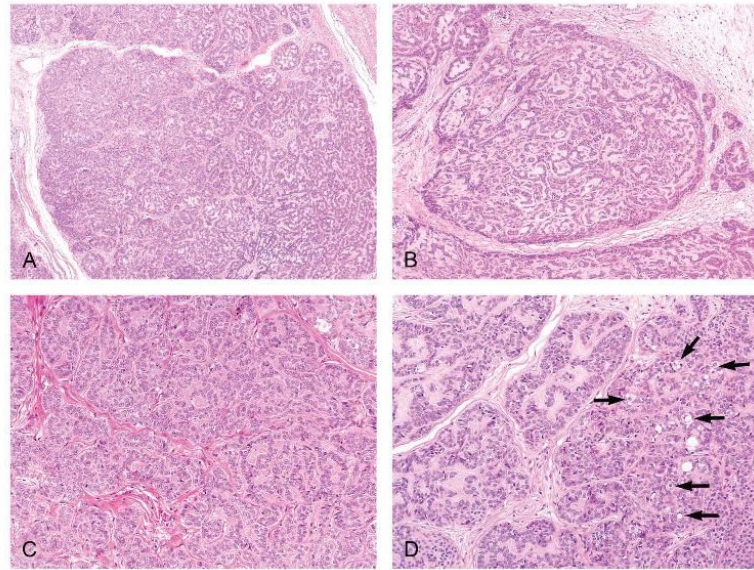
FIGURE 5. Case with a predominant petaloid pattern (A), showing in addition areas labyrinthine/sinusoidal (B), and carcinoid-like areas (C), with occasional mature sebocytes (arrows) (D).

significant mitotic activity, focal areas showed highly pleomorphic cells with atypical mitoses, these features perhaps favoring a carcinoma. The follow-up of this patient did not reveal recurrent or metastatic disease (range 6–329 months, mean 94 months), nor did the patient meet criteria for MTS (thus far). Such borderline cases have been described in the setting of MTS, but these lacked any organoid patterns as described here.[21] Recently, a case of putative sebaceous carcinoma ex sebaceoma with rippled and carcinoid-like patterns has been reported.[13]

Despite the fact that rippled and labyrinthine/sinusoidal patterns in sebaceous lesions were recognized as long as 15 years ago, and occur in a quarter of them, these and other organoid patterns seem to be underrecognized and misinterpreted, even in the literature, especially as trichoblastoma.[5,23–27] This is likely explained by the fact that sebaceomas manifesting organoid patterns usually show a paucity of mature sebocytes, especially in the rippled pattern. Several published examples of the so-called rippled trichoblastoma are clearly sebaceomas. The differential diagnosis of sebaceoma and trichoblastoma should be straightforward in an adequate biopsy specimen because trichoblastoma is a biphasic neoplasm composed of follicular germinative cells and a specific follicular stroma. The latter is never encountered in sebaceoma. Besides, follicular germinative cells in trichoblastoma are positive for Ber-Ep4, whereas immature sebocytes are not. Basal cell carcinoma may also be a differential diagnostic consideration when it shows sebaceous differentiation and/or focally displays cellular arrangements resembling the organoid patterns herein described. Recognition of conventionally appearing areas with stromal clefts filled with mucin, peripheral palisading, and positive immunoreaction for Ber-Ep4 are clues for basal cell carcinoma. Sebaceoma with numerous infundibulocystic structures (and also prominent squamous metaplasia) should not be misinterpreted as trichoadenoma or even microcystic adnexal carcinoma, particularly in a small biopsy specimen, as discussed elsewhere.[17] Sebaceomas with a carcinoid-like appearance are easily distinguished from true carcinoid tumors, which usually represent metastases from an internal malignancy; existence of true primary cutaneous carcinoids reported in the literature is a matter of debate. Neuroendocrine markers are a reliable tool to identify carcinoids and distinguish them from sebaceous tumors and from rare melanomas with a carcinoid-like pattern.[28–34]

Four sebaceomas in our series manifested focal apocrine glandular differentiation in the form of glands of various complexities. This feature has been previously described in sebaceomas with organoid patterns and in cases lacking such differentiation.[16,35] A combination of sebaceous, apocrine, and follicular differentiation is an expected feature in cutaneous adnexal neoplasms considering normal embryology and has been described in a variety of adnexal lesions.[36–47]

In conclusion, sebaceous neoplasms with organoid growth patterns are predominantly sebaceomas having a predilection for the scalp, occurring as solitary lesions in elderly patients, with a male to female ratio of 2:1. Such patterns are expected to be found in a quarter of sebaceomas. In most cases, more than 1 of the organoid patterns is present. Mature sebocytes may be inconspicuous in these lesions, requiring distinction from other cutaneous adnexal neoplasms. However, these patterns per se may serve as a clue to sebaceous differentiation. These lesions do not seem to be associated with internal malignancy or MMR deficiency in most cases. However, confirmation of the absence of any significant association with MTS will require genetic studies.

REFERENCES

1. Troy JL, Ackerman AB. Sebaceoma. A distinctive benign neoplasm of adnexal epithelium differentiating toward sebaceous cells. *Am J Dermatopathol.* 1984;6:7–13.
2. Rulon DB, Helwig EB. Cutaneous sebaceous neoplasms. *Cancer.* 1974;33:82–102.
3. Kazakov DV, Michal M, Kacerovska D, et al. Cutaneous adnexal tumors outside the skin. *Am J Dermatopathol.* 2011;33:303–315.
4. Steffen C, Ackerman AB. *Neoplasms With Sebaceous Differentiation.* Philadelphia, PA: Lea & Febiger; 1994:1994.
5. Ohata C, Ackerman AB. "Ripple pattern" in a neoplasm signifies sebaceous differentiation [sebaceoma (not trichoblastoma or trichomatricoma) if benign and sebaceous carcinoma if malignant]. *Dermatopathol Prac Conc.* 2001;7:355–362.
6. Nielsen TA, Maia-Cohen S, Hessel AB, et al. Sebaceous neoplasm with reticulated and cribriform features: a rare variant of sebaceoma. *J Cutan Pathol.* 1998;25:233–235.
7. Kazakov DV, Spagnolo DV, Kacerovska D, et al. Unusual patterns of cutaneous sebaceous neoplasms. *Diagn Histopathol.* 2010;16:425–431.
8. Ansai S, Kimura T. Rippled-pattern sebaceoma: a clinicopathological study. *Am J Dermatopathol.* 2009;31:364–366.
9. Kiyohara T, Kumakiri M, Kuwahara H, et al. Rippled-pattern sebaceoma: a report of a lesion on the back with a review of the literature. *Am J Dermatopathol.* 2006;28:446–448.
10. Kawakami Y, Ansai S, Nakamura-Wakatsuki T, et al. Case of rippled-pattern sebaceoma with clinically yellowish surface and histopathological paucity of lipid-containing neoplastic cells. *J Dermatol.* 2012;39:644–646.
11. Kurokawa I, Nishimura K, Hakamada A, et al. Rippled-pattern sebaceoma with an immunohistochemical study of cytokeratins. *J Eur Acad Dermatol Venereol.* 2007;21:133–134.
12. Nomura M, Tanaka M, Nunomura M, et al. Dermoscopy of rippled pattern sebaceoma. *Dermatol Res Pract.* 2010;2010:140486.
13. Misago N, Toda S. Sebaceous carcinoma within rippled/carcinoid pattern sebaceoma. *J Cutan Pathol.* 2016;43:64–70.
14. Kazakov DV, Kutzner H, Rutten A, et al. Carcinoid-like pattern in sebaceous neoplasms: another distinctive, previously unrecognized pattern in extraocular sebaceous carcinoma and sebaceoma. *Am J Dermatopathol.* 2005;27:195–203.
15. Kazakov DV, Calonje E, Zelger B, et al. Sebaceous carcinoma arising in nevus sebaceus of Jadassohn: a clinicopathological study of five cases. *Am J Dermatopathol.* 2007;29:242–248.
16. Kazakov DV, Calonje E, Rutten A, et al. Cutaneous sebaceous neoplasms with a focal glandular pattern (seboapocrine lesions): a clinicopathological study of three cases. *Am J Dermatopathol.* 2007;29:359–364.
17. Flux K, Kutzner H, Rutten A, et al. Infundibulocystic structures and prominent squamous metaplasia in sebaceoma-a rare feature. A clinicopathologic study of 10 cases. *Am J Dermatopathol.* 2016;38:678–682.
18. LeBoit PE, Burg G, Weedon D, et al. *World Health Organization Classification of Tumours. Pathology and Genetics of Skin Tumours.* Lyon, France: IARC Press; 2006:2006.
19. McKee PH, Calonje E, Granter SR. *Pathology of the Skin With Clinical Correlations.* 3rd ed. Philadelphia, PA: Elsevier Mosby; 2005.
20. Kazakov DV, Kutzner H, Spagnolo DV, et al. Discordant architectural and cytological features in cutaneous sebaceous neoplasms–a classification dilemma: report of 5 cases. *Am J Dermatopathol.* 2009;31:31–36.
21. Misago N, Narisawa Y. Sebaceous neoplasms in Muir-Torre syndrome. *Am J Dermatopathol.* 2000;22:155–161.
22. Misago N, Mihara I, Ansai S, et al. Sebaceoma and related neoplasms with sebaceous differentiation: a clinicopathologic study of 30 cases. *Am J Dermatopathol.* 2002;24:294–304.
23. Akasaka T, Imamura Y, Mori Y, et al. Trichoblastoma with rippled-pattern. *J Dermatol.* 1997;24:174–178.
24. Graham BS, Barr RJ. Rippled-pattern sebaceous trichoblastoma. *J Cutan Pathol.* 2000;27:455–459.
25. Hashimoto K, Prince C, Kato I, et al. Rippled-pattern trichomatricoma. Histological, immunohistochemical and ultrastructural studies of an immature hair matrix tumor. *J Cutan Pathol.* 1989;16:19–30.
26. Swick BL, Baum CL, Walling HW. Rippled-pattern trichoblastoma with apocrine differentiation arising in a nevus sebaceus: report of a case and review of the literature. *J Cutan Pathol.* 2009;36:1200–1205.
27. Yamamoto O, Hisaoka M, Yasuda H, et al. A rippled-pattern trichoblastoma: an immunohistochemical study. *J Cutan Pathol.* 2000;27:460–465.
28. Santi R, Massi D, Mazzoni F, et al. Skin metastasis from typical carcinoid tumor of the lung. *J Cutan Pathol.* 2008;35:418–422.
29. Dijk CV, Ten Seldam RE. A possible primary cutaneous carcinoid. *Cancer.* 1975;36:1016–1020.
30. Smith PA, Chappell RH. Another possible primary carcinoid tumour of skin? *Virchows Arch A Pathol Anat Histopathol.* 1985;408:99–103.
31. Collina G, Quarto F, Eusebi V. Trabecular carcinoid of the skin with cellular stroma. *Am J Dermatopathol.* 1988;10:430–435.
32. Bart RS, Kamino H, Waisman J, et al. Carcinoid tumor of skin: report of a possible primary case. *J Am Acad Dermatol.* 1990;22:366–370.
33. Sakamoto F, Ito M, Matumura G, et al. Ultrastructural study of a mucinous carcinoid of the skin. *J Cutan Pathol.* 1991;18:128–133.
34. Kacerovska D, Michal M, Sosna B, et al. Carcinoid-like pattern in melanoma: report of 4 cases. *Am J Dermatopathol.* 2009;31:542–550.
35. Misago N, Narisawa Y. Sebaceous carcinoma with apocrine differentiation. *Am J Dermatopathol.* 2001;23:50–57.
36. Requena L, Kiryu H, Ackerman AB. *Neoplasms With Apocrine Differentiation.* Philadelphia, PA: Lippincott-Raven; 1998.
37. Kazakov DV, Belousova IE, Bisceglia M, et al. Apocrine mixed tumor of the skin ("mixed tumor of the folliculosebaceous-apocrine complex"). Spectrum of differentiations and metaplastic changes in the epithelial, myoepithelial, and stromal components based on a histopathologic study of 244 cases. *J Am Acad Dermatol.* 2007;57:467–483.
38. Nakhleh RE, Swanson PE, Wick MR. Cutaneous adnexal carcinomas with divergent differentiation. *Am J Dermatopathol.* 1990;12:325–334.
39. LeBoit PE, Parslow TG, Choy SH. Hair matrix differentiation. Occurrence in lesions other than pilomatricoma. *Am J Dermatopathol.* 1987;9:399–405.
40. Kazakov DV, Kacerovska D, Michal M. Microcystic adnexal carcinoma with multiple areas of follicular differentiation toward germinative cells and specific follicular stroma (trichoblastomatous areas). *Am J Dermatopathol.* 2011;33:e47–e49.
41. McCalmont TH. A call for logic in the classification of adnexal neoplasms. *Am J Dermatopathol.* 1996;18:103–109.
42. Kazakov DV, Kutzner H, Spagnolo DV, et al. Sebaceous differentiation in poroid neoplasms: report of 11 cases, including a case of metaplastic carcinoma associated with apocrine poroma (sarcomatoid apocrine porocarcinoma). *Am J Dermatopathol.* 2008;30:21–26.
43. Gianotti R, Coggi A, Alessi E. Poral neoplasm with combined sebaceous and apocrine differentiation. *Am J Dermatopathol.* 1998;20:491–494.
44. Kazakov DV, Mukensnabl P, Michal M. An unusual hamartoma of the folliculosebaceous-apocrine unit: a case report. *J Cutan Pathol.* 2006;33:365–368.
45. Sanchez Yus E, Requena L, Simon P, et al. Complex adnexal tumor of the primary epithelial germ with distinct patterns of superficial epithelioma with sebaceous differentiation, immature trichoepithelioma, and apocrine adenocarcinoma. *Am J Dermatopathol.* 1992;14:245–252.
46. Wong TY, Suster S, Cheek RF, et al. Benign cutaneous adnexal tumors with combined folliculosebaceous, apocrine, and eccrine differentiation. Clinicopathologic and immunohistochemical study of eight cases. *Am J Dermatopathol.* 1996;18:124–136.
47. Kazakov DV, Soukup R, Mukensnabl P, et al. Brooke-Spiegler syndrome: report of a case with combined lesions containing cylindromatous, spiradenomatous, trichoblastomatous, and sebaceous differentiation. *Am J Dermatopathol.* 2005;27:27–33.

Squared-Off Nuclei and "Appliqué" Pattern as a Histopathological Clue to Periocular Sebaceous Carcinoma: A Clinicopathological Study of 50 Neoplasms From 46 Patients

Sigrid M. C. Broekaert, MD,* Katharina Flux, MD,† Liubov Kyrpychova, MD,‡
Denisa Kacerovska, MD, PhD,‡§ Doina Ivan, MD,¶ Michael P. Schön, MD,* Philipp Ströbel, MD,‖
Michal Michal, MD,‡ Natalja Denisjuk, MD,** Katrin Kerl, MD,†† and Dmitry V. Kazakov, MD, PhD‡††

Abstract: The histopathological diagnosis of periocular sebaceous carcinoma can be difficult in poorly differentiated cases showing few mature sebocytes. The authors examined 50 periocular sebaceous carcinomas from 46 patients to determine the frequency of 2 features seen in this neoplasm, namely cells with squared-off nuclei and so-called "appliqué" pattern (peritumoral subnecrosis of peripherally located neoplastic cells). Neoplastic cells with squared-off nuclei were found in varying numbers in both the intraepithelial and dermal (invasive) components in all neoplasms, whereas the appliqué pattern was observed in a third of the cases. It is concluded that these features, taken together, may serve as a clue for the diagnosis of periocular sebaceous carcinoma.

Key Words: sebaceous carcinoma, periocular, eyelid, sebaceous differentiation, squared-off nuclei, necrosis, appliqué pattern

(Am J Dermatopathol 2017;39:275–278)

INTRODUCTION

Periocular sebaceous carcinoma is a rare malignant tumor, usually affecting the elderly, mostly located on the eyelid, where most neoplasms originate from the meibomian gland. In contrast to its extraocular counterpart, periocular sebaceous carcinoma usually shows an aggressive behavior locally and metastasizes into regional lymph nodes and distant organs, most commonly the lung, liver, bone, and brain. Periocular sebaceous carcinoma can simulate various inflammatory conditions clinically and may cause diagnostic problems histologically, as unequivocal sebaceous differentiation is often absent or difficult to recognize, especially in a limited biopsy specimen, often leading to an unfavorable delay of the final diagnosis.[1–8]

In our practice, we have often observed in periocular sebaceous carcinomas features resembling those seen in germ cell tumors (classical seminoma, embryonal carcinoma, or choriocarcinoma), namely "squared-off" or angulated nuclei and so-called "appliqué" pattern due to (sub)necrosis of peripherally located tumor cells in solid aggregations of neoplastic cells.[9,10] The aforementioned features often served as a clue, forcing, when recognized, a meticulous search for areas with sebaceous differentiation in poorly differentiated neoplasms. The purpose of this study was to establish the frequency of squared-off nuclei and appliqué pattern in a large series of periocular sebaceous carcinoma.

MATERIALS AND METHODS

Fifty periocular sebaceous carcinomas from 46 patients were retrieved from our consultation, institutional, and personal files and reviewed to confirm the diagnosis and appropriate clinicopathological context. The clinical data were extracted from original pathological reports and referring pathologists. Only excisional biopsies of tumors were included; diagnostic biopsies were not studied. In 2 cases, the primary tumor and a recurrent neoplasm were available for review, and in another patient the primary tumor and 2 subsequent recurrences were analyzed. The study was based solely on light microscopy of hematoxylin and eosin–stained slides but prospectively, immunohistochemistry (epithelial membrane antigen and/or adipophilin) was performed in 32 cases, and additionally in 4 cases histochemistry (oil red O-staining) were carried out. We documented the presence of cells with squared-off nuclei in the intraepithelial (conjunctiva, epidermis, and sebaceous glands) and intradermal components and examined the peripheral parts of tumor aggregates to find peripheral (sub)necrosis of the neoplastic cells (appliqué pattern).

RESULTS

Clinical Data

The cohort included 27 women and 17 men (gender was unknown in 2 cases), ranging in age at diagnosis from 24 to 92 years (median: 70 years). Locations included the upper eyelid (n = 20), lower eyelid (n = 14), eyelid, not specified (n = 5), perirobital/periocular areas (n = 3), caruncle (n = 2), and conjunctiva (n = 1). Additionally, in 3 patients, both the upper and lower eyelids were involved, 2 of whom presented with primary disease, and in the remaining patient involvement of both eyelids occurred during a second recurrence of the neoplasm that also extended into the orbita.

Histopathological Findings

Of the 50 neoplasms, 48 represented invasive carcinomas, whereas 2 were in situ lesions. The neoplasms were composed of small to large pleomorphic basaloid cells with

FIGURE 1. Periocular sebaceous carcinoma with neoplastic cells having pale vesicular nuclei with prominent nuclear membranes containing multiple squared-off/angulated nuclei (arrows) (A). The size of the nuclei varies and some cells are in close apposition (back to back, arrows) (B). Note also the peripheral cell necrosis (asterisks) (B).

varying degrees of sebaceous differentiation identified by cells with multiple intracytoplasmic vacuoles with scalloped nuclei. Some lesions manifested rather pale vesicular nuclei. Marked nuclear pleomorphism, bizarre cells, and plentiful atypical mitoses were also seen.

Cells with squared-off or angulated nuclei were detected in all tumor specimens (100%), either as single cells or lying in clusters, sometimes "back to back." The latter were usually seen in lesions with neoplastic cells having vesicular pale nuclei, in which the squared-off/angulated nuclei could generally be identified more easily (Figs. 1A, B). In tumors mostly composed of basaloid immature sebaceous cells, identification of cells with squared-off nuclei required a meticulous search (Fig. 2).

Of the 50 specimens, 42 cases contained epithelial parts (epidermis, conjunctival, or sebaceous glands), and the epithelial component was involved in 22 lesions (52.4%), with all cases showing occasional neoplastic cells with squared-off nuclei. Overall, the intradermal (invasive) component contained more cells with squared-off nuclei compared with the intraepithelial component (Fig. 3). Cells with squared-off nuclei were usually either devoid of intracytoplasmic fat vacuoles or contained few of them or even a single intracytoplasmic vacuole (Fig. 4).

The appliqué pattern was identified in 16 of the 50 lesions (32%), and this alteration was always present in the dermal invasive component of the neoplasms. The extent of this feature varied from only occasional neoplastic nodules with peripheral cell (sub)necrosis to rare lesions where most neoplastic cell aggregations displayed it (Figs. 1B, 5).

DISCUSSION

We have studied 50 tumors of periocular sebaceous carcinoma and found cells with squared-off nuclei in all cases, independent from the degree of sebaceous differentiation. The number of cells varied from case to case, and in tumors with pale vesicular nuclei and conspicuous nuclear
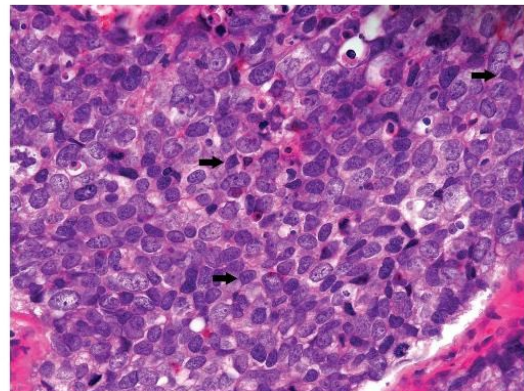

FIGURE 2. A neoplasm mainly composed of basaloid immature sebaceous cells. Cells with squared-off/angulated nuclei is more difficult to detect in such lesions.

67
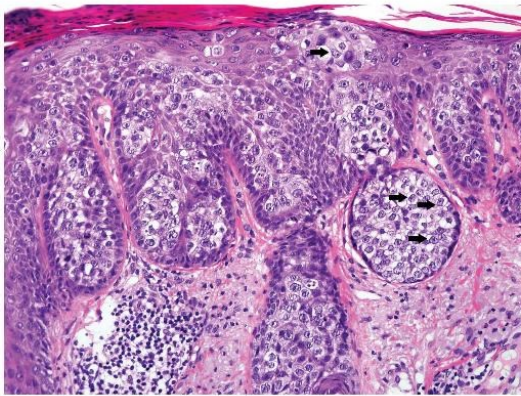
FIGURE 3. Sebaceous carcinoma with a prominent intra-epithelial spread of neoplastic cells with numerous cells with squared-off nuclei (arrows).

membranes, the angulated shape was detected more easily, wherein clusters of neoplastic cells with squared-off nuclei occurred. These cells were present both in the invasive parts of the neoplasm and in the intraepithelial portions, albeit in the latter location they were a less conspicuous feature.

The appliqué pattern was found in a third of the cases examined (16 of 50 cases) and appeared to be less specific. Although we did not formally study a control group, we observed on occasion in the past peripheral cell (sub)necrosis in some other tumor types composed of basaloid cells, for example, in Merkel cell carcinoma. Taken together, however, we suggest that both features can serve as a quite characteristic, simple diagnostic clue for periocular sebaceous carcinomas, especially in a limited biopsy specimen where mature sebocytes may be absent, thus limiting also the usage of immunohistochemical staining with epithelial membrane antigen and adipophilin that label only mature sebaceous cells. In the
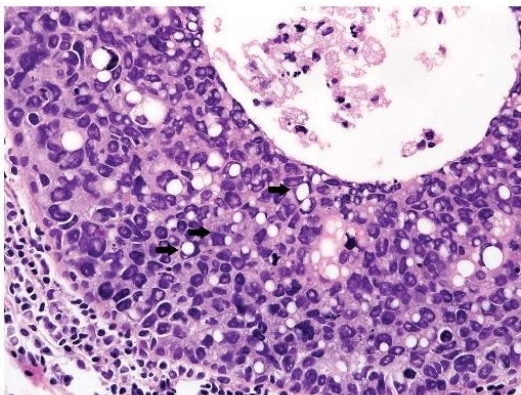
FIGURE 4. Cells with squared-off nuclei containing fat vacuoles (arrows).
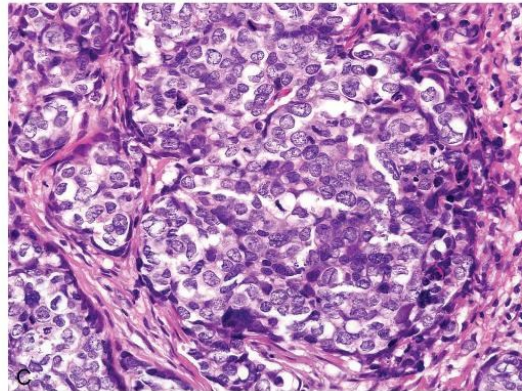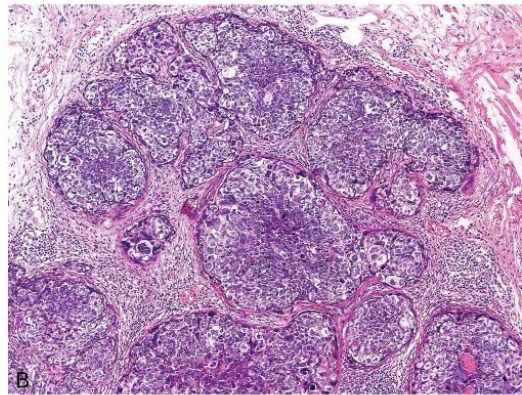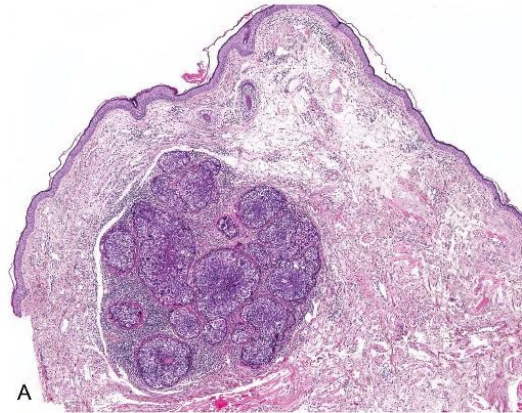
FIGURE 5. Periocular sebaceous carcinoma with the appliqué pattern seen in every tumor nodules (A and B). Note karyopyknosis and karyorrhexis of the neoplastic cells at the periphery of the neoplastic nodules (C).

authors' experience, cells with squared-off nuclei are some-times easier to identify on hematoxylin and eosin–stained slides than mature sebocytes with intracytoplasmic vacuoles.

In conclusion, neoplastic sebocytes with squared-off nuclei are a common feature in periocular sebaceous carci-nomas, which can serve as a diagnostic clue. The appliqué pattern less common but seen in combination with squared-off/angulated cells should prompt a search for signs of mature sebaceous differentiation in undifferentiated tumors located in the periocular area.

REFERENCES

1. Deprez M, Uffer S. Clinicopathological features of eyelid skin tumors. A retrospective study of 5504 cases and review of literature. *Am J Derma-topathol*. 2009;31:256–262.
2. Shields JA, Demirci H, Marr BP, et al. Sebaceous carcinoma of the eyelids: personal experience with 60 cases. *Ophthalmology*. 2004;111: 2151–2157.
3. Shields JA, Demirci H, Marr BP, et al. Sebaceous carcinoma of the ocular region: a review. *Surv Ophthalmol*. 2005;50:103–122.
4. Honavar SG, Shields CL, Maus M, et al. Primary intraepithelial seba-ceous gland carcinoma of the palpebral conjunctiva. *Arch Ophthalmol*. 2001;119:764–767.
5. Rao NA, Hidayat AA, McLean IW, et al. Sebaceous carcinomas of the ocular adnexa: a clinicopathologic study of 104 cases, with five-year follow-up data. *Hum Pathol*. 1982;13:113–122.
6. Ni C, Searl SS, Kuo PK, et al. Sebaceous cell carcinomas of the ocular adnexa. *Int Ophthalmol Clin*. 1982;22:23–61.
7. Jakobiec FA, Zimmerman LE, La Piana F, et al. Unusual eyelid tumors with sebaceous differentiation in the Muir-Torre syndrome. Rapid clin-ical regrowth and frank squamous transformation after biopsy. *Ophthal-mology*. 1988;95:1543–1548.
8. Doxanas MT, Green WR. Sebaceous gland carcinoma. Review of 40 cases. *Arch Ophthalmol*. 1984;102:245–249.
9. Ulbright TM, Amin MB, Young RH. *Tumors of the Testis, Adnexa, Spermatic Cord, and Scrotum*. Washington, DC: AFIP; 1999.
10. Kazakov DV, Michal M, Kacerovska D, et al. *Cutaneous Adnexal Tumors*. Philadelphia, USA: LWW; 2012:814.

69

1.2 LESIONS OF ANOGENITAL MAMMARY-LIKE GLANDS

Anogenital mammary-like glands (AGMLG) have long been regarded as ectopic or supernumerary breast tissue, but are now considered a normal constituent of the anogenital area. AGMLG are not visible clinically, but they are often found incidentally in pathological specimens from the anogenital region. They mainly located in the sulcus between the labia minora and labia majora. (43), (44) Although lesions affecting AGMLG are rare, they are of clinical importance because they are suggested to be the origin for certain benign and malignant lesions, and also may serve as a pathway for carcinomas spreading to deeper tissues. (45), (46) Our studies on AGMLG have resulted in 5 articles.

The first paper titled «*Anogenital mammary-like glands: a study of their normal histology with emphasis on glandular depth, presence of columnar epithelial cells, and distribution of elastic fibers*» extends our knowledge on the normal histology of AGMLG. The material represented 148 AGMLG identified in 133 paraffin blocks sampled from 64 wide vulvar excision or vulvectomy specimens. The authors studied the following features: a glandular depth, presence of columnar epithelium resembling columnar cell change/hyperplasia as defined in mammary pathology, and distribution of elastic fibers, all of which have not been previously investigated. It was found that the depth of AGMLG ranged from 0.64 to 3.9 mm. Epithelial columnar cell change was noted in 33.1% of all AGMLG, whereas columnar cell hyperplasia was detected in 10.1%. Of 22 specimens stained for elastic fibers, in only 6 (27.3%) cases were elastic fibers found around glands. Our study contributed novel data by documenting for the first time the depth to which AGMLG may extend, which has important implications when planning topical and surgical therapies for lesions evolving from AGMLG. Alterations identical to columnar cell change appear to be a frequent normal variation of AGMLG. Less commonly, normal glands may manifest changes analogous to columnar cell hyperplasia of the breast.

The second article, «*An immunohistochemical study of anogenital mammary-like glands*», describing a detailed immunoprofile of these structures, with a total of 45 antibodies used, including broad-spectrum cytokeratins (both low-and high-molecular weight), myoepithelial markers, steroid receptors markers, and others. We found that the immunoprofile of AGMLG is similar to normal breast tissue.

The third article, «*Molecular alterations in lesions of anogenital mammary-like glands and their mammary counterparts including hidradenoma papilliferum, intraductal papilloma, fibroadenoma, and phyllodes tumor*», is based on the study in which we compared the underlying molecular mechanisms in lesions of AGMLG and their mammary counterparts. We analyzed the mutational profile of 16 anogenital neoplasms including hidradenomas papilliferum, lesions with hybrid features of hidradenomas papilliferum and fibroadenoma, fibroadenomas, phyllodes tumors and 18 analogous breast lesions (6 intraductal papillomas, 9 fibroadenomas, and 3 phyllodes tumors) by high-coverage next-generation sequencing (NGS) using a panel comprising 50 cancer-

related genes. Additionally, all cases were analyzed for the presence of a mutation in the *MED12* gene. All detected mutations with allele frequencies over 20% were independently validated by Sanger sequencing (concordance: 100%). We documented several hitherto unreported mutations and concluded that *AKT1* or *PIK3CA* mutation of PI3K-AKT cascade plays a role both in tumors of AGMLG and their mammary counterparts, indicating that some histopathologically similar anogenital and breast lesions develop along similar molecular pathways.

The remaining two articles are focused on primary extramammary Paget disease (EMPD) which is a rare malignant neoplasm usually involving the anogenital area, most commonly the vulva. (47) The histogenesis of primary EMPD is still uncertain. Cutaneous adnexa, clear cells of Toker, pluripotent stem cells have been previously proposed as possible sites of origin. (48)

The goals of our study, «*Spectrum of changes in anogenital mammary-like glands in primary extramammary (anogenital) Paget disease and their possible role in the pathogenesis of the disease*», were to identify and describe the spectrum of involvement of AGMLG and their ducts in cases of primary anogenital EMPD, and to determine whether a subset of primary EMPD may originate in AGMLG, analogous to breast carcinoma. All patients were women, ranging in age from 38 to 93 years and all but one tumor were located on the vulva. In 33 specimens from 31 patients, various alterations of AGMLG were found, including columnar cell change and columnar cell hyperplasia which occur in normal AGMLG. In addition, other alterations as usual ductal hyperplasia, oxyphilic (apocrine) metaplasia and atypical duct hyperplasia were detected. In four cases with invasive mammary-type carcinomas, AGMLG displayed a range of alterations including ductal carcinoma in situ, columnar cell change, and columnar cell hyperplasia, with the subsequent upward migration of the neoplastic cells into the epidermis, similar to cases of mammary Paget disease. Colonization of AGMLG by neoplastic Paget cells was noted in 6 cases. We concluded that, by analogy with mammary Paget disease, rare cases of primary EMPD might originate in AGMLG. Usual ductal hyperplasia and atypical duct hyperplasia can then be regarded as earlier precursor lesions, linking both ends of the spectrum.

Since adnexal involvement (hair follicles and eccrine ducts) in primary EMPD is a very common feature and serves as a pathway for carcinoma to spread into deeper tissue, we studied the depth of carcinomatous spread along the appendages and the patterns of adnexal involvement in 178 lesions from 146 patients with primary EMPD. The results have been published in the article entitled «*Depth and Patterns of Adnexal Involvement in Primary Extramammary (Anogenital) Paget Disease: A Study of 178 Lesions From 146 Patients*». There were 114 women and 32 men, ranging in age at the diagnosis from 40 to 95 years. The most common location of EMPD in women were vulva (89.4%) and less frequently the perianal (5.3%) regions, whereas, in men, EMPD mostly involved the scrotum and groin. Of the 178 specimens, 165 were in situ EMPD, and 13 were invasive EMPD with the dermal depth of invasion >1 mm in 4 cases. The most commonly affected adnexa by carcinoma cells were hair follicles, involved in 92.8% of large resection specimens and the most deeply involved structures were eccrine ducts, which most frequently manifested as infiltration of the acrosyringium in 97.7%. The maximal depth of involvement in

this study was 3.6 mm, which provides important information for local treatment of EMPD with topical drugs such as imiquimod, 5-fluorouracil, and retinoic acid, alone or in combination. For example, 5-fluorouracil penetrates the skin to a depth of 1–2 mm, therefore our results showing the deeper adnexal involvement in EMPD should be taken into account when planning topical therapy or developing novel local treatment modalities for EMPD. (49)

Anogenital Mammary-Like Glands: A Study of Their Normal Histology With Emphasis on Glandular Depth, Presence of Columnar Epithelial Cells, and Distribution of Elastic Fibers

Anastasia M. Konstantinova, MD, PhD,*†‡ Liubov Kyrpychova, MD,§ Irena E. Belousova, MD, PhD,*‡¶ Dominic V. Spagnolo, MBBS, FRCPA,‖** Denisa Kacerovska, MD, PhD,§†† Michal Michal, MD,§†† Katrin Kerl, MD,‡‡ and Dmitry V. Kazakov, MD, PhD§††‡‡

Abstract: The normal histology of anogenital mammary-like glands (AGMLG) has been studied previously, but some aspects, including glandular depth, presence of columnar epithelium resembling columnar cell change/hyperplasia as defined in mammary pathology, and distribution of elastic fibers, have not been previously investigated. To address these issues, we studied 148 AGMLG identified in 133 paraffin blocks sampled from 64 vulvar wide excision or vulvectomy specimens (64 patients, various indications for surgery). The depth of AGMLG ranged from 0.64 to 3.9 mm. Epithelial columnar cell change was noted in 33.1% of all AGMLG, whereas columnar cell hyperplasia was detected in 10.1%. Occasionally, combinations of cuboidal epithelium and columnar cell change were seen within 1 histological section. Of 22 specimens stained for elastic fibers, in only 6 (27.3%) cases were elastic fibers found around glands. Periductal elastic fibers were demonstrated around 3 of the only 5 ducts, which were available for analysis in slides stained for elastic fibers. The depth of AGMLG should be taken into account when planning topical and surgical therapies for lesions derived or evolving from AGMLG. Alterations identical to columnar cell change may represent a normal variation of AGMLG.

Key Words: anogenital mammary–like glands, depth, adnexa, vulva, columnar cell change, columnar cell hyperplasia

From the *Department of Pathology, Clinical Research and Practical Center for Specialized Oncological Care, Saint-Petersburg, Russia; †Department of Pathology, Medical Faculty, Saint-Petersburg State University, Saint-Petersburg, Russia; ‡Department of Pathology, Saint-Petersburg Medico-Social Institute, Saint-Petersburg, Russia; §Sikl's Department of Pathology, Medical Faculty in Pilsen, Charles University in Prague, Pilsen, Czech Republic; ¶Department of Dermatology, Medical Military Academy, Saint-Petersburg, Russia; ‖PathWest Laboratory Medicine WA, QEII Medical Centre, Nedlands, WA, Australia; **School of Pathology and Laboratory Medicine, University of Western Australia, Nedlands, WA, Australia; ††Bioptical Laboratory, Pilsen, Czech Republic; and ‡‡Dermatopathology Unit, Department of Dermatology, Zurich University Hospital, Zurich, Switzerland.

INTRODUCTION

Long regarded as ectopic or supernumerary breast tissue, anogenital mammary-like glands (AGMLG) are now considered a normal constituent of the anogenital area.[1–5] Mainly located in the sulcus between the labia minora and labia majora, AGMLG are not visible clinically, but they are often found incidentally in pathological specimens from the anogenital area. Although lesions affecting AGMLG are rare, they are of clinical importance because they are suggested to be the origin for certain benign and malignant lesions, in addition to being a pathway for carcinomas spreading to deeper tissues.[6–8]

Normal AGMLG vary from simple glandular structures with round lumina surrounded by loose or dense fibrotic stroma to more complex units closely imitating breast tissue, although lacking lobules comparable to those seen in breast.[1,3,7] However, there are several aspects that have never been addressed. First, the depth to which AGMLG normally extend has never been studied; this is important and should be taken into account when planning topical or surgical therapy. Thus, our primary goal was to establish the depth to which AGMLG may extend into the dermis. Second, the epithelium lining AGMLG, especially in remnants of AGMLG associated with neoplasms arising from them, often manifest a columnar appearance resembling columnar cell change (CCC) or columnar cell hyperplasia (CCH) in various benign breast lesions.[9,10] Our second goal, therefore, was to determine whether CCC/CCH may be a feature of normal AGMLG, outside the setting of any accompanying neoplasia. Finally, we sought to study the presence of elastic fibers to establish if there are similarities in the distribution of elastic fibers between AGMLG and breast, which typically displays periductal but not perilobular elastic fibers.

MATERIAL AND METHODS

Case Selection

A search in the consultation, routine institutional, and personal files of the authors between 1997 and 2016 yielded 6733 biopsies from the vulva. Of these, 212 cases represented wide vulvar surgical excisions or vulvectomy specimens performed for vulvar intraepithelial neoplasia, invasive squamous carcinoma, or extramammary Paget disease (EMPD).

Histological slides were reviewed to identify any AGMLG. Excluded from the study were 148 cases lacking AGMLG or in which AGMLG occurred under a damaged epidermis, were in company with an invasive neoplasm, or were associated with any pathological process that potentially could displace them or alter their appearances. Thus, the study cohort consisted of 64 specimens (133 paraffin blocks) from 64 patients. Age at diagnosis ranged from 23 to 92 years (median, 61.5 years; mean, 61.9 years).

Light Microscopy

The study was based on the assessment of hematoxylin and eosin–stained slides. Twenty-two cases were stained histochemically for the presence of elastic fibers. The number of tissue blocks per case ranged from 1 to 8 (median, 2; mean, 2.1).

We recorded the presence of changes compatible with CCC or CCH as defined in breast pathology. CCC was defined as variably dilated lumina lined by 1–2 cell layers of elongated to ovoid columnar epithelial cells oriented perpendicularly to the basement membrane, having apical cytoplasmic blebs or snouts. CCH appeared as variably dilated lumina lined by more than 2 cell layers of elongated to ovoid columnar epithelial cells oriented perpendicularly to the basement membrane, having apical cytoplasmic blebs or snouts.[7]

The depth of AGMLG was measured from the granular layer of intact epidermis to the deepest point of extension of AGMLG, using an ocular micrometer. When it was not possible to distinguish between glandular and ductal elements of AGMLG, they were arbitrarily designated as glands and their depth recorded. Depths of a total of 148 AGMLG were measured in 133 blocks.

RESULTS

A total of 148 AGMLG were identified, occurring in 133 paraffin blocks taken from the 64 resection specimens. The mean depth of AGMLG was 1.7 mm (median, 1.55 mm; range, 0.64–3.9 mm) (Fig. 1A, B). In line with previous studies, AGMLG exhibited varying cytoarchitectural complexity and were lined by a simple cuboidal epithelium surrounded by an outer myoepithelial layer (Fig. 2A–C). Features compatible with CCC were found in 49 (33.1%) of 148 AGMLG (Fig. 3A), whereas CCH was detected in 15 (10.1%) AGMLG (Fig. 3B). Occasionally, combinations of the cuboidal epithelium and CCC were seen within 1 histologic section. Loosely or densely fibrotic stroma was invariably present around AGMLG, and in 6 (27.3%) cases, elastic fibers were found (Fig. 4A, B).

Only 5 ducts were available for analysis in sections stained for elastic fibers, and 3 of these were surrounded by elastic fibers (Fig. 4A). In 2 cases, distinct small clear cells (Toker cells) arranged as single cells or in small clusters in the lower epidermis around the openings of the ducts were recognized.

DISCUSSION

AGMLG are presumed to be a source for various benign and malignant lesions occurring in the anogenital region, including hidradenoma papilliferum, fibroadenoma, phyllodes tumor, mammary-type invasive carcinomas, and other lesions.[3,6–8,10–24] Additionally, a subset of primary EMPD may originate in AGMLG, with subsequent upward migration of the neoplastic cells into the epidermis similar to cases of so-called invasive mammary Paget disease.[6,25] AGMLG, along with other adnexa, may provide a path for carcinoma spreading to deeper tissues, especially in cases of EMPD.[6,8] We found that the maximal depth of AGMLG is 3.9 mm, with a range of 0.64–3.9 mm. This is an important finding indicating that in superficial biopsies, alterations in deeper AGMLG may go undetected. Besides, it can be assumed that in cases of invasive tumors originating in AGMLG, the neoplastic cells can rapidly access lymphatic vessels, increasing the risk of development of metastatic disease. Although we did find the depth of lymphatic vessels in
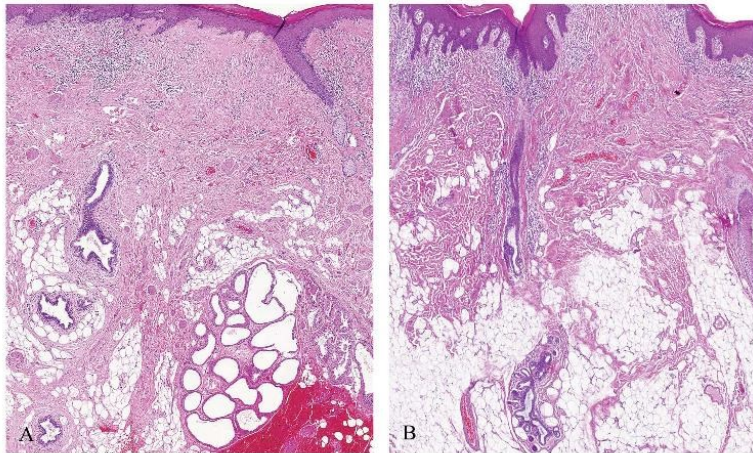
FIGURE 1. A deeply located AGMLG and its excretory ducts (A, B).

74
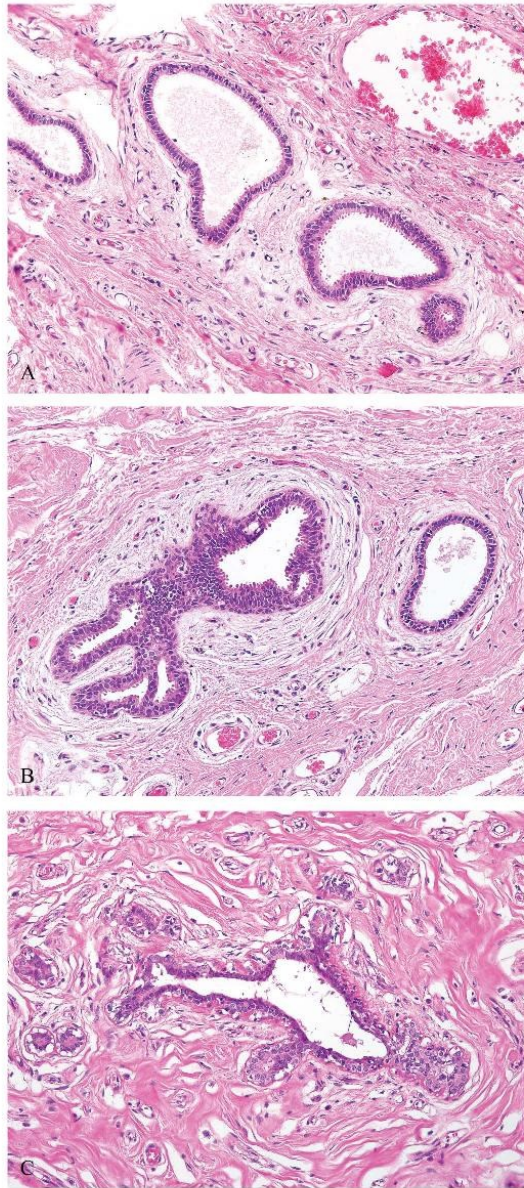
FIGURE 2. Microscopic variations of AGMLG. Simple bilayered glands lined by a luminal columnar to low cuboidal epithelium showing decapitation secretion and surrounded by a layer of myoepithelial cells (A, B). B, Note CCC of the epithelium. C, A more complex AGMLG with out pouchings.
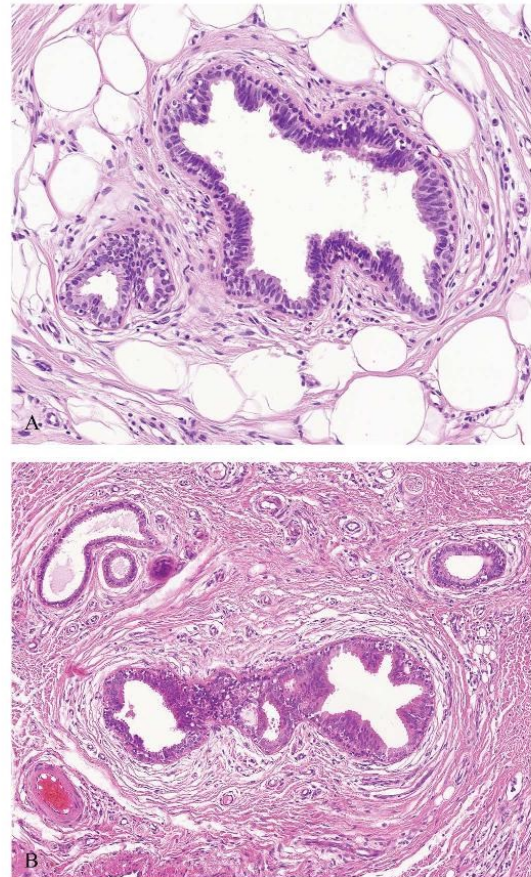
FIGURE 3. Columnar cell change (A) and columnar cell hyperplasia (B) of AGMLG.

the anogenital area in the literature, in the skin elsewhere, these are usually located at/below the depth of 0.75–1 mm.

We found that the epithelium lining normal AGMLG often manifested changes compatible with CCC (33.1%) or CCH (10.1%) as defined in breast pathology. Sometimes cuboidal epithelium and CCH/CCH coexisted. A similar morphological spectrum has been described in AGMLG adjacent to hidradenoma papilliferum or some carcinomas, suggesting that CCC/CCH may be a precursor lesion.[10] In the breast, a low level of allelic imbalance was demonstrated in columnar cell lesions using the microdissection approach. None of the cases of CCC had loss of heterozygosity, whereas CCH had a low (0%–15%) fractional mutation percentage.[26] Another study showed a lower level of copy number changes in CCC relative to CCH.[27] The frequent occurrence of features identical to CCC in normal AGMLG (one-third of all AGMLG found) indicates that this is likely
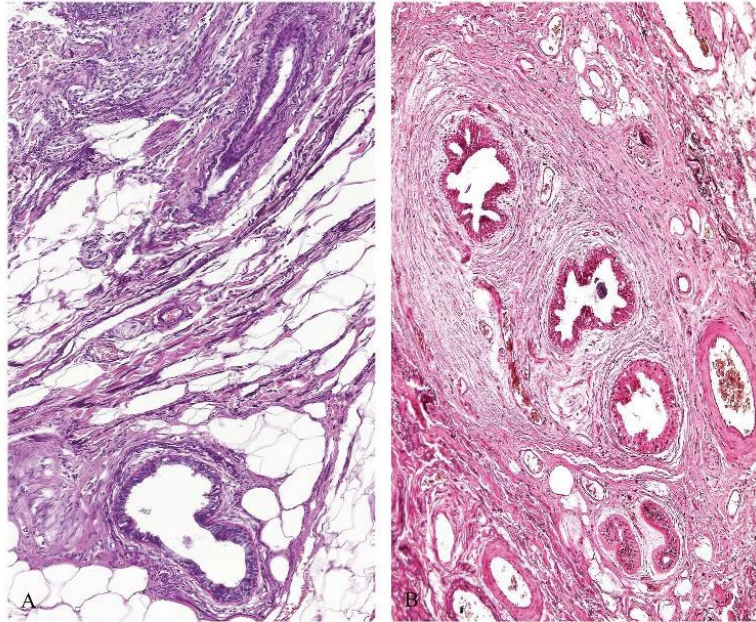
FIGURE 4. A, Elastic fibers in the stroma surrounding AGMLG and excretory duct. B, Absence of elastic fibers in the stroma surrounding AGMLG.

a normal variation in the histologic spectrum of normal AGMLG. In the breast, periductal elastic fibers are seen frequently.[28]

We also found elastic fibers surrounding excretory ducts of AGMLG in 3 of the 5 studied specimens. On the contrary, elastic fibers around anogenital glands were found only in 6 (27.3%) cases. Invasive mammary ductal carcinoma may elicit prominent elastosis manifest grossly as white streaks (chalky streaks). This feature has not been emphasized in mammary-type carcinomas of AGMLG, although prominent stromal elastosis in a case of tubulolobular carcinoma of AGMLG has been reported.[29]

In conclusion, our study contributes novel data by documenting for the first time the depth to which AGMLG may extend, which has important implications when planning topical and surgical therapies for lesions evolving from AGMLG. It appears that alterations identical to CCC are a frequent normal variation of AGMLG, and less commonly, normal glands may manifest changes analogous to CCH of the breast.

REFERENCES

1. van der Putte SC. Anogenital "sweat" glands. Histology and pathology of a gland that may mimic mammary glands. *Am J Dermatopathol.* 1991; 13:557–567.
2. van der Putte SC. Ultrastructure of the human anogenital "sweat" gland. *Anat Rec.* 1993;235:583–590.
3. van der Putte SC. Mammary-like glands of the vulva and their disorders. *Int J Gynecol Pathol.* 1994;13:150–160.
4. van der Putte SC, van Gorp LH. Cysts of mammarylike glands in the vulva. *Int J Gynecol Pathol.* 1995;14:184–188.
5. van der Putte SC. Clear cells of Toker in the developing anogenital region of male and female fetuses. *Am J Dermatopathol.* 2011;33: 811–818.
6. Belousova IE, Kazakov DV, Michal M, et al. Vulvar toker cells: the long-awaited missing link: a proposal for an origin-based histogenetic classification of extramammary paget disease. *Am J Dermatopathol.* 2006;28:84–86.
7. Kazakov DV, Spagnolo DV, Kacerovska D, et al. Lesions of anogenital mammary-like glands: an update. *Adv Anat Pathol.* 2011;18: 1–28.
8. Konstantinova AM, Shelekhova KV, Stewart CJ, et al. Depth and patterns of adnexal involvement in primary extramammary (anogenital) Paget disease: a study of 178 lesions from 146 patients. *Am J Dermatopathol.* 2016. [Epub ahead of print].
9. Kazakov DV, Michal M, Kacerovska D, et al. *Cutaneous Adnexal Tumors.* Philadelphia, PA: Lippincot Williams & Wilkins; 2012.
10. Konstantinova AM, Michal M, Kacerovska D, et al. Hidradenoma papilliferum: a clinicopathologic study of 264 tumors from 261 patients, with emphasis on mammary-type alterations. *Am J Dermatopathol.* 2016;38: 598–607.
11. Hayes MM, Konstantinova AM, Kacerovska D, et al. Bilateral gigantomastia, multiple synchronous nodular pseudoangiomatous stromal hyperplasia Involving breast and bilateral axillary accessory breast tissue, and perianal mammary-type hamartoma of anogenital mammary-like glands: a case report. *Am J Dermatopathol.* 2016;38:374–383.
12. Kazakov DV, Belousova IE, Sima R, et al. Mammary type tubulolobular carcinoma of the anogenital area: report of a case of a unique tumor presumably originating in anogenital mammarylike glands. *Am J Surg Pathol.* 2006;30:1193–1196.
13. Kazakov DV, Bisceglia M, Mukensnabl P, et al. Pseudoangiomatous stromal hyperplasia in lesions involving anogenital mammary-like glands. *Am J Surg Pathol.* 2005;29:1243–1246.
14. Kazakov DV, Bisceglia M, Sima R, et al. Adenosis tumor of anogenital mammary-like glands: a case report and demonstration of clonality by HUMARA assay. *J Cutan Pathol.* 2006;33:43–46.
15. Kazakov DV, Hugel H, Vanecek T, et al. Unusual hyperplasia of anogenital mammary-like glands. *Am J Dermatopathol.* 2006;28:134–137.

76

16. Kazakov DV, Mikyskova I, Kutzner H, et al. Hidradenoma papilliferum with oxyphilic metaplasia: a clinicopathological study of 18 cases, including detection of human papillomavirus. *Am J Dermatopathol.* 2005;27:102–110.
17. Kazakov DV, Spagnolo DV, Stewart CJ, et al. Fibroadenoma and phyllodes tumors of anogenital mammary-like glands: a series of 13 neoplasms in 12 cases, including mammary-type juvenile fibroadenoma, fibroadenoma with lactation changes, and neurofibromatosis-associated pseudoangiomatous stromal hyperplasia with multinucleated giant cells. *Am J Surg Pathol.* 2010;34:95–103.
18. Konstantinova AM, Hayes MM, Stewart CJ, et al. Syringomatous structures in extramammary Paget disease: a potential diagnostic pitfall. *Am J Dermatopathol.* 2016;38:653–657.
19. Konstantinova AM, Kacerovska D, Michal M, et al. A tumoriform lesion of the vulva with features of mammary-type fibrocystic disease. *Am J Dermatopathol.* 2013;35:e124–e127.
20. Konstantinova AM, Kacerovska D, Michal M, et al. A composite neoplastic lesion of the vulva with mixed features of fibroadenoma and hidradenoma papilliferum combined with pseudoangiomatous stromal hyperplasia containing multinucleated giant cells. *Am J Dermatopathol.* 2014;36:e171–e174.
21. Konstantinova AM, Kacerovska D, Stewart CJ, et al. Syringocystadenocarcinoma papilliferum in situ-like changes in extramammary Paget disease: a report of 11 cases. *Am J Dermatopathol.* 2016. [Epub ahead of print].
22. Willman JH, Golitz LE, Fitzpatrick JE. Vulvar clear cells of Toker: precursors of extramammary Paget's disease. *Am J Dermatopathol.* 2005;27:185–188.
23. Vazmitel M, Pavlovsky M, Kacerovska D, et al. Pseudoangiomatous stromal hyperplasia in a complex neoplastic lesion involving anogenital mammary-like glands. *J Cutan Pathol.* 2009;36:1117–1120.
24. Vazmitel M, Spagnolo DV, Nemcova J, et al. Hidradenoma papilliferum with a ductal carcinoma in situ component: case report and review of the literature. *Am J Dermatopathol.* 2008;30:392–394.
25. Duan X, Sneige N, Gullett AE, et al. Invasive paget disease of the breast: clinicopathologic study of an underrecognized entity in the breast. *Am J Surg Pathol.* 2012;36:1353–1358.
26. Dabbs DJ, Carter G, Fudge M, et al. Molecular alterations in columnar cell lesions of the breast. *Mod Pathol.* 2006;19:344–349.
27. Simpson PT, Gale T, Reis-Filho JS, et al. Columnar cell lesions of the breast: the missing link in breast cancer progression? A morphological and molecular analysis. *Am J Surg Pathol.* 2005;29:734–746.
28. Farahmand S, Cowan DF. Elastosis in the normal aging breast. A histopathologic study of 140 cases. *Arch Pathol Lab Med.* 1991;115:1241–1246.
29. Fernandez-Figueras MT, Michal M, Kazakov DV. Mammary-type tubulolobular carcinoma of anogenital mammary-like glands with prominent stromal elastosis. *Am J Surg Pathol.* 2010;34:1224–1226.

An Immunohistochemical Study of Anogenital Mammary-Like Glands

Anastasia M. Konstantinova, MD, PhD,*†‡ Colin J. R. Stewart, FRCPA,§ Liubov Kyrpychova, MD,¶ Irena E. Belousova, MD, PhD,*‡‖ Michal Michal, MD,¶** and Dmitry V. Kazakov, MD, PhD¶**

Abstract: Although the normal histology of anogenital mammary-like glands (AGMLG) has been studied, no systemic investigation has been performed on the immunoprofile of these structures. We studied intact AGMLG with a broad panel of antibodies. The immunoprofile of AGMLG is similar to that of a normal breast tissue, and there are similarities to eccrine glands and coils about cytokeratin expression. Our immunohistochemical data may contribute to understanding of the pathogenesis of lesions arising from AGMLG.

Key Words: anogenital mammary-like glands, immunohistochemistry, vulva, steroid receptors, myoepithelial cells

(*Am J Dermatopathol* 2017;39:599–605)

INTRODUCTION

Long regarded as ectopic or supernumerary breast tissue, anogenital mammary-like glands (AGMLG) are nowadays considered to be a normal constituent of the anogenital area[1–5]. AGMLG are presumed to be the origin for various benign and malignant lesions occurring in the anogenital region which manifest a striking similarity to their mammary counterparts, including hidradenoma papilliferum, fibroadenoma, phyllodes tumor, mammary-type invasive carcinomas, and other lesions[3,6–23]. Although the histology of normal AGMLG has been previously documented, there are limited data regarding the immunohistochemical profile of these structures[1,14,21]. Most reports have described the immunohistochemical findings in AGMLG adjacent to benign or malignant tumors, but no systemic study of the immunoprofile of normal AGMLG has been performed[4,24–28]. Our aims were to

characterize the immunoprofile of AGMLG with a broad panel of antibodies and compare the immunohistological features with those of normal breast tissue and with normal eccrine/apocrine glands.

MATERIALS AND METHODS

Case Selection

Two hundred twelve surgical excisions or vulvectomy specimens performed for the treatment of vulvar intraepithelial neoplasia and/or invasive squamous cell carcinoma were recruited from 6733 vulval specimens in our consultation, routine institutional, and personal files accessioned between 1997 and 2016. The histological slides were reviewed to detect the presence of intact AGMLG in blocks where the glands were not involved or altered by another pathologic process including the primary neoplasm, lichen sclerosus, scar, or inflammation. Included in the study were 15 randomly selected cases with intact AGMLG. The age at diagnosis ranged from 37 to 89 years (mean, 63.2 years).

Immunohistochemistry

The following primary antibodies were used using a Ventana Benchmark XT automated stainer (Ventana Medical System Inc, Tucson, AZ).

1. Broad-spectrum cytokeratins (CKs): AE1/AE3 (AE1-AE3, monoclonal; Ventana; RTU), MNF 116 (MNF 116, monoclonal; DakoCytomation, Carpinteria, CA; 1:50), and OSCAR (IsoType:IgG2a; BioLegend, Dedham, MA; 1:100).
2. Low molecular weight (LMW) CKs: CAM 5.2 (CAM 5.2, monoclonal; Ventana; RTU), CK7 (OV-TL12/30, monoclonal; DakoCytomation, Carpinteria, CA; 1:200), CK8 (35ßH11; Cell Marque, Rockin, CA; RTU), CK18 (DC10; DakoCytomation, Carpinteria, CA; RTU), CK19 (A53-B/A2.26; Cell Marque, Rockin, CA; RTU), and CK20 (Ks20.8; DakoCytomation, Carpinteria, CA; 1:100).
3. High molecular weight (HMW) CKs: K903 (34&223; E12; DakoCytomation, Carpinteria, CA; 1:200), CK5 (XM26; Novocastra, Newcastle, United Kingdom; 1:400), CK5/6 (D5/16B4; DakoCytomation, Glostrup, Denmark; 1:100), CK10/13 (DE-K13; DakoCytomation, Carpinteria, CA; 1:100), CK14 (LL002; Novocastra, Newcastle, United Kingdom; 1:40), and CK17 (E3; DakoCytomation, Carpinteria, CA; 1:40).

TABLE 1. Summary of Immunohistochemical Analysis of AGMLG*

	Glandular Part			Excretory Duct		
	No. Cases Available for Analysis	Myoepithelial Cells	Luminal Cells	No. Cases Available for Analysis	Myoepithelial Cells	Luminal Cells
Wide-spectrum CK						
AE1/AE3	11	+	+++	3	+(++)	+++(++)
CK MNF 116	9	−(+)	+++(++)	4	−(+)	+++
OSCAR	11	+(−)	+++	4	−(+)	+++(++)
LMW CK						
CAM 5,2	13	−(+)	+++	3	−	++(+++)
CK7	10	−	+++	4	−(+)	+++
CK8	8	−	+++(++)	4	−	++/+++
CK18	9	−	+++(++)	4	−	+++(+/++)
CK19	10	−	+++	3	−	+++
CK20	11	−	−	4	−	−
HMW CK						
K 903	9	+(−)	++,foc (+,foc)	5	0(+)	++(+,foc)
CK CK5	10	−(+,foc)	−(+,foc)	4	−(+,foc)	−(+,foc)
CK 5/6	8	+(−/foc)	+(++,foc/−)	5	++(+)	+(−/++,foc)
CK10/13	11	−	−	3	−	−
CK14	11	++(+/+++)	+,foc(−)	2	++/+++	+,foc/−
CK17	9	++,foc(−)	−(+,foc)	3	+(−)	−
Myoepithelial markers						
MSA	10	++(+/+++)	−	5	+(+++)	−
ASMA	10	+++(++)	−	3	+(+++)	−
Caldesmon	13	++(+)	−	3	+(++)	−
Calponin	12	++(+/+++)	−	3	+	−
EGFR	9	+(−)	−	2	+	−
p63	8	+++	−	5	+++	−
NGFR	7	++	−	4	++	−
Steroid receptors						
AR	12	−	+++(−)	5	−	−(+)
ER	9	−	+++(+)	6	−	++(−/+++)
PR	7	−	++(+++)	3	−	+(+++)
Others						
BerEP4	11	−	−(+)	4	−	−(+)
Calretinin	12	−	−(+,foc)	3	−	−
CD138	11	++(+)	++(−/+)	2	+	+(−)
CDX2	10	−	−	3	−	−
COX-2	9	−	−	4	−	−
E-cadherin	9	++(+)	+++(+/++)	3	+	++
EMA	9	−	++(+++)	6	−	++(+++)
GCDFP-15	11	−	+++(++), foc	5	−	+++(++)
GFAP	10	−(+)	−	4	−	−
HER 2/neu	11	−	−(+)	5	−	−(+)
Mammaglobin	10	−	+++(++), foc	4	−	++/+++, foc
MUC 1	11	−	+++(+/++)	5	−	++(+/+++)
MUC 2	9	−	−	2	−	−
MUC 5	9	−	−(+,foc)	2	−	−
MUC 6	9	−	−(+)	2	−	−(+,foc)
p16	10	−	+++(−/++), foc	5	−	+++(−)
S100 protein	8	++(+++)	−	3	++	−

79

TABLE 1. (*Continued*) Summary of Immunohistochemical Analysis of AGMLG*

	Glandular Part			Excretory Duct		
	No. Cases Available for Analysis	Myoepithelial Cells	Luminal Cells	No. Cases Available for Analysis	Myoepithelial Cells	Luminal Cells
MSH2	8	+++	+++	6	+++	+++
GATA3	8	−	++/+++(+)	3	−	+++

Score before in brackets indicates the most commonly seen reaction, whereas score in brackets indicates less common variation(s).
*+++ indicates strong positivity; ++, intermediate positivity; +, weak positivity; −, negative; foc, focal; MSA, muscle-specific actin; GFAP, glial fibrillary acidic protein.
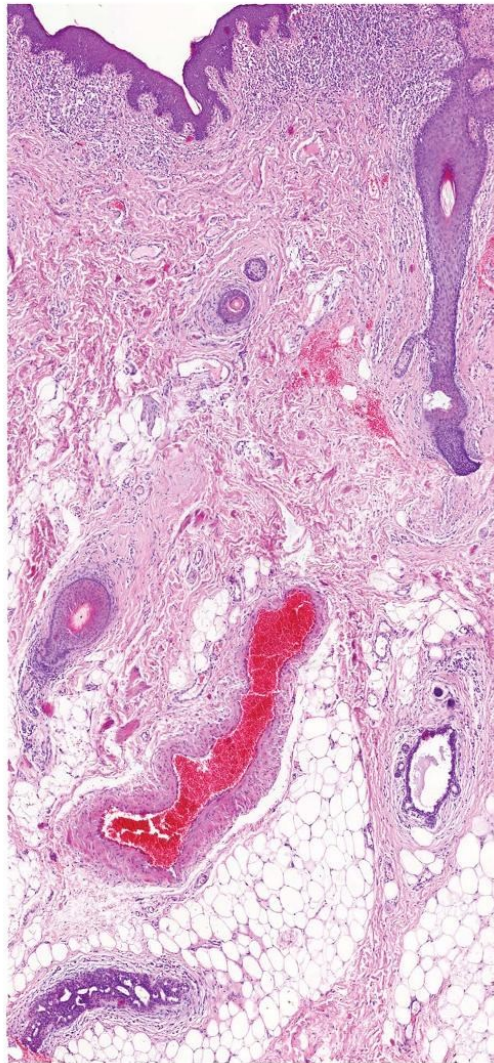

FIGURE 1. An AGMLG and its duct.

4. Myoepithelial markers: anti-smooth muscle actin (ASMA) (1A4; DakoCytomation, Carpinteria, CA; 1:1000), muscle-specific actin (HHF-35; DakoCytomation, Carpinteria, CA; 1:200), caldesmon (E89; Cell Marque, Rockin, CA; RTU); calponin (EP798Y; Ventana; RTU), EGFR (5B7; Ventana; RTU), p63 (4A4; Neomarkers, Fremon, CA; 1:500), and NGFR (MRQ-21; Cell Marque, Rockin, CA; RTU).

5. Steroid receptors: androgen receptors (ARs) (SP107; Cell Marque, Rockin, CA; RTU), estrogen receptors (ERs) (SP1; Ventana; RTU), and progesterone receptors (PRs) (1E2; Ventana; RTU).

6. Others: BerEP4 (BerEP4; DakoCytomation, Carpinteria, CA; 1:200), calretinin (5A5; Ventana; RTU), CD 138 (MI15; Cell Marque, Rockin, CA; RTU), CDX2 (CDX2-88; Cell Marque, Rockin, CA; RTU), COX-2 (CX-294; DakoCytomation, Carpinteria, CA; 1:100), E-cadherin (36; Ventana; RTU), epithelial membrane antigen (EMA) (E29; DakoCytomation, Glostrup, Denmark; 1:400), GCDFP-15 (BRST 2) (EP1582Y; Ventana; RTU), glial fibrillary acidic protein (6F2; DakoCytomation, Carpinteria, CA; RTU), HER 2/neu (4B5; Ventana; RTU), mammaglobin (304-1A5; DakoCytomation, Carpinteria, CA; RTU), MUC 1 (Ma695; Ventana; RTU), MUC 2 (Ccp58; Cell Marque, Rockin, CA; RTU), MUC 5 (MRQ-19; Cell Marque, Rockin, CA; RTU), MUC 6 (CLH5; Cell Marque, Rockin, CA; RTU), p16 (R19-D; Ventana; RTU), S100 protein (polyclonal, Ventana, RTU), MSH2 (G219-1129; Cell Marque, Rockin, CA; RTU), and GATA3 (L50-823, Biocare Medical, 1:100).

The staining patterns in the glandular and ductal components of the AGMLG were assessed separately. When it was not possible to distinguish these components, they were arbitrarily designated as glands. The staining was scored as follows: strong positivity (+++), intermediate positivity (++), weak positivity (+), and negative (−). Also, diffuse versus focal positivity was recorded.

RESULTS

The immunohistochemical data are summarized in Table 1. Two cases were excluded because of poor staining or loss of tissue. The glandular and excretory components of the AGMLG were both lined by a luminal epithelium and an underlying myoepithelial layer. The luminal epithelial cells were cuboidal to columnar in appearances, focally resembling
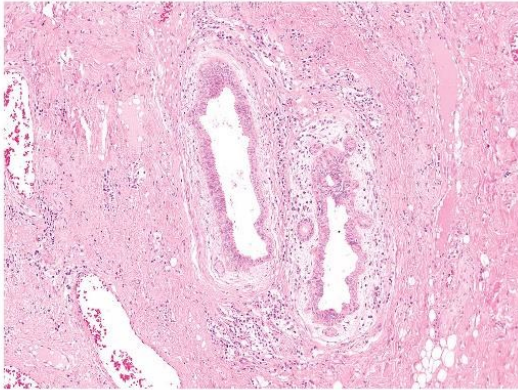
FIGURE 2. Microscopic variations of AGMLG. One simple bilayer glands lined by a luminal columnar to low-cuboidal epithelium showing decapitation secretion and surrounded by a layer of myoepithelial cells. Note columnar cell change of the epithelium. The second more complex AGMLG with outpouchings.

in some cases columnar cell change as defined in mammary pathology. The glands and ducts had round to oval lumina, sometimes with outpouchings and were surrounded by a loose stroma (Figs. 1, 2). There were no major differences between the immunohistochemical profiles of the cells according to their glandular or ductal distribution.

The luminal cells showed intermediate to strong expression of LMW CKs (CAM5.2, CK7, CK8, CK18, and CK19), EMA, steroid receptors, GCDFP-15, mammaglobin, MUC1, and GATA3. In 9 of the 10 studied cases (90%), the luminal epithelial cells were focally positive for p16 (Figs. 3–5). The basal/myoepithelial cells were positive for myoepithelial markers, S100 protein, and in most cases for the HMW CKs (K903, CK5/6, CK14, and CK17) (Figs. 5, 6).

Both cell layers were positive for E-cadherin, CD138, and MSH2. There was no expression of CK10/13, CK20, MUC2, COX2, and CDX2 in either the luminal or the myoepithelial cells, while calretinin decorated stromal cells close to the AGMLG and mast cells.

In two cases, distinct small CK7-positive cells (Toker cells), arranged as single cells, were identified. In one case, these were located along ducts lined by squamous epithelium.
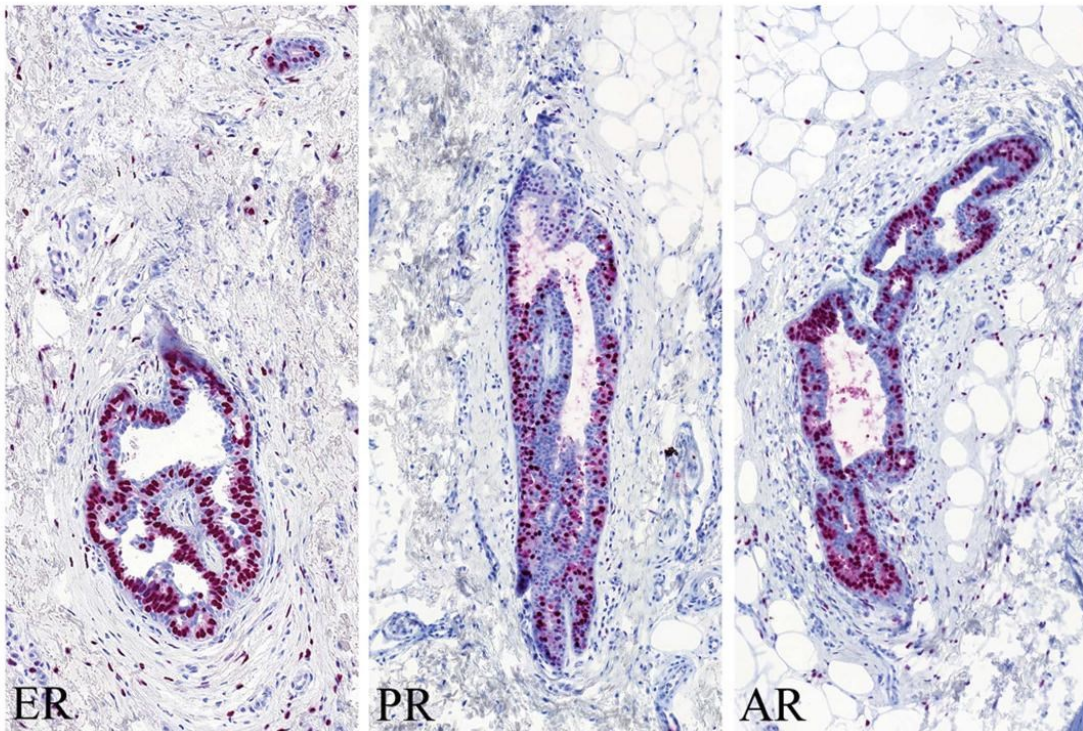
FIGURE 3. A composite figure showing immunoreaction of luminal cells of AGMLG are for steroid receptors.
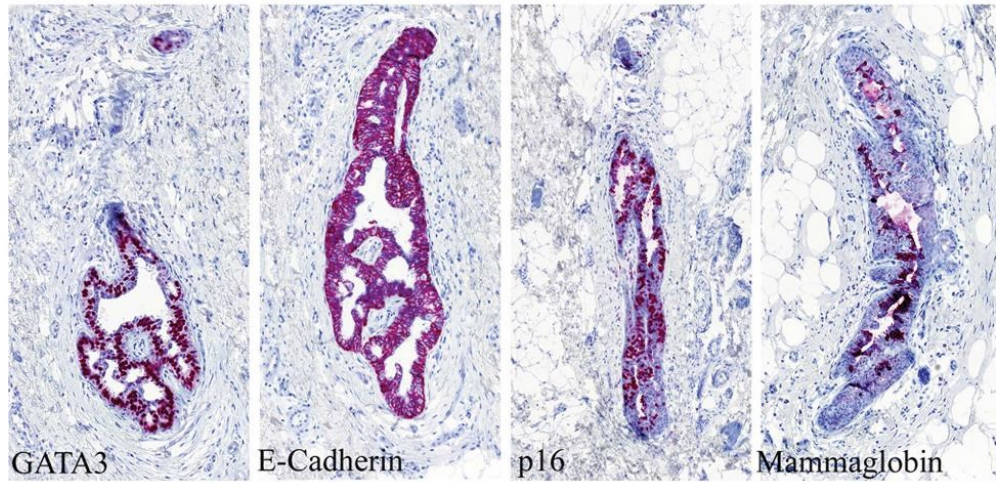
FIGURE 4. A composite figure demonstrating diffuse immunoreaction of the epithelial cells of AGMLG for GATA3 and E-cadherin and focal positivity for p16 and mammaglobin. E-cadherin also stains myoepithelial cells.
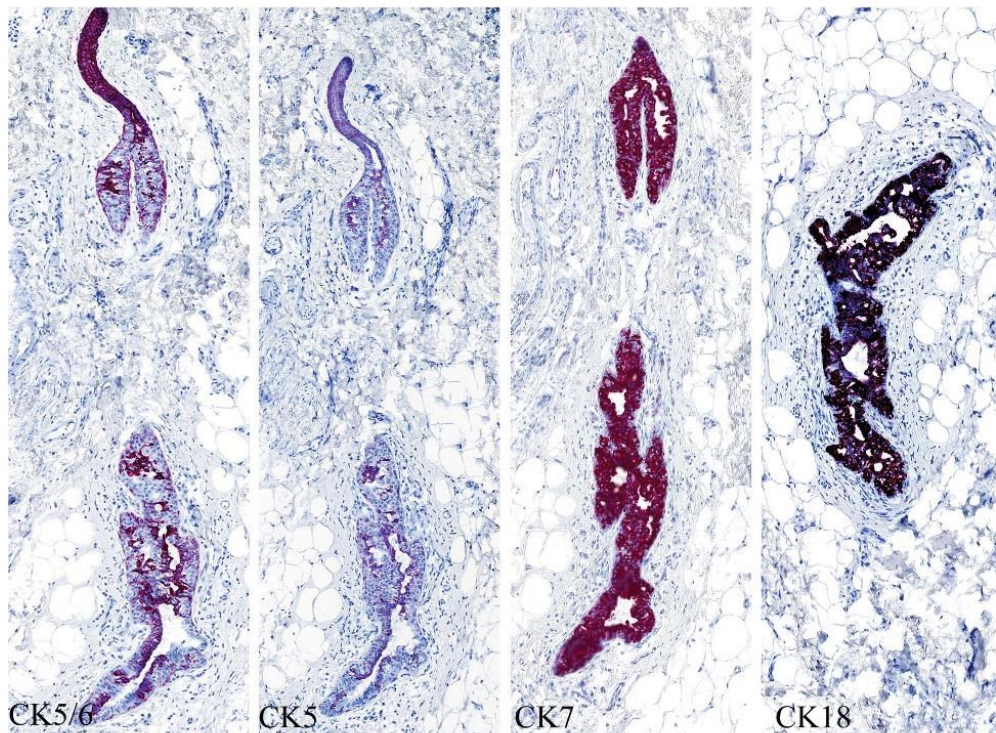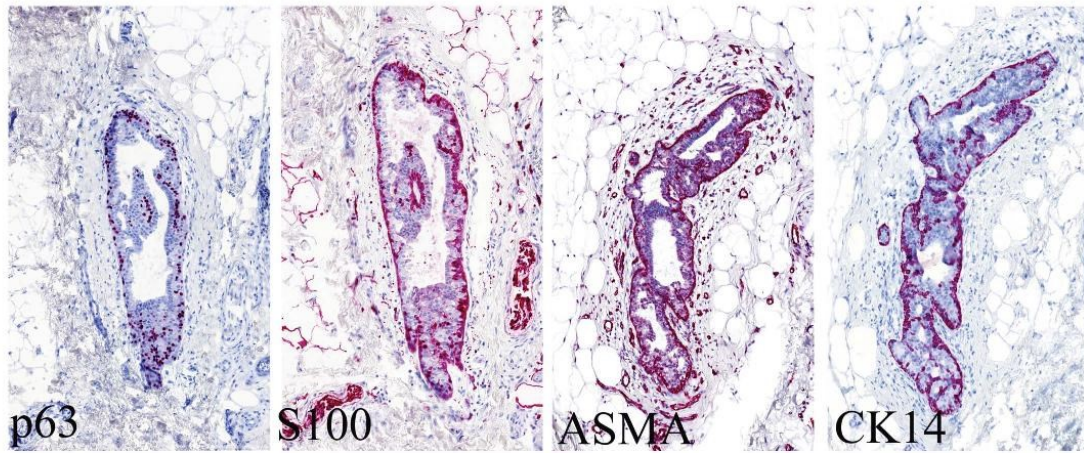

FIGURE 5. A composite figure showing focal expression of CK5 and CK5/6 by both luminal and myoepithelial cells in AGMLG and its duct. Note also strong expression of CK7 and CK18 by epithelial cells.

FIGURE 6. Composite figure illustrating immunoreaction of the cells of the myoepithelial layer for p63, S100 protein, ASMA (alpha smooth muscle actin) and CK14.

DISCUSSION

Two immunohistochemically different cell layers in AGMLG were recognized initially by van der Putte who showed that cells lining the acini, ducts, and typical cylindrical cells with snouts were positive for LMW CKs, HMFG, and CEA, whereas the abluminal myoepithelial cells were positive for actin and S100 protein.[1] Subsequently, expression of ER, PR, GCDFP-15, CEA, HMFG-2, CK7, EMA, and AE1/3 has been described in the luminal cell layer.[4,14,21,24–28]

In our study, we also identified distinct luminal cells which showed intermediate to strong expression of LMW CKs ("luminal" keratins), and basal cells which were usually positive for myoepithelial markers and mostly for HMW CKs ("basal" keratins). Furthermore, some cells in the luminal layer were positive for the HMW CKs, CK5, CK5/6, CK14, and CK17.[29,30] These could correspond to the intermediate glandular cell lineage described in mammary tissue.[31–33]

The luminal cells of AGMLG showed intermediate to strong expression of EMA, GCDFP-15, mammaglobin, MUC1 and GATA3, similar to the findings described in breast tissue.[34–39] In 9 of the 10 cases (90%), the epithelial cells were also positive for p16 which is also expressed in the normal breast.[40] Similarly, both layers of cells were positive for E-cadherin, CD138, and MSH2.[41–43]

With respect to hormone receptor expression, most epithelial cells in our study showed strong ER, PR, and AR positivity, which is in agreement with most previously published data.[24–27] However, Offidiani et al reported that AGMLG did not express AR.[27]

There was no expression of MUC2, COX2, and CDX2 in AGMLG, similar to previous findings in normal breast tissue.[44–46]

Expression of CKs in the secretory coils of eccrine and apocrine glands was similar to that seen in the glandular component of AGMLG. However, the luminal cells of AGMLG were positive for CK8 and CK18[47] in contrast to the findings in normal adnexal ducts.

Calretinin is a calcium-binding protein member of the EF-hand family which expression has been demonstrated in certain stages of the cellular cycle in many normal and neoplastic tissues. With respect to normal skin, calretinin has been found to be expressed in the innermost cell layer of the outer root sheath in anagen hair follicle, in sebaceous ducts, eccrine secretory coil, and in mast cells of the stroma.[48] In breast glands, weak expression of calretinin by luminal cells has been demonstrated in one study.[49] We found focal calretinin expression in the stroma of AGMLG and rarely in luminal epithelial cells.

In conclusion, our study contributes novel immunohistochemical data of AGMLG, which were hitherto not previously documented. In general, the immunohistochemical profile of AGMLG is similar to that seen in a normal breast tissue.

REFERENCES

1. van der Putte SC. Anogenital "sweat" glands. Histology and pathology of a gland that may mimic mammary glands. *Am J Dermatopathol.* 1991; 13:557–567.
2. Van der Putte SC. Ultrastructure of the human anogenital "sweat" gland. *Anat Rec.* 1993;235:583–590.
3. van der Putte SC. Mammary-like glands of the vulva and their disorders. *Int J Gynecol Pathol.* 1994;13:150–160.
4. van der Putte SC, van Gorp LH. Cysts of mammarylike glands in the vulva. *Int J Gynecol Pathol.* 1995;14:184–188.
5. van der Putte SC. Clear cells of Toker in the developing anogenital region of male and female fetuses. *Am J Dermatopathol.* 2011;33:811–818.
6. Belousova IE, Kazakov DV, Michal M, et al. Vulvar toker cells: the long-awaited missing link: a proposal for an origin-based histogenetic classification of extramammary paget disease. *Am J Dermatopathol.* 2006;28:84–86.
7. Hayes MM, Konstantinova AM, Kacerovska D, et al. Bilateral gigantomastia, multiple synchronous nodular pseudoangiomatous stromal hyper-

plasia involving breast and bilateral axillary accessory breast tissue, and perianal mammary-type hamartoma of anogenital mammary-like glands: a case report. *Am J Dermatopathol.* 2016;38:374–383.

8. Kazakov DV, Spagnolo DV, Kacerovska D, et al. Lesions of anogenital mammary-like glands: an update. *Adv Anat Pathol.* 2011;18:1–28.

9. Konstantinova AM, Michal M, Kacerovska D, et al. Hidradenoma papilliferum: a clinicopathologic study of 264 tumors from 261 patients, with emphasis on mammary-type alterations. *Am J Dermatopathol.* 2016;38:598–607.

10. Konstantinova AM, Shelekhova KV, Stewart CJ, et al. Depth and patterns of adnexal involvement in primary extramammary (anogenital) Paget disease: a study of 178 lesions from 146 patients. *Am J Dermatopathol.* 2016. [Epub ahead of print].

11. Kazakov DV, Belousova IE, Sima R, et al. Mammary type tubulolobular carcinoma of the anogenital area: report of a case of a unique tumor presumably originating in anogenital mammarylike glands. *Am J Surg Pathol.* 2006;30:1193–1196.

12. Kazakov DV, Bisceglia M, Mukensnabl P, et al. Pseudoangiomatous stromal hyperplasia in lesions involving anogenital mammary-like glands. *Am J Surg Pathol.* 2005;29:1243–1246.

13. Kazakov DV, Bisceglia M, Sima R, et al. Adenosis tumor of anogenital mammary-like glands: a case report and demonstration of clonality by HUMARA assay. *J Cutan Pathol.* 2006;33:43–46.

14. Kazakov DV, Hugel H, Vanecek T, et al. Unusual hyperplasia of anmogenital ammary-like glands. *Am J Dermatopathol.* 2006;28:134–137.

15. Kazakov DV, Mikyskova I, Kutzner H, et al. Hidradenoma papilliferum with oxyphilic metaplasia: a clinicopathological study of 18 cases, including detection of human papillomavirus. *Am J Dermatopathol.* 2005;27:102–110.

16. Kazakov DV, Spagnolo DV, Stewart CJ, et al. Fibroadenoma and phyllodes tumors of anogenital mammary-like glands: a series of 13 neoplasms in 12 cases, including mammary-type juvenile fibroadenoma, fibroadenoma with lactation changes, and neurofibromatosis-associated pseudoangiomatous stromal hyperplasia with multinucleated giant cells. *Am J Surg Pathol.* 2010;34:95–103.

17. Konstantinova AM, Hayes MM, Stewart CJ, et al. Syringomatous structures in extramammary paget disease: a potential diagnostic pitfall. *Am J Dermatopathol.* 2016;38:653–657.

18. Konstantinova AM, Kacerovska D, Michal M, et al. A tumoriform lesion of the vulva with features of mammary-type fibrocystic disease. *Am J Dermatopathol.* 2013;35:e124–127.

19. Konstantinova AM, Kacerovska D, Michal M, et al. A composite neoplastic lesion of the vulva with mixed features of fibroadenoma and hidradenoma papilliferum combined with pseudoangiomatous stromal hyperplasia containing multinucleated giant cells. *Am J Dermatopathol.* 2014;36:e171–174.

20. Konstantinova AM, Kacerovska D, Stewart CJ, et al. Syringocystadenocarcinoma papilliferum in situ-like changes in extramammary Paget disease: a report of 11 cases. *Am J Dermatopathol.* 2016. [Epub ahead of print].

21. Willman JH, Golitz LE, Fitzpatrick JE. Vulvar clear cells of Toker: precursors of extramammary Paget's disease. *Am J Dermatopathol.* 2005;27:185–188.

22. Vazmitel M, Pavlovsky M, Kacerovska D, et al. Pseudoangiomatous stromal hyperplasia in a complex neoplastic lesion involving anogenital mammary-like glands. *J Cutan Pathol.* 2009;36:1117–1120.

23. Vazmitel M, Spagnolo DV, Nemcova J, et al. Hidradenoma papilliferum with a ductal carcinoma in situ component: case report and review of the literature. *Am J Dermatopathol.* 2008;30:392–394.

24. Castro C, Deavers M. Ductal carcinoma in-situ arising in mammary-like glands of the vulva. *Int J Gynecol Pathol.* 2001;20:277–283.

25. Kennedy DA, Hermina MS, Xanos ET, et al. Infiltrating ductal carcinoma of the vulva. *Pathol Res Pract.* 1997;193:723–726.

26. Nishie W, Sawamura D, Mayuzumi M, et al. Hidradenoma papilliferum with mixed histopathologic features of syringocystadenoma papilliferum and anogenital mammary-like glands. *J Cutan Pathol.* 2004;31:561–564.

27. Offidani A, Campanati A. Papillary hidradenoma: immunohistochemical analysis of steroid receptor profile with a focus on apocrine differentiation. *J Clin Pathol.* 1999;52:829–832.

28. Tresserra F, Grases P, Izquierdo M, et al. Fibroadenoma phyllodes arising in vulvar supernumerary breast tissue: report of two cases. *Int J Gynecol Pathol.* 1998;17:171–173.

29. Bocker W, Bier B, Freytag G, et al. An immunohistochemical study of the breast using antibodies to basal and luminal keratins, alpha-smooth muscle actin, vimentin, collagen IV and laminin. Part I: normal breast and benign proliferative lesions. *Virchows Arch A Pathol Anat Histopathol.* 1992;421:315–322.

30. Yeh IT, Mies C. Application of immunohistochemistry to breast lesions. *Arch Pathol Lab Med.* 2008;132:349–358.

31. Bocker W, Moll R, Poremba C, et al. Common adult stem cells in the human breast give rise to glandular and myoepithelial cell lineages: a new cell biological concept. *Lab Invest.* 2002;82:737–746.

32. Boecker W, Buerger H. Evidence of progenitor cells of glandular and myoepithelial cell lineages in the human adult female breast epithelium: a new progenitor (adult stem) cell concept. *Cell Prolif.* 2003;36(suppl 1):73–84.

33. Bocker W, Burger H, Buchwalow IB, et al. Ck5-positive cells are precursor cells of glandular and myoepithelial cell lineages in the human breast epithelium. A new cell concept as a basis for a better understanding of proliferative breast disease? *Verh Dtsch Ges Pathol.* 2005;89:45–47.

34. Sloane JP, Ormerod MG. Distribution of epithelial membrane antigen in normal and neoplastic tissues and it value in diagnostic tumor pathology. *Cancer.* 1981;47:1786–1795.

35. Mazoujian G, Pinkus GS, Davis S, et al. Immunohistochemistry of a gross cystic disease fluid protein (GCDFP-15) of the breast. A marker of apocrine epithelium and breast carcinomas with apocrine features. *Am J Pathol.* 1983;110:105–112.

36. Sasaki E, Tsunoda N, Hatanaka Y, et al. Breast-specific expression of MGB1/mammaglobin: an examination of 480 tumors from various organs and clinicopathological analysis of MGB1-positive breast cancers. *Mod Pathol.* 2007;20:208–214.

37. Lu X, Li H, Xu K, et al. MUC-1-/ESA+ progenitor cells in normal, benign and malignant human breast epithelial cells. *Histol Histopathol.* 2009;24:1381–1390.

38. Pereira MB, Dias AJ, Reis CA, et al. Immunohistochemical study of the expression of MUC5AC and MUC6 in breast carcinomas and adjacent breast tissues. *J Clin Pathol.* 2001;54:210–213.

39. Liu H, Shi J, Wilkerson ML, et al. Immunohistochemical evaluation of GATA3 expression in tumors and normal tissues: a useful immunomarker for breast and urothelial carcinomas. *Am J Clin Pathol.* 2012;138:57–64.

40. Shan M, Zhang X, Liu X, et al. P16 and p53 play distinct roles in different subtypes of breast cancer. *PLoS One.* 2013;8:e76408.

41. Goldstein NS, Bassi D, Watts JC, et al. E-cadherin reactivity of 95 noninvasive ductal and lobular lesions of the breast. Implications for interpretation of problematic lesions. *Am J Clin Pathol.* 2001;115:534–542.

42. Barbareschi M, Maisonneuve P, Aldovini D, et al. High syndecan-1 expression in breast carcinoma is related to an aggressive phenotype and to poorer prognosis. *Cancer.* 2003;98:474–483.

43. Hussein MR, Ismael HH. Alterations of p53, Bcl-2, and hMSH2 protein expression in the normal breast, benign proliferative breast disease, in situ and infiltrating ductal breast carcinomas in the upper Egypt. *Cancer Biol Ther.* 2004;3:983–988.

44. Boland GP, Butt IS, Prasad R, et al. COX-2 expression is associated with an aggressive phenotype in ductal carcinoma in situ. *Br J Cancer* 2004;90:423–429.

45. Moskaluk CA, Zhang H, Powell SM, et al. Cdx2 protein expression in normal and malignant human tissues: an immunohistochemical survey using tissue microarrays. *Mod Pathol.* 2003;16:913–919.

46. Walsh MD, McGuckin MA, Devine PL, et al. Expression of MUC2 epithelial mucin in breast carcinoma. *J Clin Pathol.* 1993;46:922–925.

47. Kazakov DV, Michal M, Kacerovska D, et al. *Cutaneous Adnexal Tumors.* Philadelphia, PA: Lippincott Williams & Wilkins; 2012.

48. Gonzalez-Guerra E, Kutzner H, Rutten A, et al. Immunohistochemical study of calretinin in normal skin and cutaneous adnexal proliferations. *Am J Dermatopathol.* 2012;34:491–505.

49. Lugli A, Forster Y, Haas P, et al. Calretinin expression in human normal and neoplastic tissues: a tissue microarray analysis on 5233 tissue samples. *Hum Pathol.* 2003;34:994–1000.
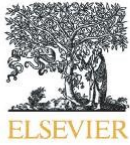
84

Molecular alterations in lesions of anogenital mammary-like glands and their mammary counterparts including hidradenoma papilliferum, intraductal papilloma, fibroadenoma and phyllodes tumor ☆

Anastasia M. Konstantinova [a,b,c], Tomas Vanecek [d,e], Petr Martinek [d,e], Liubov Kyrpychova [f], Dominic V. Spagnolo [g,h], Colin J.R. Stewart [i], Francesca Portelli [j], Michal Michal [f,k], Dmitry V. Kazakov [f,k,*]

[a] Department of Pathology, Clinical research and practical center for specialized oncological care, Saint-Petersburg, Russia
[b] Department of Pathology, Medical Faculty, Saint-Petersburg State University, Russia
[c] Department of Pathology, Medico-Social Institute, St.-Petersburg, Russia
[d] Departments of Pathology, Charles University, Medical Faculty and Charles University Hospital, Pilsen, Czech Republic
[e] Department of Molecular Genetics, Bioptical Laboratory Ltd., Pilsen, Czech Republic
[f] Sikl's Department of Pathology, Medical Faculty in Pilsen, Charles University in Prague, Pilsen, Czech Republic
[g] PathWest Laboratory Medicine WA, QEII Medical Centre, Nedlands, WA, Australia
[h] University of Western Australia, School of Pathology and Laboratory Medicine, Nedlands, WA, Australia
[i] Department of Histopathology, King Edward Memorial Hospital, Perth, Western Australia, Australia
[j] Division of Anatomic Pathology, University of Palermo, Italy
[k] Bioptical Laboratory, Pilsen, Czech Republic

ARTICLE INFO

ABSTRACT

Lesions affecting anogenital mammary–like glands (AGMLG) are histopathologically very similar to those seen in the breast but whether this morphological similarity is also reflected at the genetic level is unknown. To compare the underlying molecular mechanisms in lesions of AGMLG and their mammary counterparts, we analyzed the mutational profile of 16 anogenital neoplasms including 5 hidradenomas papilliferum (HP), 1 lesion with features of HP and fibroadenoma (FA), 7 FA, 3 phyllodes tumors (PhT)) and 18 analogous breast lesions (6 intraductal papillomas (IDP), 9 FA, and 3 PhT) by high-coverage next generation sequencing (NGS) using a panel comprising 50 cancer-related genes. Additionally, all cases were analyzed for the presence of a mutation in the *MED12* gene. All detected mutations with allele frequencies over 20% were independently validated by Sanger sequencing (concordance: 100%). Mutations in *PIK3CA, AKT1, MET, ABL1* and *TP53* genes were found in lesions of AGMLG and also their mammary counterparts. The *PI3K-AKT* cascade plays a role in tumors arising at both sites. It appears that some histopathologically similar anogenital and breast lesions develop along similar molecular pathways.

© 2017 Published by Elsevier Inc.

1. Introduction

Lesions affecting anogenital mammary–like glands (AGMLG), epithelial or mesenchymal, benign or malignant are histopathologically very similar to those encountered in the breast [1-12]. Hidradenoma papilliferum (HP), the most common benign tumor of the female anogenital area is regarded as the cutaneous counterpart of mammary intraductal papilloma (IDP) [9,13,14,15,16]. Fibroepithelial neoplasms of AGMLG including fibroadenoma (FA), lesions with features of both

HP and FA (HP/FA) and phyllodes tumor (PhT) are also microscopically identical to their mammary counterparts but are rare in comparison to their breast analogues [17]. One may speculate whether the morphological similarity between tumors of AGMLG and their mammary counterparts is also reflected at the genetic level. To compare underlying molecular mechanisms in lesions of AGMLG and their mammary counterparts, we analyzed the mutational profiles of 16 anogenital neoplasms, including HP, FA and PhT and 18 analogous breast lesions.

2. Material and methods

2.1. Case selection

Sixteen lesions of AGMLG (5 HP, 1 HP/FA, 7 FA and 3 PhT) and 18 breast neoplasms (6 IDP, 9 FA and 3 PhT) were selected from the

routine, consultation and institutional files of the authors. Hematoxy-lin–eosin–stained slides and clinical data (extracted from the medical charts) were reviewed to confirm the diagnosis. The size of the tumors, when not available in the charts, was measured on histopathological slides directly. One HP (case 5), the single HP/FA (case 12), five FA (cases 14, 16–19) and 2 PhT (cases 20 and 21) were the subjects of previous publications [9,17,18]. Cases 2 and 3 had also been previously analyzed for the presence of *BRCA1/BRCA2* founder mutations using allele-specific PCR testing [19] (Table 1).

2.2. DNA extraction

DNA was extracted from formalin-fixed, paraffin-embedded material. Genomic DNA was isolated using the NucleoSpin tissue isolation kit (Macherey-Nagel, Düren, Germany), according to the manufacturer's protocols.

2.3. Mutation screening

The concentration and purity of the isolated DNA were measured using the NanoDrop ND-1000 (NanoDrop Technologies, Inc., Wilmington, DE, USA). DNA integrity was examined by the amplification of control genes in multiplex PCR, producing fragments from 100 to 600 bp [20]. All samples were tested for hotspot mutations in *MED12*, however only cases with DNA integrity equal or higher than 200 bp were selected for mutational analysis (Table 2) using Ion AmpliSeq Cancer Hotspot Panel v2 by massively parallel sequencing on Ion Torrent PGM (Life Technologies, part of Thermo Fisher Scientific, Waltham, MA, USA). Extracted DNA (10 ng) was amplified, and adapters were ligated using the Ampliseq library preparation kit. The fusion primer library for detection of hotspot mutations in *MED12* was generated using specific primers published by Mishima et al. [21] according to the manufacturer's protocol (Life Technologies, USA). Sequencing beads were templated and enriched using the Hi-Q Template OT2 200 Kit, and sequencing was performed on 318v2 chips using the Hi-Q Sequencing kit (Life Technologies) according to manufacturer's protocols. Signal processing, mapping and quality control were performed with Torrent Suite v.5.0 (Life Technologies). Sequence variants were called using Ion Reporter v5.2 employing AmpliSeq CHPv2 single sample workflow and default settings. Variants were subsequently filtered to include only exonic, non-synonymous variants with allele frequencies >5%. All filtered variants were annotated using HGVS nomenclature according to transcripts listed in Table 2. Mutations found with at least 15% allele frequency were confirmed by Sanger sequencing.

3. Results

3.1. Clinical data

The main clinicopathological features are summarized in Table 3. All patients were females with solitary lesions in the anogenital area or breast.

3.2. Histopathological data

All HP and IDP had a similar microscopic appearance (Fig. 1A, B). They were solid-cystic nodules with a complex pattern of branching and anastomosing tubules interconnected in a labyrinthine manner, with bands of fibrous tissue between them, focally forming papillae with fibrovascular stalks invested by a layer of myoepithelial cells and overlying epithelial cells (Fig. 1). Variably present in HP and breast IDP were oxyphilic (apocrine) metaplasia (1 HP, 4 breast IDP; Fig. 1A), focal myoepithelial clear cell change (4 HP, 2 IDP), usual ductal hyperplasia (3 HP, 4 IDP), focal squamous metaplasia (1 HP) and sclerosing adenosis (1 mammary IDP).

The complex mixed HP/FA lesion of the AGMLG, which also exhibited pseudoangiomatous stromal hyperplasia (PASH), has been discussed and illustrated previously [18].

Anogenital and breast fibroepithelial neoplasms were microscopically identical (Fig. 2A, B). FA were well-circumscribed neoplasms having pericanalicular and/or intracanalicular growth patterns and lacked pleomorphism in either epithelial or stromal components (Fig. 2A, B).

One vulvar FA (case 14) had papillary architecture and showed focal lactation-like change and PASH, while case 19 had features consistent with those seen in mammary juvenile FA (discussed and illustrated previously [22]).

PhT of AGMLG and mammary PhT were histologically identical. Of the 3 PhT of AGMLG, 1 was benign whilst 2 were low- grade malignant tumors having a typical leaf-like intracanalicular growth pattern, stromal hypercellularity and variable stromal atypia (Fig. 3A, B). In all three cases, areas of PASH were identified, and two contained multinucleated giant cells as described elsewhere [17].

3.3. Molecular genetic findings (Table 3)

Sequenced cases that passed all quality controls during the library preparation and with average sequencing coverage over 1500× were labeled as positive or negative in the results, whilst the remainder were labeled as not analyzable. The resulting pathogenic or untested mutations are listed in Table 3 together with their allele frequencies detected in each sample.

Table 1
Overview of the 50 cancer genes assessed for mutations in lesions of AGMLG and their mammary counterparts.

Gene	Exon-s	Gene	Exones	Gene	Exones
ABL1	4,5,6,7	FGFR3	7,9,14,16,18	NOTCH1	26,27,34
AKT1	3,6	FLT3	11,14,16,20	NPM1	11
ALK	23,25	GNA11	5	NRAS	2,3,4
APC	16	GNAQ	5	PDGFRA	12,14,15,18
ATM	8,9,12,17,26,34,35,36,39,50,54,55,56,59,61,63	GNAS	8,9	PIK3CA	2,5,7,8,10,14,19,21
BRAF	11,15	HNF1A	3,4	PTEN	1,3,5,6,7,8
CDH1	3,8,9	HRAS	2,3	PTPN11	3,13
CDKN2A	2	IDH1	4	RB1	4,6,10,11,14,17,18,20, 21,22
CSF1R	7,22	IDH2	4	RET	10,11,13,15,16
CTNNB1	3	JAK2	14	SMAD4	3,4,5,6,8,9,10,11,12
EGFR	3,7,15,18,19,20,21	JAK3	4,13,16	SMARCB1	2,4,5,9
ERBB2	19,20,21	KDR	6,7,11,19,21, 26,27,30	SMO	3,5,6,9,11
ERBB4	3,4,6,7,8,9,15,23	KIT	2,9,10,11,13, 14,15,17,18	SRC	14
EZH2	16	KRAS	2,3,4	STK11	1,4,4/5,6,8
FBXW7	5,8,9,10,11	MET	2,11,14,16,19	TP53	2,4,5,6,7,8,10
FGFR1	4,7	MLH1	12	VLH	1,2,3
FGFR2	7,9,12	MPL	10		

Table 2
Mutated genes in lesions of AGMLG and their mammary counterparts.

Case	Location	Diagnosis	Age (years)	Tumor size (cm)	Gene* (MED12 NM_005120.2)	Mutation protein effect	Mutation cDNA reference sequence	Allele frequency (%)	Coverage	COSMIC ID
1	Vulva	HP*	25	0.8	PIK3CA (no mutation)	p.Glu545Lys	c.1633G>A NM_006218.2	33,2	945	COSM763
2	Vulva	HP	37	0.6	No mutation (no mutation)					
3	Vulva	HP	45	1.0	No mutation (no mutation)					
4	Vulva	HP	38	0.9	No mutation (no mutation)					
5	Vulva	HP	31	1.2	NA* (no mutation)					
6	Breast	IDP	68	0.6	AKT1 (no mutation)	p.Glu17Lys	c.49G>A NM_005163.2	31,7	1317	COSM33765
7	Breast	IDP	56	1.0	AKT1 (no mutation)	p.Glu17Lys	c.49G>A NM_005163.2	38,7	701	COSM33765
8	Breast	IDP	44	1.5	AKT1 (no mutation)	p.Glu17Lys	c.49G>A NM_005163.2	26,5	1421	COSM33765
9	Breast	IDP	53	1.0	No mutation (no mutation)					
10	Breast	IDP	75	0.6	NA (no mutation)					
11	Breast	IDP	50	0.5	NA (no mutation)					
12	Vulva	FA + HP	63	1.0	NP (no mutation)					
13	Perianal	FA	68	1.0	AKT1 (no mutation)	p.Glu17Lys	c.49G>A NM_005163.2	27,4	445	COSM33765
14	Vulva	FA	30	3.0	MET (no mutation)	p.Arg988Cys	c.2962C>T NM_001127500.1	47	1642	COSM1666978
15	Vulva	FA	49	0.5	NP (no mutation)					
16	Perineum	FA	42	2.0	NP (no mutation)					
17	Vulva	FA	50	3.0	NP (no mutation)					
18	Vulva	FA	45	2.5	No mutation (no mutation)					
19	Vulva	FA	45	3.0	NP (no mutation)					
20	Vulva	PhT low-grade	31	2.0	ABL1	p.Lys266Arg	c.797A>G NM_007313.2,	53	2000	no entry
					TP53 (no mutation)	p.Arg110Cys	c.328C>T NM_000546.5	7	348	COSM43682
21	Vulva	PhT low-grade	38	4.0	NA (no mutation)					
22	Perineum	PhT	44	2.6	No mutation (no mutation)					
23	Breast	FA	33	2.0	No mutation (MED12)	(p.G44D)	(c.131G>A)	(11)	(4000)	(COSM131596)
24	Breast	FA	23	2.0	NP (no mutation)					
25	Breast	FA	33	1.5	NP (no mutation)					
26	Breast	FA	37	3.5	No mutation (no mutation)					
27	Breast	FA	34	2.5	NP (no mutation)					
28	Breast	FA	22	2.0	NP (MED12)	(p.Gly44Cys)	(c.130G>T)	(21)	(37114)	(COSM131593)
29	Breast	FA	53	1.3	NA (no mutation)					
30	Breast	FA	52	1.1	NA (no mutation)					
31	Breast	FA	25	1.3	No mutation (MED12)	(p.Gly44Ser)	(c.130G>A)	(24)	(56784)	(COSM131594)
32	Breast	PhT	42	2.5	SMAD4 (No mutation)	p.Gln256Leu	c.767A>T NM_005359.5	16	553	COSM5546625
33	Breast	PhT	51	1.2	KIT	p.Asp816Asn	c.2446G>A NM_000222.2	11	249	COSM1313
					FBXW7	p.Thr482Ala	c.1444A>G NM_018315.4	6	258	COSM1169213
					RET (no mutation)	p.Ser767Asn	c.2300G>A NM_020630.4	6	180	no entry
34	Breast	PhT	48	1.5	No mutation (no mutation)					

NA – not available; NP – not performed, FA - fibroadenoma, PhT- Phyllodes tumor.
*As studied by Ion AmpliSeq Cancer Hotspot Panel v2 by massively parallel sequencing on Ion Torrent PGM.

In lesions of AGMLG, we detected mutations in 1/5 HP (20%), in 2/7 FA (28.6%) and in 1/2 low-grade malignant PhT (50%) (33% of all PhT). In breast counterparts, mutations were found in 3/6 IDP (50%) and in 2/3 benign PhT (66.7%).

Among the 50 cancer genes interrogated, a missense mutation (p.E545K) in PIK3CA was found in one HP and a recurrent missense mutation (p.E17K) in AKT1 was found in 3 breast IDP and in 1 perianal FA. A mutation in MET was found in 1 vulvar FA (case 14). One vulvar low-grade PhT (case 20) showed mutations in ABL1 (p.K247R) and TP53 (p.R110C). Mutations in KIT (p.D816N), FBXW7 (p.T482P) and RET (p.S767N) were found in one breast PhT (case 33), whereas a mutation in SMAD4 (p.Q256L) was found in another mammary PhT (case 32).

In addition, point mutations at G44 (p.G44S, p.G44C, and p.G44D) in the MED12 gene were identified in 3 of the 9 breast FA (33.3%).

Table 3
Salient clinicopathological features.

	HP	Breast intraductal papilloma	Anogenital FA and 1 HP/FA	Breast FA	Anogenital PhT	Breast PhT
Number of cases	5	6	8	9	3	3
Age, years mean (range)	35.2 (25–45)	57.7 (44–75)	49 (30–63)	34.7 (22–53)	37.7 (31–44)	47 (42–51)
Size, cm mean (range)	0.9 (0.6–1.2)	0.9 (0.5–1.5)	2 (0.5–3)	1.9 (1.1–3.5)	2.9 (2–4)	1.7 (1.2–2.5)
Location						
— Vulva	5		6		2	
— Perineum	–		1		1	
— Perianal			1		–	

*One case had combined features of HP and FA.
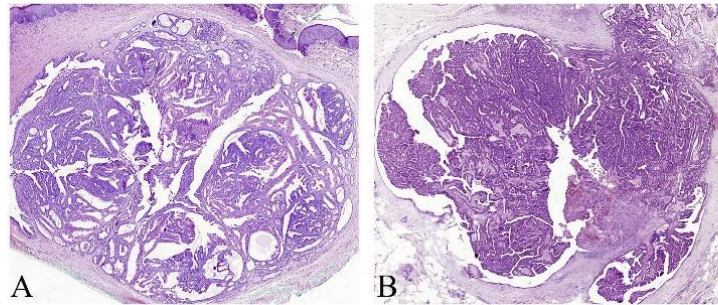
Fig. 1. Hidradenoma papilliferum (A) and breast intraductal papilloma (B) appearing as an intradermal solid-cystic neoplasm with a complex pattern of branching and anastomosing tubules and papillae. Note oxyphilic (apocrine) metaplasia in hidradenoma papilliferum (A).

All mutations with allele frequencies over 20%, were independently validated by Sanger sequencing (concordance: 100%, Fig. 4A–E).

4. Discussion

We undertook this study to determine if the morphological similarity between some neoplasms of AGMLG and their mammary counterparts might also be reflected at the genetic level. The study comprised cases of cutaneous and mammary HP/IDP, FA and PhT. Data on the molecular mechanisms driving HP are scarce, whereas there is no information regarding molecular alterations in FA and PhT of AGMLG. Previous studies of HP have found mutations in genes of the PI3K-AKT cascade [23,24,25].

The *PIK3CA* gene on chromosome 3q26.32 encodes a p110α protein which is a catalytic subunit of phosphatidylinositol 3-kinase (PI3K) [26,27]. The *AKT1* gene on chromosome 14q32.33 encodes serine/threonine-protein kinase (AKT1 kinase) [28]. The PI3K/AKT pathway is implicated in cell proliferation, protein translation, cell metabolism, and antiapoptosis [24].

Mutations involving the PI3K-AKT cascade were found in 5 (14.7%) of 34 cases. A missense mutation p.E17K in *AKT1* was found in 3 (50%) of 6 IDP and in one perianal FA (12.5%), and a p.E545K missense mutation in *PIK3CA* was found in 1 (20%) of 5 HP.

In respect of HP and IDP, *PIK3CA* and *AKT1* mutations have been detected in up to 33% of mammary IDP and in 29% (*PIK3CA*) and 14% (*AKT1*) of HP. [23] It appears that a subgroup of HP and benign papillary breast lesions are driven by mutations in the PI3K-AKT cascade with

prevalence of H1047R/L mutation in *PIK3CA* in HP and E17K mutation in *AKT1* in breast IDP [25,24,29] Mutations in *PIK3CA* have also been found in extramammary Paget disease (EMPD), invasive mammary-type adenocarcinomas, in breast ductal adenoma and in malignant PhT of the breast [19,30,31,32,33,34,35]. Mutant *AKT1* (p.E17K) has been reported in EMPD and in breast ductal adenomas [32,33]. Whilst the p.E17K mutation in *AKT1* occurs in a proportion of breast cancers, and may be a driver in some, it is a rare finding in other common malignancies including colorectal, lung, gastric and hepatocellular carcinomas and acute leukaemias [36,37].

Recurrent missense mutations p.H1047R/L and E542/5 in the oncogene *PIK3CA* are highly prevalent in breast cancer and also occur in primary ovarian, colorectal, gastric and others cancers [27,38-41].

Thus, point mutations in *PIK3CA* and *AKT1* genes of the PI3K-AKT cascade are relatively common both in tumors of AGMLG and their mammary counterparts with predominance of p.H1047R/L mutations of *PIK3CA* in HP and p.E17K mutations in *AKT1* gene in anogenital FA and breast papillomas.

In addition to the PI3K-AKT cascade, we found mutations in *MET* in 1 vulvar FA and alterations in *ABL1* and *TP53* in one vulvar PhT of low-grade malignant potential. To the best of our knowledge, mutations in *MET* and *ABL1* have not been previously reported in lesions of AGMLG nor in fibroepithelial neoplasms of the breast.

The *MET* gene on chromosome 7q21-31 encodes tyrosine-protein kinase Met (c-Met) that activates a wide range of different cellular signaling pathways including those involved in proliferation, motility, migration and invasion [42]. *MET* proto-oncogene is dysregulated in
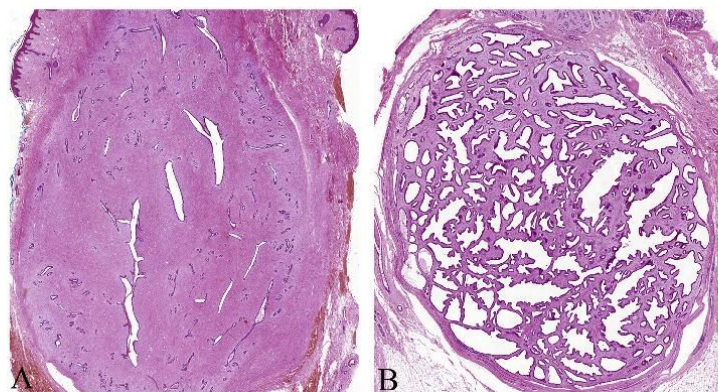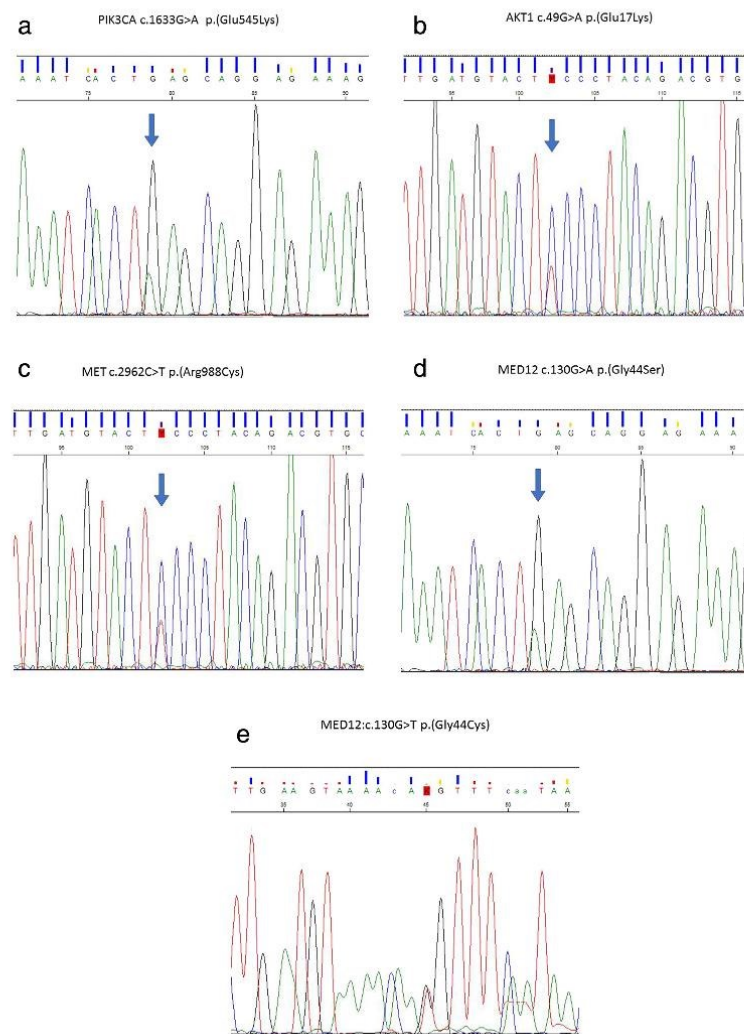

Fig. 2. Fibroadenoma of the vulva (A) and breast (B) are well-circumscribed neoplasms with no pleomorphism either in the epithelial or stromal components.
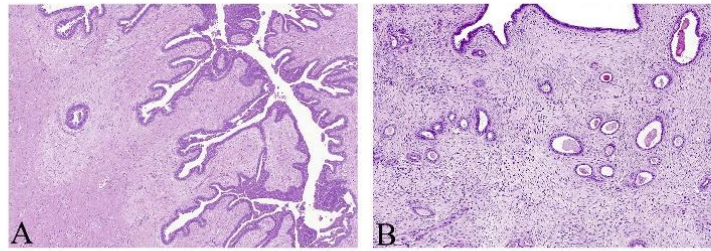
Fig. 3. Benign phyllodes tumors of the vulva (A) and breast (B) with a leaf-like intracanalicular growth pattern and stromal hypercellularity.

Fig. 4. Valiadation of detected mutations using Sanger sequencing: PIK3CA: c.1633G>A p.(Glu545Lys) (A); AKT1: c.49G>A p.(Glu17Lys) (B); MET: c.2962C>T p.(Arg988Cys) (C); MED12: c.130G>A p.(Gly44Ser) (D); MED12:c.130G>T p.(Gly44Cys) (E).

89

many types of human malignancies, including cancers of lung, kidney, liver, stomach, breast and anaplastic large cell lymphoma. (31) A mutation in *MET* has also been identified in breast tubular adenoma [33].

The *ABL1* gene located on chromosome 9q34.1 encodes protein tyrosine kinase ABL1, involved in cell differentiation, cell division, cell adhesion and stress response [43]. Alterations in proto-oncogene *ABL1* are associated with chronic myelogenous leukemia and also occur rarely in invasive breast cancer [44].

TP53 on chromosome 17p13.1 encodes the tumor suppressor protein p53 [43]. More than 50 percent of human neoplasms have mutated or deleted cellular tumor protein p53 (TP53) [45]. *TP53* is frequently mutated in malignant PhT of the breast and *TP53* mutations also occur in hereditary and nonhereditary breast cancer [34,35,46,47].

In addition to the above-mentioned mutations in lesions of AGMLG, a *BRAF V600E* mutation has been found in an HP that also had a *PIK3CA* H1047R mutation [25]. Praff et al. showed mutations in driver genes encoding *MAPK* signaling in 2 cases of HP [25].

MED12 is a human gene found on the X chromosome and it encodes the protein mediator complex subunit 12. This component of the Mediator complex is involved in the regulated transcription of nearly all RNA polymerase II-dependent genes. The MED12 domain connects cyclin C-CDK8 to the core of the mediator complex, which activates CDK8 kinase and thus regulates expression of several genes including *TP53*, *WNT*, and *SHH* in various signaling pathways [48,49].

Somatic mutations in *MED12* have not been investigated in tumors of AGMLG but have been identified in 60% of breast FA and 70% of breast PhT [35,50]. Whereas 3 of the 9 mammary FA in our study harbored a point mutation at G44, *MED12* mutations were not detected in any of the lesions of AGMLG. *MED12* mutations have also been reported in other tumor types such as hematological cancers (chronic lymphoid leukemia), uterine leiomyomas and leiomyosarcomas [51].

Two mammary PhT in our study harbored mutations in *SMAD4, KIT, RET* and *FBXW7,* whereas the samples from their anogenital homologues did not reveal alterations in these genes.

The *SMAD4* gene on chromosome 18q21.2 encodes a member of the Smad family of signal transduction proteins. SMAD 4 (DPC4) forms a complex with SMAD 3 which can bind to DNA and modify the expression of several genes related to cellular activities such as proliferation or differentiation [52]. Point mutations of *SMAD4* have only rarely been observed in breast cancer and skin melanomas [53,54].

The *KIT* gene on chromosome 4q11 encodes a receptor tyrosine kinase protein c-Kit (CD117) which plays an essential role in the regulation of cell survival and proliferation, hematopoiesis, stem cell maintenance, gametogenesis, mast cell development, migration and function and melanogenesis [55-57]. Although many fibroepithelial breast tumors and cancers express C-kit protein, *KIT* mutations in these tumors are very rare [58,59] whereas they are implicated in melanomas, especially in acral lentiginous and mucosal melanoma [60].

The *RET* proto-oncogene on chromosome 10q11.21 [61], a member of the cadherin superfamily, encodes one of the receptor tyrosine kinases, which are cell-surface molecules that transduce signals for cell growth and differentiation. This gene plays a crucial role in neural crest development, and it can undergo oncogenic activation [62,63]. Activating point mutations in *RET* can give rise to the hereditary cancer syndrome known as multiple endocrine neoplasia type 2 (MEN 2) [64]. Also mutations in *RET* were found in one case of breast cancer and in cutaneous spitzoid neoplasms and melanomas [65-67].

The *FBXW7* gene located on chromosome 4q31.3 encodes F-box/WD repeat-containing protein 7 (FBW7) [68]. FBW7 is the substrate recognition component of an evolutionarily conserved SCF (complex of SKP1, CUL1 and F-box protein)-type ubiquitin ligase that functions in cellular growth and division pathways [69].

Mutations of the tumor suppressor gene *FBXW7* have been identified in the malignant recurrence of a benign PhT of breast [70], some breast carcinomas [71] and in various cutaneous malignancies (melanomas, basal cell and squamous cell carcinomas) [72-74].

In summary, we have demonstrated various genetic alterations in a series of lesions arising from AGMLG and their mammary counterparts. We document several hitherto unreported mutations. Our study expands the spectrum of lesions of AGMLG harboring mutations in the genes encoding the PI3K-AKT cascade. *AKT1* or *PIK3CA* mutation of PI3K-AKT cascade plays a role both in tumors of AGMLG and their mammary counterparts. We provide evidence that some histopathologically similar anogenital and breast lesions appear to develop along similar molecular pathways. Of note, most mutations have been identified in several genes coding for various kinases. Whilst most tumors in our study were benign, future studies may reveal kinase gene mutations in malignant neoplasms as well (for example malignant PhT). This provides a potential for the use of targeted or multi-kinase inhibitors in the treatment of these neoplasms.

References

[1] Van der Putte S. Anogenital "sweat" glands. Histology and pathology of a gland that may mimic mammary glands. Am J Dermatopathol 1991;13:557–67.
[2] Van der Putte S. Mammary-like glands of the vulva and their disorders. Int J Gynecol Pathol 1994;13:150–60.
[3] Belousova IE, Kazakov DV, Michal M, Suster S. Vulvar toker cells: the long-awaited missing link: a proposal for an origin-based histogenetic classification of extramammary Paget disease. Am J Dermatopathol 2006;28:84–6.
[4] Kazakov DV, Bisceglia M, Mukensnabl P, Michal M. Pseudoangiomatous stromal hyperplasia in lesions involving anogenital mammary-like glands. Am J Surg Pathol 2005;29:1243–6.
[5] Kazakov DV, Bisceglia M, Sima R, Michal M. Adenosis tumor of anogenital mammary-like glands: a case report and demonstration of clonality by HUMARA assay. J Cutan Pathol 2006;33:43–6.
[6] Kazakov DV, Hugel H, Vanecek T, Michal M. Unusual hyperplasia of anogenital mammary-like glands. Am J Dermatopathol 2006;28:134–7.
[7] Hayes MM, Konstantinova AM, Kacerovska D, Michal M, Kreuzberg B, Suvova B, et al. Bilateral gigantomastia, multiple synchronous nodular pseudoangiomatous stromal hyperplasia involving breast and bilateral axillary accessory breast tissue, and perianal mammary-type hamartoma of anogenital mammary-like glands: a case report. Am J Dermatopathol 2016;38:374–83.
[8] Konstantinova AM, Kacerovska D, Michal M, Kazakov DV. A tumoriform lesion of the vulva with features of mammary-type fibrocystic disease. Am J Dermatopathol 2013;35:e124–7.
[9] Konstantinova AM, Michal M, Kacerovska D, Spagnolo DV, Stewart CJ, Kutzner H, et al. Hidradenoma papilliferum: a clinicopathologic study of 264 tumors from 261 patients, with emphasis on mammary-type alterations. Am J Dermatopathol 2016;38:598–607.
[10] Vazmitel M, Pavlovsky M, Kacerovska D, Michal M, Kazakov DV. Pseudoangiomatous stromal hyperplasia in a complex neoplastic lesion involving anogenital mammary-like glands. J Cutan Pathol 2009;36:1117–20.
[11] Vazmitel M, Spagnolo DV, Nemcova J, Michal M, Kazakov DV. Hidradenoma papilliferum with a ductal carcinoma in situ component: case report and review of the literature. Am J Dermatopathol 2008;30:392–4.
[12] Konstantinova AM, Kyrpychova L, Belousova IE, Spagnolo DV, Kacerovska D, Michal M, et al. Anogenital mammary-like glands: a study of their normal histology with emphasis on glandular depth, presence of columnar epithelial cells, and distribution of elastic fibers. Am J Dermatopathol 2016.
[13] Meeker JH, Neubecker RD, Helwig EB. Hidradenoma papilliferum. Am J Clin Pathol 1962;37:182–95.
[14] Kazakov DV, Mikyskova I, Kutzner H, Simpson RH, Hes O, Mukensnabl P, et al. Hidradenoma papilliferum with oxyphilic metaplasia: a clinicopathological study of 18 cases, including detection of human papillomavirus. Am J Dermatopathol 2005;27:102–10.
[15] Sington J, Chandrapala R, Manek S, Hollowood K. Mitotic count is not predictive of clinical behavior in hidradenoma papilliferum of the vulva: a clinicopathologic study of 19 cases. Am J Dermatopathol 2006;28:322–6.
[16] Scurry J, van der Putte SC, Pyman J, Chetty N, Szabo R. Mammary-like gland adenoma of the vulva: review of 46 cases. Pathology 2009;41:372–8.
[17] Kazakov DV, Spagnolo DV, Stewart CJ, Thompson J, Agaimy A, Magro G, et al. Fibroadenoma and phyllodes tumors of anogenital mammary-like glands: a series of 13 neoplasms in 12 cases, including mammary-type juvenile fibroadenoma, fibroadenoma with lactation changes, and neurofibromatosis-associated pseudoangiomatous stromal hyperplasia with multinucleated giant cells. Am J Surg Pathol 2010;34:95–103.
[18] Konstantinova AM, Kacerovska D, Michal M, Kazakov DV. A composite neoplastic lesion of the vulva with mixed features of fibroadenoma and hidradenoma papilliferum combined with pseudoangiomatous stromal hyperplasia containing multinucleated giant cells. Am J Dermatopathol 2014;36:e171–4.
[19] Konstantinova AM, Shelekhova KV, Imyanitov EN, Iyevleva AG, Kacerovska D, Michal M, et al. Study of selected BRCA1, BRCA2 and PIK3CA mutations in benign and malignant lesions of anogenital mammary-like glands. Am J Dermatopathol 2016 (accepted for publication).
[20] van Dongen JJ, Langerak AW, Bruggemann M, Evans PA, Hummel M, Lavender FL, et al. Design and standardization of PCR primers and protocols for detection of clonal

immunoglobulin and T-cell receptor gene recombinations in suspect lymphoproliferations: report of the BIOMED-2 concerted action BMH4-CT98-3936. Leukemia 2003;17:2257–317.

[21] Mishima C, Kagara N, Tanei T, Naoi Y, Shimoda M, Shimomura A, et al. Mutational analysis of MED12 in fibroadenomas and phyllodes tumors of the breast by means of targeted next-generation sequencing. Breast Cancer Res Treat 2015;152:305–12.

[22] Kazakov DV, Spagnolo DV, Kacerovska D, Michal M. Lesions of anogenital mammary-like glands: an update. Adv Anat Pathol 2011;18:1–28.

[23] Goto K, Maeda D, Kudo-Asabe Y, Hibiya T, Hayashi A, Fukayama M, et al. PIK3CA and AKT1 mutations in hidradenoma papilliferum. J Clin Pathol 2016.

[24] Liau JY, Lan J, Hong JB, Tsai JH, Kuo KT, Chu CY, et al. Frequent PIK3CA-activating mutations in hidradenoma papilliferums. Hum Pathol 2016;55:57–62.

[25] Pfarr N, Sinn HP, Klauschen F, Flechtenmacher C, Bockmayr M, Ridinger K, et al. Mutations in genes encoding PI3K-AKT and MAPK signaling define anogenital papillary hidradenoma. Genes Chromosomes Cancer 2016;55:113–9.

[26] Hiles ID, Otsu M, Volinia S, Fry MJ, Gout I, Dhand R, et al. Phosphatidylinositol 3-kinase: structure and expression of the 110 kd catalytic subunit. Cell 1992;70:419–29.

[27] Karakas B, Bachman KE, Park BH. Mutation of the PIK3CA oncogene in human cancers. Br J Cancer 2006;94:455–9.

[28] Staal SP, Huebner K, Croce CM, Parsa NZ, Testa JR. The AKT1 proto-oncogene maps to human chromosome 14, band q32. Genomics 1988;2:96–8.

[29] Troxell ML, Levine J, Beadling C, Warrick A, Dunlap J, Presnell A, et al. High prevalence of PIK3CA/AKT pathway mutations in papillary neoplasms of the breast. Mod Pathol 2010;23:27–37.

[30] Barth P, Dulaimi Al-Saleem E, Edwards KW, Millis SZ, Wong YN, Geynisman DM. Metastatic extramammary Paget's disease of scrotum responds completely to single agent trastuzumab in a hemodialysis patient: case report, molecular profiling and brief review of the literature. Case Rep Oncol Med 2015;2015:895151.

[31] Kang Z, Xu F, Zhang QA, Lin J, Wu Z, Zhang X, et al. Correlation of DLC1 gene methylation with oncogenic PIK3CA mutations in extramammary Paget's disease. Mod Pathol 2012;25:1160–8.

[32] Kang Z, Xu F, Zhang QA, Wu Z, Zhang X, Xu J, et al. Oncogenic mutations in extramammary Paget's disease and their clinical relevance. Int J Cancer 2013;132:824–31.

[33] Volckmar AL, Leichsenring J, Flechtenmacher C, Pfarr N, Siebolts U, Kirchner M, et al. Tubular, lactating, and ductal adenomas are devoid of MED12 Exon2 mutations, and ductal adenomas show recurrent mutations in GNAS and the PI3K-AKT pathway. Genes Chromosomes Cancer 2017;56:11–7.

[34] Liu SY, Joseph NM, Ravindranathan A, Stohr BA, Greenland NY, Vohra P, et al. Genomic profiling of malignant phyllodes tumors reveals aberrations in FGFR1 and PI-3 kinase/RAS signaling pathways and provides insights into intratumoral heterogeneity. Mod Pathol 2016;29:1012–27.

[35] Tan J, Ong CK, Lim WK, Ng CC, Thike AA, Ng LM, et al. Genomic landscapes of breast fibroepithelial tumors. Nat Genet 2015;47:1341–5.

[36] Kim MS, Jeong EG, Yoo NJ, Lee SH. Mutational analysis of oncogenic AKT E17K mutation in common solid cancers and acute leukaemias. Br J Cancer 2008;98:1533–5.

[37] Dunlap J, Le C, Shukla A, Patterson J, Presnell A, Heinrich MC, et al. Phosphatidylinositol-3-kinase and AKT1 mutations occur early in breast carcinoma. Breast Cancer Res Treat 2010;120:409–18.

[38] Bachman KE, Argani P, Samuels Y, Silliman N, Ptak J, Szabo S, et al. The PIK3CA gene is mutated with high frequency in human breast cancers. Cancer Biol Ther 2004;3:772–5.

[39] Dillon RL, White DE, Muller WJ. The phosphatidyl inositol 3-kinase signaling network: implications for human breast cancer. Oncogene 2007;26:1338–45.

[40] Stemke-Hale K, Gonzalez-Angulo AM, Lluch A, Neve RM, Kuo WL, Davies M, et al. An integrative genomic and proteomic analysis of PIK3CA, PTEN, and AKT mutations in breast cancer. Cancer Res 2008;68:6084–91.

[41] Tserga A, Chatziandreou I, Michalopoulos NV, Patsouris E, Saetta AA. Mutation of genes of the PI3K/AKT pathway in breast cancer supports their potential importance as biomarker for breast cancer aggressiveness. Virchows Arch 2016;469:35–43.

[42] Organ SL, Tsao MS. An overview of the c-MET signaling pathway. Ther Adv Med Oncol 2011;3:S7–S19.

[43] Surget S, Khoury MP, Bourdon JC. Uncovering the role of p53 splice variants in human malignancy: a clinical perspective. Onco Targets Ther 2013;7:57–68.

[44] Greuber EK, Smith-Pearson P, Wang J, Pendergast AM. Role of ABL family kinases in cancer: from leukaemia to solid tumours. Nat Rev Cancer 2013;13:559–71.

[45] Hollstein M, Soussi T, Thomas G, von Brevern MC, Bartsch. P53 gene alterations in human tumors: perspectives for cancer control. Recent Results Cancer Res 1997;143:369–89.

[46] Cani AK, Hovelson DH, McDaniel AS, Sadis S, Haller MJ, Yadati V, et al. Next-gen sequencing exposes frequent MED12 mutations and actionable therapeutic targets in phyllodes tumors. Mol Cancer Res 2015;13:613–9.

[47] Greenblatt MS, Chappuis PO, Bond JP, Hamel N, Foulkes WD. TP53 mutations in breast cancer associated with BRCA1 or BRCA2 germ-line mutations: distinctive spectrum and structural distribution. Cancer Res 2001;61:4092–7.

[48] Borggrefe T, Yue X. Interactions between subunits of the mediator complex with gene-specific transcription factors. Semin Cell Dev Biol 2011;22:759–68.

[49] Spaeth JM, Kim NH, Boyer TG. Mediator and human disease. Semin Cell Dev Biol 2011;22:776–87.

[50] Piscuoglio S, Murray M, Fusco N, Marchio C, Loo FL, Martelotto LG, et al. MED12 somatic mutations in fibroadenomas and phyllodes tumours of the breast. Histopathology 2015;67:719–29.

[51] Lae M, Gardrat S, Rondeau S, Richardot C, Caly M, Chemlali W, et al. MED12 mutations in breast phyllodes tumors: evidence of temporal tumoral heterogeneity and identification of associated critical signaling pathways. Oncotarget 2016;7:84428–38.

[52] Lin X, Liang M, Liang YY, Brunicardi FC, Melchior F, Feng XH. Activation of transforming growth factor-beta signaling by SUMO-1 modification of tumor suppressor Smad4/DPC4. J Biol Chem 2003;278:18714–9.

[53] Schutte M, Hruban RH, Hedrick L, Cho KR, Nadasdy GM, Weinstein CL, et al. DPC4 gene in various tumor types. Cancer Res 1996;56:2527–30.

[54] Riggins GJ, Kinzler KW, Vogelstein B, Thiagalingam S. Frequency of Smad gene mutations in human cancers. Cancer Res 1997;57:2578–80.

[55] Andre C, Hampe A, Lachaume P, Martin E, Wang XP, Manus V, et al. Sequence analysis of two genomic regions containing the KIT and the FMS receptor tyrosine kinase genes. Genomics 1997;39:216–26.

[56] Edling CE, Hallberg B. c-Kit—a hematopoietic cell essential receptor tyrosine kinase. Int J Biochem Cell Biol 2007;39:1995–8.

[57] Ray P, Krishnamoorthy N, Ray A. Emerging functions of c-kit and its ligand stem cell factor in dendritic cells: regulators of T cell differentiation. Cell Cycle 2008;7:2826–32.

[58] Djordjevic B, Hanna WM. Expression of c-kit in fibroepithelial lesions of the breast is a mast cell phenomenon. Mod Pathol 2008;21:1238–45.

[59] Zhu Y, Wang Y, Guan B, Rao Q, Wang J, Ma H, et al. C-kit and PDGFRA gene mutations in triple negative breast cancer. Int J Clin Exp Pathol 2014;7:4280–5.

[60] Hodi FS, Corless CL, Giobbie-Hurder A, Fletcher JA, Zhu M, Marino-Enriquez A, et al. Imatinib for melanomas harboring mutationally activated or amplified KIT arising on mucosal, acral, and chronically sun-damaged skin. J Clin Oncol 2013;31:3182–90.

[61] Ceccherini I, Bocciardi R, Luo Y, Pasini B, Hofstra R, Takahashi M, et al. Exon structure and flanking intronic sequences of the human RET proto-oncogene. Biochem Biophys Res Commun 1993;196:1288–95.

[62] Knowles PP, Murray-Rust J, Kjaer S, Scott RP, Hanrahan S, Santoro M, et al. Structure and chemical inhibition of the RET tyrosine kinase domain. J Biol Chem 2006;281:33577–87.

[63] Arighi E, Borrello MG, Sariola H. RET tyrosine kinase signaling in development and cancer. Cytokine Growth Factor Rev 2005;16:441–67.

[64] Qi XP, Ma JM, Du ZF, Ying RB, Fei J, Jin HY, et al. RET germline mutations identified by exome sequencing in a Chinese multiple endocrine neoplasia type 2A/familial medullary thyroid carcinoma family. PLoS One 2011;6:e20353.

[65] Yablonski-Peretz T, Paluch-Shimon S, Gutman LS, Kaplan Y, Dvir A, Barnes-Kedar I, et al. Screening for germline mutations in breast/ovarian cancer susceptibility genes in high-risk families in Israel. Breast Cancer Res Treat 2016;155:133–8.

[66] Wiesner T, Kutzner H. Morphological and genetic aspects of Spitz tumors. Pathologe 2015;36:37–43 [45].

[67] Miller DD, Emley A, Yang S, Richards JE, Lee JE, Deng A, et al. Mixed versus pure variants of desmoplastic melanoma: a genetic and immunohistochemical appraisal. Mod Pathol 2012;25:505–15.

[68] Winston JT, Koepp DM, Zhu C, Elledge SJ, Harper JW. A family of mammalian F-box proteins. Curr Biol 1999;9:1180–2.

[69] Welcker M, Clurman BE. FBW7 ubiquitin ligase: a tumour suppressor at the crossroads of cell division, growth and differentiation. Nat Rev Cancer 2008;8:83–93.

[70] Muller KE, Tafe LJ, de Abreu FB, Peterson JD, Wells WA, Barth RJ, et al. Benign phyllodes tumor of the breast recurring as a malignant phyllodes tumor and spindle cell metaplastic carcinoma. Hum Pathol 2015;46:327–33.

[71] Akhoondi S, Lindstrom L, Widschwendter M, Corcoran M, Bergh J, Spruck C, et al. Inactivation of FBXW7/hCDC4-beta expression by promoter hypermethylation is associated with favorable prognosis in primary breast cancer. Breast Cancer Res 2010;12:R105.

[72] Aydin IT, Melamed RD, Adams SJ, Castillo-Martin M, Demir A, Bryk D, et al. FBXW7 mutations in melanoma and a new therapeutic paradigm. J Natl Cancer Inst 2014;106:dju107.

[73] Bonilla X, Parmentier L, King B, Bezrukov F, Kaya G, Zoete V, et al. Genomic analysis identifies new drivers and progression pathways in skin basal cell carcinoma. Nat Genet 2016;48:398–406.

[74] Al-Rohil RN, Tarasen AJ, Carlson JA, Wang K, Johnson A, Yelensky R, et al. Evaluation of 122 advanced-stage cutaneous squamous cell carcinomas by comprehensive genomic profiling opens the door for new routes to targeted therapies. Cancer 2016;122:249–57.

Spectrum of Changes in Anogenital Mammary-like Glands in Primary Extramammary (Anogenital) Paget Disease and Their Possible Role in the Pathogenesis of the Disease

Anastasia M. Konstantinova, MD, PhD,*†‡ Dominic V. Spagnolo, MBBS, FRCPA,§||
Colin J.R. Stewart, FRCPA,¶ Denisa Kacerovska, MD, PhD,#** Ksenya V. Shelekhova, MD, PhD,*‡
Jose A. Plaza, MD,†† Saul Suster, MD,‡‡ Jiri Bouda, MD, PhD,§§ Liubov Kyrpychova, MD,#
Michal Michal, MD,#** Irena E. Belousova, MD, PhD,*‡||| Katrin Kerl, MD,¶¶
and Dmitry V. Kazakov, MD, PhD#¶¶

Abstract: To determine whether a subset of primary extramammary Paget disease (EMPD) may originate in anogenital mammary-like glands (AGMLG), the authors studied 181 specimens of EMPD, detailing alterations in AGMLG. The latter were identified in 33 specimens from 31 patients. All patients were women, ranging in age from 38 to 93 years (median, 65 y). In all cases, lesions involved the vulva and in 1 patient the perianal skin was affected. Histopathologically, AGMLG manifested changes identical to columnar cell change (CCC) (87.1%), usual ductal hyperplasia (22.6%), columnar cell hyperplasia (CCH) (9.7%), oxyphilic (apocrine) metaplasia (6.5%), and atypical duct hyperplasia (3.2%). Four cases (12.9%), in addition to intraepidermal carcinoma, harbored invasive carcinoma. In all 4 of these, AGMLG displayed a range of alterations including ductal carcinoma in situ, CCC, and CCH. Three further cases (9.7%) showed ductal carcinoma in situ without any definite invasive carcinoma. Colonization of AGMLG by neoplastic Paget cells was noted in 6 cases. As CCC and CCH may be encountered in normal AGMLG, these alterations are unlikely to play a significant role in the pathogenesis of the disease. However, by analogy with mammary Paget disease, rare cases of primary EMPD may originate in AGMLG with a subsequent upward migration of the neoplastic cells into the epidermis and possible later breach through the basal membrane. Usual ductal hyperplasia and atypical duct hyperplasia can then be regarded as earlier precursor lesions, linking both ends of the spectrum.

Key Words: anogenital mammary-like glands, extramammary Paget disease, vulva, columnar cell change, columnar cell hyperplasia, ductal hyperplasia, mammary-type carcinoma

(*Am J Surg Pathol* 2017;41:1053–1058)

From the *Department of Pathology, Clinical Research and Practical Center for Specialized Oncological Care; †Department of Pathology, Medical Faculty, Saint-Petersburg State University; ‡Department of Pathology, Saint-Petersburg Medico-Social Institute; ||Department of Dermatology, Medical Military Academy, Saint Petersburg, Russia; §PathWest Laboratory Medicine WA, QEII Medical Centre; ||School of Pathology and Laboratory Medicine, University of Western Australia, Nedlands; ¶PathWest Laboratory Medicine WA, King Edward Memorial Hospital, Perth, WA, Australia; #Sikl's Department of Pathology, Medical Faculty in Pilsen, Charles University in Prague; **Bioptical Laboratory; §§Department of Obstetrics and Gynecology, Charles University Medical Faculty Hospital, Pilsen, Czech Republic; ††Miraca Life Science, Irving, TX; ‡‡Department of Pathology, Division of Dermatopathology, Medical College of Wisconsin, Milwaukee, WI; and ¶¶Dermatopathology Unit, Department of Dermatology, Zurich University Hospital, Zurich, Switzerland.

Extramammary Paget disease (EMPD) is a rare neoplasm usually involving the anogenital area, most commonly the vulva.[1] EMPD can be divided into primary and secondary forms, the latter representing intraepithelial spread of an underlying carcinoma arising in the urogenital or gastrointestinal tracts.[2–5] The histogenesis of primary EMPD is uncertain. Cutaneous adnexa, clear cells of Toker, pluripotent stem cells, and anogenital mammary-like glands (AGMLG) have been proposed as possible sites of origin.[2,6–18]

Unlike in mammary Paget disease (MPD), underlying ductal carcinoma in situ (DCIS) or invasive mammary-type carcinoma are rarely associated with primary EMPD,[2,19–21] but, when present, they raise the likelihood that the pathogenesis of EMPD in these cases may be identical to that of MPD.[2] In addition to DCIS, AGMLG in cases of primary EMPD may show changes identical to those affecting ducts in the breast, including columnar cell change (CCC), columnar cell hyperplasia (CCH), usual ductal hyperplasia (UDH), and atypical duct hyperplasia (ADH).[2,7] Further, AGMLG may represent a path for carcinomatous spread into deeper tissues.[2,7,22]

The goals of our study were to identify and describe the spectrum of involvement of AGMLG and their ducts in cases of primary anogenital EMPD, and to determine

whether a subset of primary EMPD may originate in AGMLG, analogous to breast carcinoma.

MATERIALS AND METHODS

Case Selection

A search in the consultation, routine institutional, and personal files of the authors between 1993 and 2016 years yielded 202 cases coded as EMPD. Histologic slides were reviewed along with the available clinical information obtained from patients' medical records to confirm the location and the clinicopathologic context. Only cases of primary anogenital EMPD were included. Excluded from the study were 21 cases of secondary EMPD arising from carcinomas of other primary sites (rectum, urethra, prostate, etc.) and cases with insufficient clinical data.

Light Microscopy

The study was based on the assessment of hematoxylin and eosin–stained slides. All specimens were local resections, wide surgical excisions, or vulvectomies. We determined the presence and nature of involvement of AGMLG and their ducts in 181 specimens from 150 patients. Of the 181 specimens, 102 were wide surgical excisions, local resections, or vulvectomies (the number of tissue blocks ranged from 1 to 59; median, 10) and 79 were small specimens (punch, or small incisional biopsies, with a single block per case).

The following features were assessed using the same criteria applied in breast pathology[23-25]: oxyphilic metaplasia, CCC, CCH, UDH, ADH, DCIS, and colonization of AGMLG by carcinoma cells. Oxyphilic metaplasia manifests as cells with eosinophilic, glassy cytoplasm, which may have mildly pleomorphic nuclei and conspicuous nucleoli. CCC presents as variably dilated lumina lined by 1 to 2 layers of columnar epithelial cells oriented perpendicularly to the basement membrane and which have apical cytoplasmic blebs or snouts. CCH has variably dilated lumina lined by >2 layers of columnar epithelial cells as described for CCC. UDH shows solid or fenestrated intraluminal streaming cellular proliferation without atypia. ADH was defined as a marked intraluminal proliferation of uniform cuboidal epithelial cells with increased nuclear to cytoplasmic ratio, forming complex

architectural patterns including micropapillae, true papillae, cribriform spaces with Roman bridges but with mild or no cytologic atypia.[2] DCIS was defined according to Rosai, including papillary, comedocarcinoma, solid, cribriform, micropapillary, clinging, and cystic hypersecretory variants.[23] Grading of DCIS of AGMLG was according to published criteria.[26] For EMPD having both invasive carcinoma and DCIS, grading of the invasive carcinoma was performed according to the Nottingham system (Elston-Ellis modification of Scarff-Bloom-Richardson grading system).[25]

All the specimens were reviewed by a general pathologist (A.M.K.), dermatopathologist (D.V.K.), and an expert in mammary pathology (M.M.). The number of tissue blocks with changes in AGMLG ranged from 1 to 12 (median, 3) per case. All patients were women, ranging in age from 38 to 93 years (median, 65 y; mean, 64.2 y). The age of the patients was unknown in 2 cases.

All included patients were the subjects of previous publications addressing various other clinicopathologic aspects of AGMLG and EMPD.[7,22,27–29]

RESULTS

The main clinical and morphologic findings are summarized in Table 1. All lesions involved the vulva other than 1 case of UDH in the perianal skin. Alterations of AGMLG were found in 33 specimens from 31 patients. In 29 cases, the carcinoma was confined to the epidermis (in situ), whereas in the remaining 4 there was stromal microinvasion defined as invasion to a depth of no >1 mm.[30] The most common change encountered in AGMLG was CCC (87.1%) (Fig. 1). Less frequently found were UDH (22.6%), CCH (9.7%), oxyphilic (apocrine) metaplasia (6.5%), and ADH (3.2%) (Figs. 2–4). Four cases (12.9%), in addition to intraepidermal carcinoma, harbored invasive carcinoma resembling breast carcinoma (3 with invasive carcinoma of no special type [NST] [previously known as ductal carcinoma]; 1 with a tubulolobular carcinoma). In all 4 cases AGMLG displayed a range of changes including DCIS (1 case), CCC (2 cases), and CCC combined with CCH (1 case) (Figs. 5, 6). In a further 3 cases (9.7%), DCIS without definite invasion was recognized. In 2 of these, adjacent to DCIS were areas of fibrosis and elastosis, as may be found in mammary invasive carcinoma, NST (Fig. 7). DCIS morphology included solid growth with

TABLE 1. Summary of the Main Clinicopathologic Features

| Type of Change in AGMLG	No. Cases	Other Changes in AGMLG (No. Cases)	Age (y)/Median (Range)
CCC	12	—	68 (49-86) Unknown in 1 case
CCH	2	CCC (2)	61 (57-65)
UDH	5	CCC (4), OM (1)	70 (59-93)
DCIS, G2-3	3	CCC (3), AGMLG colonization (1)	51 (40-56)
ICNST, G3, and DCIS	1		74
Invasive mammary-type carcinomas, G2-3 incl. ICNST (2) and TLC (1)	3	CCC (3), CCH (1)	78 (38-78)
Colonization by neoplastic cells	5	CCC (3), UDH (2), ADH (1), OM (1)	51.5 (47-75) Unknown in 1 case

ICNST indicates invasive carcinoma, no special type (previously known as invasive ductal carcinoma); OM, oxyphilic metaplasia; TLC, tubulolobular carcinoma.

93
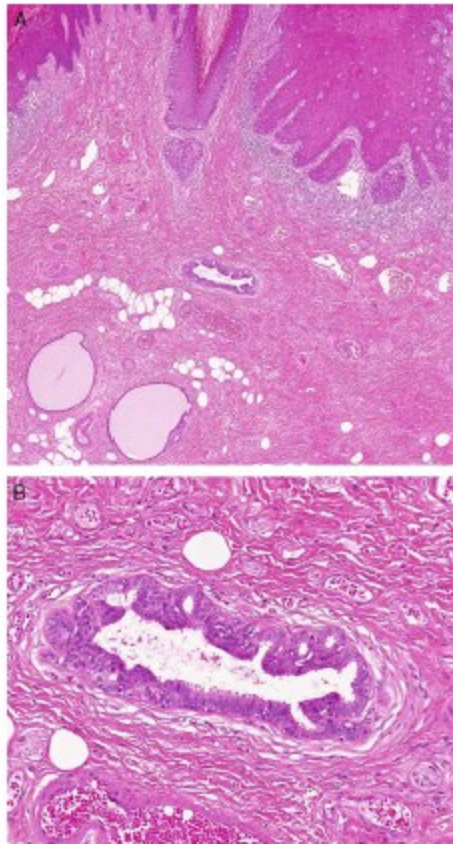
FIGURE 1. A and B, CCC of AGMLG in EMPD. Note a lumen of the gland lined by 1 to 2 cell layers of elongated to ovoid columnar epithelial cells oriented perpendicularly to the basement membrane, having apical cytoplasmic snouts.

or without comedonecrosis or a micropapillary pattern, and was of grade 2 to 3. The invasive carcinomas also were grade 2 or 3. Colonization of AGMLG by neoplastic Paget cells was noted in 6 cases (Fig. 8). In 3, single cells or small clusters of neoplastic cells focally infiltrated the glandular portion of AGMLG. One case each, respectively, showed extensive single cell infiltration of neoplastic cells beneath a preserved luminal layer in an excretory duct, similar extensive single cell infiltration in both glandular and excretory duct elements, and almost complete replacement of normal glandular luminal epithelium by solid and cribriform formations of Paget cells, with a preserved peripheral myoepithelial cell layer, occasioning resemblance to DCIS. In a further case with DCIS, there was also extensive colonization of AGMLG.
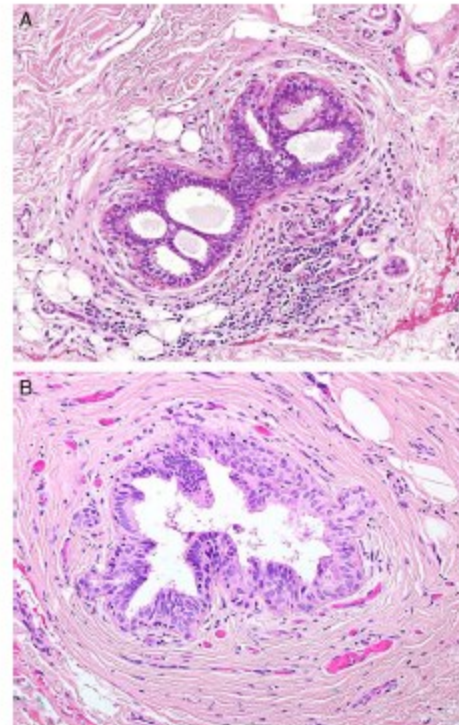

FIGURE 2. UDH of AGMLG showing irregularly shaped bridges connecting opposite portions of the wall (A) or intraluminal proliferations of relatively monomorphic cells (B).

DISCUSSION

We found alterations of AGMLG in 33 of 181 specimens (18.2%) although the actual figure may be higher, as some specimens (small biopsies) lacked AGMLG. From our findings, there seems to be a spectrum of ductal lesions ranging from CCC and CCH via UDH/ADH to DCIS and invasive carcinoma. The question is whether this finding allows a bona fide conclusion that a subset of primary EMPD may originate in AGMLG. Although in the breast, low level allelic imbalance was demonstrated in columnar cell lesions,[31] our recent study suggested that CCC and CCH may occur normally in AGMLG, as they were seen in approximately 30% and 10% of cases, respectively.[32] Admittedly, no molecular biological studies were carried out for comparison with the breast data. More remarkable is that CCC in AGMLG in the setting of EMPD is much more frequent than in "normal" AGMLG (87% vs. 33%, respectively).[32]
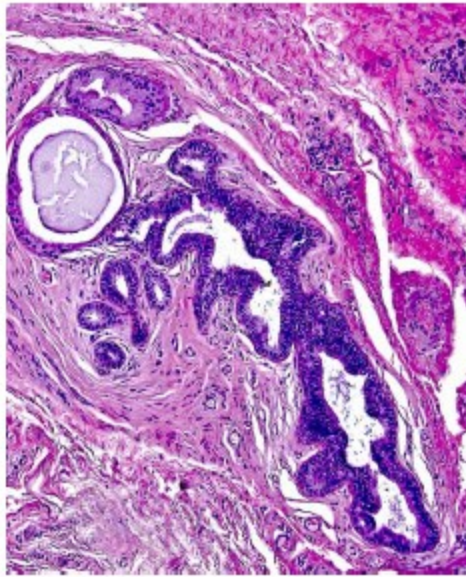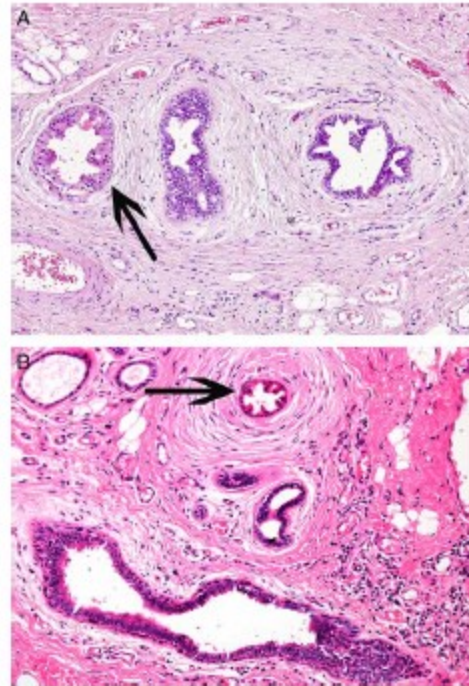
FIGURE 3. CCH of AGMLG. Note the lumina lined by >2 cell layers of elongated to ovoid columnar epithelial cells oriented perpendicularly to the basement membrane, having apical cytoplasmic snouts.

FIGURE 4. A and B, Oxyphilic metaplasia of AGMLG. Note cells with eosinophilic, glassy cytoplasm in 2 glands (arrows).

In this series, there were 4 cases of invasive mammary-type carcinomas of AGMLG and 3 cases of DCIS, suggesting that in these cases the carcinoma may have originated in AGMLG, with subsequent upward migration of the neoplastic cells into the epidermis, similar to cases of so-called invasive MPD.[7,33] In 2 of these cases, there was elastosis near the DCIS that may be a sign of stromal invasion analogous to the situation in the breast in which an invasive carcinoma of NST may elicit prominent elastosis, at times so prominent as to be appreciated grossly as white chalky streaks. If one accepts the occurrence of DCIS and invasive carcinoma as 1 path of tumor progression in EMPD, then UDH and ADH might reasonably be interpreted as precursor lesions.

In contrast, we have previously shown that cutaneous adnexa including hair follicles, sebaceous glands, and apocrine and eccrine units may present a path for carcinomatous spread into deeper tissues in cases of EMPD, as they are involved in almost all cases.[7,22] A similar situation may be presumed with respect to AGMLG. We noticed several patterns of colonization of AGMLG by neoplastic cells. Both ductal and/or glandular components were focally or diffusely infiltrated by neoplastic cells with preservation of the normal luminal cells or, as seen in one case, there was almost complete replacement of the normal luminal epithelium by solid or cribriform formations of Paget cells above a preserved peripheral myoepithelial cell layer resembling DCIS. In the latter case, it may be difficult or impossible to determine whether DCIS is the source of the EMPD or the result of colonization of these glands by the neoplastic cells of EMPD. Although we arbitrarily considered single cell spread of Paget cells in AGMLG as colonization, we cannot completely exclude that this may be an incipient (in situ) carcinomatous change within AGMLG or the result of a field effect. One can argue that the similar occurrence in cutaneous adnexa may occasion the same conclusion, but the absence of lesions compatible with DCIS in eccrine/apocrine units and involvement of different adnexa (sebaceous glands, hair follicles, etc.) militate against an adnexal origin.

In conclusion, AGMLG in primary EMPD manifest a range of changes analogous to those occurring in the breast and which may be regarded as a morphologic spectrum. As CCC and CCH may be encountered in normal AGMLG, these alterations would seem to play little, if any, role in the pathogenesis of EMPD.
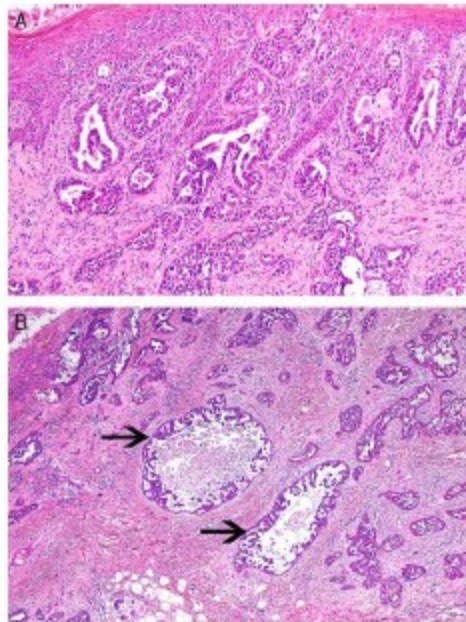
FIGURE 5. EMPD associated with underlying mammary-type invasive carcinoma of NST (previously called invasive ductal carcinoma) (A). Note DCIS of micropapillary type (arrows) (B).
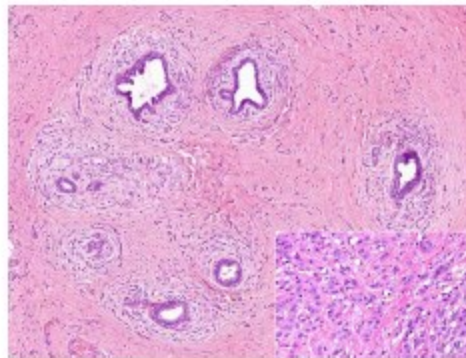

FIGURE 6. Formations of invasive tubulolobular carcinoma concentrically surrounding AGMLG with CCC. The invasive carcinoma in other areas was composed of single cell cords of round to ovoid cells intermixed with round to elongated tubules showing decapitation secretion at the luminal border, with both components positive for E-Cadherin (not shown). Inset: higher magnification of the invasive component.
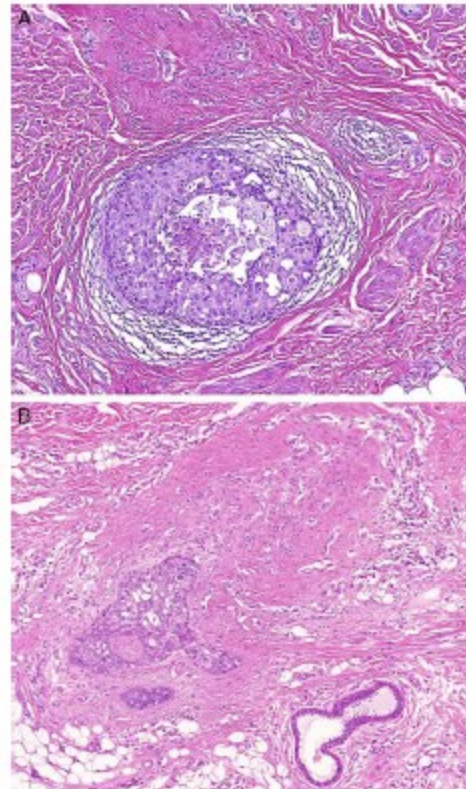
FIGURE 7. A and B, DCIS of solid type involving AGMLG with adjacent areas of fibrosis and elastosis. Note possible microinvasion (B).

However, DCIS and invasive carcinoma comprising the malignant end of the spectrum suggest, by analogy with some cases of MPD,[33] that rare cases of primary EMPD may originate in AGMLG with subsequent upward migration of the neoplastic cells into the epidermis and possible later breach through the basement membrane. UDH and ADH can then be regarded as precursor lesions, linking both ends of the spectrum. If our proposition is confirmed in subsequent studies, this may result in a reevaluation of current therapeutic approaches to primary EMPD, especially with respect to local surgical and nonsurgical treatment, which should take into consideration both the depth of secondary adnexal involvement (up to 3.6 mm) and the depth of location of AGMLG (up to 3.9 mm) as a possible source of disease, including recurrences, which have a rate that ranges currently from 12% to 57%.[3,22,32]
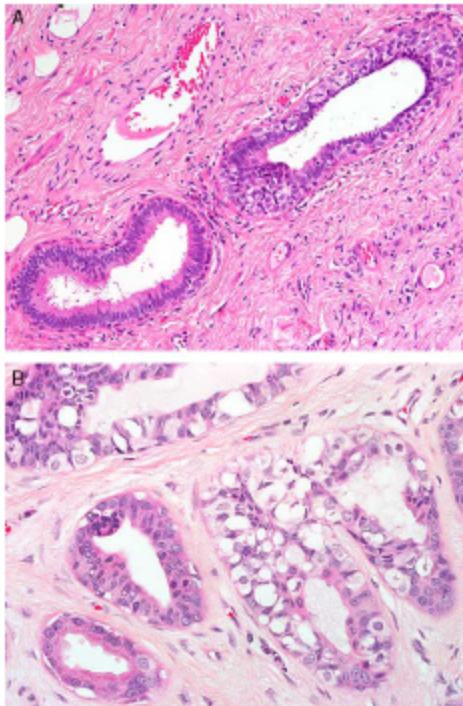
FIGURE 8. Colonization of AGMLG by Paget cells. Note the diffuse infiltration of the duct and CCC (A), and diffuse colonization of the glands (B).

REFERENCES

1. Lam C, Funaro D. Extramammary Paget's disease: summary of current knowledge. *Dermatol Clin*. 2010;28:807-826.
2. Kazakov DV, Spagnolo DV, Kacerovska D, et al. Lesions of anogenital mammary-like glands: an update. *Adv Anat Pathol*. 2011; 18:1–28.
3. Kazakov DV, Michal M, Kacerovska D, et al. *Cutaneous Adnexal Tumors*. Philadelphia, PA: Lippincott Williams & Wilkins; 2012.
4. Parker LP, Parker JR, Bodurka-Bevers D, et al. Paget's disease of the vulva: pathology, pattern of involvement, and prognosis. *Gynecol Oncol*. 2000;77:183–189.
5. Weedon D. *Weedon's Skin Pathology*, 3rd ed. London: Churchill Livingstone Elsevier; 2010.
6. van der Putte SC. Clear cells of Toker in the developing anogenital region of male and female fetuses. *Am J Dermatopathol*. 2011;33: 811–818.
7. Belousova IE, Kazakov DV, Michal M, et al. Vulvar Toker cells: the long-awaited missing link: a proposal for an origin-based histogenetic classification of extramammary paget disease. *Am J Dermatopathol*. 2006;28:84–86.
8. Willman JH, Golitz LE, Fitzpatrick JE. Vulvar clear cells of Toker: precursors of extramammary Paget's disease. *Am J Dermatopathol*. 2005;27:185–188.
9. Toker C. Clear cells of the nipple epidermis. *Cancer*. 1970;25: 601–610.
10. Guarner J, Cohen C, DeRose PB. Histogenesis of extramammary and mammary Paget cells. An immunohistochemical study. *Am J Dermatopathol*. 1989;11:313-318.
11. Hamm H, Vroom TM, Czarnetzki BM. Extramammary Paget's cells: further evidence of sweat gland derivation. *J Am Acad Dermatol*. 1986;15:1275–1281.
12. Helm KF, Goellner JR, Peters MS. Immunohistochemical stains in extramammary Paget's disease. *Am J Dermatopathol*. 1992;14: 402–407.
13. Lloyd J, Flanagan AM. Mammary and extramammary Paget's disease. *J Clin Pathol*. 2000;53:742–749.
14. Mazoujian G, Pinkus GS, Haagensen DE Jr. Extramammary Paget's disease—evidence for an apocrine origin. An immunoperoxidase study of gross cystic disease fluid protein-15, carcinoembryonic antigen, and keratin proteins. *Am J Surg Pathol*. 1984;8:43–50.
15. Merot Y, Mazoujian G, Pinkus G, et al. Extramammary Paget's disease of the perianal and perineal regions. Evidence of apocrine derivation. *Arch Dermatol*. 1985;121:750-752.
16. Nadji M, Morales AR, Girtanner RE, et al. Paget's disease of the skin. A unifying concept of histogenesis. *Cancer*. 1982;50:2203–2206.
17. Ordonez NG, Awalt H, Mackay B. Mammary and extramammary Paget's disease. An immunocytochemical and ultrastructural study. *Cancer*. 1987;59:1173–1183.
18. Urabe A, Matsukuma A, Shimizu N, et al. Extramammary Paget's disease: comparative histopathologic studies of intraductal carcinoma of the breast and apocrine adenocarcinoma. *J Cutan Pathol*. 1990;17:257–265.
19. Di Bonito L, Patriarca S, Falconieri G. Aggressive "breast-like" adenocarcinoma of vulva. *Pathol Res Pract*. 1992;188:211–216.
20. Ohira S, Itoh K, Osada K, et al. Vulvar Paget's disease with underlying adenocarcinoma simulating breast carcinoma: case report and review of the literature. *Int J Gynecol Cancer*. 2004;14: 1012–1017.
21. Piura B, Gemer O, Rabinovich A, et al. Primary breast carcinoma of the vulva: case report and review of literature. *Eur J Gynaecol Oncol*. 2002;23:21–24.
22. Konstantinova AM, Shelekhova KV, Stewart CJ, et al. Depth and patterns of adnexal involvement in primary extramammary (anogenital) Paget disease: a study of 178 lesions from 146 patients. *Am J Dermatopathol*. 2016;38:802–808.
23. Rosai J. *Rosai and Ackerman's Surgical Pathology*, 9th ed. St. Louis, MO: Elsevier Mosby; 2004.
24. Rosen P. *Rosen's Breast Pathology*, 3rd ed. Philadelphia, PA: Lippincott Williams & Wilkins; 2009.
25. Lakhani S, Ellis I, Schnitt S, et al. *World Health Organization Classification of Tumours of the Breast*. Lyon: IARC Press; 2012.
26. Lester SC, Bose S, Chen YY, et al. Protocol for the examination of specimens from patients with invasive carcinoma of the breast. *Arch Pathol Lab Med*. 2009;133:1515-1538.
27. Konstantinova AM, Hayes MM, Stewart CJ, et al. Syringomatous structures in extramammary Paget disease: a potential diagnostic pitfall. *Am J Dermatopathol*. 2016;38:653–657.
28. Konstantinova AM, Kacerovska D, Stewart CJ, et al. Syringocystadenocarcinoma papilliferum in situ-like changes in extramammary Paget disease: a report of 11 cases. *Am J Dermatopathol*. 2016;38: 882-886.
29. Konstantinova AM, Michal M, Kacerovska D, et al. Hidradenoma papilliferum: a clinicopathologic study of 264 tumors from 261 patients, with emphasis on mammary-type alterations. *Am J Dermatopathol*. 2016;38:598-607.
30. Feuer GA, Shevchuk M, Calanog A. Vulvar Paget's disease: the need to exclude an invasive lesion. *Gynecol Oncol*. 1990;38:81–89.
31. Dabbs DJ, Carter G, Fudge M, et al. Molecular alterations in columnar cell lesions of the breast. *Mod Pathol*. 2006;19:344–349.
32. Konstantinova AM, Kyrpychova L, Belousova IE, et al. Anogenital mammary-like glands: a study of their normal histology with emphasis on glandular depth, presence of columnar epithelial cells and distribution of elastic fibers. *Am J Dermatopathol*. 2016; In press.
33. Duan X, Sneige N, Gullett AE, et al. Invasive paget disease of the breast: clinicopathologic study of an underrecognized entity in the breast. *Am J Surg Pathol*. 2012;36:1353–1358.

97

Depth and Patterns of Adnexal Involvement in Primary Extramammary (Anogenital) Paget Disease: A Study of 178 Lesions From 146 Patients

Anastasia M. Konstantinova, MD, PhD,*† Ksenya V. Shelekhova, MD, PhD,*‡ Colin J. Stewart, FRCPA,§ Dominic V. Spagnolo, MBBS, FRCPA,¶‖ Heinz Kutzner, MD,** Denisa Kacerovska, MD, PhD,††‡‡ Jose A. Plaza, MD,§§ Saul Suster, MD,¶¶ Jiri Bouda, MD, PhD,‖‖ Michal Pavlovsky, MD,*** Liubov Kyrpychova, MD,†† Michal Michal, MD,††‡‡ Emmanuella Guenova, MD, PhD,††† and Dmitry V. Kazakov, MD, PhD††††

Abstract: Extramammary Paget disease (EMPD) is a rare neoplasm usually presenting in the anogenital area, most commonly in the vulva. Adnexal involvement in primary EMPD is a very common feature and serves as a pathway for carcinoma to spread into deeper tissue. The depth of carcinomatous spread along the appendages and the patterns of adnexal involvement were studied in 178 lesions from 146 patients with primary EMPD. Hair follicles and eccrine ducts were the adnexa most commonly affected by carcinoma cells. The maximal depth of involvement was 3.6 mm in this series. When planning topical therapy or developing novel local treatment modalities for EMPD, this potential for significant deep spread along adnexa should be taken into account.

Key Words: extramammary Paget disease, adnexa, invasion, vulva

(Am J Dermatopathol 2016;38:802–808)

INTRODUCTION

Extramammary Paget disease (EMPD) is a rare neoplasm usually presenting in the anogenital area, most commonly in the vulva, where it represents approximately 1% of malignant lesions.[1] EMPD can be divided into primary and secondary variants, the latter representing intraepithelial spread of an underlying carcinoma, usually from the urogenital or gastrointestinal tracts.[2–5]

Primary EMPD is a form of intraepithelial adenocarcinoma of uncertain histogenesis, for which cutaneous adnexa, clear cells of Toker, pluripotent stem cells, and anogenital mammary-like glands (AGMLG) have been proposed as possible sites of origin.[2,6–18]

Surgical excision is a widely used treatment modality for primary EMPD but this can be disfiguring and recurrences are not uncommon. Other than surgery, in recent years, topical drugs such as imiquimod, 5-fluorouracil, and retinoic acid, alone or in combination, have been used for the treatment of EMPD.[19] The application of these drugs is based on the premise that most primary EMPD represents a form of adenocarcinoma in situ, in which a proliferation of the neoplastic cells is confined to the epidermis or mucosal epithelium and can be destroyed by the drug, either directly or through immunoreactive processes. One can speculate, however, that in EMPD invading the underlying dermis, these treatments would be less effective. In addition, previous case reports and case series have demonstrated that adnexal involvement is common in EMPD and that the adnexa may serve as a pathway for carcinoma spreading to deeper tissues where local therapeutic agents are less likely to be effective.[7,20,21] Since the depth of adnexal involvement has never been previously studied, our primary goal was to establish the depth of spread of carcinomatous cells along the adnexa in primary EMPD, and also to identify previously undescribed patterns of adnexal involvement by studying 178 lesions from 146 patients with primary anogenital EMPD.

MATERIAL AND METHODS

Case Selection

A search in the consultation, routine institutional, and personal files of the authors between 1993 and 2015 years yielded 167 cases coded as EMPD. Histological slides were reviewed along with the available clinical information obtained from patients' medical records to confirm the

location and the clinicopathological context. Only cases of primary anogenital EMPD were included. Excluded from the study were 21 cases of secondary EMPD arising from carcinomas of other possible origins (rectum, urethra, prostate, etc.) as well as cases with insufficient clinical data. Thus, the study cohort consisted of 178 specimens from 146 patients with primary anogenital EMPD.

Light Microscopy

The study was based on the assessment of hematoxylin and eosin–stained slides, periodic acid-Schiff–stained and/or mucicarmine-stained sections, and immunostains for cytokeratin 7. Of the 178 specimens, 99 were wide surgical excisions, local resections, or vulvectomies (the number of tissue blocks ranged from 1 to 59; median 10) and 79 were small specimens (punch, or small incisional biopsies, with a single block per case). From 13 patients, both primary and recurrent tumors were available for study (1 recurrence in 8 patients; 2 recurrences in 4 patients; 3 recurrences in 1 patient).

Involvement of cutaneous adnexal structures including hair follicles, sebaceous, apocrine, and eccrine glands and their ducts were evaluated. Eccrine and apocrine ducts are typically indistinguishable, but in many cases their nature could be reasonably determined when they were clearly related to an underlying apocrine or eccrine secretory coil or acrosyringium (the intraepidermal part of the eccrine duct). When it was not possible to distinguish between apocrine and eccrine ducts, they were designated as "ducts, not otherwise specified". We also determined the presence and nature of involvement of AGMLG and their ducts, but these results will be the subject of a separate report.

Depth of invasion was determined on hematoxylin and eosin–stained slides from large resection specimens only (n = 99), whereas for small specimens (n = 79), only the frequency and distribution of adnexal involvement was documented. An ocular micrometer was used to measure the depth from the surface of the epidermis (cornified layer) or epithelium to the deepest located tumor cell in an involved adnexal structure. In all cases, we determined if there was microinvasion (defined as stromal invasion to a depth of no more than 1 mm below the basement membrane[22]) or if depth of invasion exceeded 1 mm. Twelve lesions were the subject of 2 previous reports.[23,24]

RESULTS

Clinical Data

The clinicopathological features of the 146 patients are summarized in Table 1. There were 114 women and 32 men. Age at diagnosis (known in 142 patients) ranged from 40 to 95 years (median, 73 years; mean, 71 years). In all but 1 case, the lesions were solitary and occurred in the anogenital area sometimes involving large areas (eg, vulva and perianal area; scrotum and groin). One patient presented with bilateral groin lesions. In women, EMPD most commonly involved the vulva (89.4%) and less frequently the perianal (5.3%) regions. In men, EMPD mostly involved the scrotum (40.6%) and groin (25%). Thirteen patients had recurrences of EMPD. In a further 2 patients with recurrent EMPD, the slides of the original biopsies were not available for review. Clinically, most lesions appeared as flat or slightly elevated

TABLE 1. Main Clinical Characteristics of 146 Study Patients

Parameter	N (%)
Age (yrs)	40–95 (median 73, mean 71.26)
Gender	
Female	114 (78.1)
Male	32 (21.9)
Location	
Genital	123 (84.2)
Vulva NOS or predominantly	93
Labium majus	8
Mons pubis	8
Scrotum (predominantly)	13
Periclitoral	1
Groin	10 (6.8)
Perianal	9 (6.2)
Anogenital, NOS	4 (2.7)

NOS, not otherwise specified.

FIGURE 1. Clinical appearance of extramammary Paget disease: Erythematous erosive areas.

TABLE 2. Frequency and Depth of Invasion of Adnexal Structures in 99 Large Postoperative Specimens

Type of Adnexa	Involved/Present (% with Involved Adnexa); {Number/ % of Cases Where it was the Deepest Involved Structure}	Depth of Adnexal Involvement in mm
Hair follicles	91/98 (92.8); {76/83.5}	0.5–3.25 (median 1.6, mean 1.64)
Sebaceous glands	29/79 (36.7); {1/3.4}	0.4–1.5 (median 1, mean 0.98)
Eccrine secretory coil	12/95 (12.6); {5/41.7}	0.8–3.2 (median 2.55, mean 2.39)
Apocrine secretory coil	1/60 (1.7); {0}	1.8 (median 1.8, mean 1.8)
Adnexal ducts		
Eccrine ducts		
Acrosyringium	87/89 (97.7)	
Straight/coiled	54/76 (71.1); {13/24.1}	0.3–3.6 (median 1.1, mean 1.28)
Apocrine ducts	6/41 (14.6); {0}	0.5–1.38 (median 0.93, mean 0.99)
Ducts, NOS	14/72 (19.4); {1/7.1}	0.4–2.5 (median 0.94, mean 0.98)

NOS, not otherwise specified.

erythematous or white-gray areas, with variable scaling, excoriations, oozing, or crusting (Fig. 1).

Histopathological Findings

Of the 178 specimens, 165 were in situ EMPD and 13 were invasive EMPD. Of the latter, 9 were minimally invasive, as defined above, and 4 had dermal invasion >1 mm in depth. Inguinal lymph node metastases occurred in 1 case only.

Adnexal involvement was a common finding in large samples (Table 2) as well as in small biopsy specimens (Table 3). The most common targets were hair follicles, involved in 92.8% of large resection specimens (91 of 98

TABLE 3. Frequency of Invasion of Adnexal Structures in 79 Small Biopsies Specimens

Type of Adnexa	Involved/Present (% With Involved Adnexa)
Hair follicle	35/56 (62.5)
Sebaceous glands	5/23 (21.7)
Eccrine glands	1/44 (2.3)
Apocrine glands	1/9 (11.1)
Adnexal ducts	
Eccrine ducts	
Acrosyringium	23/26 (88.5)
Straight/coiled	7/21 (33.3)
Apocrine ducts	1/4 (25)
Ducts NOS	8/34 (23.5)

NOS, not otherwise specified.
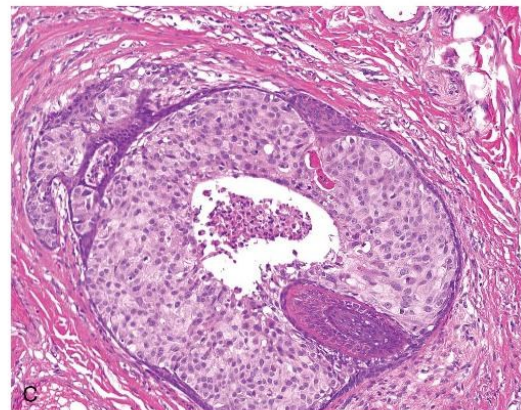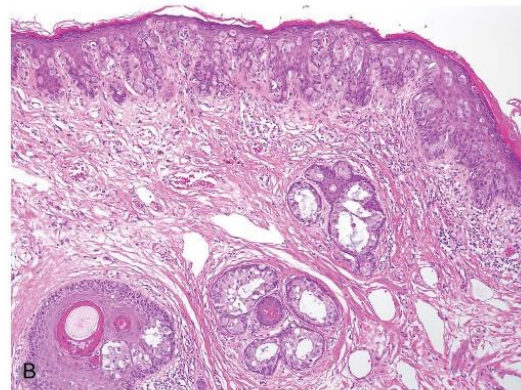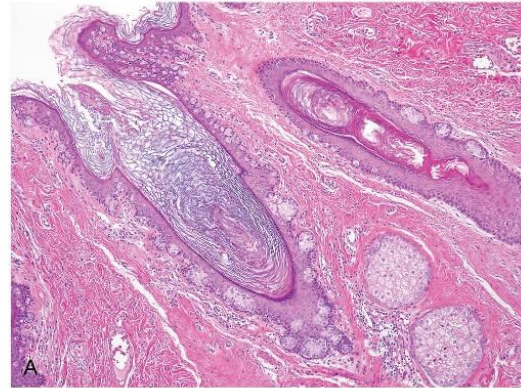
FIGURE 2. Involvement of hair follicles in EMPD. Single tumor cell infiltration and clusters of neoplastic cells involve a hair follicle (A). Gland-like structures in hair follicles, some with cribriform appearances, replacing most of native follicular epithelium (B). Prominent involvement of hair follicle with comedonecrosis (C).
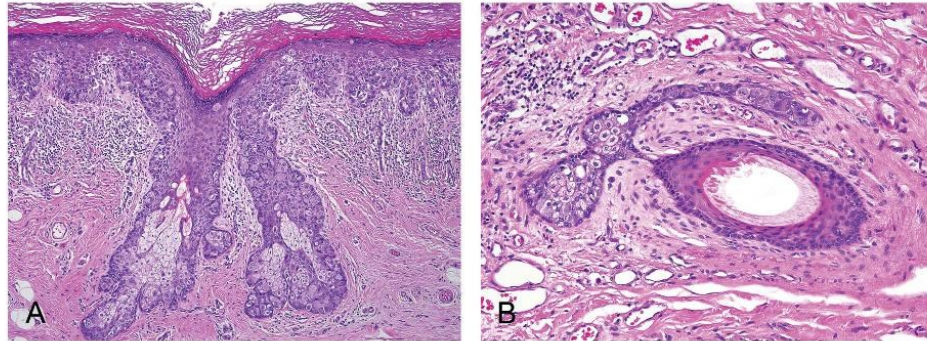
FIGURE 3. Involvement of sebaceous glands in EMPD. Dispersed single tumor cells and small clusters in mature sebaceous glands (A) and in the mantle (B).

specimens). In 76 large specimens (76.7%), the hair follicle was the adnexal structure most deeply involved (compared with sebaceous glands and apocrine or eccrine units). The maximal depth of carcinoma cells affecting hair follicles was 3.25 mm. In small biopsy specimens (n = 79), hair follicles were present in more than half of the cases, of which 62.5% (35/56) were involved by Paget cells. In most cases, neoplastic cells were dispersed in the affected hair follicles as
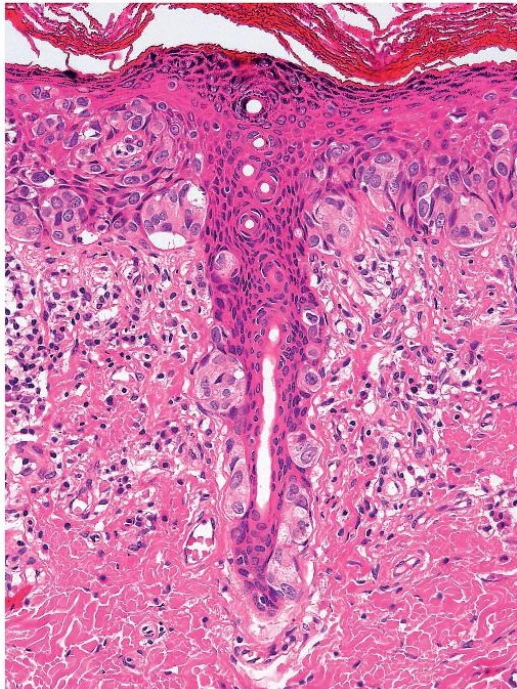

FIGURE 4. Infiltration of the acrosyringium in EMPD.

single cells or small clusters (Fig. 2A). Less commonly, gland-like structures were formed (Fig. 2B). Whereas in most cases only a minor proportion of the native follicular epithelium was replaced by the neoplastic cells, a few cases demonstrated extensive follicular involvement by the carcinoma, sometimes accompanied by comedonecrosis (Fig. 2C).

Sebaceous glands were infiltrated by Paget cells in a third of the large specimens and in a quarter of the small biopsy samples. Both mature sebaceous glands and mantles were seen to be involved by single cell spread or by small groups of tumor cells (Fig. 3), sometimes identified only after mucicarmine staining. The deepest involved sebaceous gland was located 1.5 mm below the stratum corneum.

Involvement of eccrine units most frequently manifested as infiltration of the acrosyringium (97.7%), which is logical due to its intraepidermal location (Fig. 4). Intradermal straight and coiled eccrine ducts were found in 76 large specimens and were infiltrated by tumor cells in 54 samples (71.1%) (Fig. 5), with the deepest involvement of 3.6 mm seen in 13 specimens. In most, there was single cell infiltration of the ducts but small clusters of neoplastic cells and gland-like structures were also noted less frequently (Fig. 6). Immature squamous cell metaplasia and hyperplasia of duct epithelium were occasionally encountered, and a combination of metaplasia and hyperplasia resulted rarely in cribriform formations (Fig. 7). In some cases, neoplastic cells were observed to have replaced mostly the basal/myoepithelial cells with the focal preservation of luminal cells (Fig. 8).

The eccrine secretory coils were infiltrated less frequently by tumor cells (12.6% of large specimens), in 4 cases showing the deepest involvement to be at a maximal depth of 3.2 mm. Similar to other adnexal structures, eccrine glands were seen to be colonized by single cells or groups of neoplastic cells, and rarely by gland-like structures. In some eccrine coils, complete replacement of the normal luminal epithelium by solid or cribriform formations of Paget cells, in the presence of preserved peripheral basal/myoepithelial cell layers, occasioned a resemblance to either ductal carcinoma in situ or so-called lobular cancerization as seen in mammary carcinomas (Fig. 9).

101
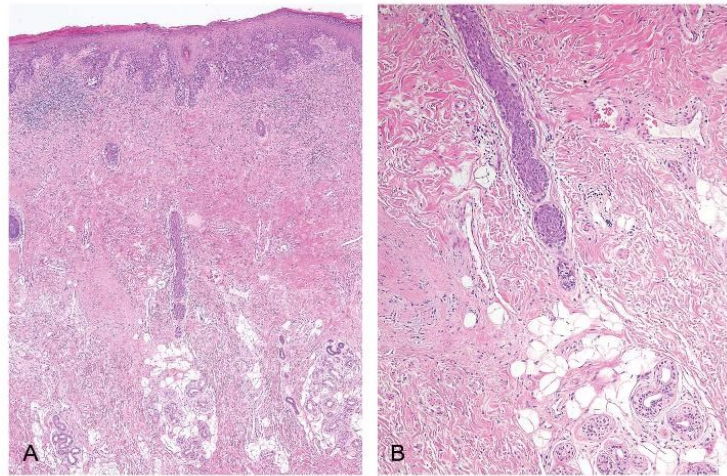
FIGURE 5. Involvement of the straight portion of eccrine duct in EMPD, mostly occurring as single cell colonization (A, B).

The apocrine secretory coils were involved in 14.6% of cases, and never were they the deepest structure affected by the carcinoma.

In 1 case, a large complex structure of uncertain derivation was involved by neoplastic cells (Figs. 10, 11), whereas in another case of recurrent EMPD involving the neovulva, carcinoma cells colonized the remnants of a Bartholin gland at a depth of 12 mm.

DISCUSSION

Our study validates the previously published observations that involvement of adnexa is a common feature in primary EMPD, likely contributing to the spread of carcinoma into deeper tissues and to the propensity for recurrence.[7,18,20,21,25] Our study contributes novel data by documenting the depth of adnexal involvement, hitherto not previously examined. We found that Paget cells may spread along the adnexa as deeply as 3.6 mm, with hair follicles and eccrine ducts/glands being the most commonly and the most deeply involved structures. This information should be taken into account when planning topical nonsurgical treatment or when developing new local treatment modalities in the future. At present, imiquimod, 5-fluorouracil, and retinoic acid are used in the treatment of EMPD attempting to substitute for alternative, often disfiguring surgical approaches. Other novel treatments including CO_2 laser, trastuzumab, alone or in combination with chemotherapy, and photodynamic therapy are being studied.[26–29] The above treatment modalities have differing mechanisms of action (eg, imiquimod acts as an immune response modifier; 5-fluorouracil is a chemotherapeutic agent; photodynamic therapy relies on light activation of a photosensitizer in neoplastic cells) but the depth of skin penetration and knowledge of the depths of tumor deposits
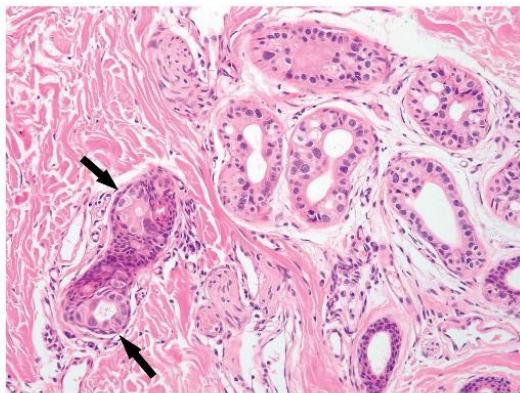
FIGURE 6. Gland-like structures in an involved eccrine duct (arrow).
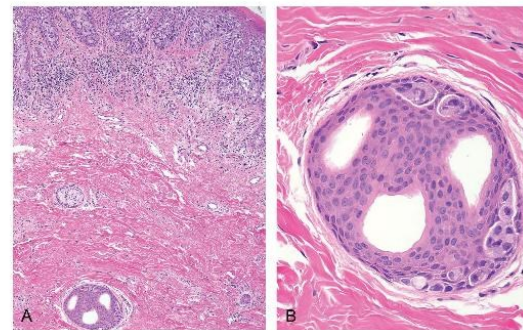
FIGURE 7. Carcinoma cell infiltration of an eccrine duct, which also shows squamous metaplasia and hyperplasia resulting in a cribriform appearance.
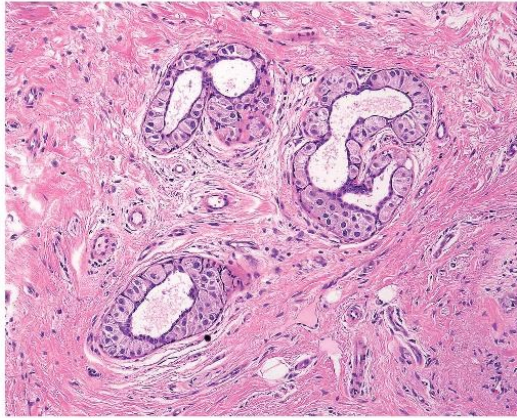
FIGURE 8. A duct showing replacement of the basal/myoepithelial cells by Paget cells.

FIGURE 10. A large complex structure of uncertain derivation involved by neoplastic cells (A, B). It clearly differs from hyperplastic eccrine or apocrine units and also from anogenital mammary-like glands depicted in Figure 11 for comparison.

are obviously essential for planning successful treatment. From our literature review, we have been unable to determine to what depth imiquimod may penetrate the skin, whereas 5-fluorouracil reportedly penetrates the skin to a depth of 1–2 mm.[30] This is manifestly insufficient for a substantial number of cases in which Paget cells extend well beyond this. Whereas data on the presenc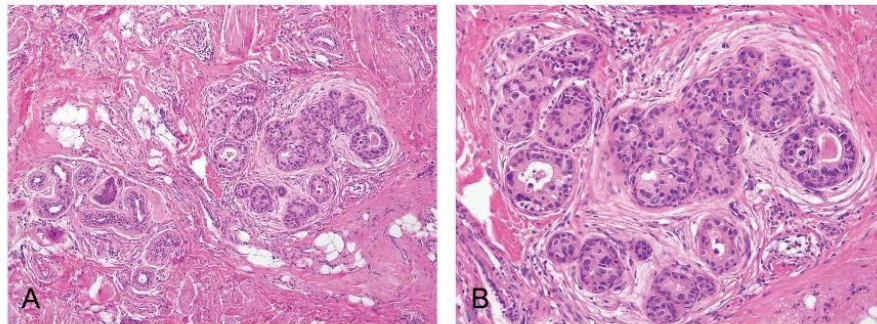e or absence of invasion are available in previously published trials, the issue of adnexal spread has not been properly addressed. Nonetheless, it has been speculated that therapeutic responses may be related to the depth of penetration of imiquimod such that thicker portions of an in situ lesion or tumor with extensive adnexal involvement or invasive disease may exhibit incomplete responses.[31]

Appendages may be colonized by neoplastic cells in different ways. We noted several patterns of adnexal involvement These include involvement or spread as single cells, small clusters, gland-like formations, substitution of luminal cells in ducts/coils with preserved peripheral basal/

myoepithelial cells resulting in ductal carcinoma in situ–like appearances, or, conversely, predominant replacement of basal/myoepithelial cells. Additionally, ductal structures may exhibit epithelial metaplasia and hyperplasia, posing potential diagnostic pitfalls. We also noted changes in AGMLG, structures mooted to play a role in the etiology and pathogenesis of primary EMPD,[7,2,3] but these results will be reported in a separate study.

In conclusion, adnexal involvement in primary EMPD is a very common feature occurring in more than 90% of cases. Hair follicles and eccrine ducts are the most commonly affected adnexa by Paget cells. In this study, the maximal depth of involvement was as much as 3.6 mm, with the median for each adnexal structure ranging from 0.93 mm (eccrine ducts) to 2.55 mm (eccrine secretory coils). Given the fact that we used for formalin-fixed tissues in the study, the actual depth of invasion in vivo is bound to be deeper. This phenomenon should be taken into account when planning topical therapy or developing novel local treatment modalities for EMPD.

FIGURE 9. Infiltration of eccrine coils occasioning a resemblance to either ductal carcinoma in situ or so-called lobular cancerization as seen in mammary carcinomas (A, B).
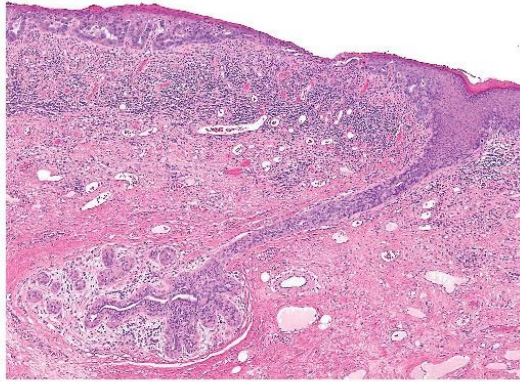
FIGURE 11. Anogenital mammary-like gland involved by carcinoma cells.

REFERENCES

1. Lam C, Funaro D. Extramammary paget's disease: summary of current knowledge. *Dermatol Clin.* 2010;28:807–826.
2. Kazakov DV, Spagnolo DV, Kacerovska D, et al. Lesions of anogenital mammary-like glands: an update. *Adv Anat Pathol.* 2011;18:1–28.
3. Kazakov DV, Michal M, Kacerovska D, et al. *Cutaneous Adnexal Tumors.* Philadelphia, PA: Lippincott Williams & Wilkins; 2012.
4. Parker LP, Parker JR, Bodurka-Bevers D, et al. Paget's disease of the vulva: pathology, pattern of involvement, and prognosis. *Gynecol Oncol.* 2000;77:183–189.
5. Weedon D. *Weedon's Skin Pathology.* 3rd ed. London, United Kingdom: Churchill Livingstone Elsevier; 2010.
6. van der Putte SC. Clear cells of Toker in the developing anogenital region of male and female fetuses. *Am J Dermatopathol.* 2011;33:811–818.
7. Belousova IE, Kazakov DV, Michal M, et al. Vulvar toker cells: the long-awaited missing link: a proposal for an origin-based histogenetic classification of extramammary paget disease. *Am J Dermatopathol.* 2006;28:84–86.
8. Willman JH, Golitz LE, Fitzpatrick JE. Vulvar clear cells of toker: precursors of extramammary paget's disease. *Am J Dermatopathol.* 2005;27: 185–188.
9. Toker C. Clear cells of the nipple epidermis. *Cancer.* 1970;25:601–610.
10. Guarner J, Cohen C, DeRose PB. Histogenesis of extramammary and mammary paget cells. An immunohistochemical study. *Am J Dermatopathol.* 1989;11:313–318.
11. Hamm H, Vroom TM, Czarnetzki BM. Extramammary paget's cells: further evidence of sweat gland derivation. *J Am Acad Dermatol.* 1986;15:1275–1281.
12. Helm KF, Goellner JR, Peters MS. Immunohistochemical stains in extramammary paget's disease. *Am J Dermatopathol.* 1992;14:402–407.
13. Lloyd J, Flanagan AM. Mammary and extramammary paget's disease. *J Clin Pathol.* 2000;53:742–749.
14. Mazoujian G, Pinkus GS, Haagensen DE Jr. Extramammary paget's disease—evidence for an apocrine origin. An immunoperoxidase study of gross cystic disease fluid protein-15, carcinoembryonic antigen, and keratin proteins. *Am J Surg Pathol.* 1984;8:43–50.
15. Merot Y, Mazoujian G, Pinkus G, et al. Extramammary paget's disease of the perianal and perineal regions. Evidence of apocrine derivation. *Arch Dermatol.* 1985;121:750–752.
16. Nadji M, Morales AR, Girtanner RE, et al. Paget's disease of the skin. A unifying concept of histogenesis. *Cancer.* 1982;50:2203–2206.
17. Ordonez NG, Awalt H, Mackay B. Mammary and extramammary paget's disease. An immunocytochemical and ultrastructural study. *Cancer.* 1987;59:1173–1183.
18. Urabe A, Matsukuma A, Shimizu N, et al. Extramammary paget's disease: comparative histopathologic studies of intraductal carcinoma of the breast and apocrine adenocarcinoma. *J Cutan Pathol.* 1990;17:257–265.
19. Micali G, Lacarrubba F, Nasca MR, et al. Topical pharmacotherapy for skin cancer: part I. *Pharmacol J Am Acad Dermatol.* 2014;70:965. e1–12.
20. Goldblum JR, Hart WR. Vulvar paget's disease: a clinicopathologic and immunohistochemical study of 19 cases. *Am J Surg Pathol.* 1997;21: 1178–1187.
21. Hart WR, Millman JB. Progression of intraepithelial paget's disease of the vulva to invasive carcinoma. *Cancer.* 1977;40:2333–2337.
22. Feuer GA, Shevchuk M, Calango A. Vulvar paget's disease: the need to exclude an invasive lesion. *Gynecol Oncol.* 1990;38:81–89.
23. Konstantinova AM, Hayes M, Stewart CJR, et al. Syringomatous structures in extramammary paget disease: a potential diagnostic pitfall. *Am J Dermatopathol.* In press.
24. Konstantinova AM, Michal M, Kacerovska D, et al. Hidradenoma papilliferum: a clinicopathologic study of 264 cases from 261 patients, with emphasis on mammary-type alterations. *Am J Dermatopathol.* In press.
25. Shiomi T, Yoshida Y, Yamamoto O, et al. Extramammary paget's disease: evaluation of the adnexal status of 53 cases. *Pol J Pathol.* 2015;66: 121–126.
26. Karam A, Berek JS, Stenson A, et al. HER-2/neu targeting for recurrent vulvar paget's disease A case report and literature review. *Gynecol Oncol.* 2008;111:568–571.
27. Takahagi S, Noda H, Kamegashira A, et al. Metastatic extramammary paget's disease treated with paclitaxel and trastuzumab combination chemotherapy. *J Dermatol.* 2009;36:457–461.
28. Shepherd V, Davidson EJ, Davies-Humphreys J. Extramammary paget's disease. *BJOG.* 2005;112:273–279.
29. Henta T, Itoh Y, Kobayashi M, et al. Photodynamic therapy for inoperable vulval paget's disease using delta-aminolaevulinic acid: successful management of a large skin lesion. *Br J Dermatol.* 1999;141: 347–349.
30. Delport ES. Extramammary paget's disease of the vulva: an annotated review of the current literature. *Australas J Dermatol.* 2013;54:9–21.
31. Green JS, Burkemper NM, Fosko SW. Failure of extensive extramammary paget disease of the inguinal area to clear with imiquimod cream, 5%: possible progression to invasive disease during therapy. *Arch Dermatol.* 2011;147:704–708.

104

PART 2 - CUTANEOUS NONEPITHELIAL TUMORS

Cutaneous nonepithelial tumors represent a large and heterogeneous group of neoplasms, including melanocytic, histiocytic, vascular, neural lesions, to name just a few. We studied several entities subdivided into three subgroups, namely lymphoproliferative disorders, mesenchymal tumors, and melanocytic neoplasms.

2.1 LYMPHOPROLIFERATIVE DISORDERS

Three papers are included in this subgroup. The article is entitled «*Mummified cells are a common finding in cutaneous Hodgkin lymphoma and can be used as a diagnostic clue*» represents the largest published series of this rare condition in a dermatopathology practice to date. (50) The microscopic diagnosis is usually based on the recognition of diagnostic Reed-Sternberg cells (large cells with abundant amphophilic cytoplasm and two or more oval lobulated nuclei containing prominent eosinophilic nucleoli) and its variants, including mononuclear Hodgkin cells and lacunar cells. (51) These specific cells express CD30 and CD15. In nodal Hodgkin lymphoma, one often encounters so-called mummified cells. (52) These cells have pyknotic eosinophilic or basophilic nuclei and condensed cytoplasm. Sometimes they are conspicuous and easy to recognize, thus serving as a clue to the diagnosis. With respect to cutaneous Hodgkin lymphoma, the presence of these cells has never been examined. Our objective was to study cases of cutaneous Hodgkin lymphoma to identify the occurrence of these specific cells. We studied 12 cases in which histopathological, immunohistochemical, and molecular genetic studies, including rearrangements for TCR, IgH genes, and EBV studies were performed. Diagnostic Reed-Sternberg cells and its variants were identified in all cases. Mummified cells were detected in 9 cases, as individual scattered cells or being conspicuous. Immunohistochemically, in all 7 cases studied mummified cells were positive for both CD30 and CD15. EBV virus was found in 2 of 7 studied cases, whereas clonal TCR or IgH gene rearrangements were detected in 3/7 and 1/7 cases, respectively. We concluded that mummified cells are encountered in many of cases of cutaneous Hodgkin lymphoma and may on occasion be conspicuous, their presence can be used as a clue to the diagnosis.

The second entity covered in this section is lymphomatoid papulosis, namely its rare and unusual variant, type E. Our article titled *«A case of lymphomatoid papulosis type E with an unusual exacerbated clinical course»* describes an exceptional clinical presentation of this lymphoproliferative entity. Lymphomatoid papulosis (LyP) belongs to the spectrum of CD30-positive cutaneous lymphoproliferative disorders. Histopathologically, LyP is characterized in most cases by atypical large lymphoid cells expressing CD30, but the clinicopathological spectrum of the disease is broad (types A, B, C, D, E, F and LyP with 6p23.5 rearrangement). (53), (54)

LyP type E is a recently delineated variant characterized by the occurrence of large necrotic "eschar"-like lesions displaying microscopically angioinvasive and angiodestructive infiltrates

composed of CD30+ lymphocytes, frequently coexpressing CD8. (55) In contrast to other variants of LyP in which lesions are small (<2 cm) and multiple, patients with LyP type E often present with one or two large (>2 cm) lesions at a given time point, often requiring the distinction from CD30+ large cell anaplastic lymphoma. We described a 34-year-old man with LyP type E with an exacerbated clinical course characterized by the occurrence of almost a hundred of lesions. The disease started with a single rapidly growing 2-cm large erythematous nodule on the forearm, which rapidly became necrotic and ulcerated after the administration of doxycycline by a dermatologist who suspected a Staphylococcus aureus infection. Additionally, multiple similar eschar-like lesions (around 100) developed all over the body. The biopsy revealed a characteristic angiocentric and angiodestructive infiltrate of CD30+ medium-sized to large pleomorphic lymphocytes. After the diagnosis was established, the antibiotic treatment was stopped, and the lesions spontaneously regressed within five months, leaving behind atrophic scars and pigmentary patches.

In the third article «*Kaposi sarcoma in association with an extracavitary primary effusion lymphoma showing unusual intravascular involvement: report of a case harboring a FAM175A germline mutation*» we described a rare case of cutaneous primary effusion lymphoma (PEL) with an unusual intravascular presentation, combined with Kaposi sarcoma (KS) involving the skin, lung and gastrointestinal tract. The patient was a 67-year-old man who presented with numerous cutaneous tumors, and mass in the left lung. He died 17 hours after the admission to the hospital. At autopsy, multiple purple patches, plaques and tumors involving the lower and upper extremities were found. In addition to the cutaneous lesions, tumors in the left lung and gastrointestinal mucosa were also detected, and no effusions in the body cavities were seen. The biopsy from the skin lesions, pulmonary and intestinal tumors revealed histological and immunohistochemical features of KS. The skin biopsy specimens contained diffuse infiltrates composed of large pleomorphic cells, with focal intravascular growth that was negative for pan-B-cell markers, weakly positive for CD38 and CD138 but expressed CD3, HHV-8, and EBV. Molecular genetic studies in this specimen revealed monoclonal rearrangements of the IgH gene, leading to the diagnosis of PEL, solid variant. NGS analysis of the tumorous and normal tissue (myocardium) detected a pathogenic germline mutation of the *FAM175A* gene and somatic mutations in *BRCA2* and *RAD51B* (in both sarcoma and lymphoma specimens), and *INPP4B and RICTOR* (in lymphoma specimen only).

Mummified Cells are a Common Finding in Cutaneous Hodgkin Lymphoma and Can Be Used as a Diagnostic Clue

Liubov Kastnerova, MD,*† Irena E. Belousova, MD, PhD,‡ Ladislav Hadravsky, MD, PhD,§
Helmut Kerl, MD,¶ Lorenzo Cerroni, MD,¶ Katrin Kerl, MD, PhD,‖ Ludmila Boudova, MD, PhD,*†
Pavel Jindra, MD, PhD,** Katerina Cerna, PhD,† Michal Michal, MD,*†
and Dmitry V. Kazakov, MD, PhD*†‖

Abstract: Specific cutaneous involvement in Hodgkin lymphoma is rare. In cutaneous lesions, the diagnosis is usually based on the recognition of diagnostic Reed–Sternberg cells and its variants. In nodal Hodgkin lymphoma, so-called mummified cells (cells with condensed cytoplasm and pyknotic eosinophilic or basophilic nuclei) are often seen. They are sometimes conspicuous and easy to recognize, thus serving as a clue to the diagnosis. Our objective was so study cases of cutaneous Hodgkin lymphoma to identify the occurrence of mummified cells. We studied 12 patients (4 women and 8 men; age range 23–80 years). In 7 patients, cutaneous and extracutaneous disease was identified almost simultaneously; in 3 patients, lymph node disease preceded cutaneous involvement; and in the remaining 2 patients, the skin lesions were the presenting sign, whereas lymph node involvement occurred later. Histopathological, immunohistochemical, and molecular-genetic studies, including rearrangements for TCR, IgH genes, and PCR for EBV, were performed. Cutaneous biopsy specimens revealed either a multinodular or diffuse infiltrate, included small lymphocytes, eosinophils, plasma cells, and macrophages, but in all cases, diagnostic Reed–Sternberg cells and its variants were identified. Mummified cells were detected in 9 cases, either as occasional scattered mummified cells often requiring a search (6 cases) or being conspicuous, grouped and therefore easily identified (3 cases). Immunohistochemically, in all 7 cases studied, mummified cells were positive for both CD30 and CD15. It is concluded that mummified cells are encountered in a majority of cases of cutaneous Hodgkin lymphoma.

Key Words: cutaneous Hodgkin, lymphoma, mummified cells, CD30

(Am J Dermatopathol 2019;00:1–5)

INTRODUCTION

Specific cutaneous involvement in Hodgkin lymphoma is rare, with a reported incidence varying from 0.1% to 3.4%.[1] Because of its rare occurrence in dermatopathology practice, the histopathological diagnosis of cutaneous Hodgkin disease may not be straightforward. The microscopic appearance of the cutaneous lesions do not usually correlate with that seen in concomitant lymph node disease in the sense that particular histopathological variants in lymph nodes (lymphocyte-rich, nodular sclerosis, mixed cellularity, and lymphocyte-depleted, etc.) do not manifest with identical changes in the skin. In cutaneous lesions, the diagnosis is usually based on the recognition of diagnostic Reed–Sternberg cells (large cells with abundant amphophilic cytoplasm and 2 or more oval lobulated nuclei containing prominent eosinophilic nucleoli) and its variants, including mononuclear Hodgkin cells (cells with a single round or oblong nucleus with large inclusion-like nucleolus) and lacunar cells (cells with an empty space around the nucleus due to shrinkage of the cytoplasm caused by formalin fixation) expressing CD30 and CD15. In addition, so-called LP cells (aka L&H," or popcorn cells) with a fluffy, lobulated nucleus with fine chromatin and small nucleoli can be encountered; these are strongly positive for CD20, variably positive for CD30, and almost always CD15 negative.[2] In nodal Hodgkin lymphoma, one often encounters so-called mummified cells (cells with condensed cytoplasm and pyknotic eosinophilic or basophilic nuclei), which are sometimes conspicuous and easy to recognize, thus serving as a clue to the diagnosis. With respect to cutaneous Hodgkin lymphoma, the presence of such elements has never been systematically evaluated. Our objective was to study cases of cutaneous Hodgkin lymphoma to identify the occurrence of mummified cells.

MATERIAL AND METHODS

Cases coded as cutaneous Hodgkin lymphoma were searched in our institutional and consultation databases. The retrieved cases were reviewed together with the available clinical information. Included were cases with specific cutaneous involvement by Hodgkin lymphoma, irrespective of temporal relationship of cutaneous and nodal (extracutaneous) disease. Cases with unspecific cutaneous involvement (no diagnostic Reed–Sternberg, Hodgkin, and lacunar cells were present) and cases in which extracutaneous disease was not

confirmed were excluded. Based on the above criteria, 12 cases were included in the study, and 5 cases were excluded. Whenever available, slides from extracutaneous lesions were also reviewed. Three included cases were subjects of 2 previous reports.[5,6]

Immunohistochemical studies were performed at the time of diagnosis and in some cases were repeated retrospectively with new markers. The immunohistochemical panel varied from case to case but CD30, CD15, CD45R0, a B-cell marker (CD20, CD79a, or PAX-5 (Fig. 1)), and a T-cell marker (CD3) were invariably used. Molecular genetic studies, including rearrangements for TCR and IgH genes, RT-PCR for EBV, were performed whenever possible, as previously described.[7–9] We have also studied the expression of the EBV-encoded RNA.[10]

RESULTS

Clinical Data

There were 8 male and 4 female patients, with the ages ranging at the time of cutaneous involvement from 23 to 80 years. Cutaneous lesions were solitary in 8 cases and involved more than one skin area in 4 cases (Fig. 2). The lesions varied in size, with the largest lesion measuring 12 cm. In 7 patients, cutaneous and extracutaneous disease was identified almost simultaneously: most patients presented with skin lesions and subsequent clinical investigations revealed extracutaneous involvement. In 3 patients, lymph node disease preceded cutaneous involvement (cases 3, 10 and 12). In one of these (case 3), cutaneous involvement occurred 33 months after the diagnosis of nodal classical Hodgkin lymphoma, and later in the course of the disease, the tonsil was involved. In the remaining 2 patients (cases 7 and 9), the skin lesions were the presenting sign, whereas lymph node involvement occurred 34 months and 6 years later, respectively. The sites of extracutaneous involvement, treatment, and follow-up are summarized for each patient in Table 1.

Histopathological Features

Cutaneous biopsy specimens revealed either a multinodular or diffuse infiltrate, and in some lesions with a multinodular architecture with a variable degree of sclerosis around the nodules (Fig. 3). The cellular composition of the infiltrate varied from case to case and included small lymphocytes, eosinophils, plasma cells, and macrophages, but in all cases, diagnostic cells Reed–Sternberg cells and its variants were identified (Fig. 4).

Mummified cells were detected in 9 cases. In 6 cases, there were only occasional scattered mummified cells requiring a meticulous search, whereas in the remaining 3 cases, mummified cells were conspicuous, grouped, and therefore easily identified. Mummified cells were binucleated or mononuclear, cells with an empty space around the nucleus, or multilobated, thus retaining the form of the corresponding diagnostic cell but being smaller (Fig. 4).

Immunohistochemically, in all 7 cases studied, mummified cells were positive for both CD30 and CD15
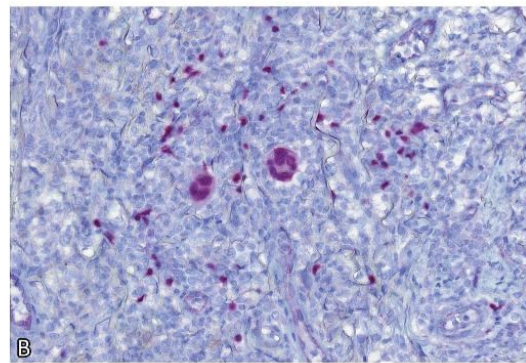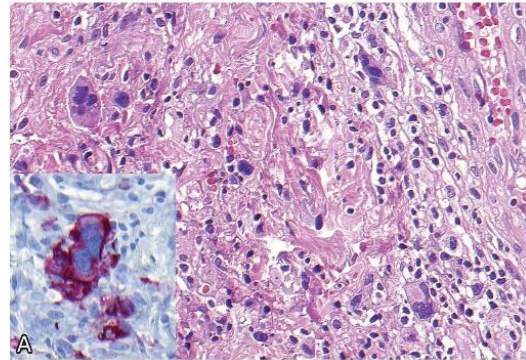

FIGURE 1. Multilobated mummified cells positive for CD30 (inset, A) and PAX-5 (B).

and for CD20 (Fig. 5). In 2 cases (cases 9 and 11), it was not possible to access this feature in retrospect as the original slides were from 1970 to 1980s.

FIGURE 2. Clinical presentation of cutaneous Hodgkin lymphoma with an ulcerated plaque (case 6).

TABLE 1. Main Clinicopathological Features and Follow-up of Patients With Specific Cutaneous Involvement by Hodgkin Lymphoma

Case	Sex/Age	Cutaneous Location and Clinical Appearance	Extracutaneous Involvement	Temporal Relationship	Histologic Type (Extracutaneous)	Stage	Treatment Follow-up
1	F/65	Back forearm	Cervical and axillary LN Tonsil	LN and tonsil and skin almost simultaneously	Mixed cellularity	I	RT 2x 30 Gy, 1x 40 GY, 6x COPP, 2x ABVD, 2x MOPP CR, then cutaneous recurrence 2 years later, DOD at 57 months
2	F/80	Flank	Retroperitoneal, paraaortal, iliac, mediastinal, cervical LN	Skin and LN almost simultaneously	NA	IIIB	4x COPP, RT 10x 3 Gy DOD 22 at months
3	M/67	Back and later axilla	Tonsil	LN→skin 33 months Skin→tonsil 34 months	NA	IIB	6 ABVD, CHOP CR at 82 months, then died of lung carcinoma
4	M/56	Groin, subcutaneous nodule 6 × 5 × 4 cm	Unguinal, iliac (bilateral) LN, sacrum	Skin and LN almost simultaneously	Mixed cellularity	IIEB	8x BEACOPP CR 73 months
5	F/56	Forearm: Mottled dark red plaque, 12 cm Back: a similar smaller lesion	Tonsil Cervical LN	Tonsil and LN and skin almost simultaneously	Mixed cellularity	IIA	4x ABVD CR, 50 months
6	M/23	Chest wall, ulcerated plaque	Cervical, axillary LN	Skin—LN almost simultaneously	Mixed cellularity	NA	8x BEACOPP CR, 72 months
7	M/70	Shin, solitary 1-cm nodule of 14 days duration	Unguinal and retroperitoneal (unilaterally) LN	Skin→LN 34 months	Nodular sclerosis	IIB	4x× ABVD CR 44 months
8	M/29	Shoulder; rapidly growing solitary tumor of 3-week duration	Axillary LN	Skin—LN almost simultaneously	Nodular sclerosis	IEA	2x ABVD, RT 15x 2 Gy CR, 17 months
9	M/54	Left lower leg, solitary nodule	Inguinal lymph node, left	Skin→LN 6 years	Mixed cellularity	NA	NA
10	M/39	Back, solitary bluish-red nodule	NA	LN→skin 10 years	NA	NA	RT, CHT (De Vita protocol), relaps in 3 years treated with De Vita protocol and leukeran, recurrence with stage IV and skin involvement, new RT and ChT. NED 109 months after skin involvement
11	M/50	Buttock, multiple gray-brown	NA	LN→skin several months	Lymphocyte depleted	NA	COPP, NED 6 months
12	F/66	Abdomen, ulcerated tumor	Cervical LN	LN→skin 51 months	Nodular sclerosis	IB	2x ABVD, RT 20 Gy Recent case

Corresponds to case 1 in Sioutus et al.

ABVD, adriamycin, bleomycin, vinblastine, and dacarbazine; BEACOPP, bleomycin, etoposide, doxorubicin, cyclophosphamide, vincristine, procarbazine, and prednisone; ChT, chemotherapy; COPP, cyclophosphamide, Oncovin, procarbazine, prednisone; CR, complete remission; DOD, dead of disease; LN, lymph nodes; MOPP, mechlorethamine, Oncovin, procarbazine, prednisone; NA, not available; RT, radiation therapy.

By RT-PCR EBV was found in 2 of the 7 studied cases. The latter 5 EBV-negative cases were further studied by for the expression of the EBV-encoded RNA and all proved negative. Clonal TCR or IgH gene rearrangements were detected in 3/7 and 1/7 cases, respectively.

DISCUSSION

Regressive cell changes in Hodgkin lymphoma were noted already in the initial articles by Sternberg and Reed.[11,12] Later studies showed that these cells occur in all disease variants.[13–15] The nature of these cells have been
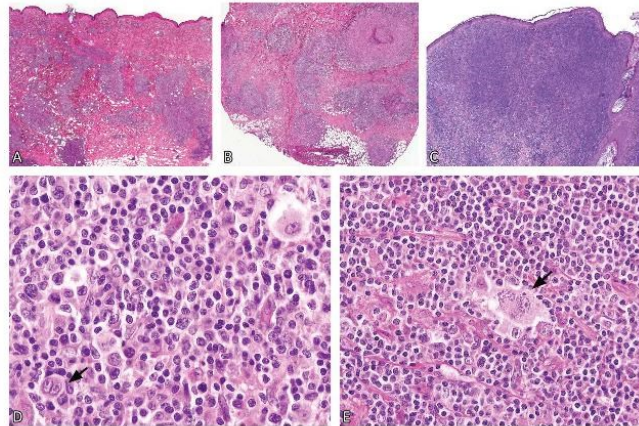
FIGURE 3. Histological features of cutaneous Hodgkin disease. The pattern of the infiltrate includes multinodular (A and B) and diffuse (C) distribution, focally with perinodular sclerosis (B). Diagnostic cells are Reed–Stenberg cell (D, arrow) and lacunar cell (E, arrow).

controversially discussed, and based on the light, immunohistochemical and electron microscopic investigations, analysis of DNA strand breaks by in situ end-labeling (ISEL), and TdT-mediated dUTP-digoxigenin nick end-labeling (TUNEL) techniques, Lorenzen et al posited that mummified cells in Hodgkin lymphoma show features of cell death different from the classical definition of apoptosis by Kerr et al.[16,17] The author suggested that mummified cells in Hodgkin lymphoma manifest features of nonclassical apoptosis ("paraapoptosis"), a concept put forward by Payne et al.[16,18]
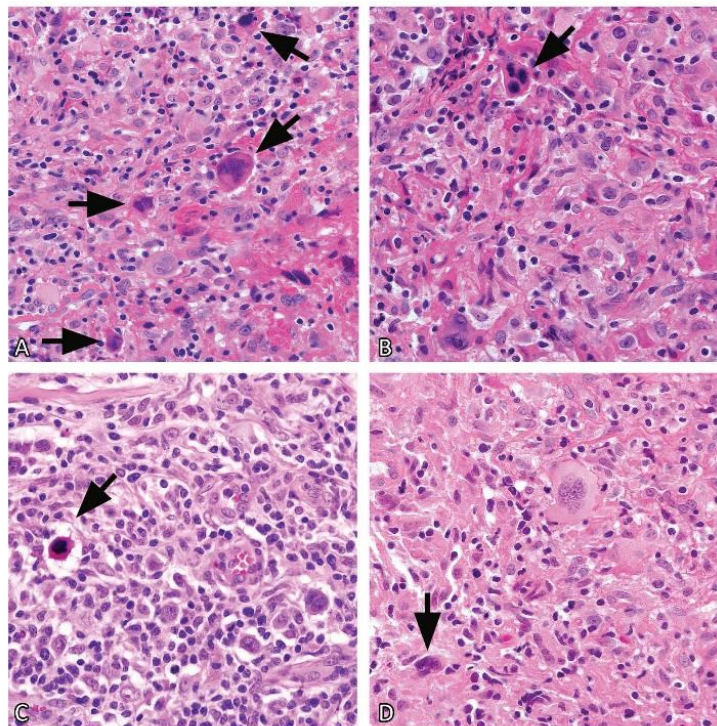
FIGURE 4. Mummified cells in cutaneous Hodgkin lymphoma (A–D, arrows). The mummified cells have varying appearances (binucleated, mononuclear, haloed, and multilobated) thus likely representing regressing cells of the correspondent diagnostic type (Reed–Sternberg cells, mononuclear Hodgkin cells, lacunar cells, and popcorn cells).
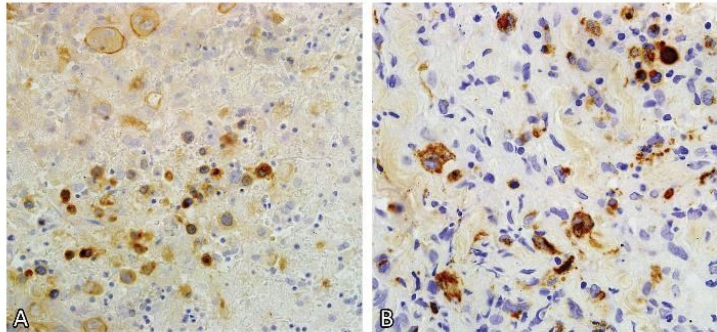
FIGURE 5. Positivity for CD30 (A) and CD15 (B) in mummified cells and intact diagnostic cells in cutaneous Hodgkin lymphoma.

Lorenzen demonstrated that classical apoptotic cells lost lineage and activation antigens such as CD3 and CD20 as well as CD15 or CD30, and DNA strand breaks were readily detected by use of either the ISEL or the TUNEL procedure. By contrast, mummified cells retained CD20, CD15, and CD30, whereas DNA strand breaks (detected by either ISEL or TUNEL) were absent.[16] In our opinion, mummified cells may be difficult to distinguish from pyknotic cells (which likely they are), but if retaining of CD30 and CD15 staining is accepted as a defining feature, then it appears that mummified cells are present in a majority of cases of cutaneous Hodgkin lymphoma. Their identification may be helpful because in some cases of cutaneous Hodgkin lymphoma, they can be recognized more readily than the diagnostic Reed–Sternberg cells, lacunar cells, and LP cells, thus providing a clue for the subsequent diagnostic workup of the lesion. The authors have occasionally observed similar pyknotic/mummified cells in CD30-positive anaplastic large cell lymphoma, and therefore, this feature per se can hardly be used to discriminate between the 2 diseases. In dermatopathology literature on cutaneous involvement in Hodgkin lymphoma, mummified cells have never been a subject of specific studies, but mummified/pyknotic cells can be recognized in the previously published material, however, without any specific comment (Figure 1 in Ref. 19).

In conclusion, mummified cells are encountered in a majority of cases of cutaneous Hodgkin lymphoma and may on occasion be conspicuous, thus serving as a clue to the diagnosis. Their strict separation from apoptotic cells on hematoxylin and eosin–stained slides is likely arbitrary.

REFERENCES

1. Smith JL Jr, Butler JJ. Skin involvement in Hodgkin's disease. *Cancer.* 1980;45:354–361.
2. White RM, Patterson JW. Cutaneous involvement in Hodgkin's disease. *Cancer.* 1985;55:1136–1145.
3. Tassies D, Sierra J, Montserrat E, et al. Specific cutaneous involvement in Hodgkin's disease. *Hematol Oncol.* 1992;10:75–79.
4. Moretti S, Pimpinelli N, Di Lollo S, et al. In situ immunologic characterization of cutaneous involvement in Hodgkin's disease. *Cancer.* 1989; 63:661–666.
5. Sioutos N, Kerl H, Murphy SB, et al. Primary cutaneous Hodgkin's disease. Unique clinical, morphologic, and immunophenotypic findings. *Am J Dermatopathol.* 1994;16:2–8.
6. Cerroni L, Beham-Schmid C, Kerl H. Cutaneous Hodgkin's disease: an immunohistochemical analysis. *J Cutan Pathol.* 1995;22:229–235.
7. van Dongen JJ, Langerak AW, Brüggemann M, et al. Design and standardization of PCR primers and protocols for detection of clonal immunoglobulin and T-cell receptor gene recombinations in suspect lymphoproliferations: report of the BIOMED-2 concerted action BMH4-CT98-3936. *Leukemia.* 2003;17:2257–2317.
8. Kazakov DV, Nemcova J, Mikyskova I, et al. Absence of Epstein-Barr virus, human papillomavirus, and simian virus 40 in patients of central european origin with lymphoepithelioma-like carcinoma of the skin. *Am J Dermatopathol.* 2007;29:365–369.
9. Watzinger F, Suda M, Preuner S, et al. Real-time quantitative PCR assays for detection and monitoring of pathogenic human viruses in immunosuppressed pediatric patients. *J Clin Microbiol.* 2004;42:5189–5198.
10. Svajdler M Jr, Kaspirkova J, Mezencev R, et al. Human papillomavirus and Epstein-Barr virus in nasopharyngeal carcinoma in a non-endemic eastern european population. *Neoplasma.* 2016;63:107–114.
11. Sternberg C Ueber eine eigenartige unter dem Bilde der Pseudoleukaemie verlaufende Tuberculose des lymphatischen Apparates. *Z Heilkunde.* 1898;19:21–90.
12. Reed DM. On the pathological changes in Hodgkin's dieae, with especial reference to its relation to tuberculosis. *Johns Hopkins Hosp Rep.* 1902;10:133–196.
13. Jackson H, Parker F. Hodgkin's disease II. Pathology. *N Engl J Med.* 1944;231:35–44.
14. Cross RM. Hodgkin's disease: histological classification and diagnosis. *J Clin Pathol.* 1969;22:165–182.
15. Kodousek R, Tichá V, Tichý M. Selective monocellular necrosis of Hodgkin's/Reed-Sternberg cells and their immunoreactivity to human serum antinuclear antibodies in NS- and MC-types of malignant lymphogranuloma. *Neoplasma.* 1992;39:205–210.
16. Lorenzen J, Thiele J, Fischer R. The mummified Hodgkin cell: cell death in Hodgkin's disease. *J Pathol.* 1997;182:288–298.
17. Kerr JF, Wyllie AH, Currie AR. Apoptosis: a basic biological phenomenon with wide-ranging implications in tissue kinetics. *Br J Cancer.* 1972;26:239–257.
18. Payne CM, Bernstein C, Bernstein H. Apoptosis overview emphasizing the role of oxidative stress, DNA damage and signal-transduction pathways. *Leuk Lymphoma.* 1995;19:43–93.
19. Gru AA, Lu D. Concurrent malignant melanoma and cutaneous involvement by classical Hodgkin lymphoma (CHL) in a 63 year-old man. *Diagn Pathol.* 2013;8:135.

A Case of Lymphomatoid Papulosis Type E With an Unusual Exacerbated Clinical Course

Irena E. Belousova, MD, PhD,* Liubov Kyrpychova, MD,† Alexey V. Samtsov, MD, PhD,* and Dmitry V. Kazakov, MD, PhD†

Abstract: Lymphomatoid papulosis (LyP) type E is a recently delineated variant characterized by the occurrence of large necrotic "eschar"-like lesions displaying microscopically angioinvasive and angiodestructive infiltrates composed of CD30$^+$ lymphocytes, frequently coexpressing CD8. In contrast to other LyP variants where patients develop multiple lesions, most patients with LyP type E present with few lesions (often 1 or 2 at a given time). In this article, we describe a 34-year-old man with LyP type E with an exacerbated clinical course characterized by the occurrence of almost a hundred of lesions. Initially, he presented with a single rapidly growing 2-cm large erythematous nodule on the forearm but after the administration of doxycycline multiple eschar-like lesions developed all over the body. Atypical lymphoid infiltrates with marked angiocentricity and angiotropism of CD30$^+$ medium-sized to large pleomorphic lymphocytes were seen histopathologically. After the withdrawal of the antibiotic, the lesions spontaneously regressed. Awareness of this rare LyP variant and its correct recognition, even if the clinical course is unusual and worrisome, is important to avoid aggressive treatment.

Key Words: lymphoma, skin, CD30, lymphomatoid papulosis, angiotropic, anaplastic large cell lymphoma

(Am J Dermatopathol 2018;40:145–147)

Lymphomatoid papulosis (LyP) belongs to the spectrum of CD30-positive cutaneous lymphoproliferative disorders. The latter also include primary cutaneous CD30$^+$ anaplastic large cell lymphoma and so-called borderline CD30$^+$ cases.[1] LyP clinically presents as recurrent erythematous and papulonecrotic eruptions with a waxing and waning course and can affect any body part. Histopathologically, LyP is characterized in most cases by atypical large lymphoid cells expressing CD30 but the clinicopathological spectrum of the disease is wide (types A, B, C, D, E, F and LyP with 6p23.5 rearrangement).[2–4] LyP type E is a recently delineated variant characterized by the occurrence of large necrotic "eschar"-like lesions displaying microscopically angioinvasive and angiodestructive infiltrates of CD30$^+$ lymphocytes, frequently coexpressing CD8.[5] To date, 22 cases of this disease variant have been reported

in the English language literature.[5–10] In most cases, patients typically presented with few lesions (often one or 2 at a given time). Here, we describe a patient with LyP type E with an exacerbated clinical course characterized by the occurrence of almost a hundred of lesions.

CASE REPORT

A 34-year-old man presented with a single rapidly growing 2-cm large erythematous nodule on the forearm (Fig. 1). Doxycycline was administered by a dermatologist who suspected a *Staphylococcus aureus* infection, but the lesion rapidly became necrotic, ulcerated, and, additionally, multiple similar eschar-like lesions (around 100) developed all over the body, sparing only the scalp, palms and soles (Figs. 2A–C). There was no peripheral lymphadenopathy, and the patient was otherwise healthy. The

FIGURE 1. An initial lesion appearing as 2-cm large erythematous nodule on the forearm.

www.amjdermatopathology.com | 145

FIGURE 2. Multiple eschar-like lesions that appeared after doxycycline intake. Overall, around 100 lesions developed on different body sites (A–C). The lesions spontaneously regressed, leaving behind atrophic scars and pigmentary patches within the course of 5 months (D).
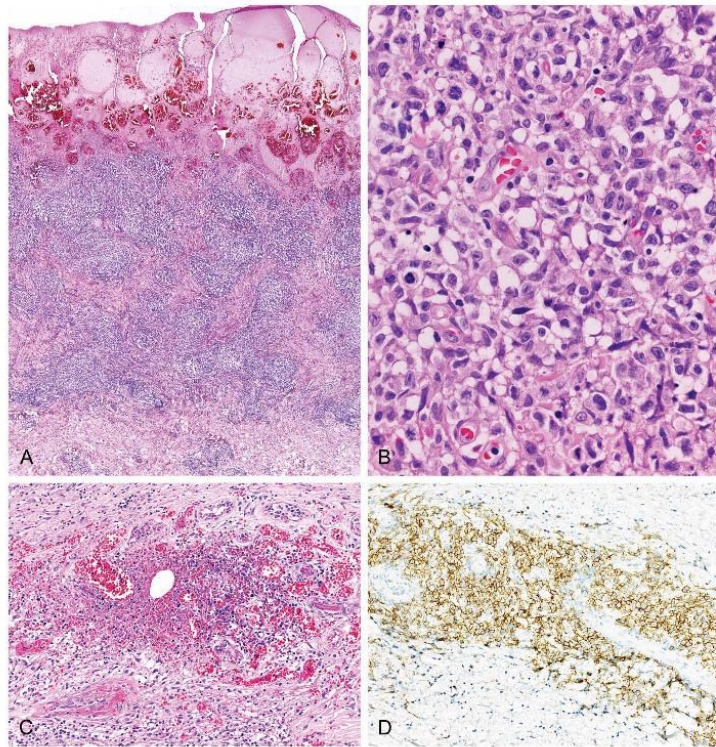
FIGURE 3. Ulcerative and necrotic epidermis, overlying an atypical lymphoid infiltrate extending throughout the reticular dermis with marked angiocentricity and angiotropism (A). The infiltrate is composed of medium-sized to large pleomorphic lymphocytes (B). Some vessels are partially or completely destroyed with extravasation of erythrocytes (C). CD30 positivity of the atypical lymphoid cells around vessels (D).

114

results of clinical investigations (routine blood tests and computer tomography) revealed no abnormalities. A biopsy was taken and after the diagnosis was established, the antibiotic was withdrawn, and the lesions spontaneously regressed within 5 months, leaving behind atrophic scars and pigmentary patches (Fig. 2D). According to the patient, he had similar but smaller lesions 16 and 13 years ago, occurring in a single fashion or as few lesions, respectively.

Histology revealed an ulcerative and necrotic epidermis, overlying an atypical lymphoid infiltrate extending throughout the reticular dermis with marked angiocentricity and angiotropism of medium-sized to large pleomorphic lymphocytes (Figs. 3A, B). Some vessels were partially or completely destroyed, and extravasation of erythrocytes was a prominent feature (Fig. 3C). There were foci of dermal necrosis. Small reactive lymphocytes, histiocytes, and neutrophils were present in the infiltrate.

Immunohistochemically, the atypical lymphoid cells were positive for CD3, CD5, CD30 (Fig. 3D), and CD4 and negative for CD8, CD56, and ALK-1. Small reactive T-lymphocytes expressed CD8 antigen; CD20+ B-lymphocytes formed small clusters on periphery of the infiltrate. About 10% of all tumor cells expressed TIA1, granzyme B, and perforin. FISH for EBER was negative. Molecular biologic studies using BIOMED 2 primers revealed monoclonal rearrangement of TCR genes.[11]

DISCUSSION

In its classic forms, LyP clinically manifests with crops of papules and small nodules (up to 2 cm), some of which are accompanied by a small and superficial ulceration, preceding spontaneous regression of the lesions. By contrast, in LyP type E, the initial papular lesions rapidly evolve into larger (up to 4 cm) ulcerations with a hemorrhagic necrotic, eschar-like appearance, often exceeding the size of the antecedent papule. Typically, only 1 or 2 ulcers are present in most cases at the time of diagnosis and during the disease course. At a later stage, the occurrence of several elements has been reported in some patients with LyP type E.[5] The clinical manifestation in our patient was unusual, in that the occurrence of a single lesion was followed by the eruption of about a hundred of large eschar-like ulcers, all of which developed within a single day after the administration of doxycycline, which seems to be a trigger factor. The diagnosis of LyP type E was confirmed histopathologically. The biopsy revealed a characteristic angiocentric and angiodestructive infiltrate of CD30+ medium-sized to large pleomorphic lymphocytes. In the original series, most cases demonstrated a cytotoxic phenotype; however, a variation with respect

to immunoreactivity of CD8/TIA-1 even within a single specimen was noted.[5] In our case, CD8 was negative, but only a single lesion was biopsied. Otherwise, the histopathological features were distinctive and permitted rendering the correct diagnosis, which was further confirmed by the typical clinical course with spontaneous regression of the lesions.

From a histopathological standpoint, the differential diagnosis of LyP type E includes several entities which present with angiocentric/angiodestructive features, including extranodal T/NK-cell lymphoma, nasal type, cutaneous gamma/delta-positive T-cell lymphoma, primary cutaneous, and systemic anaplastic large cell lymphoma. The distinction of LyP type E from these entities is discussed in details elsewhere.[5] Our case further demonstrates that the awareness of this rare LyP variant, even when if clinical course is unusual and worrisome, is important to avoid aggressive treatment.

REFERENCES

1. Willemze R. Lymphomatoid papulosis. *Dermatol Clin.* 1985;3:735–747.
2. Willemze R, Meyer CJ, Van Vloten WA, et al. The clinical and histological spectrum of lymphomatoid papulosis. *Br J Dermatol.* 1982;107:131–144.
3. Kempf W, Kazakov DV, Baumgartner HP, et al. Follicular lymphomatoid papulosis revisited: a study of 11 cases, with new histopathological findings. *J Am Acad Dermatol.* 2013;68:809–816.
4. El Shabrawi-Caelen L, Kerl H, Cerroni L. Lymphomatoid papulosis: reappraisal of clinicopathologic presentation and classification into subtypes A, B, and C. *Arch Dermatol.* 2004;140:441–447.
5. Kempf W, Kazakov DV, Schärer L, et al. Angioinvasive lymphomatoid papulosis: a new variant simulating aggressive lymphomas. *Am J Surg Pathol.* 2013;37:1–13.
6. Sharaf MA, Romanelli P, Kirsner R, et al. Angioinvasive lymphomatoid papulosis: another case of a newly described variant. *Am J Dermatopathol.* 2014;36:e75–7.
7. Wieser I, Oh CW, Talpur R, et al. Lymphomatoid papulosis: Treatment response and associated lymphomas in a study of 180 patients. *J Am Acad Dermatol.* 2016;74:59–67.
8. Kiavash K, Abner SM, Malone JC. New variant lymphomatoid papulosis type E preceding and coexisting with mycosis fungoides—a case report and review of the literature. *J Cutan Pathol.* 2015;42:1018–1023.
9. Wieser I, Wohlmuth C, Nunez CA, et al. Lymphomatoid papulosis in children and adolescents: a systematic review. *Am J Clin Dermatol.* 2016;17:319–327.
10. Uchiyama A, Motegi SI, Ishikawa O. Angioinvasive lymphomatoid papulosis (type E): a first Japanese case. *Eur J Dermatol.* 2016;26:507–508.
11. van Dongen JJ, Langerak AW, Bruggemann M, et al. Design and standardization of PCR primers and protocols for detection of clonal immunoglobulin and T-cell receptor gene recombinations in suspect lymphoproliferations: report of the BIOMED-2 Concerted Action BMH4-CT98-3936. *Leukemia.* 2003;17:2257–2317.

Kaposi Sarcoma in Association With an Extracavitary Primary Effusion Lymphoma Showing Unusual Intravascular Involvement: Report of a Case Harboring a *FAM175A* Germline Mutation

Liubov Kastnerova, MD,*† Irena E. Belousova, MD, PhD,‡ Michael Michal, MD, PhD,*†§ Nikola Ptakova, MSc,†¶ Michal Michal, MD,*† and Dmitry V. Kazakov, MD, PhD*†

Abstract: Primary effusion lymphoma (PEL) is a rare form of aggressive B-cell lymphoma characterized by a malignant serous effusion involving body cavities. It usually associated with human herpes virus–8 (HHV-8) and coexpression of Epstein–Barr virus and mostly affects patients with HIV. We report a rare case of cutaneous PEL with an unusual intravascular presentation, combined with Kaposi sarcoma involving the skin, lung, and gastrointestinal tract. The molecular genetic analysis of the sarcoma and lymphoma components, using next-generation sequencing was performed. The patient was a 67-year-old man who presented with multiple cutaneous tumors and mass in the left lung. He died 17 hours after the admission to the hospital. At autopsy, in addition to the cutaneous lesions, tumors in the left lung and gastrointestinal mucosa were also detected, and no effusions in the body cavities were seen. The biopsy from the cutaneous lesions, pulmonary, and intestinal tumors revealed histological and immunohistochemical features of Kaposi sarcoma. In addition, the skin biopsy specimens contained diffuse infiltrate composed of large pleomorphic cells, with focal intravascular growth that were negative for pan B-cell markers, weakly positive for CD38 and CD138 but expressed CD3, HHV-8, and Epstein–Barr virus. Molecular genetic studies in this specimen revealed monoclonal rearrangements of the IgH gene. The diagnosis of PEL, solid variant, was made. Next-generation sequencing analysis of the tumorous and normal tissue detected a pathogenic germline mutation of the *FAM175A* gene and somatic mutations in *BRCA2* and *RAD51B* (in both sarcoma and lymphoma specimens), and *INPP4B* and *RICTOR* (in lymphoma specimen only).

Key Words: primary effusion lymphoma, extracavitary solid tissue lymphoma, intravascular, HHV-8, EBV, sarcoma Kaposi

From the *Department of Pathology, Charles University, Faculty of Medicine in Pilsen, Pilsen, Czech Republic; †Bioptical Laboratory, Pilsen, Czech Republic; ‡Department of Dermatology, Medical Military Academy, Saint Petersburg, Russia; §Biomedical Center, Charles University, Faculty of Medicine in Pilsen, Pilsen, Czech Republic; and ¶Second Faculty of Medicine, Charles University, Prague, Czech Republic.

Correspondence: Dmitry V. Kazakov, MD, Sikl's Department of Pathology, Charles University Medical Faculty Hospital, Alej Svobody 80, 304 60 Pilsen, Czech Republic (e-mail: kazakov@medima.cz).

INTRODUCTION

Primary effusion lymphoma (PEL) is a rare and aggressive large B-cell lymphoma presenting in cavity serous effusions and is associated with herpes virus–8 (HHV-8) and coexpression of Epstein–Barr virus in 80% of cases.[1] Histopathologically, extracavitary PEL is characterized by large atypical cells with a plasmablastic, immunoblastic, or anaplastic morphology and an unusual phenotype, including negative immunoreaction for some or all B-cell lineage markers (CD20, CD19, and Pax5), aberrant expression of T-cell markers (CD3, CD4, and CD7), and positivity for one or more markers associated with terminal B-cell differentiation (CD38, CD138, and/or MUM-1).[2] It was originally described in patients with HIV/AIDS who developed body cavity effusions containing pleomorphic malignant cells.[3] PEL has also been reported in patients with severe immunodeficiency, recipients of solid organ transplants,[4] and also can occur in the absence of immunodeficiency, usually in elderly patients.[5] Given their common viral etiology, patients with PEL may have concurrent Kaposi sarcoma (KS). HHV-8–positive cases occur as solid masses rather than serous effusions and are classified as extracavitary or solid variant of PEL.[6] Extracavitary tumors with the morphological and phenotypic characteristics similar to those of PEL can occur in extranodal sites, including the gastrointestinal tract, skin, lungs, and central nervous system.[1] Solid organ involvement may occur without lymphomatous effusions during the course of the disease or precede or follow it. Associated KS may involve different or the same anatomical sites as solid PEL.[7] According to a recent study with a review of the literature, 10 cases of cutaneous extracavitary/solid variant of PEL have been described in the literature to date,[8] but only 2 of them had previous or concomitant KS.[9,10] We present a case of cutaneous PEL with intravascular involvement combined with KS affecting the skin, lung, and gastrointestinal tract, including the results of next generating sequencing (NGS) on both the sarcoma and lymphoma components.

CASE REPORT

A 67-year-old patient was admitted to our hospital in a severe condition with hypotension, hyposaturation, and somnolence. He

had multiple cutaneous patches, nodules, and tumors. An X-ray of the lung revealed a 29 × 31-mm large mass located paracardially on the left side. The patient died 17 hours after the admission. The patient history was significant for progressive multiple sclerosis, marked malnutrition, and a duodenal ulcer. His medication included, among others, a long-term corticosteroid therapy. Three years before the current admission, the patient developed multiple red-violet flat and exophytic lesions on both legs and on the right hand. A skin biopsy from the lower leg was taken at that time and interpreted as acroangiodermatitis Mali in another department.

At autopsy, multiple purple patches, plaques, and tumors involving the lower and upper extremities were found (Fig. 1). The tumor size ranged from 0.5 to 2 cm in the greatest dimension. Some lesions coalesced into large conglomerates. On the distal part of the right lower leg, there were multiple yellowish white confluent nodules with maceration that formed verrucous areas with toes' deformation. On both upper limbs, especially on the forearms, multiple bluish-like large macules and plaques were present. The above mentioned pulmonary lesion identified by the X-ray appeared grossly as a dark-red homogeneous firm nodule in the lower lobe of the left lung.

In addition, there were multiple exophytic lesions ranging from 0.8 to 3 cm on the mucosa of the gastroduodenal junction, duodenum, and small intestine. In the small intestine, the lesions involved approximately 50 cm of its length. No effusions in the body cavities were detected. No lymphadenopathy was found.

Several skin specimens taken from the lower leg demonstrated the dermal proliferation of spindled cells with eosinophilic cytoplasm and intracytoplasmic eosinophilic hyaline globules, forming numerous irregular, slit-like, vascular spaces. Extravasated erythrocytes were seen (Fig. 2). The spindled cells were immunohistochemically positive for CD31, D2-40, and demonstrated dot-like nuclear staining for HHV-8.

In addition, some cutaneous specimens contained a diffuse infiltrate composed of large pleomorphic cells showing numerous mitotic figures. The tumor cells had large round irregular nuclei, prominent nucleoli, and abundant eosinophilic cytoplasm. Some of the neoplastic cells had eccentrically located nuclei, perinuclear clearing, corresponding to the plasmablastic morphology. There were areas with an intravascular location of the neoplastic cells. Immunohistochemically, the atypical lymphoid cells were negative for pan B-cell markers (CD20, PAX-8, and CD79a) but showed aberrant expression of the T-cell marker CD3 and manifested strong nuclear immunoreaction for HHV-8 and Epstein–Barr virus. In addition, occasional neoplastic cells were weakly positive for CD38 and CD138 (Fig. 3). The tumor cells were negative for CD45, CD30, TIA, Granzyme B, Perforin, *BCL6*, CD5, CD7, CD4, CD8, and MUM-1. Ki-67 immunostaining demonstrated positivity in about 90% of the neoplastic cells.

The specimens from the pulmonary and intestinal tumors revealed features of KS without an infiltration of atypical lymphoid cells. We also review the previous cutaneous biopsy interpreted as acroangiodermatitis Mali, and it proved to be a misdiagnosed KS, confirmed retrospectively in our department by HHV-8–positive staining.

Molecular genetic studies using the BIOMED 2 primers[11] were performed on the lymphoma specimen and revealed monoclonal rearrangement of IgH, IgK, IgL, whereas no monoclonal rearrangements of TCR genes were found.

FIGURE 1. Multiple violaceous macules, plaques, and tumors on the lower and upper limbs (A, B), accompanied by multiple yellowish white confluent nodules with toes' deformation (C).
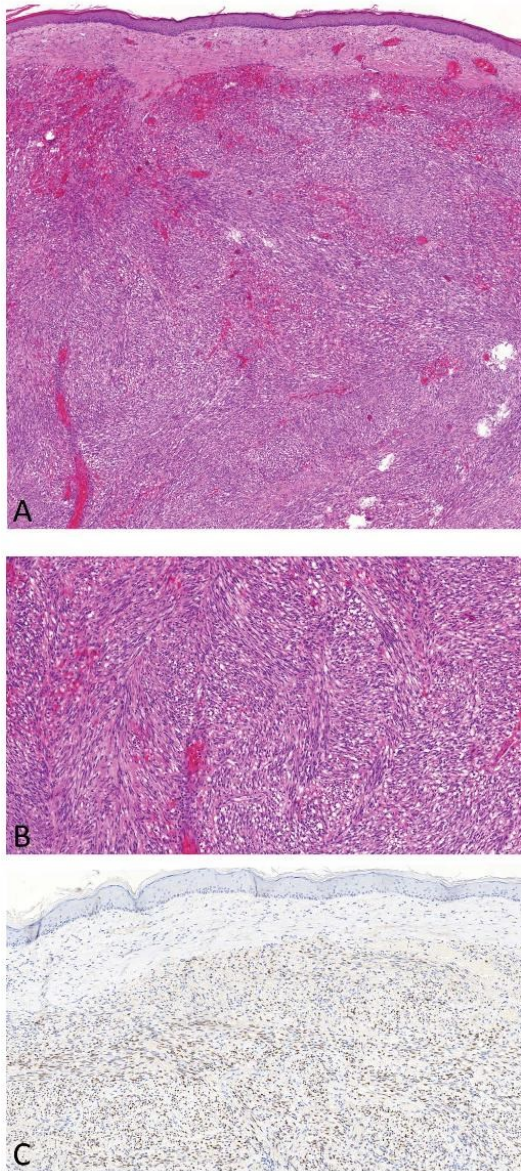
FIGURE 2. Kaposi sarcoma. At low-magnification, a well-defined dermal nodule consisting of fascicles of spindled cell (A) with irregular vascular spaces and extravasated erythrocytes is seen (B). The dot-like nuclear staining with HHV-8 in the spindled cells (C).

The FusionPlex Sarcoma and Lymphoma kits (ArcherDX Inc, Boulder, CO) were used to construct cDNA library for detection fusion transcripts, and TruSight Solid Tumor 170 (Illumina, San Diego, CA) was used for somatic mutation detection. All libraries were prepared in accordance with manufacturer's protocols and sequenced on an Illumina platform as described previously.[12] The Archer FusionPlex Sarcoma kit is a targeted sequencing assay to simultaneously detect and identify fusions of 26 genes associated with soft-tissue cancers (*ALK, CAMTA1, CCNB3, CIC, EPC1, EWSR1, FOXO1, FUS, GLI1, HMGA2, JAZF1, MEAF6, MKL2, NCOA2, NTRK3, PDGFB, PLAG1, ROS1, SS18, STAT6, TAF15, TCF12, TFE3, TFG, USP6,* and *YWHAE*). The Archer FusionPlex Lymphoma kit is a targeted NGS assay to simultaneously detect and identify fusions, point mutations, and expression levels in 125 genes linked to lymphomas, namely fusions in *ALK, BCL2, BCL6, BCR, BIRC3, CBFB, CCND1, CCND3, CDK6, CHIC2, CIITA, CREBBP, DEK, DUSP22, EIF4A1, ETV6, FGFR1, JAK2, KMT2A, MALT1, MKL1, MLF1, MLLT10, MYC, NFKB2, NOTCH1, P2RY8, PDCD1LG2, PDGFRA, PRDM16, STIL, TCF3,* and *TP63*; mutations in *AKT3, ALK, BAX, BCL2, BIRC3, BRAF, BTK, CARD11, CCND1, CD79B, CREBBP, DNMT3A, ETV6, EZH2, FBXW7, IDH1, IDH2, JAK1, JAK2, JAK3, KRAS, MYD88, NOTCH1, NOTCH2, NRAS, PDGFRA, PLCG1, PLCG2, RHOA, SF3B1, STAT3, STAT5B, STAT6, WT1,* and *XPO1*; and expression of *E2F2, ENTPD1, EXOC2, FAM216A, FOXP1, FUT8, IL16, IRF4, IRF8, ITPKB, KIAA0101, LIMD1, LMO2, LRMP, LZTS1, MAL, MAML3, MME, MUC1, MYBL1, MYC, NEK6, NFKB1, NME1, PAICS, PDCD1, PDCD1LG2, PIM1, PIM2, PPAT, PRKAR2B, PTPN1, PYCR1, RAB29, RAG1, RAG2, RANBP1, S1PR2, SERPINA9, SH3BP5, STRBP, TNFRSF13B, TNFSF4,* and *WT1*.

The Illumina TruSight Tumor 170 Panel, includes both the DNA and RNA parts, targeting the following genes *AKT1, AKT2, AKT3, ALK, APC, AR, ARID1A, ATM, ATR, BAP1, BARD1, BCL2, BCL6, BRAF, BRCA1, BRCA2, BRIP1, BTK, CARD11, CCND1, CCND2, CCND3, CCNE1, CD79A, CD79B, CDH1, CDK12, CDK4, CDK6, CDKN2A, CEBPA, CREBBP, CSF1R, CTNNB1, DDR2, DNMT3A, EGFR, EP300, ERBB2, ERBB3, ERBB4, ERCC1, ERCC2, ERG, ESR1, EZH2, FAM175A, FANCI, FANCL, FBXW7, FGF1, FGF10, FGF14, FGF19, FGF2, FGF23, FGF3, FGF4, FGF5, FGF6, FGF7, FGF8, FGF9, FGFR1, FGFR2, FGFR3, FGFR4, FLT1, FLT3, FOXL, GEN1, GNA11, GNAQ, GNAS, HNF1A, HRAS, CHEK1, CHEK2, IDH1, IDH2, INPP4B, JAK2, JAK3, KDR, KIT, KRAS, LAMP1, MAP2K1, MAP2K2, MCL1, MDM2, MDM4, MET, MLH1, MLL, MLLT3, MPL, MRE11A, MSH2, MSH3, MSH6, MTOR, MUTYH, MYC, MYCL1, MYCN, MYD88, NBN, NF1, NOTCH1, NOTCH2, NOTCH3, NPM1, NRAS, NRG1, PALB2, PDGFRA, PDGFRB, PIK3CA, PIK3CB, PIK3CD, PIK3CG, PIK3R1, PMS2, PPP2R2A, PTEN, PTCH1, PTPN11, RAD51, RAD51B, RAD51C, RAD51D, RAD54L, RAF1, RB1, RET, RICTOR, ROS1, RPS6KB1, SLX4, SMAD4, SMARCB1, SMO, SRC, STK11, TERT, TET2, TFRC, TP53, TSC1, TSC2, VHL,* and *XRCC2.* The quality of the extracted DNA was checked by qPCR using the Illumina FFPE QC kit, whereas the quality of RNA was tested using Agilent RNA 6000 Nano Kit on bioanalyzer 4200 TapeStation.

The detected mutations are listed in Table 1. A nontumoral specimen of normal heart tissue was tested to facilitate confirmation of the somatic and germline status of the mutations.

DISCUSSION

We describe a patient with extracavitary PEL associated with KS. Apart from the diffuse infiltrate, the lymphoma cells were located within blood vessels, which is a rare feature. Two cases of a cutaneous intravascular variant of extracavitary PEL have been described in the literature.[13,14] The neoplastic cells were mainly negative for B-cell–specific antigens with focal and subtle expression of CD138 and CD38, but the

118
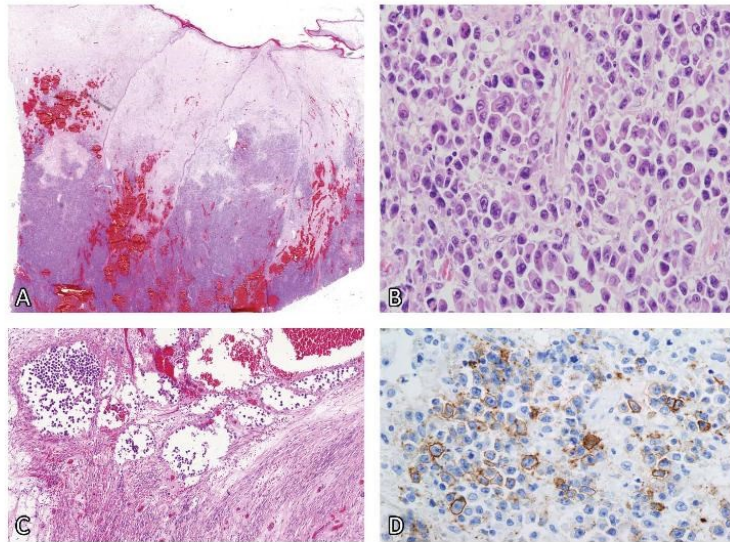
FIGURE 3. Primary effusion lymphoma, solid type. The skin biopsy contains a diffuse infiltrate in the deep dermis (A) composed of large atypical cells with prominent nucleoli, abundant eosinophilic cytoplasm with some features of a plasmablastic morphology (B). Note intravascular neoplastic cells (C). A weak positive immunoreaction for CD138 in neoplastic cells (D).

tumor cell lineage was confirmed by monoclonal IgH gene rearrangement. The histopathologic diagnosis of PEL can be difficult due to the unusual immunophenotype with aberrant expression of T-cell markers and monoclonal T-cell population. The presence of an intravascular component requires consideration of a differential diagnosis, which encompasses other intravascular B- and T/NK-cell lymphomas and intravascular lymphoid proliferations. In our case, however, the cells in the dermal infiltrate had the same histopathologic characteristics as the intravascular cells. A similar histological picture with dermal and intralymphatic tumor cells may be encountered in cutaneous anaplastic CD30+ large-cell lymphoma, but the latter expresses CD30, is of T-cell lineage, and is negative for HHV-8 and EBER.

Cases of PEL with an anaplastic morphology should be differentiated from the anaplastic variant of KS. Anaplastic or pleomorphic KS is poorly documented in the literature, possibly because of its rarity. Malignant transformation of KS, characterized by increased mitoses and marked cellular pleomorphism, was first described in 1959 by Cox and Helwig.[15] A "monomorphic" variant was identified by Templeton[16] in several cases of African KS. In a review of KS cases from Uganda, investigators distinguished KS with a "monocellular pattern" (resembling anaplastic KS) from a so-called "anaplastic variant pattern" (resembling angiosarcoma).[17] Anaplastic histopathological features have been described in the context of classic, African, and AIDS-associated KS.[18] In some of these reports, the picture demonstrating the anaplastic morphology of tumor cells is difficult to distinguish from the anaplastic variant of PEL without confirming the immunophenotype (eg, Fig. 3 in Ref. 19). Furthermore, some illustrations of purported anaplastic KS are rather suggestive of PEL (Fig. 4 in Ref. 20).

As far as we are aware, no previous cases of KS associated with PEL have been studied by means of NGS. The genetic analysis revealed that our patient harbored a pathogenic germline mutation of the *FAM175A* gene, which was of a clinical significance (Table 1). This gene is located

TABLE 1. Germline and Somatic Mutations Detected in Normal Tissue, Kaposi Sarcoma, and Lymphoma Specimens

	Germline Mutations	Somatic Mutations
Nontumor tissue (myocardium)	*FAM175A c.1106dupG*, CSF1R c.2746 G>A, TSC1 c.346T>G.*	None
Kaposi sarcoma (2277-19)	*FAM175A c.1106dupG*, CSF1R c.2746 G>A, TSC1 c.346T>G.*	*BRCA2 c.3096_3098delAGAinsTAT, RAD51B c.1111C>T.*
Lymphoma (2278-19)	*FAM175A c.1106dupG*, CSF1R c.2746 G>A, TSC1 c.346T>G.*	*BRCA2 c.3096_3098delAGAinsTAT, RAD51B c.1111C>T, INPP4B c.727C>A, RICTOR c.2335 G>A.*

Variant annotation was performed according to databases and in-silicon prediction software, including somatic database COSMIC, My Cancer Genome, and TCGA and predictive softwares SIFT, PolyPhen2, MutTaster, and CADD.
*Pathogenic mutations.

on chromosome 4q21.23 and codes for ABRAXAS (FA-M175A), a coiled-coil domain-containing protein involved in DNA damage resistance, G2/M checkpoint control, and DNA repair.[21] Germline mutations of *FAM175A* have been associated with ovarian carcinomas[22] and an increased breast cancer risk; they have also been found in rare types of cancer, including lip, upper aerodigestive tract, and pulmonary carcinomas and lymphoma of the throat.[23,24] To the best of our knowledge, no patient with cutaneous lymphoma or KS with a germline mutation in *FAM175A* has been described. The patient was childless, both his siblings died relatively young (cause of death remained unknown), as did parents; so, no further clarification of possible morbidities in the family was possible.

The other 2 germline variants detected were classified as of uncertain significance and involved the genes *CSF1R* (colony-stimulating factor–1 receptor) located on chromosome 5q32 and *TSC1* (tumor sclerosis complex–1) located in chromosome 9q34.13. *CSF1R* encodes a tyrosine kinase growth factor receptor for colony-stimulating factor–1, the macrophage- and monocyte-specific growth that controls the production, differentiation, and function of macrophages. Mutations in *CSF1R* have been associated with a predisposition to myeloid malignancy but have also been reported in lymphoproliferative disorders including Hodgkin lymphoma and CD30 $^+$ anaplastic large-cell lymphoma.[25,26]

TSC1 is a tumor suppressor gene that encodes the growth inhibitory protein hamartin, which interacts with and stabilizes the GTPase-activating protein tuberin. This hamartin–tuberin complex negatively regulates mammalian target of rapamycin complex–1 (mTORC1) signaling, which is a major regulator of anabolic cell growth. The main diseases associated with *TSC1* include tuberous sclerosis and focal cortical dysplasia, type I. *TSC1/2* is highly expressed in Burkitt's lymphoma cell lines.[27] Amplification of the angiogenic signal through the activation of the TSC/mTOR/HIF axis by the virus has been found in KS.[28]

Somatic mutations were detected in *BRCA2*, *RAD51B*, *INPP4B*, and *RICTOR*, and 2 of them were seen in both the sarcoma and the lymphoma specimens (Table 1). *BRCA2* is located on chromosome 13q13.1 and codes for the BRCA2 protein that contains several copies of a 70 aa motif called the BRC motif; these motifs mediate binding to the RAD51 recombinase, which functions in DNA repair. Alterations in *BRCA2* have been described in familial breast-ovarian cancer susceptibility 2,[29,30] in prostate cancer,[31] pancreatic adenocarcinoma,[32] and chronic lymphocytic leukemia[33] to name but a few.

Mutations of *RAD51B*, located on chromosome 14q24.1, have been reported in male breast cancer[34] and prostatic lesions.[35]

INPP4B is linked to 4q31.21 and encodes the inositol polyphosphate 4-phosphatase type II, one of the enzymes involved in phosphatidylinositol signaling pathways. Diseases associated with *INPP4B* include vulvar adenocarcinoma and tumors of the thyroid glands. *INPP4B* LOH has been found to be associated with more aggressive behavior in breast cancer and with a poorer prognosis.[36,37]

RICTOR is located on chromosome 5p13.1. Its protein, RICTOR, alone with MTOR is a component of a protein

[AU5]

complex that integrates nutrient- and growth factor–derived signals to regulate cell growth. It is related to the PI3K–AKT–mTOR signaling pathway. Alterations in the *RICTOR* gene have been found on leiomyosarcoma, osteosarcoma, and some cases of small cell lung cancer.[38–41]

In summary, we have reported a new case of KS-associated extracavitary PEL, supplementing the histopathological results by the NGS analysis.

REFERENCES

1. Swerdlow SH, Campo E, Harris NL, et al. *WHO Classification of Tumours of Haematopoietic and Lymphoid Tissues*. Lyon, France: IARC Press; 2017:323–324.
2. Chadburn A, Hyjek E, Mathew S, et al. KSHV-positive solid lymphomas represent an extra-cavitary variant of primary effusion lymphoma. *Am J Surg Pathol*. 2004;28:1401–1416.
3. Knowles DM, Inghirami G, Ubriaco A, et al. Molecular genetic analysis of three AIDS-associated neoplasms of uncertain lineage demonstrates their B-cell derivation and the possible pathogenetic role of the Epstein-Barr virus. *Blood*. 1989;73:792–799.
4. Nador RG, Cesarman E, Chadburn A, et al. Primary effusion lymphoma: a distinct clinicopathologic entity associated with the Kaposi's sarcoma-associated herpes virus. *Blood*. 1996;88:645–656.
5. Teruya-Feldstein J, Zauber P, Setsuda JE, et al. Expression of human herpesvirus-8 oncogene and cytokine homologues in an HIV-seronegative patient with multicentric Castleman's disease and primary effusion lymphoma. *Lab Invest*. 1998;78:1637–1642.
6. Pan ZG, Zhang QY, Lu ZB, et al. Extracavitary KSHV-associated large B-cell lymphoma: a distinct entity or a subtype of primary effusion lymphoma? study of 9 cases and review of an additional 43 cases. *Am J Surg Pathol*. 2012;36:1129–1140.
7. Zhang H, Yang XY, Hong T, et al. Kaposi sarcoma-associated herpesvirus (human herpesvirus type 8)-associated extracavitary lymphoma: report of a case in an HIV-positive patient with simultaneous kaposi sarcoma and a review of the literature. *Acta Haematol*. 2010;123:237–241.
8. Pielasinski U, Santonja C, Rodriguez-Pinilla SM, et al. Extracavitary primary effusion lymphoma presenting as a cutaneous tumor: a case report and literature review. *J Cutan Pathol*. 2014;41:745–753.
9. Aboulafia DM. HHV-8- and EBV-associated nonepidermotrophic large B-cell lymphoma presenting as a foot rash in a man with AIDS. *AIDS Patient Care STDS*. 2002;16:139–145.
10. Deloose ST, Smit LA, Pals FT, et al. High incidence of Kaposi sarcoma-associated herpesvirus infection in HIV-related solid immunoblastic/plasmablastic diffuse large B-cell lymphoma. *Leukemia*. 2005;19:851–855.
11. van Dongen JJ, Langerak AW, Bruggemann M, et al. Design and standardization of PCR primers and protocols for detection of clonal immunoglobulin and T-cell receptor gene recombinations in suspect lymphoproliferations: report of the BIOMED-2 Concerted Action BMH4-CT98-3936. *Leukemia*. 2003;17:2257–2317.
12. Skalova A, Vanecek T, Martinek P, et al. Molecular profiling of mammary analog secretory carcinoma revealed a subset of tumors harboring a novel ETV6-RET translocation: report of 10 cases. *Am J Surg Pathol*. 2018;42:234–246.
13. Crane GM, Ambinder RF, Shirley CM, et al. HHV-8-positive and EBV-positive intravascular lymphoma: an unusual presentation of extracavitary primary effusion lymphoma. *Am J Surg Pathol*. 2014;38:426–432.
14. Crane GM, Xian RR, Burns KH, et al. Primary effusion lymphoma presenting as a cutaneous intravascular lymphoma. *J Cutan Pathol*. 2014;41:928–935.
15. Cox FH, Helwig EB. Kaposi's sarcoma. *Cancer*. 1959;12:289–298.
16. Templeton AC. Kaposi's sarcoma. *Pathol Annu*. 1981;16:315–336.
17. Taylor JF, Templeton AC, Vogel CL, et al. Kaposi's sarcoma in Uganda: a clinico-pathological study. *Int J Cancer*. 1971;8:122–135.
18. Grayson W, Pantanowitz L. Histological variants of cutaneous Kaposi sarcoma. *Diagn Pathol*. 2008;3:31.
19. O'Connell KM. Kaposi's sarcoma: histopathological study of 159 cases from Malawi. *J Clin Pathol*. 1977;30:687–695.

120

20. Chapalain M, Goldman-Levy G, Kramkimel N, et al. Anaplastic Kaposi's sarcoma: 5 cases of a rare and aggressive type of Kaposi's sarcoma. *Ann Dermatol Venereol*. 2018;145:21–28.
21. Wang B, Matsuoka S, Ballif BA, et al. Abraxas and RAP80 form a BRCA1 protein complex required for the DNA damage response. *Science*. 2007;316:1194–1198.
22. Pennington KP, Walsh T, Harrell MI, et al. Germline and somatic mutations in homologous recombination genes predict platinum response and survival in ovarian, fallopian tube, and peritoneal carcinomas. *Clin Cancer Res*. 2014;20:764–775.
23. Solyom S, Aressy B, Pylkas K, et al. Breast cancer-associated Abraxas mutation disrupts nuclear localization and DNA damage response functions. *Sci Transl Med*. 2012;4:122ra123.
24. McKay JD, Truong T, Gaborieau V, et al. A genome-wide association study of upper aerodigestive tract cancers conducted within the INHANCE consortium. *PLoS Genet*. 2011;7:e1001333.
25. Ridge SA, Worwood M, Oscier D, et al. FMS mutations in myelodysplastic, leukemic, and normal subjects. *Proc Natl Acad Sci U S A*. 1990; 87:1377–1380.
26. Lamprecht B, Walter K, Kreher S, et al. Derepression of an endogenous long terminal repeat activates the CSF1R proto-oncogene in human lymphoma. *Nat Med*. 2010;16:571–579.
27. Hartleben G, Muller C, Kramer A, et al. Tuberous sclerosis complex is required for tumor maintenance in MYC-driven Burkitt's lymphoma. *EMBO J*. 2018;37. AU6
28. Jham BC, Ma T, Hu J, et al. Amplification of the angiogenic signal through the activation of the TSC/mTOR/HIF axis by the KSHV vGPCR in Kaposi's sarcoma. *PLoS One*. 2011;6:e19103.
29. Wooster R, Bignell G, Lancaster J, et al. Identification of the breast cancer susceptibility gene BRCA2. *Nature*. 1995;378:789–792.
30. Miki Y, Katagiri T, Kasumi F, et al. Mutation analysis in the BRCA2 gene in primary breast cancers. *Nat Genet*. 1996;13:245–247.
31. Edwards SM, Kote-Jarai Z, Meitz J, et al. Two percent of men with early-onset prostate cancer harbor germline mutations in the BRCA2 gene. *Am J Hum Genet*. 2003;72:1–12.
32. Schutte M, da Costa LT, Hahn SA, et al. Identification by representational difference analysis of a homozygous deletion in pancreatic carcinoma that lies within the BRCA2 region. *Proc Natl Acad Sci U S A*. 1995;92:5950–5954.
33. Garcia-Marco JA, Caldas C, Price CM, et al. Frequent somatic deletion of the 13q12.3 locus encompassing BRCA2 in chronic lymphocytic leukemia. *Blood*. 1996;88:1568–1575.
34. Orr N, Lemnrau A, Cooke R, et al. Genome-wide association study identifies a common variant in RAD51B associated with male breast cancer risk. *Nat Genet*. 2012;44:1182–1184.
35. Nowacka-Zawisza M, Wisnik E, Wasilewski A, et al. Polymorphisms of homologous recombination RAD51, RAD51B, XRCC2, and XRCC3 genes and the risk of prostate cancer. *Anal Cell Pathol (Amst)*. 2015;2015:828646.
36. Tokunaga E, Yamashita N, Kitao H, et al. Biological and clinical significance of loss of heterozygosity at the INPP4B gene locus in Japanese breast cancer. *Breast*. 2016;25:62–68.
37. Kofuji S, Kimura H, Nakanishi H, et al. INPP4B is a PtdIns(3,4,5)P3 phosphatase that can act as a tumor suppressor. *Cancer Discov*. 2015;5:730–739.
38. Sarbassov DD, Ali SM, Kim DH, et al. Rictor, a novel binding partner of mTOR, defines a rapamycin-insensitive and raptor-independent pathway that regulates the cytoskeleton. *Curr Biol*. 2004;14:1296–1302.
39. El Shamieh S, Saleh F, Moussa S, et al. RICTOR gene amplification is correlated with metastasis and therapeutic resistance in triple-negative breast cancer. *Pharmacogenomics*. 2018;19:757–760.
40. Cote GM, He J, Choy E. Next-generation sequencing for patients with sarcoma: a single center experience. *Oncologist*. 2018;23:234–242.
41. Ross JS, Wang K, Elkadi OR, et al. Next-generation sequencing reveals frequent consistent genomic alterations in small cell undifferentiated lung cancer. *J Clin Pathol*. 2014;67:772–776.

121

2.2 MESENCHYMAL TUMORS

This section included a single article *«ALK gene fusions in epithelioid fibrous histiocytoma: a study of 14 cases, with new histopathological findings»*. Epithelioid fibrous histiocytoma (EFH) is a variant of benign fibrous histiocytoma mostly composed of epithelioid cells. (56) Previous studies showed that ALK is often positive in epithelioid fibrous histiocytoma. (57), (58) Our objective was to study a series of EFH to describe histopathological variations of EFH, identify potentially novel *ALK* gene fusions and determine whether there is a correlation between the morphology and a particular gene fusion. Microscopically, all but two lesions were polypoid and composed of epithelioid cells with ample cytoplasm with a variable number of bi-, tri- or multinucleated, spindled, multilobated, cells with eccentric nuclei, cells with nuclear pseudoinclusions, mucinous and grooved cells. The remaining two neoplasms were composed of pale eosinophilic to clear cells, occasioning a resemblance to PEComa or leiomyoma. Immunohistochemically, all cases expressed ALK, and 11 were positive for TFE-3. The break apart test for *ALK* was positive in 11 cases, whereas specimens from the remaining 3 cases were not analyzable. *ALK* genes fusions were found in all but 3 cases and included *SQSTM1-ALK*, *VCL-ALK*, *TMP3-ALK*, *PRKAR2A-ALK*, *MLPH-ALK*, and *EML4-ALK*, 4 representing novel fusions. No correlation between the histological features and the type of *ALK* fusion was found. *TFE-3* break apart test was negative. In conclusion, ALK-positive EFH frequently shows *ALK* gene fusions, and rare variants consist instead of spindled "non-epithelioid" cells, thus occasioning a resemblance to PEComa or leiomyoma.

ALK Gene Fusions in Epithelioid Fibrous Histiocytoma: A Study of 14 Cases, With New Histopathological Findings

Dmitry V. Kazakov, MD, PhD,*† Liubov Kyrpychova, MD,*† Petr Martinek, PhD,*†
Petr Grossmann, PhD,*† Petr Steiner,*† Tomas Vanecek, PhD,*† Michal Pavlovsky, MD,‡
Vladimir Bencik, MD,§ Michael Michal, MD,*† and Michal Michal, MD*†

Abstract: Previous studies showed that ALK is often positive in epithelioid fibrous histiocytoma (EFH). Two cases of EFH with *ALK* gene fusions have been recorded. Our objective was to study a series of EFH to present histopathological variations of EFH, identify novel *ALK* gene fusions, and determine whether there is a correlation between histopathological features and particular gene. We investigated 14 cases of EFH, all ALK immunopositive. The cases were assessed histopathologically as well as for *ALK* and *TFE-3* rearrangements using FISH and *ALK* gene fusions using next-generation sequencing. The analysis of the sequencing results was performed using the Archer Analysis software (v5; ArcherDX Inc). The study group consisted of 8 female and 6 male patients, ranging in age from 18 to 79 years (mean 42 years; median 37.5 years). All presented with a solitary lesion. Microscopically, most lesions were polypoid and composed of epithelioid cells with ample cytoplasm. In addition, a variable number of bi-, tri-, or multinucleated, spindled, multilobated, cells with eccentric nuclei, cells with nuclear pseudoinclusions, mucinous, and grooved cells were admixed. In 5 cases, the predominant epithelioid cell component consisted of rather small cells, whereas spindled cells dominated in 3 cases. Of these, 2 lesions were composed rather of pale eosinophilic to clear cells, occasioning a resemblance to PEComa or leiomyoma. Immunohistochemically, all cases expressed ALK and 11 were positive for TFE-3. The break apart test for *ALK* was positive in 11 cases, whereas specimens from the remaining 3 cases were not analyzable. *ALK* genes fusions were found in all but 3 cases and included *SQSTM1-ALK* (3), *VCL-ALK* (3), *TMP3-ALK* (2), *PRKAR2A-ALK* (1), *MLPH-ALK* (1), and *EML4-ALK* (1). No correlation between histological features and type of *ALK* fusion was found. *TFE-3* break apart test was negative. It is concluded that ALK-immunopositive EFH shows *ALK* gene fusions that involve various protein-coding genes, implicated in a variety of biological processes. Rare variants of EFH rather consist of spindled "non-epithelioid" cells.

Key Words: epithelioid fibrous histiocytoma, ALK, TFE-3, gene fusions, Spitz nevus

From the *Sikl's Department of Pathology, Medical Faculty in Pilsen, Charles University in Prague, Pilsen, Czech Republic; †Bioptical Laboratory, Pilsen, Czech Republic; ‡Department of Pathology, Regional Hospital Most, Czech Republic; and §Ben Labor, Ostrava, Czech Republic.

INTRODUCTION

Epithelioid fibrous histiocytoma (EFH) is considered as a variant of benign fibrous histiocytoma in which more than 50% of cells are epithelioid.[1,2] In contrast to benign fibrous histiocytoma (dermatofibroma), EFH usually lacks collagen entrapment at the periphery of the lesion, xanthomatized cells and epidermal hyperpigmentation above the lesion. EFH usually presents as a polypoid lesion, often with an epidermal collarette. Previously published material and our own experience indicate certain histopathological heterogeneity of EFH, regarding cytological features, architectural features and immunoprofile.[3–6] With respect to the latter, a subset of EFH shows ALK expression on immunohistochemistry.[7,8] Doyle et al detected this feature in 29 of 33 cases, and in all 13 studied ALK-positive lesions, FISH demonstrated *ALK* rearrangements.[9] Two cases of EFH with *ALK* gene fusions have been recently recorded.[10] Our objective was to study a series of EFH to present histopathological variations of EFH, identify potentially novel *ALK* gene fusions, and determine whether there is a correlation between the histopathological features and a particular gene fusion.

MATERIAL AND METHODS

Case Selection

A search in the joint consultation files of 2 authors (M. M. and D.V.K.) yielded 46 cases coded as EFH and lesions in which EFH was a diagnostic consideration. Cases with available blocks were retrieved and reviewed. Apart from tissue availability, included in the study were only ALK-immunopositive lesions. A total of 14 cases meeting the selection criteria were included for a further investigation.

Immunohistochemical Studies

A new staining for ALK was performed for all selected cases. In most cases, 2 clones, namely ALK01 and D5F3 (both prediluted; Ventana, Tuscon, AZ), were used. Also, all lesions were stained for TFE-3 (MRQ-37, prediluted; Cell Marque, Rocklin, CA), as we have previously noted frequently positivity of EFH for TFE-3. In most cases, other various markers, including melanocytic, epithelial, vascular, neural, follicular dendritic, Langerhans cell, and others were performed at the time of the original diagnosis; these were not repeated.

TABLE 1. Summary of the Main Clinicopathological, Immunohistochemical, and Molecular Biological Features

Case	Sex/Age	Location	Clinical Data/Size (mm)	Architecture	Cell Arrangement	Cells
1	F/49	Back	Tumor, 2 yrs duration/5	Polypoid with epidermal collaret	Sheets	Small epithelioid cells*; multilobated cells; cells with eccentric nuclei; spindled cells; intranuclear pseudoinclusions
2	M/38	Shin	Fibrous tumor/8	Polypoid with epidermal collaret	Sheets, nests	Large epithelioid cells with ample cytoplasm*; multinucleated cells; grooved cells; intranuclear pseudoinclusions
3	M/35	Chest wall	Nevus/10	Polypoid with epidermal collaret	Sheets	Large epithelioid cells with ample cytoplasm*; multinucleated cells; grooved cells; mucinous; intranuclear pseudoinclusions
4	F/45	Thigh	Nodule/8	Polypoid with epidermal collaret	Sheets, fascicles	Spindled cells*; large epithelioid cells with ample cytoplasm; grooved cells; intranuclear pseudoinclusions
5	F/79	Thigh	Fibroma/17	Polypoid, ulcerated	Sheets, perivascular cuffs	Small epithelioid cells*; multilobated cells; multinucleated cells; spindled cells; grooved cells
6	M/18	Back	Bleeding pyogenic granuloma, 1-mo duration/12	Polypoid, ulcerated	Sheets, perivascular cuffs	Small epithelioid cells*; spindled cells; multinucleated cells; mucinous cells
7	F/37	Flank	Dermatofibroma? Keratoacanthoma? 1-yr duration/5	Intradermal, nonpolypoid	Nested, focally fascicular	Small epithelioid cells*; cells with eccentric nuclei; spindled cells; grooved cells; intranuclear pseudoinclusions
8	M/48	Thigh	Amelanotic melanoma? BCC? 3-mo duration/10	Polypoid	Sheets, focally storiform with vague whorling	Large epithelioid cells with ample cytoplasm*; multinucleated cells; spindled cells; cells with eccentric nuclei; intranuclear pseudoinclusions
9	M/74	Back	BCC/10	Polypoid with epidermal collaret	Fascicular, single cell files, nested	Small epithelioid and spindled cells*; multinucleated cells; intranuclear pseudoinclusions
10	F/31	Thigh	Nodule/10	Polypoid with epidermal collaret	Sheets, focally nested	Large epithelioid cells with ample cytoplasm*; cells with eccentric nuclei mucinous cells; spindled cells; multinucleated cells; grooved cells; intranuclear pseudoinclusions
11	F/55	Earlobe	Tumor/7	Polypoid	Sheets	Large epithelioid cells with ample cytoplasm*; multinucleated cells; cells with eccentric nuclei; spindled cells; grooved cells; intranuclear pseudoinclusions
12	M/21	Trunk	Wart/20	Intradermal	Sheets, focally plexiform, fascicular	Clear spindled cells*; spindled cells; nuclear pseudoinclusions
13	F/28	Shin	Verrucous nevus/8	Polypoid with epidermal collaret	Sheets, fascicular	Clear spindled cells*; cigar-like cells
14	F/28	Chest wall	Nodule, 6-mo duration/8	Polypoid with epidermal collaret	Sheets	Large epithelioid cells with ample cytoplasm*; multinucleated cells; cells with eccentric nuclei; mucinous cells

Case	Stroma	Vasculature	Reactive Cells	IHC ALK/TFE-3	FISH *ALK/TFE-3* Ba	Gene Fusion
1	Scant	Inconspicuous	Lymphocytes	+/+	+/−	*SQSTM1-ALK*
2	Focally collagenous	Inconspicuous	Lymphocytes	+/+	+/−	*SQSTM1-ALK*
3	Scant, focally fibrotic	Focally prominent	Lymphocytes	+/+	+/−	*VCL-ALK*
4	Focally fibrotic	Focally prominent	Lymphocytes	+/+	+/−	*TPM3-ALK*
5	Scant, focally myxoid	Prominent	Lymphocytes; neutrophils	+/+	+/−	*VCL-ALK*

124

TABLE 1. (*Continued*) Summary of the Main Clinicopathological, Immunohistochemical, and Molecular Biological Features

Case	Stroma	Vasculature	Reactive Cells	IHC ALK/TFE-3	FISH *ALK/TFE-3* Ba	Gene Fusion
6	Scant	Prominent	Lymphocytes; neutrophils	+/+	+/−	VCL-ALK
7	Collagenous, focally myxoid	Inconspicuous	Lymphocytes	+/-	NA	SQSTM1-ALK
8	Scant	Inconspicuous	Lymphocytes; emperiopolesis	+/+	+/−	NA
9	Collagenous	Inconspicuous	Lymphocytes	+/-	+/−	PRKAR2A-ALK
10	Collagenous, especially perivascular	Prominent	Lymphocytes; emperiopolesis	+/+	NA	NA
11	Scant, focally myxoid	Focally prominent	Lymphocytes; plasma cells; emperiopolesis	+/+	+/−	MLPH-ALK
12	Scant, focally collagenous	Inconspicuous	Lymphocytes; plasma cells	+/+	+/−	TMP3-ALK
13	Scant	Focally prominent	Lymphocytes	+/+	+/−	EML4-ALK
14	Scant	Focally prominent	Lymphocytes; plasma cells	+/−	NA	NA

*Predominant cell type.
ba, break apart; NA, not analyzable.

FISH for *ALK* and *TFE3* Rearrangements

Four-micrometer thick formalin-fixed paraffin-embedded sections were placed onto positively charged slides. The unstained slides were routinely deparaffinized and incubated in the 1× Target Retrieval Solution Citrate pH 6 (Dako, Glostrup, Denmark) at 95°C for 40 minutes and subsequently cooled for 20 minutes at a room temperature in the same solution. The slides were washed in deionized water for 5 minutes and digested in protease solution with Pepsin (0.5 mg/mL; Sigma Aldrich, St. Louis, MO) in 0.01 M HCl at 37°C for 35–60 minutes, according the sample conditions. The slides were then placed into deionized water for 5 minutes, dehydrated in a series of ethanol solution (70%, 85%, and 96% for 2 minutes each) and air-dried. For the detection of *ALK* and *TFE3* breaks, the Vysis ALK Break Apart Probe Kit (Vysis/Abbott Molecular, Des Plaines, IL) and ZytoLight SPEC TFE3 Dual Color Break Apart Probe (ZytoVision GmbH, Bremerhaven, Germany) were used, respectively. An appropriate amount of factory premixed probe was applied on a specimen, covered with a glass coverslip, and sealed with rubber cement. The slides were incubated in the ThermoBrite instrument (StatSpin/Iris Sample Processing, Westwood, MA) with co-denaturation at 85°C for 8 minutes and hybridization at 37°C for 16 hours. The rubber cemented coverslip was then removed and the slide was placed in post-hybridization wash solution (2xSSC + 0.3% NP-40) at 72°C for 2 minutes. The slides were air-dried in the dark, counterstained with 4′,6′-diamidino-2-phenylindole DAPI (Vysis/Abbott Molecular), coverslipped and immediately examined with an Olympus BX51 fluorescence microscope (Olympus Corporation, Tokyo, Japan) using a 100× objective and filter sets triple band pass (DAPI/SpectrumGreen/SpectrumOrange), dual band pass (SpectrumGreen/SpectrumOrange), and single band pass (SpectrumGreen or SpectrumOrange). A minimum of 100 randomly selected nonoverlapping tumor cell nuclei were counted. For both the *ALK* break apart and *TFE-3* break apart tests, the presence of yellow (normal) and separated (break) orange and/or green fluorescent signals was evaluated.

Samples were considered positive when more than 10% of nuclei showed break signals (mean + 3 standard deviation in normal nonneoplastic control tissues).
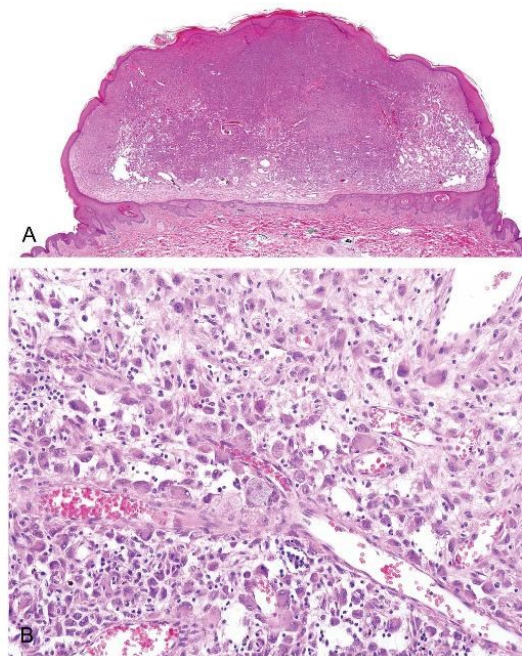
FIGURE 1. EFH (case 13). A polyploid lesion with epidermal collarette and prominent vasculature at the periphery (A) composed of large epithelioid cells with ample cytoplasm, with focal accentuation around the vessels (B). Note binucleated cells and occasional cells with mucinous cytoplasm (B).
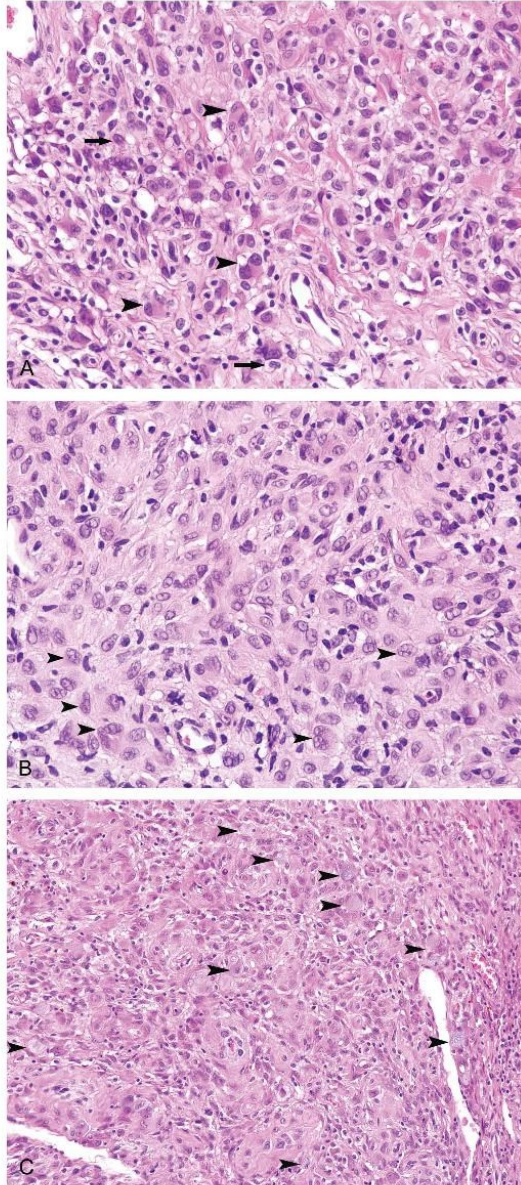
FIGURE 2. Cytological variations in EFH. Note cells with nuclear grooves (arrows) and numerous bi- or tri-nucleated cells (arrowheads) (A), cells with lobulated nuclei (arrowheads, B), and numerous mucinous cells (arrowheads, C).
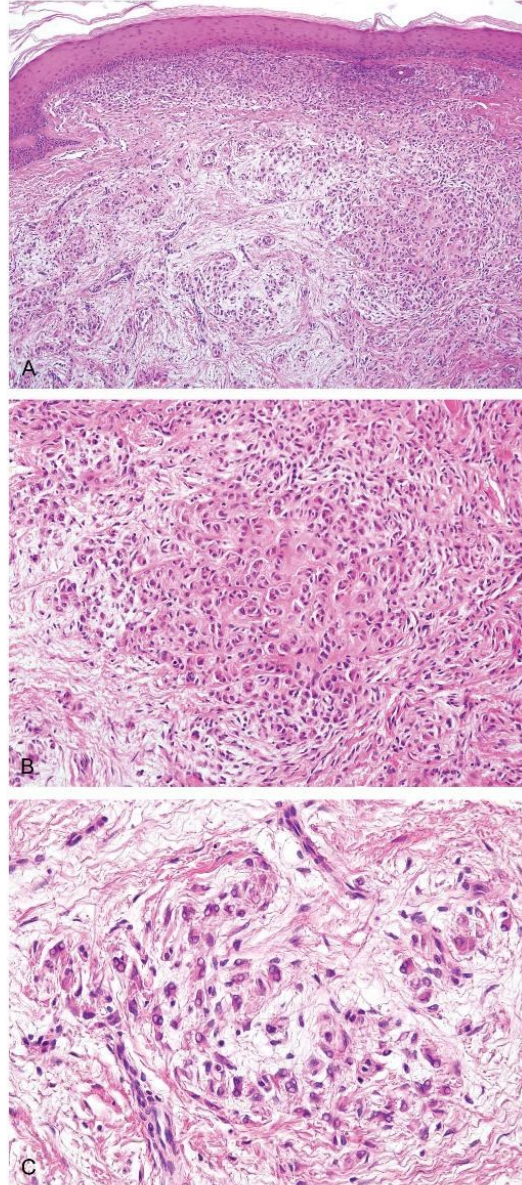
FIGURE 3. EFH (case 7) with nested pattern (A, B), focally resembling a melanocytic lesion. Note plentiful cells with intranuclear pseudoinclusions in less cellular (C) compared with the nested area (B).

126

Gene Fusion Detection Using Next-Generation Sequencing

Depending on the sample size, up to 3 formalin-fixed paraffin-embedded sections (10 μm thick) were macrodissected and total nucleic acid was extracted using the Agencourt For-maPure Kit (Beckman Coulter, Brea, CA) with modifications recommended by ArcherDX (ArcherDX Inc, Boulder, CO). Total nucleic acid was quantified using the Qubit Broad Range RNA Assay Kit (ThermoFisher Scientific, Waltham, MA) and input for each sample's library preparation was set to 250 ng. The PreSeq RNA QC Assay using iTaq Universal SYBR Green Supermix (Biorad, Hercules, CA) was performed to assess sample quality. Samples with the cycle threshold value smaller than 30 continued with target enrichment. The Comprehensive Thyroid Lung kit (ArcherDX Inc, Boulder, CO) containing 195 targets in 40 genes was used, and all steps were performed following the Archer's Fusion Plex Protocol for Illumina (ArcherDX Inc). Final libraries were quantified following the Library Quantification for Illumina Libraries protocol (KAPA, Wilmington, MA) assuming a 200 bp fragment length. Up to 32 samples were multiplexed per run on a NextSeq sequencer (Illumina, San Diego, CA) spiked with 20% PhiX control. The analysis of the sequencing results was performed using the Archer Analysis software (v5; ArcherDX Inc). Fusion parameters were set to a minimum of 5 valid fusion reads with a minimum of 3 unique start sites within the valid fusion reads.

RESULTS

Clinical Data

There were 8 female and 6 male patients, ranging in age from 18 to 79 years (mean 42 years; median 37.5 years). All presented with a solitary lesion. The clinical diagnoses included a melanocytic nevus, pyogenic granuloma, derma-tofibroma, basal cell carcinoma, wart, keratoacanthoma, or mere description as a nodule or tumor. The locations included the trunk (7 cases), lower extremities (6 cases), and face (1 case). Grossly, the lesions varied in sized from 5 to 20 mm (mean 9.9 mm; median 9 mm) (Table 1).

Histopathological Findings

The lesions were mostly polypoid, with (n = 8) or without (n = 4) an epidermal collarette (Fig. 1A). Two cases exhibited a nonpolypoid architecture with an intradermal proliferation of the neoplastic cells. The predominant cell types were mononucleated medium-sized to large epithelioid cells with ample eosinophilic to amphophilic cytoplasm. In addition, a variable number of bi-, tri-, or multinucleated (rarely), spindled, multilobated, cells with eccentric nuclei, cells with nuclear pseudoinclusions, mucinous, and grooved cells, likely representing a variation of a single cell type were admixed (Figs. 1B, 2–4) The cells were usually arranged in well-demarcated sheets, rarely with a focal nested/whirling pattern, fascicular areas, and perivascular cuffs. Subtle variations of cell arrangement were noted in some cases within a single lesion. In cases, where focal stromal edema was prominent, the cells were arranged in a more dyscohesive fashion (Figs. 1B, 2–4). In 5 cases, the predominant epithelioid cell component consisted of rather small cells, whereas spindled cells dominated in 3 cases (Fig. 5). Of these, 2 lesions were composed of pale eosinophilic to clear cells, occasioning a resemblance to PEComa or leiomyoma (Fig. 6). The stroma was usually scant, focally myxoid, or sclerotic. In 7 cases, a vascular component was conspicuous. Admixed with the neoplastic cells were occasional lymphocytes, plasma cells, and, rarely,
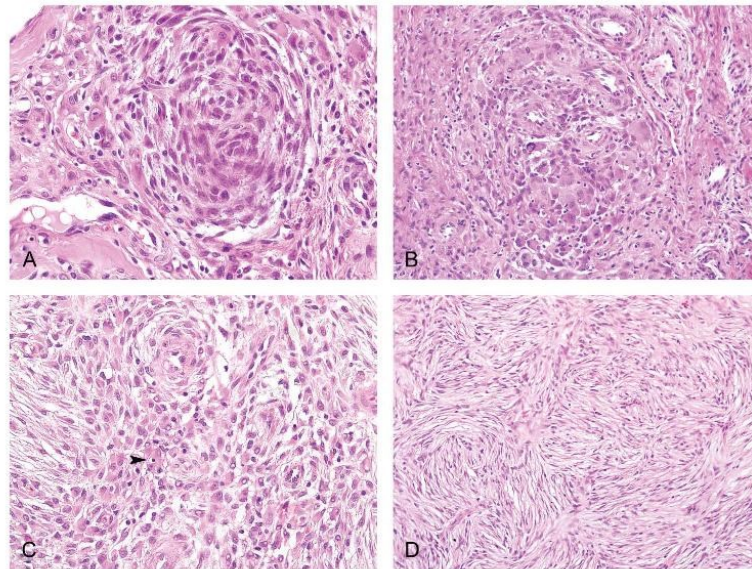
FIGURE 4. Pattern variation in EFH. A nest with vague whorling of the neoplastic cells with some spindling (A) and a more sharply circumscribed nodule composed of large round epithelioid cells (B). Both areas (A, B) are from the same lesion (case 10). Solid and vague storiform patterns with slender spindled cells occurring in the same lesion (case 8) (C, D). Note intracytoplasmic lymphocyte (emperipolesis, C, arrowhead).

127
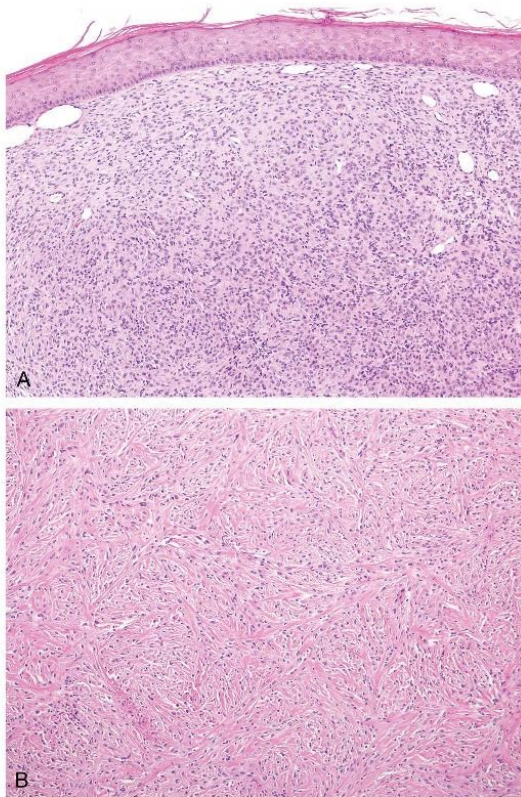
FIGURE 5. EFH composed predominantly of small epithelioid (A) (case 1) and small, spindled cells on a fibrous background (B) (case 9).

neutrophils. In 3 cases, single intracytoplasmic lymphocytes were identified, a feature consistent with emperipolesis (Fig. 4C).

Immunohistochemical Findings

ALK was positive in all 14 cases, whereas TFE-3 was positive in 11 lesions (>50% of cells). In the 3 cases labeled as negative for TFE-3, only focal nuclear positivity was noted.

FISH Findings

A break apart test for *ALK* was positive in 11 cases, whereas specimens from the remaining 3 cases were not analyzable (Table 1). Of the 11 positive cases, 10 manifested the classical break apart pattern, whereas one case (case 1) showed a FISH positive pattern with deletion of the 5′-ALK probe that hybridizes centromerically of the breakpoint (Fig. 7). TFE-3 rearrangements were not found in none of the 11 analyzable cases.
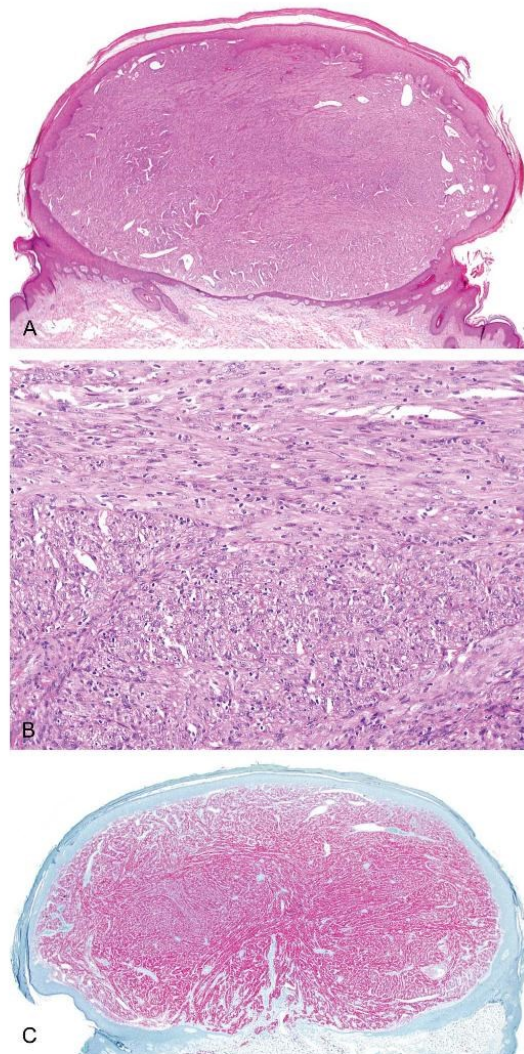
FIGURE 6. This example (case 13) manifests a typical polypoid architecture (A) but is composed of densely packed pale to clear spindled cells arranged in fascicles resembling a leiomyoma (B). ALK staining (C).

ALK Gene Fusions

Genes fusions were found in all 11 analyzable samples and included *SQSTM1-ALK* (n = 3), *VCL-ALK* (n = 3), *TMP3-ALK* (n = 2), *PRKAR2A-ALK* (n = 1), *MLPH-ALK* (n = 1), and *EML4-ALK* (n = 1) (Fig. 8, Tables 1 and 2).
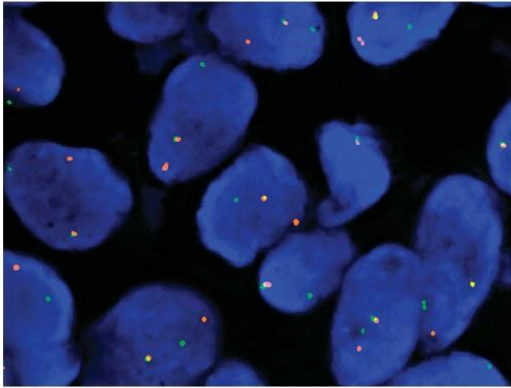
FIGURE 7. FISH analysis of the *ALK* locus using Vysis ALK break apart probe. Nuclei with 1 normal yellow fusion and separated 1 orange and 1 green signal pattern indicates the rearrangement (break) of 1 copy in the *ALK* gene region.

TABLE 2. Details of Next-Generation Sequencing Analysis

Case	Fusions	Exons	Reads	%	Start Sites
1	*SQSTM1-ALK*	5–20	1389	88	155
2	*SQSTM1-ALK*	5–20	672	93.2	138
3	*VCL-ALK*	16–20	2959	43.4	205
4	*TPM3-ALK*	6–20	1200	69.2	202
5	*VCL-ALK*	16–20	102	83.6	50
6	*VCL-ALK*	16–20	41	75.9	9
7	*SQSTM1-ALK*	5–20	21	53.9	6
8	NA				
9	*PRKAR2A-ALK*	2–20	112	100	25
10	NA	NA	NA	NA	NA
11	*MLPH-ALK*	11–20	277	58.9	54
12	*TMP3-ALK*	6–20	17	94.4	7
13	*EML4-ALK*	2–20	80	88.9	33
14	NA				

%, percentage of the reads supporting the fusion; exons, number of exons involved in the fusion, respectively; NA, not analyzable; reads, number of reads supporting the fusion; start sites, number of unique start sites of reads supporting the fusion.

DISCUSSION

Our study confirms the finding of Doyle et al[9] that all ALK-immunopositive cases manifest *ALK* gene rearrangements as detected by FISH. Also, in all analyzable cases, we detected *ALK* gene fusions. Six fusion types were identified, including 2 previously reported by Jedrych et al and 4 being novel fusions in EFH. Table 3 summarizes the main characteristics of the involved genes, proteins encoded by these genes, and their role and conditions in which these gene fusions or gene mutations have previously been detected.[10–31]

Our study revealed no correlation between the histopathological features and a particular fusion type, but we have found some hitherto unreported microscopic features in EFH. Two lesions were composed of closely packed, plexiform, or fascicular proliferations of pale to clear spindled cells and thus resembled PEComa or leiomyoma. The typical epithelioid cell component was absent and in both cases, the original diagnosis of EFH was rendered as an "exclusion" diagnosis after a broad spectrum of antibodies had been performed to exclude possible tumors of other lineages. We consider these lesions EFH, as we have noted similar cytological features, albeit never prominent, in more conventional EFH. ALK positivity and *ALK* gene fusion support the classification of these lesions as EFH. Both cases were more cellular and in this respect resemble those reported by Glusac et al as the cellular variant of EFH.[6] Thus, PEComa and leiomyoma can be added to the list of the differential diagnosis of EFH, which at present also include perineurioma,
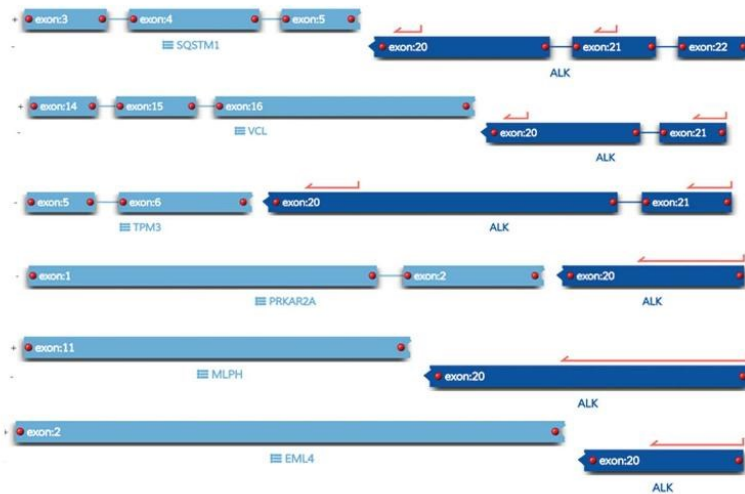
FIGURE 8. Schematic visualization of the detected fusion transcripts: (1) *SQSTM1-ALK*, (2) *VCL-ALK*, (3) *TPM3-ALK*, (4) *PRKAR2A-ALK*, (5) *MLPH-ALK*, and (6) *EML4-ALK*. In all cases, a 5′ fusion partner is joined with exons 20–29 of *ALK* containing the tyrosine kinase domain.

TABLE 3. Brief Overview of Location of the Involved Genes, Encoded Proteins, Their Function, and Roles and Conditions Associated With Fusions and Gene Mutations

Gene	Location/Type	Protein Function	Role	Conditions with Gene Fusions and Mutations Tumors/Diseases
VCL; Vinculin	10q22/protein coding	A cytoskeletal protein (vinculin) is associated with cell–cell and cell–matrix junctions, functioning as one of several interacting proteins involved in anchoring F-actin to the membrane	Regulates cell adhesion and migration; links extracellular matrix to the actomyosin cytoskeleton	*VCL-ALK*: renal cell carcinoma, EFH; *VCL* mutations: dilated cardiomyopathy
SQSTM1; Sequestosome	5q35/protein coding	A multifunctional protein that binds ubiquitin and regulates activation of the nuclear factor kappa-B (NF-κB) signaling pathway, functioning as a scaffolding/adaptor protein in concert with TNF receptor-associated factor 6 to mediate activation of NF-κB in response to upstream signals	Participate in processes of autophagy, cell signalling and differentiation	*SQSTM1-ALK*: diffuse large B-cell lymphoma, EFH; *SQSTM1* mutations: sporadic and familial Paget disease of bone
TPM3; Tropomyosin 3	1q21.3/protein coding	Tropomyosin family of actin-binding proteins are dimers of coiled-coil proteins that provide stability to actin filaments	Regulates access of other actin-binding proteins	*TPM3-ALK*: inflammatory myofibroblastic tumor, TFE3-positive renal cell carcinoma, spitzoid melanocytic leisons; gene mutations: nemaline myopathy and other muscle disorders
PRKAR2A; Protein kinase cAMP-dependent type II regulatory subunit alpha	3p21.31/protein coding	cAMP activates the cAMP-dependent protein kinase, which transduces the signal through phosphorylation of different target proteins. The protein encoded by this gene is one of the regulatory subunits of the inactive kinase holoenzyme	Participates in a variety of cellular functions, including regulation of protein transport from endosomes to the Golgi apparatus and further to the endoplasmic reticulum	*PRKAR2A-ALK*: not reported
MLPH; Melanophilin	2q37.3/protein coding	A member of the exophilin subfamily of Rab effector proteins that forms a ternary complex with the small Ras-related GTPase Rab27A in its GTP-bound form and the motor protein myosin Va	Ties melanosomes to the actin cytoskeleton in melanocytes	*MLPH-ALK*: not reported; *MLPH* mutations: Griscelli syndrome type 3
EML4; Echinoderm microtubule-associated protein like 4	2p21/protein coding	Echinoderm microtubule-associated protein (EMAP)-like (EML) family proteins are microtubule-associated proteins that have a conserved hydrophobic EMAP-like protein (HELP) domain and multiple WD40 domains	May be involved in microtubule formation; participates in mitotic spindle organization and for microtubule-kinetochore attachment	*EML4-ALK*: nonsmall cell lung carcinomas, esophageal carcinoma, breast and colorectal carcinomas, epithelioid inflammatory myofibroblastic sarcoma, large-cell neuroendocrine carcinoma

melanocytic tumors and other entities as discussed in details elsewhere.[1–3,32]

We also found some minor novel cytological variations, including cells with multilobulated nuclei, nuclear grooves, and mucinous cells. The latter appear similar to the elements described and depicted by Singh et al as foamy cells. In a subset of cases, we identified cells with intranuclear pseudoinclusions and eccentric nuclei. Although these cells were never emphasized on in the previously published material, they can be found in several illustrations (Figs. 2, 3 in Ref. 6; Fig. 4 in Ref. 2). In 3 cases, occasional areas with emperiopolesis of single lymphocytes were noted, which is another hitherto unreported feature in EFH. With respect to the skin, emperipolesis is a typical finding in Rosai-Dorfman

130

disease, granulomatous slack skin, and myxoinflammatory fibroblastic sarcoma.[33,34] In the latter, it can be very conspicuous with numerous engulfed cells easily recognizable at first glance or discrete, requiring a meticulous search.[35] Cyclin D1 has been shown to be useful for identification of cells with such a discrete single cell emperiopolesis by leaving the engulfed intracytoplasmic cells unstained.[36] We stained 3 cases of EFH with Cyclin D1 and observed a similar feature in one case with positive immunostaining.

A remarkable feature was TFE-3 immunopositivity of EFH in a majority of cases. TFE-3 positive mesenchymal tumors include epithelioid hemangioma, visceral PEComa alveolar soft part sarcoma, to name but a few.[37–39] The significance of this feature in EFH is unclear but, given frequent immunopositivity, this marker can additionally be used in the diagnosis of this neoplasm. Parenthetically, while selecting cases for inclusion, we observed more lesions with a TFE-3 +/ALK-phenotype compared with TFE-3+/ALK+ lesions. Despite frequent TFE-3 imunopositivity, the molecular analysis by FISH with *TFE3* break apart probe and by ArcherDX next-generation sequencing detecting all possible *TFE3* transcript partners, revealed neither gene alterations nor fusion transcripts. The most probable explanation of TFE-3 immunopositivity, if we exclude false positivity, is the activation of some upstream gene(s). Of note, concurrent *ALK* and *TFE-3* rearrangements are seen in some renal cell carcinoma, and remarkably these neoplasms are characterized by an epithelioid cell morphology.[13,31]

In conclusion, ALK-positive EFH shows frequently *ALK* gene fusions that involve various protein-coding genes, implicated in a variety of biological processes. Rare variants of EFH rather consist of spindled "non-epithelioid" cells, thus occasioning a resemblance to PEComa or leiomyoma. Inclusion of such lesions into the spectrum of EFH must be validated by further observations. TFE-3 is expressed in a majority of ALK-positive EFH; however, *TFE-3* rearrangement is not a feature.

REFERENCES

1. Jones EW, Cerio R, Smith NP. Epithelioid cell histiocytoma: a new entity. *Br J Dermatol.* 1989;120:185–195.
2. Singh Gomez C, Calonje E, Fletcher CD. Epithelioid benign fibrous histiocytoma of skin: clinico-pathological analysis of 20 cases of a poorly known variant. *Histopathology.* 1994;24:123–129.
3. Doyle LA, Fletcher CD. EMA positivity in epithelioid fibrous histiocytoma: a potential diagnostic pitfall. *J Cutan Pathol.* 2011;38:697–703.
4. Mehregan AH, Mehregan DR, Broecker A. Epithelioid cell histiocytoma. A clinicopathologic and immunohistochemical study of eight cases. *J Am Acad Dermatol.* 1992;26:243–246.
5. Glusac EJ, McNiff JM. Epithelioid cell histiocytoma: a simulant of vascular and melanocytic neoplasms. *Am J Dermatopathol.* 1999;21:1–7.
6. Glusac EJ, Barr RJ, Everett MA, et al. Epithelioid cell histiocytoma. A report of 10 cases including a new cellular variant. *Am J Surg Pathol.* 1994;18:583–590.
7. Walther C, Hofvander J, Nilsson J, et al. Gene fusion detection in formalin-fixed paraffin-embedded benign fibrous histiocytomas using fluorescence in situ hybridization and RNA sequencing. *Lab Invest.* 2015;95:1071–1076.
8. Creytens D, Ferdinande L, Van Dorpe J. ALK rearrangement and overexpression in an unusual cutaneous epithelioid tumor with a peculiar whorled "perineurioma-like" growth pattern: epithelioid fibrous histiocytoma. *Appl Immunohistochem Mol Morphol.* 2017;25:e46–e48.
9. Doyle LA, Marino-Enriquez A, Fletcher CD, et al. ALK rearrangement and overexpression in epithelioid fibrous histiocytoma. *Mod Pathol.* 2015;28:904–912.
10. Jedrych J, Nikiforova M, Kennedy TF, et al. Epithelioid cell histiocytoma of the skin with clonal ALK gene rearrangement resulting in VCL-ALK and SQSTM1-ALK gene fusions. *Br J Dermatol.* 2015;172:1427–1429.
11. Debelenko LV, Raimondi SC, Daw N, et al. Renal cell carcinoma with novel VCL-ALK fusion: new representative of ALK-associated tumor spectrum. *Mod Pathol.* 2011;24:430–442.
12. Zhang H, Erickson-Johnson M, Wang X, et al. Malignant high-grade histological transformation of inflammatory myofibroblastic tumour associated with amplification of TPM3-ALK. *J Clin Pathol.* 2010;63:1040–1041.
13. Thorner PS, Shago M, Marrano P, et al. TFE3-positive renal cell carcinomas are not always Xp11 translocation carcinomas: report of a case with a TPM3-ALK translocation. *Pathol Res Pract.* 2016;212:937–942.
14. Takeuchi K, Soda M, Togashi Y, et al. Identification of a novel fusion, SQSTM1-ALK, in ALK-positive large B-cell lymphoma. *Haematologica.* 2011;96:464–467.
15. d'Amore ES, Visco C, Menin A, et al. STAT3 pathway is activated in ALK-positive large B-cell lymphoma carrying SQSTM1-ALK rearrangement and provides a possible therapeutic target. *Am J Surg Pathol.* 2013;37:780–786.
16. Ali SM, Hensing T, Schrock AB, et al. Comprehensive genomic profiling identifies a subset of crizotinib-responsive ALK-rearranged non-small cell lung cancer not detected by fluorescence in situ hybridization. *Oncologist.* 2016;21:762–770.
17. Lin E, Li L, Guan Y, et al. Exon array profiling detects EML4-ALK fusion in breast, colorectal, and non-small cell lung cancers. *Mol Cancer Res.* 2009;7:1466–1476.
18. Jiang Q, Tong HX, Hou YY, et al. Identification of EML4-ALK as an alternative fusion gene in epithelioid inflammatory myofibroblastic sarcoma. *Orphanet J Rare Dis.* 2017;12:97.
19. Xia N, An J, Jiang QQ, et al. Analysis of EGFR, EML4-ALK, KRAS, and c-MET mutations in Chinese lung adenocarcinoma patients. *Exp Lung Res.* 2013;39:328–335.
20. Sokai A, Enaka M, Sokai R, et al. Pulmonary inflammatory myofibroblastic tumor harboring EML4-ALK fusion gene. *Jpn J Clin Oncol.* 2014;44:93–96.
21. Lawrence B, Perez-Atayde A, Hibbard MK, et al. TPM3-ALK and TPM4-ALK oncogenes in inflammatory myofibroblastic tumors. *Am J Pathol.* 2000;157:377–384.
22. van de Krogt JA, Vanden Bempt M, Finalet Ferreiro J, et al. ALK-positive anaplastic large cell lymphoma with the variant RNF213-, ATIC- and TPM3-ALK fusions is characterized by copy number gain of the rearranged ALK gene. *Haematologica.* 2017;102:1605–1616.
23. Cools J, Wlodarska I, Somers R, et al. Identification of novel fusion partners of ALK, the anaplastic lymphoma kinase, in anaplastic large-cell lymphoma and inflammatory myofibroblastic tumor. *Genes Chromosomes Cancer.* 2002;34:354–362.
24. Bayliss R, Choi J, Fennell DA, et al. Molecular mechanisms that underpin EML4-ALK driven cancers and their response to targeted drugs. *Cell Mol Life Sci.* 2016;73:1209–1224.
25. Woo CG, Seo S, Kim SW, et al. Differential protein stability and clinical responses of EML4-ALK fusion variants to various ALK inhibitors in advanced ALK-rearranged non-small cell lung cancer. *Ann Oncol.* 2017;28:791–797.
26. Soda M, Choi YL, Enomoto M, et al. Identification of the transforming EML4-ALK fusion gene in non-small-cell lung cancer. *Nature.* 2007;448:561–566.
27. Choi YL, Takeuchi K, Soda M, et al. Identification of novel isoforms of the EML4-ALK transforming gene in non-small cell lung cancer. *Cancer Res.* 2008;68:4971–4976.
28. Busam KJ, Kutzner H, Cerroni L, et al. Clinical and pathologic findings of Spitz nevi and atypical Spitz tumors with ALK fusions. *Am J Surg Pathol.* 2014;38:925–933.
29. Wiesner T, He J, Yelensky R, et al. Kinase fusions are frequent in Spitz tumours and spitzoid melanomas. *Nat Commun.* 2014;5:3116.
30. Omachi N, Shimizu S, Kawaguchi T, et al. A case of large-cell neuroendocrine carcinoma harboring an EML4-ALK rearrangement with resistance to the ALK inhibitor crizotinib. *J Thorac Oncol.* 2014;9:e40–e42.

131

31. Cajaiba MM, Jennings LJ, Rohan SM, et al. ALK-rearranged renal cell carcinomas in children. *Genes Chromosomes Cancer*. 2016;55:442–451.

32. Busam KJ, Granter SR, Iversen K, et al. Immunohistochemical distinction of epithelioid histiocytic proliferations from epithelioid melanocytic nevi. *Am J Dermatopathol*. 2000;22:237–241.

33. Rosai J, Dorfman RF. Sinus histiocytosis with massive lymphadenopathy: a pseudolymphomatous benign disorder. Analysis of 34 cases. *Cancer*. 1972;30:1174–1188.

34. Belousova IE, Nikonova SM, Sima R, et al. Granulomatous slack skin with clonal T-cell receptor-gamma gene rearrangement in skin and lymph node. *Br J Dermatol*. 2007;157:405–407.

35. Kinkor Z, Mukensnabl P, Michal M. Inflammatory myxohyaline tumor with massive emperipolesis. *Pathol Res Pract*. 2002;198:639–642.

36. Michal M, Kazakov DV, Hadravsky L, et al. High-grade myxoinflammatory fibroblastic sarcoma: a report of 23 cases. *Ann Diagn Pathol*. 2015;19:157–163.

37. Flucke U, Vogels RJ, de Saint Aubain Somerhausen N, et al. Epithelioid Hemangioendothelioma: clinicopathologic, immunhistochemical, and molecular genetic analysis of 39 cases. *Diagn Pathol*. 2014; 9:131.

38. Llamas-Velasco M, Mentzel T, Requena L, et al. Cutaneous PEComa does not harbour TFE3 gene fusions: immunohistochemical and molecular study of 17 cases. *Histopathology*. 2013;63:122–129.

39. Kacerovska D, Michal M, Nemcova J, et al. Crystal-deficient alveolar soft-part sarcoma with cutaneous involvement: a case report. *Am J Dermatopathol*. 2009;31:272–277.

132

2.3 MELANOCYTIC TUMORS

Considering our interest in the genetic mechanisms underlying melanocytic tumor development, we studied a series of Spitz tumor with a rare fusion which resulted in the article titled *«Spitz tumors with ROS1 fusions: a clinicopathological study of 6 cases, including FISH for chromosomal copy number alterations and mutation analysis using next-generation sequencing».* Spitz tumors represent a heterogeneous group of melanocytic neoplasms characterized by large epithelioid and/or spindled melanocytes arranged in fascicles or nests, sometimes accompanied by characteristic epidermal and stromal changes, with a spectrum of biological behavior ranging from benign (Spitz nevus) to malignant (spitzoid melanoma, or malignant Spitz tumor). (59), (60) Recently, mutually exclusive activating kinases fusions, involving *ALK, NTRK1, NTRK3, RET, MET, ROS1,* and *BRAF* have been found in a subset of spitzoid lesions. (4) Several studies revealed a certain correlation of the histopathological features in spitzoid neoplasms and particular kinase fusions. (61), (62), (63) The goal of this study was to identify possible distinctive histopathological features that correlate with *ROS1* fusions and study chromosomal copy number alterations and *TERT-p* mutation analysis to find out whether these can be used in risk stratification of these lesions. All six cases were compound symmetric melanocytic neoplasms with a nested pattern of growth with the confluence of whorling nests, predominant spindle-cell morphology, striking transepidermal elimination of whole melanocytic nests. Myxoid changes, Kamino bodies, multinucleated cells, increased mitotic figures, and usually moderate pleomorphism were found. We found three different 5' fusion partners involving the tyrosine kinase receptor *ROS1.* The most common rearrangement in Spitz tumor *PWWP2A-ROS1* was detected in 4 cases, confirming the previously published finding. (4) The two novel 5' fusion partners were *FIP1L1,* and *CAPRIN1* were detected. In addition to the above-mentioned fusions, alterations in other genes were identified by NGS. It is concluded that *ROS1* fused spitzoid neoplasms appear to have no distinctive histopathological features, although consistent findings were spindled melanocytes arranged in confluent whorling nests, prominent transepidermal elimination of melanocytic nests and myxoid/mucinous changes.

In the second article *«Polypoid atypical Spitz tumor with a fibrosclerotic stroma, CLIP2-BRAF fusion and homozygous loss of 9p21»* we presented an extraordinary case report of a polypoid atypical Spitz tumor with a prominent fibrosclerotic stromal component, harboring a *CLIP2-BRAF* fusion, which has hitherto not been reported in melanocytic lesions. Recently, two cases of unclassified sclerosing malignant melanomas with an AKAP9-BRAF gene fusion have been described, but to our eyes, both neoplasms rather represent spitzoid lesions. (64) The patient we reported was a 78-year-old male with a dermal, barely symmetrical, polypoid lesion composed mainly of moderately pleomorphic epithelioid cells with ample amphophilic cytoplasm arranged in nests and fascicles. The mitoses (2/mm²) were confined to the upper part of the lesion. The Breslow thickness was 2.3 mm. The stroma contained conspicuous fibroblasts and thickened

collagen bundles, with focal sclerotic areas and dilated medium-sized vessels. Despite strong nuclear and cytoplasmic positivity of p16, FISH revealed homozygous loss in locus 9p21. A *CLIP2-BRAF* fusion was found by NGS. No other genetic alterations, including *TERT*-promoter mutation, was found. The patient is disease-free without recurrence or evidence of metastatic disease after five years and two months of follow-up.

Spitz Tumors With *ROS1* Fusions: A Clinicopathological Study of 6 Cases, Including FISH for Chromosomal Copy Number Alterations and Mutation Analysis Using Next-Generation Sequencing

Michele Donati, MD,* Liubov Kastnerova, MD,†‡ Petr Martinek, PhD,†‡ Petr Grossmann, PhD,†‡ Eva Sticová, MD,§ Ladislav Hadravský, MD, PhD,¶ Tomas Torday, MD,‖ Jitka Kyclova, MD,** Michal Michal, MD,†‡ and Dmitry V. Kazakov, MD, PhD†‡

Abstract: Spitz tumors represent a heterogeneous group of melanocytic neoplasms with a spectrum of biological behavior ranging from benign (Spitz nevus) to malignant (spitzoid melanoma). Prediction of the behavior of these lesions based on their histological presentation is not always possible. Recently, mutually exclusive activating kinase fusions, involving *ALK, NTRK1, NTRK3, RET, MET, ROS1,* and *BRAF,* have been found in a subset of spitzoid lesions. Some of these genetic alterations were associated with specific morphological features. Here, we report the histological presentation of 6 Spitz tumors with *ROS1* fusion. The age of the patients ranged from 6 to 34 years, with strong female prevalence (5:1). All neoplasms were compound melanocytic proliferations with a predominant dermal growth but a conspicuous junctional component displaying atypical microscopic features qualifying them as atypical Spitz. *FIP1L1* and *CAPRIN1* were identified as 2 novel 5′-fusion partners of *ROS1* along with the known *PWWP2A–ROS1* fusion. FISH for copy number changes of 9p21, 6p25, and 11q13 was negative in all but 1 neoplasm harboring isolated gain of 8q24. *TERT*-promoter hotspot mutation analysis was negative in all tumors. All patients were disease-free after a mean follow-up period of 24.5 months. It is concluded that *ROS1*-fused spitzoid neoplasms seem to have no distinctive histopathological features although consistent findings were spindled melanocytes arranged in confluent whorling nests, prominent transepidermal elimination of melanocytic nests, and myxoid/mucinous changes.

Key Words: melanocytic lesions, spitzoid melanoma, malignant Spitz tumor, nevus, kinase, *TERT*

(Am J Dermatopathol 2019;00:1–11)

INTRODUCTION

Spitz tumors are a group of melanocytic neoplasms characterized by large epithelioid and/or spindled melanocytes arranged in fascicles or nests sometimes accompanied by characteristic epidermal and stromal changes. They include Spitz nevi, with well-defined bland histological aspects and benign behavior, and frankly malignant lesions called spitzoid melanomas or malignant Spitz tumors that can lead to metastasis and patient's death.[1] The term atypical Spitz tumors (AST) is often applied to lesions that manifest atypical histological features that however do not suffice for the diagnosis of an overt malignancy. ASTs mostly affect young patients and may involve regional lymph nodes[2]; albeit these lesions mainly follow an indolent course, cases of metastasis and death have been recorded.[3–5] Several studies have demonstrated that the classification of Spitz tumors along the spectrum of benign to malignant shows a poor interobserver reproducibility and a poor correlation with the clinical outcomes.[6–9] To improve diagnostic accuracy, molecular tests and cytogenetic analysis, such as comparative genomic hybridization or fluorescence in situ hybridization (FISH), have emerged as useful ancillary methods. These are based on the fact that melanomas harbor complex chromosomal aberrations, whereas most Spitz nevi present none or single isolated chromosomal abnormalities.[10] In particular, homozygous deletion of 9p21 and *TERT* promoter (*TERT-p*) mutation have been described as potential features suggesting an aggressive course of spitzoid lesions.[11,12] Moreover, Spitz tumors generally have no mutations in the most common oncogenes associated with melanomas, such as *BRAF, NRAS,* or *KIT*.[13]

Recently, it has been demonstrated that a subset of Spitz tumors harbors mutually exclusive genomic rearrangements involving the tyrosine kinase receptors *ALK, NTRK1, NTRK2, NTRK3, MET, RET, ROS1,* and the threonine kinase *BRAF*.[14] Fusions involving these genes produce chimeric, constitutively active proteins that play a pivotal role in the oncogenesis of a wide range of neoplasms.[15–19] Activating kinase fusions have been detected across the entire spectrum of spitzoid lesions, suggesting that they represent an early oncogenic event in the development of these neoplasms.[14]

Furthermore, specific molecular alterations have been linked to different subgroups and variants of both nonspitzoid and spitzoid melanocytic lesions.[13,20–22] Several studies revealed certain correlation of histopathological features in spitzoid neoplasms and particular kinase fusions. For example, Spitz tumors with *ALK* fusions have been shown to manifest a plexiform dermal growth of intersecting fascicles of fusiform melanocytes with radial orientation toward the base of the lesion[23,24]; *NTRK1*-fused cases present predominantly with smaller spindle melanocytes arranged as smaller nests, occasionally forming rosettes[25]; *BRAF* fusion cases have a predominance of epithelioid cells commonly with a sheet-like growth pattern or dysplastic Spitz architecture and most likely have melanocytes with high-grade nuclear atypia.[25] *NTRK3* fusions have recently been identified in 57% of pigmented spindle-cell nevus of Reed, a morphologic variant of Spitz nevi.[26]

AU3

Although in the series reported by Wiesner et al,[14] *ROS1* fusions had a high frequency among spitzoid lesions (17.1%), little is known regarding the histological characteristics of this subset of neoplasms.[27] We undertook this study (1) to identify possible distinctive histopathological features that correlate with *ROS1* fusions, (2) to study chromosomal copy-number alterations and *TERT-p* mutation analysis to find out whether these can be used in risk stratification of these lesions, and (3) to study their mutation landscape.

MATERIAL AND METHODS

Six spitzoid tumors with *ROS1* fusions confirmed by FISH and next-generation sequencing (NGS) were identified in our institutional and consultations files.

Histopathological features were individually assessed by 2 dermatopathologists (D.V.K. and M.D.). The assessment parameters included the silhouette of the lesion (polypoid, verrucous, dome-shaped, or flat), symmetry, tumor thickness (Breslow index), epidermal changes (regular/irregular hyperplasia, ulceration, consumption, pagetoid spread, or irritation), junctional component, if present (confluence of nests, horizontal orientation of nests, or Kamino bodies), growth patterns (plexiform, fascicular, tubular/cord-like, or confluent nests/sheets of melanocytes in the dermis), cytological features (spindled or epithelioid cells), degree of nuclear pleomorphism (mild, moderate, or severe), cellular maturation and zonation, mitotic rate, mitosis distribution, including mitoses in the deep portion of the lesion, atypical mitotic figures, involvement of adnexal structures, vascular or perineural extension, lymphocytic infiltrate (absent, scarce, moderate, or heavy), presence of intratumoral melanin (marked, patchy, or none), and vascular and/or sclerotic stromal changes. Some of their cytological or architectural features were also recorded if encountered. Clinical follow-up was obtained from the patients, their physicians, or from referring pathologists.

Immunohistochemistry and Special Stains

Immunohistochemical staining was performed on 4-μm sections cut from formalin-fixed, paraffin-embedded tissue using Ventana Benchmark XT automated stainer (Ventana Medical System, Inc, Tucson, AZ), according to the manufacturer's protocol. Staining for p16 was performed for all

cases. In most cases, 2 clones, namely E6H4 and R19-D (both prediluted, RTU; Ventana, Tucson, AZ), were used. Alcian blue special stain was performed to assess mucin deposits.

Fluorescence In Situ Hybridization

The hybridization procedures with multicolor FISH probe sets for detecting melanoma outlined below were performed, as previously described.[28] Two separate hybridizations were performed, 1 using the 4-probe FISH assay targeting 6p25 (*RREB1*), 6q23 (*MYB*), 11q13, and Cep6 and a second using the 4-probe FISH assay targeting 6p25 (*RREB1*), 9p21 (*CNDK2A*), 11q13 (*CCND1*), and 8q24 (*MYC*).[30] *ROS1* rearrangements were confirmed using the ZytoLight SPEC *ROS1* Dual Color Break Apart Probe (ZytoVision GmbH). AU4

Gene Fusion Detection Using NGS

Depending on the sample size, up to 3 formalin-fixed paraffin-embedded sections (10 μm thick) were macrodissected, and total nucleic acid (NA) was extracted using the Agencourt FormaPure Kit (Beckman Coulter, Brea, CA) with modifications recommended by ArcherDX (ArcherDX, Inc, Boulder, CO). Total NA was quantified using the Qubit Broad Range RNA Assay Kit (ThermoFisher Scientific, Waltham, MA), and input for each sample's library preparation was set to 250 ng. The PreSeq RNA QC Assay using iTaq Universal SYBR Green Supermix (Biorad, Hercules, CA) was performed to assess the sample quality. Samples with a cycle threshold value smaller than 30 were set as valid and continued with target enrichment. The FusionPlex Solid Tumor kit (ArcherDX) containing 288 targets in 53 genes was used, and all steps were performed following the Archer's FusionPlex protocol for Illumina (ArcherDX, Inc). The targeted genes included (*AKT3, ALK, ARHGAP26, AXL, BRAF, BRD3, BRD4, EGFR, ERG, ESR1, ETV1, ETV4, ETV5, ETV6, EWSR1, FGFR1, FGFR2, FGFR3, FGR, INSR, MAML2, MAST1, MAST2, MET, MSMB, MUSK, MYB, NOTCH1, NOTCH2, NRG1, NTRK1, NTRK2, NTRK3, NUMBL, NUTM1, PDGFRA, PDGFRB, PIK3CA, PKN1, PPARG, PRKCA, PRKCB, RAF1, RELA, RET, ROS1, RSPO2, RSPO3, TERT, TFE3, TFEB, THADA,* and *TMPRSS2*). Final libraries were quantified following the Library Quantification for Illumina Libraries protocol (KAPA, Wilmington, MA) assuming a 200-bp fragment length. Samples were multiplexed and spiked with 20% PhiX control and sequenced on a NextSeq 500 (Illumina, San Diego, CA) to achieve at least 3 million reads per sample. The analysis of the sequencing results was performed using the Archer Analysis software (version 5.1.7; ArcherDX Inc). Fusion parameters were set to a minimum of 5 valid fusion reads with a minimum of 3 unique start sites within the valid fusion reads.

TERT Mutation Analysis

Hotspot mutations in the promoter of *TERT* gene including all hotspots listed in[31] were analyzed using PCR and Sanger sequencing, as described previously.[32] AU5

NGS Mutation Analysis

A panel of 275 cancer-related genes (Comprehensive Cancer Panel; Qiagen, Hilden, Germany) was used to analyze

tumor tissue samples, which were obtained using macro dissection from formalin-fixed paraffin-embedded blocks. The panel included the following genes: *ABL1, ACVR1B, AKT1, AKT2, AKT3, ALK, AMER1, APC, AR, ARAF, ARID1A, ARID1B, ARID2, ASXL1, ATM, ATR, ATRX, AURKA, AURKB, AURKC, AXIN1, AXIN2, B2M, BAP1, BCL2, BCL2L1, BCL6, BCOR, BCORL1, BCR, BIRC3, BLM, BRAF, BRCA1, BRCA2, BRIP1, BTK, CALR, CARD11, CBL, CBLB, CBLC, CCND1, CCND3, CCNE1, CD274, CD79A, CD79B, CDC73, CDH1, CDK12, CDK4, CDK6, CDKN2A, CDKN2B, CDKN2C, CEB-PA, CIC, CREBBP, CRLF2, CSF1R, CSF3R, CTCF, CTNNA1, CTNNB1, CUX1, CXCR4, CYLD, DAXX, DDR2, DICER1, DNM2, DNMT3A, DOT1L, EED, EGFR, EGLN1, EP300, EPAS1, EPHA3, EPHA5, ERBB2, ERBB3, ERBB4, ERG, ESR1, ETV6, EXO1, EZH2, FAM175A, FAM46C, FANCA, FANCC, FANCD2, FANCE, FANCF, FANCG, FAS, FBXW7, FGF4, FGF6, FGFR1, FGFR2, FGFR3, FGFR4, FH, FLCN, FLT3, FLT4, FOXL2, FUBP1, GALNT12, GATA1, GATA2, GATA3, GEN1, GNA11, GNAQ, GNAS, GREM1, GRIN2A, H3F3A, HGF, HIST1H3B, HNF1A, HOXB13, HRAS, HSP90AA1, CHEK1, CHEK2, ID3, IDH1, IDH2, IGF1R, IKZF1, IKZF3, IL7R, INHBA, IRF4, JAK1, JAK2, JAK3, KAT6A, KDM5C, KDM6A, KDR, KEAP1, KIT, KMT2A, KMT2B, KMT2C, KMT2D, KRAS, LRP1B, MAP2K1, MAP2K2, MAP2K4, MAP3K1, MAP3K14, MAPK1, MCL1, MDM2, MDM4, MED12, MEF2B, MEN1, MET, MITF, MLH1, MPL, MRE11A, MSH2, MSH6, MTOR, MUTYH, MYC, MYCL, MYCN, MYD88, NF1, NF2, NFE2L2, NFKBIA, NKX2-1, NOTCH1, NOTCH2, NOTCH3, NPM1, NRAS, NSD1, NTRK1, NTRK2, NTRK3, PAK3, PALB2, PAX5, PBRM1, PDGFRA, PDGFRB, PHF6, PIK3CA, PIK3R1, PIK3R2, PIM1, PLCG1, PMS1, PMS2, POLD1, POLE, PPM1D, PPP2R1A, PRDM1, PRKAR1A, PRKDC, PRSS1, PTEN, PTCH1, PTPN11, RAC1, RAD21, RAD50, RAD51, RAF1, RB1, RET, RHEB, RHOA, RIT1, RNF43, ROS1, RUNX1, SC2, SDHB, SETBP1, SETD2, SF3B1, SMAD2, SMAD4, SMARCA4, SMARCB1, SMC1A, SMC3, SMO, SOCS1, SOX2T, SOX9, SPOP, SRC, SRSF2, STAG2, STAT3, STK11, SUFU, SUZ12, TAL1, TCF3, TERT, TET2, TGFBR2, TNFAIP3, TNFRSF14, TP53, TRAF3, TSC1, TSHR, U2AF1, U2AF2, VHL, WHSC1, WT1, XPO1, XRCC2, XRCC3, ZNF217,* and *ZRSR2.* DNA was isolated using the Qiagen DNA mini kit, and 250 ng of DNA was used to construct the library. Library was sequenced on an Illumina's NextSeq 500, aiming at average coverage 350× after deduplication of molecular identifiers. Variants were called using Qiagen's proprietary pipeline using following filters: synonymous SNVs, variant depth after deduplication <6, allele frequency >0.05, allele population frequency ≤0.002 in the GnomAD data set,[33] and known "benign" clinical consequence according to the ClinVar database.[34] The remaining subset was checked visually, and suspected artefactual variants were excluded.

RESULTS

Clinical Findings

There were 1 male and 5 female patients, with the mean age of 17.8 years at the diagnosis (range from 6 to 34 years), with 4 of the 6 patients being in the first 2 decades of life (Table 1). Locations included lower extremities (n = 3), back (n = 1), upper lip (n = 1), and shoulder (n = 1).

The clinical presentation was a flesh-colored polypoid/verrucous (3 cases) or dome-shaped (2 cases) nodule, whereas 1 lesion was flat. Two cases (cases 3 and 5) were slightly pigmented.

All tumors were completely excised; no lymph node enlargement was clinically evident at the time of diagnosis. Patients are disease-free with a mean follow-up period of 30 months. In 1 patient with the tumor on the right shoulder (case 4), an enlarged (9 × 4 mm) lymph node was detected by a sonography in the right axilla, but no biopsy was performed. Otherwise, clinical investigation was negative. Six months later, a control sonography detected a decrease in size of the lymph node (7.3 × 3.7 mm).

Microscopic Features

All the lesions were relatively symmetrical, compound-type melanocytic proliferations with an average Breslow thickness of 1.76 mm (range 0.97–3 mm) and an uneven flat base (Table 2).

Junctional nests, both vertically and horizontally arranged, were present in all cases, with 2 lesions (cases 2 and 5) manifesting additionally a lentiginous proliferation of melanocytes extending beyond the dermal component. Kamino bodies were encountered in all but one case (case 5). The epidermis showed irregular hyperplasia in all neoplasms. The melanocytes were predominantly spindled with eosinophilic cytoplasm, with only 1 case entirely composed of epithelioid cells (case 4) (Figs. 1 and 2). Five cases exhibited moderate degree of pleomorphism, whereas a single lesion (case 2) showed severe cellular pleomorphism. Large eosinophilic nucleoli, nuclear pseudoinclusions, and a variable number of multinucleated melanocytes were also observed (Fig. 3). Small vesicle-like spaces were noted inside and between the cells of all neoplasms (Fig. 4), whereas a variable degree of myxoid change was noted in 5 lesions. Pigmentation was scarce; coarse intracytoplasmic melanin granules confined to the upper part of the lesions were observed in only 1 lesion (case 3), whereas in 2 neoplasms, pigment was present in scattered melanophages (cases 2 and 5).

Lateral pagetoid spread of single melanocytes was noted only in 1 neoplasm (case 2) located on an acral site, whereas in 2 cases, there was single-cell pagetoid spread in the central part of the lesion (case 5). Transepidermal elimination of entire melanocytic nests was a prominent finding in all 6 lesions (Figs. 2C, 4A, 5B). All neoplasms featured impaired maturation of melanocytes. The mitotic rate was >2 mm² in 4 cases (cases 1, 3, 4, and 6); cases 4 and 6 showed 8 and 6 mitoses/mm², respectively, including atypical mitotic figures (Figs. 1C, 2C). Mitoses were confined to the upper or middle portion of the lesion; none was observed near the base of the neoplasm.

A lymphocyte-predominant inflammatory infiltrate was observed in 5 cases with variable intensity, being heavy in 2 lesions (cases 1 and 4) (Fig. 1C). Atypical features for each case are listed in Table 1. There were some differences between polypoid and dome-shaped and flat lesions (cases 2 and 5). The polypoid lesions presented with large and confluent junctional nests of melanocytes pushing the overlying

TABLE 1. Summary of the Main Clinical Features, Atypical Histopathological Features, and Genetic Analysis

Case	Sex/ Age	Location	Clinical Diagnosis	Atypical Features	IHC p16	FISH ROS1	FISH Melanoma	FUSION	TERT-p Hotspot Mutations	Treatment/ Follow-up
1	F/7	Back	Spitz nevus	Confluent nests Atypical mitoses 3/mm² Large eosinophilic nucleoli Heavy inflammatory infiltrate Impaired maturation	+ (Checkerboard pattern)	+	Neg.	*PWWP2A–ROS1*	Neg.	Excision NED 18 mo
2	F/15	Shin	Pigmented nevus	Confluent nest (focal) Lateral pagetoid spread Severe nuclear pleomorphism Large eosinophilic nucleoli Impaired maturation	+ (Checkerboard pattern)	+	8q24 (MYC)	*FIP1L1–ROS1*	Neg.	Excision NED 18 mo
3	F/26	Thigh	Intradermal nevus? Blue nevus?	Confluent nests Large eosinophilic nucleoli Dermal mitoses 3/mm² Impaired maturation	+ (Checkerboard pattern)	+	Neg.	*PWWP2A–ROS1*	Neg.	Excision NED 3 yrs
4	F/34	Right shoulder	Granuloma	Confluent nests Large eosinophilic nucleoli Dermal mitoses 8/mm² (atypical 4/mm²) Heavy inflammatory infiltrate Impaiered maturation	+ (Checkerboard pattern)	+	Neg.	*CAPRIN1–ROS1*	Neg.	Excision Enlarged (9 × 4 mm) LN in the right axilla on sonography. Staging negative. No LN biopsy was not performed NED 9 mo
5	M/19	Foot (dorsal part)	Nevus	Size 1.1 cm Confluent nests (focal) Large eosinophilic nucleoli (focal) Impaired maturation	+ (Checkerboard pattern)	+	Neg.	*PWWP2A–ROS1*	Neg.	Excision NED 15 mo
6	F/6	Upper lip	Nevus? Pyogenic granuloma?	Confluent nests Eosinophilic nucleoli (focal) Dermal mitoses 6/mm² Impaired maturation	+ (Checkerboard pattern)	+	Neg.	*PWWP2A–ROS1*	Neg.	Excision NED 7 yrs

With respect to mitotic figures, atypical features included an increased mitotic rate (>2 mitoses/mm² for adults and >6 mitoses/mm² for children) and any number of atypical mitotic figures.

*NED, not evidence of disease.

LN, lymph node.

epidermis, leading to its focal consumption. The melanocytes, when transversally cut, showed small round nuclei in the center of the nests and were surrounded by whorling spindled melanocytes (Fig. 1B). Groups of necrotic melanocytes were seen inside the nests in all 6 cases, usually in 2–3 nests throughout the lesion (Fig. 2B). Polypoid lesions with a high mitotic rate showed several groups of necrotic melanocytes within large nests. The cases with a flat or dome-shaped silhouette showed a broad junctional component with a shoulder formation over the dermal component. Melanocytes inside the nests were arranged in a more discohesive fashion. Small dermal nests and focally single melanocytes were surrounded by retraction artifact, assuming a lacunar aspect (Fig. 3B).

Immunohistochemistry and Special Stain

All cases showed strong p16 nuclear stain with a checkerboard pattern (Fig. 5C).

Alcian blue was performed in 5 cases with myxoid change, confirming the presence of mucin in both nests and stroma in all lesions (Fig. 2D).

Fluorescence In Situ Hybridization

A break-apart probe for *ROS1* confirmed the presence of a rearrangement in all tumors.

FISH analysis for chromosomal numeric aberrations revealed copy number gain in locus 8q24 (*MYC*) in case 2, whereas all the remaining 5 neoplasms were negative (Table 1).

RNA and DNA Sequencing

RNA sequencing identified 3 different 5′ fusion partner genes for *ROS1*, including 2 previously unreported fusion transcripts *FIP1L1–ROS1* (case 2) and *CAPRIN1–ROS1* (case 4).

138

TABLE 2. Summary of Histopathological Features

Feature	Frequency
Thickness (mm)	
Range	0.97–3 mm
Mean/median	2.21/1.55 mm
Silhouette	
Polypoid	2/6 (33%)
Verrucous	1/6 (17%)
Dome-shaped	2/6 (33%)
Flat	1/6 (17%)
Epidermal changes	
Epidermal hyperplasia	6/6 (100%)
Epidermal atrophy/consumption	6/6 (100%)
Ulceration	0/6
Pagetoid spread (lateral)	1/6 (17%)
Irritation	0/6
Junctional component	
Junctional nests present	6/6 (100%)
Confluence of nests (focal)	6/6 (100%)
Horizontal arrangement of nests (focal)	6/6 (100%)
Kamino bodies	5/6 (83%)
Architecture and growth patterns	
Plexiform (predominant)	0/6
Fascicular (focal)	0/6
Tubular/cord-like growth (focal)	0/6
Confluence of nests/sheets of melanocytes	6/6 (100%)
Cytological features	
Spindling	5/6 (83%)
Pleomorphism	
Mild	0/6
Moderate	5/6 (83%)
Severe	1/6 (17%)
Nuclei with large eosinophilic nucleoli	6/6 (100%)
Multinucleated melanocytes	5/6 (83%)
Individual or grouped necrotic melanocytes	6/6 (100%)
Mitotic rate	
≤2 mitoses per 1 mm^2	2/6 (33%)
>2 mitoses per 1 mm^2	4/6 (66%)
Mitoses near base	0/6
Adnexal, vascular, or perineural extension	
Apocrine/eccrine unit involvement	2/6 (33%)
Follicular/sebaceous extension	4/6 (66%)
M. arrector pili involvement	0/6
Perineural invasion	0/6
Intravascular invasion	0/6
Other	
Inflammatory response	
Absent	1/6 (17%)
Scarce	2/6 (33%)
Moderate	1/6 (17%)
Heavy	2/6 (33%)
Impaired maturation	6/6 (100%)
Vascular and/or sclerotic stroma	6/6 (100%)
Myxoid change	5/6 (83%)
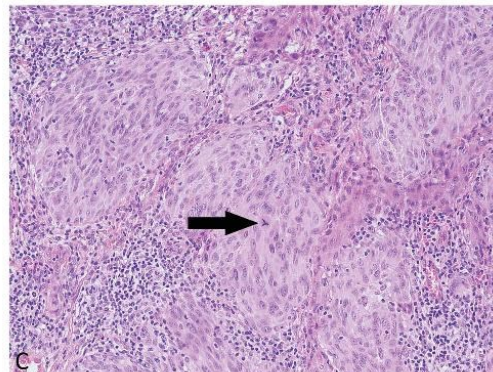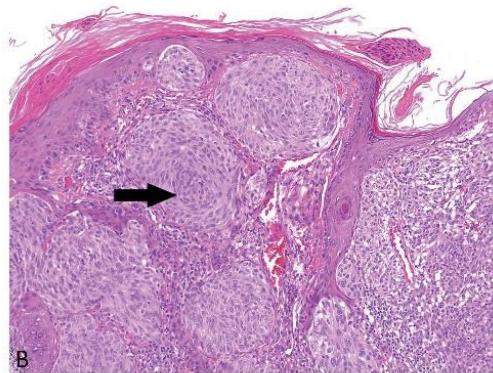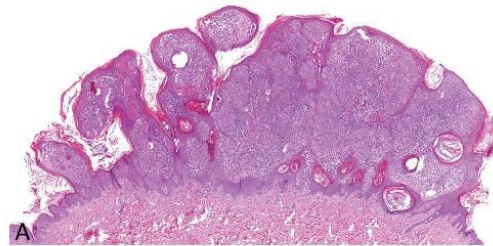
FIGURE 1. Case 1. Verrucous lesion composed of large and confluent junctional and dermal nests (A). Transversally cut, focally coalescing nests composed of spindled melanocytes with small round nuclei. Note whorling of peripherally located melanocytes around smaller cell in the center (arrow) (B). Tripolar atypical mitotic figure (arrow) and a heavy inflammatory infiltrate in the background (C).

The remaining 3 lesions harbored *PWWP2A–ROS1* fusion (Table 3).

TERT-Promoter Mutation Analysis

TERT-p hotspot mutation analysis was negative in all patients. In 1 case, a *TERT* mutation of unknown significance
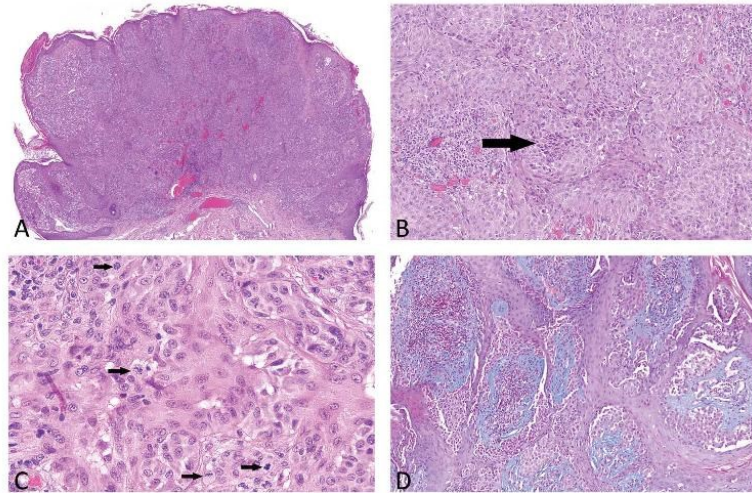
FIGURE 2. Case 4. Polypoid lesion on the shoulder of a 34-year-old woman showing a relatively symmetrical silhouette and a growth pattern of large confluent nests (A). Melanocytes are mostly epithelioid. Note a group of necrotic melanocytes (arrow) inside a large nest (B). Numerous mitotic figures (arrows) are observed in the upper part of the lesion (C). Alcian blue stain highlights mucin deposits both in the stroma (predominantly) and within melanocytic nests (D).

was identified using NGS in the coding sequence of *TERT* (c.3164C>T p.Ser1055Leu).

NGS Mutation Analysis

The mutation analysis revealed mutations in different genes (the number of mutations ranged from 4 to 10). The distribution of mutations and particular mutations is shown in Table 4.

DISCUSSION

We analyzed 6 Spitz tumors harboring *ROS1* fusion with the aim to identify specific histopathological features. These were compound symmetric melanocytic neoplasms with a nested pattern of growth with the confluence of whorling nests, predominant spindle-cell morphology, striking transepidermal elimination of whole melanocytic nests, myxoid changes, Kamino bodies, multinucleated cells, increased mitotic figures, and usually moderate pleomorphism. All these features have been described in Spitz tumors,[35,36] thus permitting no recognition of histopathological features that would be specifically linked to *ROS1* fusions. Some of the detected microscopic features are still worthy of a short comment. Transepidermal elimination of melanocytic nests is reported between 10% and 36% of Spitz nevi[37,38] and is more common on acral sites.[39] In all neoplasms of our series, transepidermal elimination of melanocytic nests was a constant and prominent finding, not limited to the central part of the
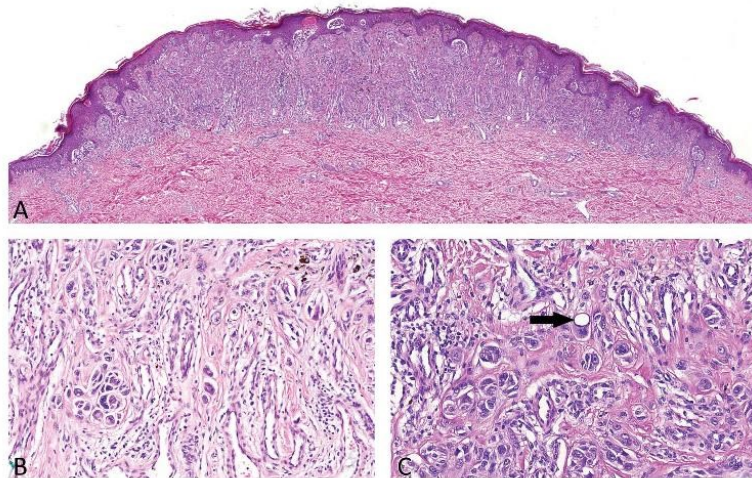
FIGURE 3. Case 2. Slightly elevated lesion from the shin of a 15-year-old girl composed of relatively small nests with only focal confluence set in a fibrovascular stroma (A). Close-up views showing small nests composed of highly pleomorphic melanocytes with surrounding cleft-like spaces imparting a lacunar appearance and a cell with prominent nuclear pseudoinclusion (arrow) (B and C).
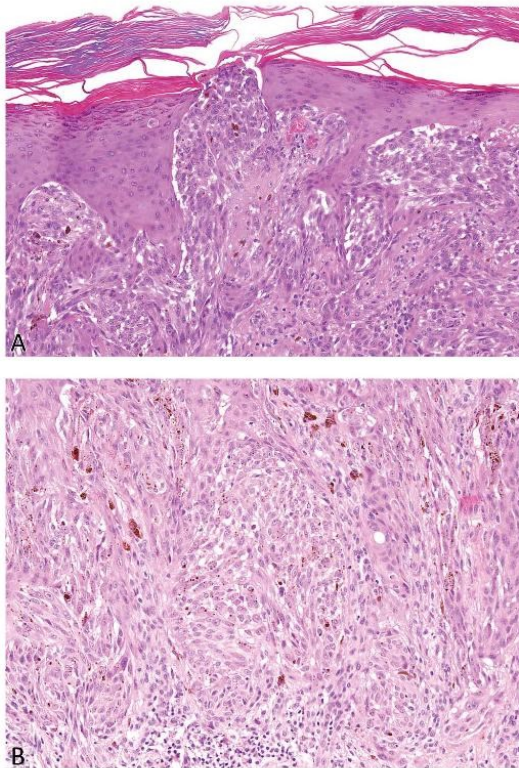
FIGURE 4. Case 3. Transepidermal elimination of a large nest (A). Large confluent nests of spindled melanocytes containing intracytoplasmic vacuoles and occasional melanin granules (B).

lesion but also involving the follicular infundibulum and acrosyringium. Melanocytes in these nests are almost always pyknotic and ascending large, and confluent nests with a full-thickness breach toward the epidermal surface simulate ulceration on histology.[40] Lack of fibrin deposition and neutrophils in the vicinity of the eliminated nests supports this view.

Myxoid change was another constant finding. Spitzoid lesions with similar features have been reported as myxoid Spitz nevi.[41–43] Recently, Perron et al[44] have identified a group of melanocytic spitzoid neoplasms harboring *ALK* fusion, characterized by myxoid changes. These lesions were mainly amelanotic, occurred on the extremities of young men and presented with spindle-cell morphology and a plexiform architecture. Although clinical and histological differences exist between our cases and those in the aforementioned series, our findings suggest that myxoid alterations are not kinase-specific.

Albeit our cohort was limited to only 6 cases, it seems that 2 main architectural patterns may be delineated in *ROS1*-fused spitzoid tumors, which possibly related to the anatomical sites (acral vs. nonacral). Nonacral lesions (cases 1, 3, 4,

and 6) seem to be polypoid to verrucous composed of large and confluent junctional and dermal nests of melanocytes pushing the overlying epidermis, leading to its focal consumption. The melanocytes, when transversally cut, showed small round nuclei in the center of the nests and were surrounded by whorling spindled melanocytes. Groups of necrotic melanocytes were often inside the nests, and inflammatory infiltrate was moderate/heavy in all but one of these cases, and the mitotic rate was high. Acral lesions (cases 2 and 5) showed a broad junctional component forming shoulders over the dermal component. Melanocytes inside the nests were arranged in a more discohesive fashion. In the dermis, small nests and single melanocytes presented retraction artifact conferring a lacunar aspect and were surrounded by a fibrovascular regression-like stromal changes. Inflammatory infiltrate was scarce or absent, as were mitotic figures. Similar relationship between histopathological type and location has been reported.[42] Two patterns of presentation with similar findings were also described in *BRAF*-fused Spitz tumors.[25]

We found 3 different 5′ fusion partners involving the tyrosine kinase receptor ROS1, including 2 novel translocations. Fusion transcript *PWWP2A–ROS1* with exons 1–36 was detected in 4 cases, confirming the previously published finding that it represents the most common rearrangement for *ROS1* in Spitz tumor.[14] The 2 novel 5′ fusion partners were *FIP1L1* and *CAPRIN1*. To the best of our knowledge, fusion transcripts *FIP1L1–ROS1* or *CAPRIN1–ROS1* have not been described. Both fusions are in frame; their sequencing details and transcript Refseq numbers are listed in Table 3. Both novel breakpoints are predicted to be in canonical sites (introns 35 and 34), which implies that ROS1 kinase constitutional activation is likely to occur similarly as in other described *ROS1* fusions in Spitz tumors.[14] Of interest, both *FIP1L1* and *CAPRIN1* are rearranged with *PDGFRβ* in chronic eosinophilic leukemia.[45,46] It has recently been proposed that intracellular downstream signaling might differ depending on the fusion partner of *ROS1*.[47] We compared the 4 neoplasms harboring *PWWP2A–ROS1* translocation with the other 2 lesions harboring different 5′ fusion partners and identified no clinicopathological differences.

In the series by Wiesner et al,[14] *ROS1* fusion was detected mainly in benign Spitz nevi (19/24) compared with ASTs or spitzoid melanomas (5/24). In our series, all lesions manifested at least 1 atypical feature deviating from a conventional Spitz nevus (Table 1).

Many attempts have been made to establish clinical, histological, and molecular parameters to stratify the risk of progression in Spitz tumors,[11,48–51] but none of them is uniformly adopted. Taking into account the clinical and histological features alone,[48,49] only 1 case (case 4) in our series had an intermediate risk of progression. The patient, a 34-year-old woman presented with a polypoid lesion with a high mitotic rate (8 mitoses/mm^2), atypical mitotic figures, and a heavy inflammatory infiltrate. During clinical investigation, a single enlarged lymph node (9 × 4 mm) was detected on sonography, but a lymph node biopsy was not performed. The patient had no evidence of the disease at a 9-month follow-up.

However, it has also been stated that the histological diagnosis of Spitz tumors is a matter of prospective, leaving

141

FIGURE 5. Case 5. Lesion on the dorsal part of the foot of a 19-year-old boy showing a flat symmetrical silhouette with a broad junctional component and shoulder formation over the dermal component (A). Somewhat discohesive melanocytes forming nests separated by clefts from the surrounding epidermis, transepidermal migration of nests and singles cell, multinucleated melanocytes (arrow), and fibrovascular regression-like stromal changes in the absence of inflammatory infiltrate are seen. (B) P16 staining with both positive and negative nuclear immunoreaction.
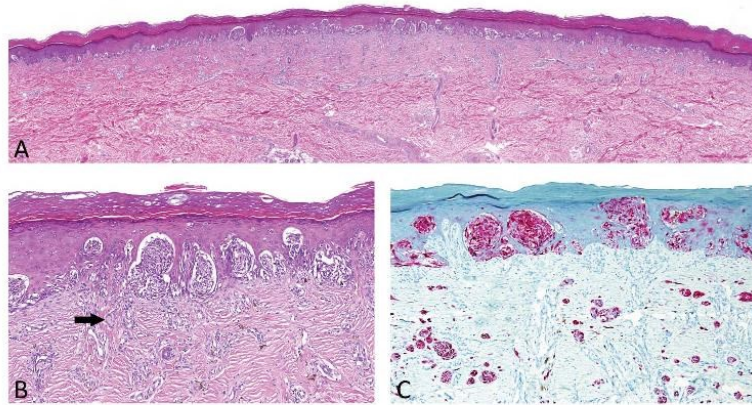
to molecular analysis the challenge to predict biological behavior.[52]

Currently, several studies focused on FISH analysis in Spitz tumors. Biallelic deletion of 9p21 has been reported to correlate with a potentially aggressive disease,[11,53–55] whereas the significance of other FISH probes such as 6p25 and 11q13 has been found to be decreased especially on the multivariate analysis.[54] Isolated loss of 6q23 has been related to the high frequency of sentinel node involvement but with an overall excellent prognosis.[56] To the best of our knowledge, no studies have so far been performed on numeric chromosome aberration in *ROS1*-fused spitzoid lesions. In our series, 1 lesion (case 2) showed an isolated gain of 8q24, which seems a very rare event in Spitz tumors. In a series of 75 spitzoid lesions, only 1 case showed 8q24 gain but it was also accompanied by 11q13, 6p25 gain, and biallelic loss of 9p21; the patient developed distant metastasis and died after 35 months from the diagnosis,[11] emphasizing that not all chromosomal changes are of equal value and increasing genetic complexity correlates with a more adverse outcome.[57]

8q24 gain has been observed mainly in amelanotic nodular melanomas occurring in nonchronically sun-damaged skin, following an aggressive clinical course.[53,58,59] In our series, the tumor with 8q24 gain was an amelanotic lesion arising in nonchronically sun-damaged skin, with highly pleomorphic melanocytes having large irregular nuclei, large eosinophilic nucleoli, and nuclear pseudoinclusions but showing no mitotic figures. To date, the patient is disease-free at 18 months of follow-up. Larger series with a longer follow-up are needed to evaluate the prognostic significance of this isolated alteration of 8q24 in atypical spitzoid lesions. Anyway, our findings suggested that this alteration occurs also in spitzoid lesions and could provide a useful marker for aneuploidy.

Recently, Lee et al[12] confirmed that acquisition of biallelic deletion of *CDKN2A* reflects tumor progression in term of nodal metastases, but only *TERT* promoter mutations in their series strongly correlated with an aggressive behavior and patient death. None of the tumors in our series yielded 9p21 loss, and no mutation was detected in *TERT-p*.

We also studied p16 expression by immunohistochemistry to evaluate the concordance with status of homozygous 9p21 deletion. In line with previous reports, Yazdan et al and Harms et al,[54,60] all neoplasms in our series showed strong positive nuclear staining with a checkerboard alteration of p16-positive and p16-negative melanocytes.

One lesion in our study harbored a mutation in the *TERT* gene c.3164C>T p.Ser1055Leu. This mutation has been labeled as of uncertain significance in the ClinVar database. Apart from the aforementioned *TERT* mutation, the NGS analysis revealed a pattern of different mutations in

TABLE 3. Details of Gene Fusions

Case	GL	Fusion	Exons	Reads	%	Start Sites	Gene 1 Transcript
1	74/18	*PWWP2A–ROS1*	1–36	277	84	99	NM_001,130,864.1
2	75/18	*FIP1L1–ROS1*	10–36	25	100	13	NM_030917.3
3	9498/17	*PWWP2A–ROS1*	1–36	5	50	4	NM_001,130,864.1
4	9403/17	*CAPRIN1–ROS1*	01/07/35	211	89	8	
5	2264/18	*PWWP2A–ROS1*	1–36	33	58	26	NM_001,130,864.1
6	9403/17	*PWWP2A–ROS1*	1–36	5	100	5	NM_001,130,864.1

Exons, number of exons involved in the fusion, respectively; reads, number of reads supporting the fusion; %, percentage of the reads supporting the fusion; start sites, number of unique start sites of reads supporting the fusion; Gene 1 transcript, RefSeq mRNA sequence record number; Gene2 (ROS1) Refseq number is NM_002944.2.

TABLE 4. Mutated Genes in Particular Cases Listed Alphabetically

Gene/case	1	2	3	4	5	6
AR						R
ARID1A	G					
ARID1B					G	
AXIN1			G			
BCORL1			G			
CDH1	G					
CIC						G
CRLF2	G					
DICER1	G					
EGFR					G	
EP300		R				
ERBB2	G					
ESR1						G
FANCD2				G		
FANCE				G		
FH					R	
FLT3				G		
FLT4	G					
GNAS						G
IL7R				G		
KMT2A			G			
KMT2D				G		
LRP1B	G			G		
MAP2K1						G
MEF2B						G
MPL		R				
MSH2		G				
NOTCH2		G	G			
NOTCH3				G		
NRAS			G			
POLD1						G
RB1	G					
ROS1		G			G	
RUNX1	G					
SETBP1				G		
TERT			G			
TNFRSF14				G		
ZNF217	G					
total	10	5	6	9	4	7

Green color denotes subtitutions, and red denotes indels.

143

genes specific for each sample listed in Table 4. The spectrum of affected pathways included especially the *PI3K-Akt* and *MAPK* signaling pathways, both of which have been found to be involved in spitzoid melanoma.[61] Of note, in 2 neoplasms, *ROS1* mutations were also detected (cases 2 and 5). One was labeled as likely pathogenic for abnormalities of brain morphology with recessive inheritance (rs61743088); no phenotype has been for the other variant.

In conclusion, *ROS1*-fused spitzoid neoplasms seem to have no distinctive histopathological features that would enable their recognition on conventional microscopy alone. In our series, all neoplasms occurred in patients younger than 40 years and displayed atypical microscopic features deviating from conventional Spitz nevi and that qualifying them as AST. They lacked homozygous 9p21 deletion or *p-TERT* mutation. Our study extends the range of *ROS1* fusions documented in Spitz tumors by listing 2 hitherto unreported 5′ partners, namely *FIP1L1* and *CAPRIN1*. The neoplasms harbor several additional mutations in other genes in which the role is unclear at the moment and require further studies.

REFERENCES

1. Zedek DC, McCalmont TH. Spitz nevi, atypical spitzoid neoplasms, and spitzoid melanoma. *Clin Lab Med.* 2011;31:311–320.
2. Busam KJ, Murali R, Pulitzer M, et al. Atypical spitzoid melanocytic tumors with positive sentinel lymph nodes in children and teenagers, and comparison with histologically unambiguous and lethal melanomas. *Am J Surg Pathol.* 2009;33:1386–1395.
3. Barnhill RL. The spitzoid lesion: the importance of atypical variants and risk assessment. *Am J Dermatopathol.* 2006;28:75–83.
4. Ludgate MW, Fullen DR, Lee J, et al. The atypical Spitz tumor of uncertain biologic potential: a series of 67 patients from a single institution. *Cancer.* 2009;115:631–641.
5. Hung T, Piris A, Lobo A, et al. Sentinel lymph node metastasis is not predictive of poor outcome in patients with problematic spitzoid melanocytic tumors. *Hum Pathol.* 2013;44:87–94.
6. Ackerman AB. Discordance among expert pathologists in diagnosis of melanocytic neoplasms. *Hum Pathol.* 1996;27:1115–1116.
7. Barnhill RL, Argenyi ZB, From L, et al. Atypical spitz nevi/tumors: lack of consensus for diagnosis, discrimination from melanoma, and prediction of outcome. *Hum Pathol.* 1999;30:513–520.
8. Kempf W, Haeffner AC, Mueller B, et al. Experts and gold standards in dermatopathology: qualitative and quantitative analysis of the self-assessment slide seminar at the 17th colloquium of the International Society of Dermatopathology. *Am J Dermatopathol.* 1998;20:478–482.
9. Wechsler J, Bastuji-Garin S, Spatz A, et al. Reliability of the histopathologic diagnosis of malignant melanoma in childhood. *Arch Dermatol.* 2002;138:625–628.
10. Bastian BC, Wesselmann U, Pinkel D, et al. Molecular cyto-genetic analysis of Spitz nevi shows clear differences to melanoma. *J Invest Dermatol.* 1999;113:1065–1069.
11. Gerami P, Scolyer RA, Xu X, et al. Risk assessment for atypical spitzoid melanocytic neoplasms using FISH to identify chromosomal copy number aberrations. *Am J Surg Pathol.* 2013;37:676–684.
12. Lee S, Barnhill RL, Dummer R, et al. TERT promoter mutations are predictive of aggressive clinical behavior in patients with spitzoid melanocytic neoplasms. *Sci Rep.* 2015;5:11200.
13. Bastian BC. The molecular pathology of melanoma: an integrated taxonomy of melanocytic neoplasia. *Annu Rev Pathol Mech Dis.* 2014;9: 239–271.
14. Wiesner T, He J, Yelensky R, et al. Kinase fusions are frequent in Spitz tumors and spitzoid melanomas. *Nat Commun.* 2014;5:3116.
15. Takeuchi K, Soda M, Togashi Y, et al. RET, ROS1 and ALK fusions in lung cancer. *Nat Med.* 2012;18:378–381.
16. Rabes HM, Demidchik EP, Sidorow JD, et al. Pattern of radiation-induced RET and NTRK1 rearrangements in 191 post-chernobyl papil-

17. lary thyroid carcinomas: biological, phenotypic, and clinical implications. *Clin Cancer Res.* 2000;6:1093–1103.
17. Birchmeier C, Sharma S, Wigler M. Expression and rearrangement of the ROS1 gene in human glioblastoma cells. *Proc Natl Acad Sci U S A.* 1987;84:9270–9274.
18. Antonescu CR, Sumeijer AJH, Zhang L, et al. Molecular characterization of inflammatory myofibroblastic tumors with frequent ALK and ROS1 fusions and rare novel RET gene rearrangement. *Am J Surg Pathol.* 2015; 39:957–967.
19. Morris SW, Kirstein MN, Valentine MB, et al. Fusion of a kinase gene, ALK, to a nucleolar protein gene, NPM, in non-Hodgkin's lymphoma. *Science.* 1994;263:1281–1284.
20. Yeh I, Lang UE, Durieux E et al. Activation of MAP kinase pathway and β-catenin signaling cause deep penetrating nevi. *Nat Commun.* 2017;21; 8:644.
21. Wiesner T, Murali R, Fried I, et al. A distinct subset of atypical Spitz tumors is characterized by BRAF mutation and loss of BAP1 expression. *Am J Surg Pathol.* 2012;36:818–830.
22. Bastian BC, LeBoit PE, Pinkel D. Mutations and copy number increase of HRAS in Spitz nevi with distinctive histopathological features. *Am J Pathol.* 2000;157:967–972.
23. Busam KJ, Kutzner H, Cerroni L, et al. Clinical and pathologic findings of Spitz nevi and atypical Spitz tumors with ALK fusions. *Am J Surg Pathol.* 2014;38:925–933.
24. Yeh I, de la Fouchardiere A, Pissaloux D, et al. Clinical, histopathologic, and genomic features of Spitz tumors with ALK fusions. *Am J Surg Pathol.* 2015;39:581–591.
25. Amin SM, Haugh AM, Lee CY, et al. A Comparison of morphologic and molecular features of BRAF, ALK, and NTRK1 fusion Spitzoid neoplasms. *Am J Surg Pathol.* 2016;41:491–498.
26. VandenBoom T, Quan VL, Zhang B, et al. Genomic fusions in pigmented spindle cell nevus of reed. *Am J Surg Pathol.* 2018;42:1042–1051.
27. Wiesner T, Kutzner H. Morphological and genetic aspects of Spitz tumors. *Pathologie.* 2015;36:37–43.
28. Gerami P, Jewell SS, Morrison LE, et al. Fluorescence in situ hybridization (FISH) as an ancillary diagnostic tool in the diagnosis of melanoma. *Am J Surg Pathol.* 2009;33:1146–1156.
29. Gerami P, Li G, Pouryazdanparast P, et al. A highly specific and discriminatory FISH assay for distinguishing between benign and malignant melanocytic neoplasms. *Am J Surg Pathol.* 2012;36:808–817.
30. Thomas NE, Edmiston SN, Tsai YS, et al. Utility of TERT promoter mutation for cutaneous primary melanoma. *Am J Dermatopathol.* 2019; 41:264–272.
31. Zhong M, Tian W, Zhuge J, et al. Distinguishing nested variants of urothelial carcinoma from benign mimickers by TERT promoter mutation. *Am J Surg Pathol.* 2015;39:127–131.
32. Lek M, Karczewski KJ, Minikel EV, et al. Analysis of protein-coding genetic variation in 60,706 humans. *Nature.* 2016;536:285–291.
33. Landrum MJ, Lee JM, Benson M, et al. Improving access to variant interpretations and supporting evidence. *Nucleic Acids Res.* 2018;46: D1062–D1067.
34. Spitz S. Melanomas of childhood. *Am J Pathol.* 1948;24:591–609.
35. Massi G, LeBoit PE. Spitz nevus. In: Massi G, LeBoit PE, eds. *Histological Diagnosis of Nevi and Melanoma.* 2nd ed. New York, NY: Springer-Verlag; 2014:155–184.
36. Barnhill RL. Spitz nevus. In: Barnhill RL, Piepkorn M, Busam KL, eds. *Pathology of Melanocytic Nevi and Malignant Melanoma.* 3rd ed. New York, NY: Springer-Verlag; 2014:205–269.
37. Kantor GR, Wheeland RG. Transepidermal elimination of nevus cells: a possible mechanism of nevus involution. *Arch Dermatol.* 1987;123: 1371–1374.
38. Weedon D, Little JH. Spindle and epithelioid cell nevi in children and adults. A review of 211 cases of the Spitz nevus. *Cancer.* 1977;40:217–225.
39. Wiedemeyer K, Guadagno A, Davey J, et al. Acral spitz nevi: clinico-pathologic study of 50 cases with immunohistochemical analysis of P16 and P21 expression. *Am J Surg Pathol.* 2018;42:821–827.
40. Spatz A, Cook MG, Elder DE, et al. Interobserver reproducibility of ulceration assessment in primary cutaneous melanomas. *Eur J Cancer.* 2003;39:1861–1865.
41. Hoang MP. Myxoid spitz nevus. *J Cutan Pathol.* 2003;30:566–568.

AU6

42. Requena C, Requena L, Kutzner H, et al. Spitz nevus: a clinicopathological study of 349 cases. *Am J Dermatopathol*. 2009;31:107–116.

43. Fernandez-Flores A, Riveiro-Falkenbach E, Cassarino DS. Myxoid spitz nevi: report of 6 cases. *Am J Dermatopathol*. 2018;40:30–35.

44. Perron E, Pissaloux D, Charon Barra C, et al. Melanocytic myxoid spindle cell tumor with ALK rearrangement (MMySTAR): report of 4 cases of a nevus variant with potential diagnostic challenge. *Am J Surg Pathol*. 2018;42:595–603.

45. Vandenberghe P, Wlodarska I, Michaux L, et al. Clinical and molecular features of FIP1L1-PDFGRA (+) chronic eosinophilic leukemias. *Leukemia*. 2004;18:734–742.

46. Walz C, Metzgeroth G, Haferlach C, et al. Characterization of three new imatinib-responsive fusion genes in chronic myeloproliferative disorders generated by disruption of the platelet-derived growth factor receptor beta gene. *Haematologica*. 2007;92:163–169.

47. Jun HJ, Johnson H, Bronson RT, et al. The oncogenic lung cancer fusion kinase CD74-ROS activates a novel invasiveness pathway through E-Syt1 phosphorylation. *Cancer Res*. 2012;72:3764–3774.

48. Spatz A, Calonje E, Handfield-Jones S, et al. Spitz tumors in children: a grading system for risk stratification. *Arch Dermatol*. 1999;135:282–285.

49. Barnhill RL. The Spitzoid lesion: rethinking Spitz tumors, atypical variants, "Spitzoid melanoma" and risk assessment. *Mod Pathol*. 2006; 19(suppl 2):S21–S33.

50. Cerroni L, Barnhill R, Elder D, et al. Melanocytic tumors of uncertain malignant potential: results of a tutorial held at the XXIX Symposium of the International Society of Dermatopathology in Graz, October 2008. *Am J Surg Pathol*. 2010;34:314–326.

51. Urso C. Diagnostic problems in spitzoid neoplasms. *Pathology*. 2017;49: 325–326.

52. Cerroni L. Spitzoid tumors: a matter of perspective? *Am J Dermatopathol*. 2004;26:1–3.

53. Gerami P, Cooper C, Bajaj S, et al. Outcomes of atypical spitz tumors with chromosomal copy number aberrations and conventional melanomas in children. *Am J Surg Pathol*. 2013;37:1387–1394.

54. Yazdan P, Cooper C, Sholl LM, et al. Comparative analysis of atypical Spitz tumors with heterozygous versus homozygous 9p21 deletions for clinical outcomes, histomorphology, BRAF mutation, and p16 expression. *Am J Surg Pathol*. 2014;38:638–645.

55. Lee CY, Sholl LM, Zhang B, et al. Atypical spitzoid neoplasms in childhood: a molecular and outcome study. *Am J Dermatopathol*. 2017;39: 181–186.

56. Shen L, Cooper C, Bajaj S, et al. Atypical spitz tumors with 6q23 deletions: a clinical, histological, and molecular study. *Am J Dermatopathol*. 2013;35:804–812.

57. Massi D, Tomasini C, Senetta R, et al. Atypical Spitz tumors in patients younger than 18 years. *J Am Acad Dermatol*. 2015;72:37–46.

58. Pouryazdanparast P, Cowen DP, Beilfuss BA, et al. Distinctive clinical and histologic features in cutaneous melanoma with copy number gains in 8q24. *Am J Surg Pathol*. 2012;36:253–264.

59. Gerami P, Jewell SS, Pouryazdanparast P, et al. Copy number gains in 11q13 and 8q24 [corrected] are highly linked to prognosis in cutaneous malignant melanoma. *J Mol Diagn*. 2011;13:352–358.

60. Harms PW, Hocker TL, Zhao L, et al. Loss of p16 expression and copy number changes of CDKN2A in a spectrum of spitzoid melanocytic lesions. *Hum Pathol*. 2016;58:152–160.

61. Lazova R, Pornputtapong N, Halaban R, et al. Spitz nevi and Spitzoid melanomas—exome sequencing and comparison to conventional melanocytic nevi and melanomas. *Mod Pathol*. 2017;30:640–649.

Jun 29 2019 02:12:43:573AM

RE: AJD-D-19-00216R1, titled "Polypoid atypical Spitz tumor with a fibrosclerotic stroma, CLIP2-BRAF fusion and homozygous loss of 9p21"

Dear Dr Kazakov,

I am pleased to inform you that your work has now been accepted for publication in The American Journal of Dermatopathology. All manuscript materials will be forwarded to the production staff for placement in an upcoming issue.

OPEN ACCESS
If you indicated in the revision stage that you would like your submission, if accepted, to be made open access, please go directly to step 2. If you have not yet indicated that you would like your accepted article to be open access, please follow the steps below to complete the process:
1. Notify the journal office via email that you would like this article to be available open access. Please send your Email to caklapak@wakehealth.edu. Please include your article title and manuscript number.
2. A License to Publish (LTP) form must be completed for your submission to be made available open access. Please download the form from http://links.lww.com/LWW-ES/A49, sign it, and Email the completed form to the journal office.
3. **Within 48 hours of receiving this e-mail:** Go to http://wolterskluwer.qconnect.com to pay for open access. If you have not previously used this site to place an order, you will need to register for an account (your login will be different from your Editorial Manager login). When placing your order, you will be asked for the following information. Please enter exactly as shown:
a. Article Title - Polypoid atypical Spitz tumor with a fibrosclerotic stroma, CLIP2-BRAF fusion and homozygous loss of 9p21
b. Manuscript Number - AJD-D-19-00216R1

Thank you for submitting your interesting and important work to the journal.

https://www.editorialmanager.com/ajd/

Your username is: ********
****

With Kind Regards,

Dr. Omar P. Sangüeza
Editor-in-Chief
The American Journal of Dermatopathology

Polypoid atypical Spitz tumor with a fibrosclerotic stroma, *CLIP2-BRAF* fusion and homozygous loss of 9p21.

Michele Donati (1), Liubov Kastnerova, MD (2,3), Nikola Ptakova, MSc (2,4), Michal Michal, MD (2,3) and Dmitry V. Kazakov, MD, PhD (2, 3)

1. Department of Pathology, University Hospital Campus Bio-Medico, Rome, Italy

2.   Sikl's Department of Pathology, Medical Faculty in Pilsen, Charles University in Prague, Pilsen, Czech Republic

3.   Bioptical Laboratory, Pilsen, Czech Republic

4. Second Faculty of Medicine, Charles University, Prague, Czech Republic

Short title: CLIP2-BRAF fused atypical spitzoid tumor

Address for correspondence: D. V. Kazakov, MD, Sikl's Department of Pathology, Charles University Medical Faculty Hospital, Alej Svobody 80, 304 60 Pilsen, Czech Republic

Cellular phone: +420-737220405, Direct: +420-377104651, Fax: +420-377104650, E-mail:kazakov@medima.cz

Abstract

We report a case of a polypoid atypical Spitz tumor a with prominent fibrosclerotic stromal component, harboring a *CLIP2-BRAF* fusion, which has hitherto been not reported in melanocytic lesions. The neoplasm occurred in a 78-year-old male patient and appeared microscopically as a predominantly dermal, barely symmetrical, polypoid lesion composed mainly of epithelioid cells showing moderate degree of nuclear pleomorphism with ample amphophilic cytoplasm arranged in nests, fascicles or single units. The mitotic rate was 2/mm² and mitoses were confined to the upper portion of the lesion. The Breslow thickness was 2.3 mm. The stroma contained conspicuous plumped fibroblasts and thickened collagen bundles associated with dilated medium-sized vessels. Focally, sclerotic areas were found. A moderately dense, lymphocyte predominant inflammatory infiltrate scattered through the whole lesion was seen. Despite strong nuclear and cytoplasmic positivity of p16 was, FISH revealed homozygous loss in locus 9p21. A *CLIP2-BRAF* fusion was found by next generation sequencing. No other genetic alterations including *TERT*-promoter mutation was found. The patient is disease-free without recurrence or evidence of metastatic disease after 5 years and 2 months of follow-up.

Introduction

Spitz neoplasms represent a heterogeneous group of melanocytic lesions histologically characterized by large epithelioid and/or spindled melanocytes with ample cytoplasm associated with specific epidermal and stromal changes, exhibiting a range of cytological and architectural variability that results in variable morphologic presentations (1). Thanks to the new data on the molecular alterations, our understanding of these neoplasms and their classification is undergoing a revision (2). Specifically, mutually exclusive genomic rearrangements involving the tyrosine kinase receptors *ALK, NTRK1, NTRK2, NTRK3, MET, RET,* and *ROS1* and the serine-threonine kinase *BRAF* are frequently involved in Spitz lesions (3) and some of them appear to be associated with specific histological features (4-8). Since the study by Wiesner et al. in 2010 (3), few detailed morphological descriptions of Spitz neoplasms with *BRAF* fusions have been reported. A *BRAF* fusion is estimated to be present in around 5% of Spitz tumors; a correlation with specific morphological changes has not yet been clearly defined, although some studies consistently revealed a combination epithelioid cell morphology and conspicuous sclerotic stroma (4, 9). Recently, two cases of unclassified sclerosing malignant melanomas with an *AKAP9-BRAF* gene fusion have been described (10). The illustrations of that paper suggest a spitzoid phenotype. We hereby report a case of an ambiguous polypoid Spitz tumor with a prominent fibrosclerotic stromal component, harboring a *CLIP2-BRAF* fusion that has not been reported to date in melanocytic lesions.

Case Report

A 78-year old man with no personal or family history of melanoma presented with 0.6 cm nodule on his left/right thigh that had been present for 3 years, slowly increasing in size over time. The lesion was surgically excised, and the histological examination showed a predominantly dermal, barely symmetrical, polypoid melanocytic neoplasm composed mainly of epithelioid cells, with copious amphophilic cytoplasm showing moderate degree of nuclear pleomorphism. Melanocytes with prominent eosinophilic nucleoli were also observed. The cells were arranged in nests and fascicles, with no or minimal confluence. Singular cells surrounded by stroma were focally seen. The mitotic rate was 2/mm². The mitoses were confined to the upper dermal portion of the lesion. No atypical mitotic figures were seen. Breslow thickness was 2.3 mm. The lesion was amelanotic and displayed an uneven flat base, not reaching the subcutaneous tissue. Maturation was preserved. The stroma

contained conspicuous plumped fibroblasts and thickened collagen bundles associated with dilated medium-sized vessels. Focally, sclerotic areas were found. A moderately dense, lymphocyte predominant inflammatory infiltrate scattered through the whole lesion was seen. The epidermis overlying the lesion was slightly hyperplastic, with an increased number of medium-sized epithelioid melanocytes at the dermo-epidermal junction not extending beyond the dermal component. No junctional nests, Kamino bodies or pagetoid spread was seen. No perineural or intravascular involvement was observed.

Immunohistochemistry showed a diffuse positivity of the neoplastic cells for S-100 protein and tyrosinase, whereas Melan A was only focally expressed in the upper part of the lesion. Diffuse and strong nuclear and cytoplasmic positivity of p16 was observed in almost all the melanocytes.

FISH assay for chromosomal numeric aberrations revealed homozygous loss in locus 9p21 (*CDKN2A*), whereas no other alterations were detected, using probes targeting 6p25 (*RREB1*), 6q23 (*MYB*), 6p25 (*RREB1*), 11q13 (*CCND1*), and 8q24 (*MYC*), as described elsewhere (11).

TERT-promoter (*TERT*-p) hotspot mutation analysis, carried out with PCR and Sanger sequencing, was negative (12).

The Illumina TruSight Tumor 170 (TS170) panel was used for genomic rearrangement and somatic mutations detection as previously described (13). The TruSight Tumor 170 Panel, both DNA and RNA parts, targets the following genes *AKT1, AKT2, AKT3, ALK, APC, AR, ARID1A, ATM, ATR, BAP1, BARD1, BCL2, BCL6, BRAF, BRCA1, BRCA2 ,BRIP1, BTK, CARD11, CCND1, CCND2, CCND3, CCNE1, CD79A, CD79B, CDH1, CDK12, CDK4, CDK6, CDKN2A, CEBPA, CREBBP, CSF1R, CTNNB1, DDR2, DNMT3A, EGFR, EP300, ERBB2, ERBB3, ERBB4, ERCC1, ERCC2, ERG, ESR1, EZH2, FAM175A, FANCI, FANCL,FBXW7, FGF1, FGF10, FGF14, FGF19, FGF2, FGF23, FGF3,FGF4, FGF5, FGF6, FGF7,FGF8, FGF9, FGFR1, FGFR2, FGFR3, FGFR4, FLT1, FLT3, FOXL, GEN1, GNA11, GNAQ, GNAS, HNF1A, HRAS, CHEK1, CHEK2, IDH1, IDH2, INPP4B, JAK2, JAK3, KDR, KIT, KRAS, LAMP1, MAP2K1, MAP2K2, MCL1, MDM2, MDM4, MET, MLH1, MLL, MLLT3, MPL, MRE11A, MSH2, MSH3, MSH6, MTOR, MUTYH, MYC, MYCL1, MYCN, MYD88, NBN, NF1, NOTCH1, NOTCH2, NOTCH3, NPM1, NRAS, NRG1, PALB2, PDGFRA, PDGFRB, PIK3CA, PIK3CB, PIK3CD, PIK3CG, PIK3R1, PMS2, PPP2R2A, PTEN, PTCH1 ,PTPN11, RAD51, RAD51B, RAD51C, RAD51D, RAD54L, RAF1, RB1, RET, RICTOR, ROS1, RPS6KB1, SLX4, SMAD4, SMARCB1, SMO, SRC, STK11, TERT, TET2, TFRC, TP53, TSC1, TSC2, VHL*, and *XRCC2*. The quality of the extracted DNA was checked by qPCR using the Illumina FFPE QC kit, whereas the quality of RNA was tested using Agilent RNA 6000 Nano Kit on bioanalizer 4200 TapeStation.

RNA sequencing identified a *CLIP2-BRAF* fusion. A complementary FISH study with a BRAF break-apart probe confirmed the presence of this gene rearrangement. DNA sequencing for the detection of somatic mutations in 153 genes commonly involved in solid tumors was negative.

Given the histological and molecular findings, a diagnosis of atypical Spitz tumor was made. No sentinel lymph node biopsy was performed. The patient is disease-free without recurrence after 5 years and 2 months of follow-up.

Discussion

The largest series on the histopathological features of *BRAF*-fused spitzoid lesions reported to date was published by Amin et al. who described 14 *BRAF*-fused Spitz tumors and compared their molecular and morphological features with Spitz tumors harboring *ALK* and *NTRK*1 fusion (4). In comparison to the other 2 groups, *BRAF*-positive cases were predominantly composed of epithelioid melanocytes with moderate to high-grade nuclear atypia with a sheet-like growth pattern in the dermis, with some cases showing single cells dispersed with a sclerotic stroma at the base. Moreover, the dysplastic Spitz architecture was also observed only in the *BRAF* fusion group. These lesions showed more likely copy number gains involving the kinase domain of the fusion protein and positive result with the melanoma FISH assay (4).

Recently, two cases of unclassified sclerosing malignant melanoma harboring *AKAP9-BRAF* gene fusion have been reported (10). The first case was a dermatofibroma-like lesion occurred in the lumbar region of a 47-year old man that histologically mimicked a desmoplastic melanoma (DM). The second case was a 42-year old woman presenting with an exophytic genital lesion. A biopsy specimen exhibited a complex morphology, with junctional nests composed of large spindled cells and a dermal component of nevoid melanocytes surrounded by a dense fibrous/sclerotic background. Both the cases harbored numerous partial chromosomal gains and losses suggesting a diagnosis of melanoma. To our eye, the cytological details of the two cases may be regarded as those of spitzoid lesions. Further studies reported the presence of *BRAF*-fusion in spitzoid and non-spitzoid melanocytic tumors (9, 14-17), including metastatic and lethal cases (18, 19).

The case we report further expands the molecular and morphological variations associated with *BRAF*-fused Spitz neoplasms. Histologically, the tumor presented as a large polypoid lesion with well-formed medium size vessels and a prominent fibrosclerotic stromal component, reminiscent of previously described polypoid Spitz nevus (20). The prominent feature was the presence of fascicles

of plumped fibroblasts alternating with nests and single cells of moderately pleomorphic epithelioid melanocytes with brisk mitotic activity. As the lesion occurred in in a 78-year old male patient, it raised a concern of a malignant neoplasm (21) and prompted us to perform further studies for risk stratification to establish whether the neoplasm harbor molecular alterations associated with an aggressive behavior, including homozygous deletion 9p21 and *TERT*-p mutations (22, 23). The FISH analysis revealed homozygous loss of 9p21, which was unexpected due to strong and diffuse nuclear staining for p16 on immunohistochemistry (previous studies reported a good correlation between "checkerboard nuclear pattern" and 9p21 preservation at FISH assay) (24, 25). Although several studies described a strong association between homozygous deletion of 9p21 and an aggressive clinical course in Spitz tumors, (22, 23, 26, 27) its prognostic value has been questioned, and *TERT*-p hotspot mutations have been proposed as a more reliable predictive marker (23). In our neoplasm, we observed no *TERT-p* mutation. Moreover, DNA sequencing of 153 genes commonly involved in solid tumors failed to identify any somatic mutation. In a previous mutational landscape study, a low somatic mutation burden were reported in both Spitz and conventional nevi (34.41±9.42), whereas both spitzoid (747.22±137.55) and conventional melanoma (758.03±96.76) showed a high somatic mutation rate (28). The low mutation burden in our case can be explained by the different methodologies used in our study and in that of Lazova et al who performed whole exome sequencing (28) but may still be used as an additional argument against the diagnosis of spitzoid melanoma. Correlating these molecular data with the uneventful clinical course and taking into account atypical histological features that are not however sufficient to make the diagnosis of an overt malignancy, we consider the lesion as atypical Spitz tumor.

TS170 RNA sequencing for the detection of fusion transcripts in 55 genes yielded a *CLIP2-BRAF* fusion, extending the list of 5' fusion partner of the *BRAF* gene. To date, 33 different 5' fusion partner have been described for BRAF in melanocytic tumors, including *AGK, AGT7, AKAP9, AGAP3, ARMC10, BAIAP2L1, BGTF21, CCDC91,CDC27, CEP89, CUX1, DGKI, DYNC112, EML4, FCHSD1, KCTD7, KIAA1549, LSM14A, MAD1L1, MZT1, NFIC, NUDCD3, PAPSS1, PLIN3, RAD18, SLC12A7, SOX6, TAX1BP1, TNEM178, TRIM24, ZNF767, ZKSCAN1* and *ZKSCAN5* (3, 4, 9, 12, 14-19, 29, 30). To the best of our knowledge, the *CLIP2-BRAF* fusion has never been reported in melanocytic lesions, but has been described in patients with histiocytic disorders and was implicated in constitutive MAPK pathway activation (31, 32) A possible role of 5' fusion partner in the determination of the biological behavior has been hypothesized in other solid tumors (33). As the catalytic domain of the kinases is preserved in the rearrangements, the N-terminal fusion partner may determine the function of the gene product (34).

In conclusion, we have described a case of polypoid atypical Spitz tumor with fibrosclerotic stroma, homozygous loss of 9p21, p16 immunopositivity and a *CLIP2-BRAF* fusion that has not been previously described in melanocytic lesions.

Reference

1. Barnhill RL. Spitz Nevus. In: Barnhill RL, Piepkorn M, Busam KL, eds. Pathology of Melanocytic Nevi and Malignant Melanoma, 3nd ed. New York, PA: Springer-Verlag; 2014: 155–184

2. WHO Classification of Skin Tumours. 4th Edn. Lyon: World Health Organization; 2018.

3. Wiesner T, Yelensky R, Esteve-Puig R, et al. Kinase fusions are frequent in Spitz tumours and spitzoid melanomas. *Nat Commun*. 2014; 5:3116

4. Amin SM, Haugh AM, Lee CY, et al. A Comparison of morphologic and molecular features of BRAF, ALK, and NTRK1 fusion Spitzoid neoplasms. *Am J Surg Pathol* 2017; 41: 491-8

5. Busam KJ, Kutzner H, Cerroni L, et al. Clinical and Pathologic Findings of Spitz Nevi and Atypical Spitz Tumors with ALK Fusions. *J Surg Pathol*. 2014; 38:925–933.

6. Yeh I, de la Fouchardiere A, Pissaloux D, et al. Clinical, histopathologic, and genomic features of Spitz tumors with ALK fusions. *Am J Surg Pathol*. 2015; 39:581–591

7. Yeh I, Busam K J, Mccalmont, et al. Filigree-like Rete Ridges, Lobulated Nests, Rosette-like Structures, and Exaggerated Maturation Characterize Spitz Tumors with NTRK1 Fusion. *Am J Surg Pathol*. 2019

8. Vandenboom T, Quan VL, Zhang B et al. Genomic fusions in pigmented spindle cell nevus of reed. *Am J Surg Pathol*, 2018; 42, 1042–1051.

9. Botton T, Yeh I, Nelson T, Vemula SS, et al. Recurrent BRAF kinase fusions in melanocytic tumors offer an opportunity for targeted therapy. *Pigment Cell Melanoma Res*. 2013; 26:845–851

10. Perron E, Pissaloux D, Neub A, et al. Unclassified sclerosing malignant melanomas with AKAP9-BRAF gene fusion: a report of two cases and review of BRAF fusions in melanocytic tumors. *Virchow Arch*. 2018; 472: 469–476.

11. Gerami P, Li G, Pouryazdanparast P, et al. A highly specific and discriminatory FISH assay for distinguishing between benign and malignant melanocytic neoplasms. *Am J Surg Pathol.* 2012; 36:808–817

12. Thomas NE, Edmiston SN1, Tsai YS, et al. Utility of TERT promoter mutation for cutaneous primary melanoma. *Am J Dermatopathol.* 2019 ;41:264–272

13. Skalova A, Vanecek T, Martinek P et al. Molecular Profiling of Mammary Analog Secretory Carcinoma Revealed a Subset of Tumors Harboring a Novel ETV6-RET Translocation: Report of 10 Cases. *Am J Surg Pathol.* 2018;42:234–246

14. Dessars B, De Raeve LE, El HH, et al. Chromosomal translocations as a mechanism of BRAF activation in two cases oflarge congenital melanocytic nevi. *J Invest Dermatol.* 2007; 127:1468–1470

15. Kim HS, Jung M, Kang HN, et al. Oncogenic BRAF fusions in mucosal melanomas activate the MAPK pathway and are sensitive to MEK/PI3K inhibition or MEK/CDK4/6 inhibition. *Oncogene.* 2017; 36:3334–3345.

16. Turner J, Couts K, Sheren J, et al. Kinase gene fusions in defined subsets of melanoma. *Pigment Cell Melanoma Res.* 2017; 30:53–62.

17. Ross JS, Wang K, Chmielecki J, et al. The distribution of BRAF gene fusions in solid tumors and response to targeted therapy. *Int J Cancer* 2016; 138:881–890

18. Menzies AM, Yeh I, Botton T, et al. Clinical activity of the MEK inhibitor trametinib in metasta- tic melanoma containing BRAF kinase fusion. *Pigment Cell Melanoma Res.* 2015; 28:607–610

19. HutchinsonKE, Lipson D, Stephens PJ, et al. BRAF fusions define a distinct molecular subset of melanomas with potential sensitivity to MEK inhibition. *Clin Cancer Res.* 2013; 19:6696–6702

20. Massi G, LeBoit PE. Spitz Nevus Variants, Polypid Spitz Nevus In: Massi G, LeBoit PE, Histological Diagnosis of Nevi and Melanoma, New York, PA: Springer, 2014; 188.

21. Ludgate MW, Fullen DR, Lee J, et al. The atypical Spitz tumor of uncertain biologic potential: a series of 67 patients from a single institution. *Cancer* 2009; 115:631–41

22. Gerami P, Scolyer RA, Xu X, et al. Risk assessment for atypical spitzoid melanocytic neoplasms using FISH to identify chromosomal copy number aberrations. *Am J Surg Pathol.* 2013; 37:676–84

23. Lee S, Barnhill RL, Dummer R, et al. TERT Promoter Mutations Are Predictive of Aggressive Clinical Behavior in Patients with Spitzoid Melanocytic Neoplasms. Sci Rep.2015; *Sci Rep.* 2015 10;5:11200

24. Yazdan P, Cooper C, Sholl LM, et al. Comparative analysis of atypical Spitz tumors with heterozygous versus homozygous 9p21 deletions for clinical outcomes, histomorphology, BRAF mutation, and p16 expression. *Am J Surg Path.* 2014; 38:638–45.

25. Harms PW, Hocker TL, Zhao L, et al. Loss of p16 expression and copy number changes of CDKN2A in a spectrum of spitzoid melanocytic lesions. *Hum Pathol.* 2016; 58:152–160

26. Gerami P, Cooper C, Bajaj S, et al. Outcomes of atypical Spitz tumors with chromosomal copy number aberrations and conventional melanomas in children. *Am J Surg Pathol* 2013; 37:1387

27. Lee CY, Sholl LM, Zhang B, et al. Atypical Spitzoid neoplasms in childhood: a molecular and outcome study. *Am J Dermatopathol* 2016; 39:181–6

28. Lazova R, Pornputtapong N, Halaban R, et al. Spitz nevi and Spitzoid melanomas: exome sequencing and comparison to conventional melanocytic nevi and melanomas. *Mod Pathol.* 2017; 30: 640–649

29. Busam KJ, Shah KN, Gerami P, et al. Reduced H3K27me3 expression is common in nodular melanomas of childhood associated with congenital melanocytic nevi but not in proliferative nodules. *Am J Surg Pathol.* 2017; 41:396–404.

30. Wu G, Barnhill RL, Lee S, et al. The landscape of fusion transcripts in spitzoid melanoma and biologically indeterminate spitzoid tumors by RNA sequencing. *Mod Pathol.* 2016; 29:359–69

31. Diamond EL, Durham BH, Haroche J, et al. Diverse and targetable kinase alterations drive histiocytic neoplasms. *Cancer Discov.* 2016; 6:154–165

32. Chakraborty R, Burke TM, Hampton OA, et al. Alternative genetic mechanisms of BRAF activation in Langerhans cell histiocytosis. *Blood.* 2016; 128:2533–2537

33. Jun, H. J., Johnson, H., Bronson, R. Tet al. The oncogenic lung cancer fusion kinase CD74-ROS activates a novel invasiveness pathway through E-syt1 phosphorylation. *Cancer Res.* 2012; 72: 3764–3774

34. Hallberg B, Palmer RH. The role of the ALK receptor in cancer biology. *Ann Oncol* 2016; 27:iii4–iii15.

Figure legends

Figure 1. A barely symmetrical, polypoid neoplasm showing a predominantly dermal growth without subcutaneous tissue involvement, with fibrosclerotic stroma contraining dilated medium-sized vessels (A). Small to medium size nests and short fascicles of melanocytes surrounded by fibrosclerotic stroma and moderate lymphocytic infiltrate can be seen. (B). A close-up view of the lesion: epithelioid melanocytes with copious amphophilic cytoplasm and moderate degree of nuclear pleomorphism intimately associated with plumped fibroblasts and thickened collagen bundles are evident. (C). Note mitotic figures activity (arrows) (D).

Figure 2. Schematic presentation of the *CLIP2-BRAF* fusion transcript as revealed by next generation sequencing. The upper section: the scheme of joining of exon 8 of *CLIP2* gene and exon 9 of *BRAF* gene. The lower section: the sequencing coverage of point of fusion in grey, several unique reads in red and blue respectively.

Figure 1
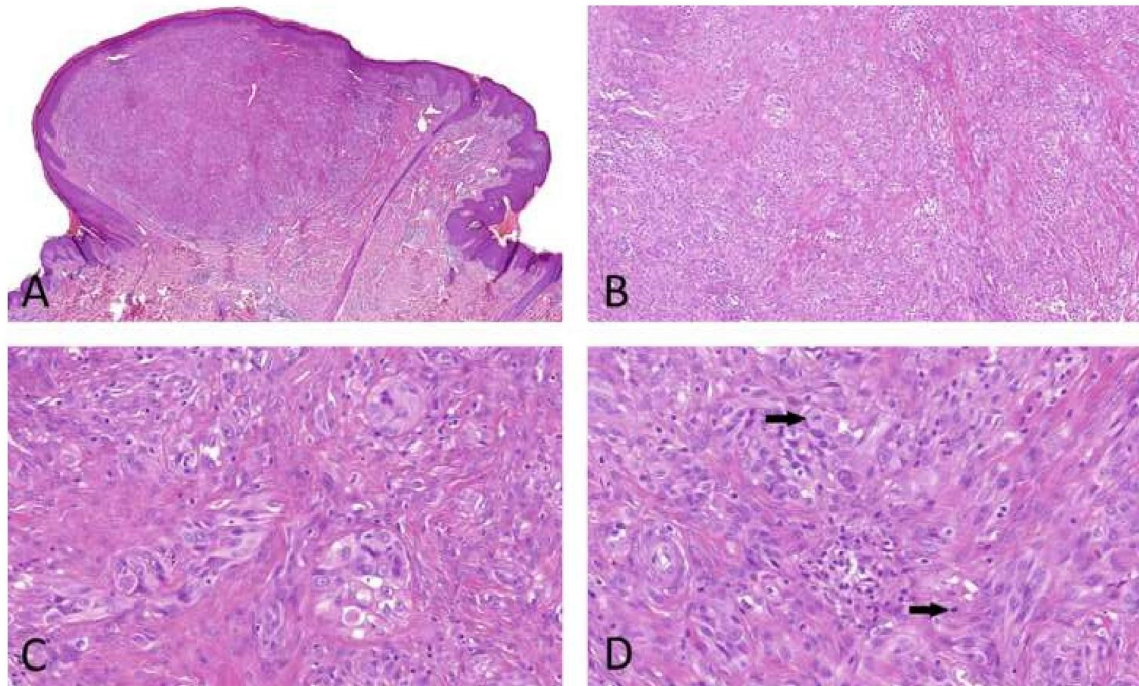
Figure 2
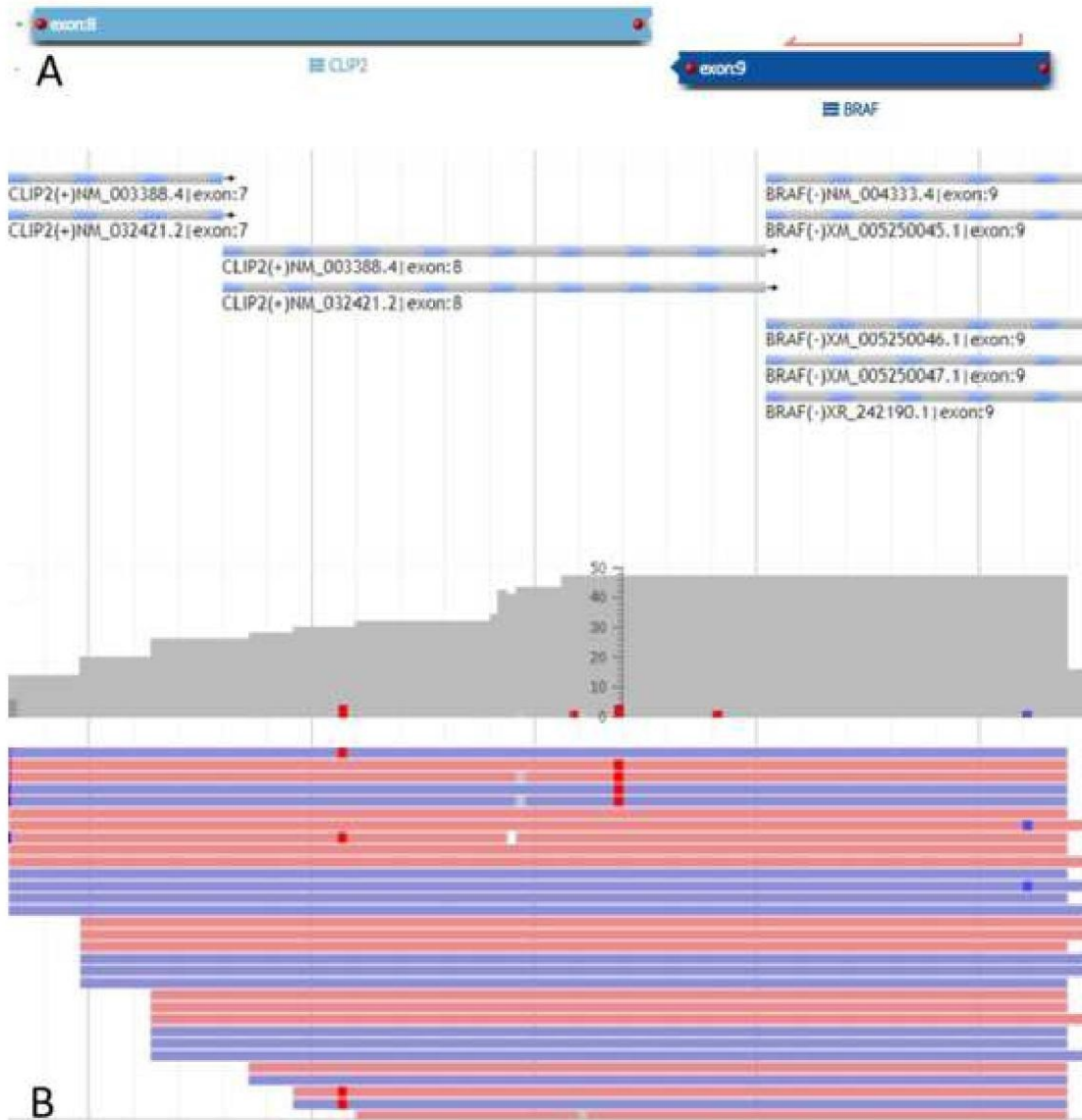
LIST OF OWN PUBLICATIONS

1. **Kyrpychova L**, Kacerovska D, Vanecek T, Grossmann P, Michal M, Kerl K, Kazakov DV. Cutaneous hidradenoma: a study of 21 neoplasms revealing neither correlation between the cellular composition and CRTC1-MAML2 fusions nor presence of CRTC3-MAML2 fusions. *Ann Diagn Pathol*. 2016 Aug;23:8-13.

2. Konstantinova AM, Shelekhova KV, Stewart CJ, Spagnolo DV, Kutzner H, Kacerovska D, Plaza JA, Suster S, Bouda J, Pavlovsky M, **Kyrpychova L**, Michal M, Guenova E, Kazakov DV. Depth and Patterns of Adnexal Involvement in Primary Extramammary (Anogenital) Paget Disease: A Study of 178 Lesions From 146 Patients. *Am J Dermatopathol*. 2016 Nov;38(11):802-808.

3. Konstantinova AM, Vanecek T, Martinek P, **Kyrpychova L**, Spagnolo DV, Stewart CJR, Portelli F, Michal M, Kazakov DV. Molecular alterations in lesions of anogenital mammary-like glands and their mammary counterparts including hidradenoma papilliferum, intraductal papilloma, fibroadenoma and phyllodes tumor. *Ann Diagn Pathol*. 2017 Jun; 28:12-18.

4. Konstantinova AM, Spagnolo DV, Stewart CJR, Kacerovska D, Shelekhova KV, Plaza JA, Suster S, Bouda J, **Kyrpychova L**, Michal M, Belousova IE, Kerl K, Kazakov DV. Spectrum of Changes in Anogenital Mammary-like Glands in Primary Extramammary (Anogenital) Paget Disease and Their Possible Role in the Pathogenesis of the Disease. *Am J Surg Pathol*. 2017 Aug;41(8):1053-1058

5. Konstantinova AM, Stewart CJ, **Kyrpychova L**, Belousova IE, Michal M, Kazakov DV. An Immunohistochemical Study of Anogenital Mammary-Like Glands. Am J Dermatopathol. 2017 Aug;39(8):599-605.

6. **Kyrpychova L**, Carr RA, Martinek P, Vanecek T, Perret R, Chottová-Dvořáková M, Zamecnik M, Hadravsky L, Michal M, Kazakov DV. Basal Cell Carcinoma With Matrical Differentiation: Clinicopathologic, Immunohistochemical, and Molecular Biological Study of 22 Cases. *Am J Surg Pathol*. 2017 Jun;41(6):738-749.

7. Broekaert SM, Flux K, **Kyrpychova L**, Kacerovska D, Ivan D, Schön MP, Ströbel P, Michal M, Denisjuk N, Kerl K, Kazakov DV. Squared-Off Nuclei and "Appliqué" Pattern as a Histopathological Clue to Periocular Sebaceous Carcinoma: A Clinicopathological Study of 50 Neoplasms From 46 Patients. *Am J Dermatopathol*. 2017 Apr;39(4):275-278.

8. **Kyrpychova L**, Kacerovska D, Michal M, Kazakov DV. Sporadic Trichoblastomas and Those Occurring in the Setting of Multiple Familial Trichoepithelioma/Brooke-Spiegler Syndrome Show No BAP1 Loss. *Am J Dermatopathol*. 2017 Oct;39(10):793-794.

9. Konstantinova AM, **Kyrpychova L**, Belousova IE, Spagnolo DV, Kacerovska D, Michal M, Kerl K, Kazakov DV. Anogenital Mammary-Like Glands: A Study of Their Normal Histology With Emphasis on Glandular Depth, Presence of Columnar Epithelial Cells, and Distribution of Elastic Fibers. *Am J Dermatopathol*. 2017 Sep;39(9):663-667.

10. Wiedemeyer K, **Kyrpychova L**, Tanas O, Spagnolo DV, Kutzner H, Rütten A, Fernandez-Figueras MT, Denisjuk N, Suster S, Pavlovsky M, Petersson F, Michal M, Lee J, Kerl K, Kazakov DV. Sebaceous Neoplasms With Rippled, labyrinthine/Sinusoidal, Petaloid, and Carcinoid-Like Patterns: A Study of 57 Cases Validating Their Occurrence as a Morphological Spectrum and Showing No Significant Association With Muir–Torre Syndrome or DNA Mismatch Repair Protein Deficiency. *Am J Dermatopathol*. 2018 Jul;40(7):479-485.

11. Kazakov DV, **Kyrpychova L**, Martinek P, Grossmann P, Steiner P, Vanecek T, Pavlovsky M, Bencik V, Michal M, Michal M. ALK gene fusions in epithelioid fibrous histiocytoma: a study of 14 cases, with new histopathological findings. *Am J Dermatopathol*. 2018 Nov;40(11):805-814.

12. **Kyrpychova L**, Vanecek T, Grossmann P, Martinek P, Steiner P, Hadravsky L, Belousova IE, Shelekhova KV, Svajdler M, Dubinsky P, Michal M, Kazakov DV. Small Subset of Adenoid Cystic Carcinoma of the Skin Is Associated With Alterations of the MYBL1 Gene Similar to Their Extracutaneous Counterparts. *Am J Dermatopathol*. 2018 Oct;40(10):721-726.

13. **Kyrpychova L,** Šteiner P, Michal M, Kazakov DV. Lack of Deletion of 1p36 in 8 Cases of Primary Adenoid Cystic Carcinoma of the Skin. *Am J Dermatopathol*. 2019 Jan 11. [Epub ahead of print]

14. Belousova IE, **Kyrpychova L**, Samtsov AV, Kazakov DV. A Case of Lymphomatoid Papulosis Type E With an Unusual Exacerbated Clinical Course. *Am J Dermatopathol*. 2018 Feb;40(2):145-147

15. Konstantinova AM, **Kyrpychova L**, Nemcova J, Sedivcova M, Bisceglia M, Kutzner H, Zamecnik M, Sehnalkova E, Pavlovsky M, Zateckova K, Shvernik S, Spurkova Z, Michal M, Kerl K, Kazakov DV. Syringocystadenoma Papilliferum of the Anogenital Area and

Buttocks: A Report of 16 Cases, Including Human Papillomavirus Analysis and HRAS and BRAF V600 Mutation Studies. *Am J Dermatopathol*., 2019 April; 41(4):281-285.

16. **Kastnerova L,** Luzar B, Goto K, Grishakov V, Gatalica Z, Kamarachev J, Martinek P, Hájková V, Grossmann P, Imai H, Fukui H, Michal M, Kazakov DV. Secretory carcinoma of the skin: report of 6 cases, including a case with a novel *NFIX-PKN1* translocation. *Am J Surg Pathol*. 2019 Aug;43(8):1092-1098.

17. **Kastnerova L**, Belousova IE, Hadravsky L, Kerl H, Cerroni L, Kerl K, Boudova L, Jindra P, Cerna K, Michal M, Kazakov DV Mummified cells are a common finding in cutaneous Hodgkin lymphoma and can be used as a diagnostic clue. *Am J Dermatopathol*., 2019 [Epub ahead of print]

18. **Kastnerova L**, Belousova IE, Michal M, Ptakova N, Michal M, Kazakov DV. Kaposi sarcoma in association with an extracavitary primary effusion lymphoma showing unusual intravascular involvement: report of a case harboring a FAM175A germline mutation. Am J Dermatopathol., 2019 [Accepted for publication]

19. Donati M, **Kastnerova L**, Martinek M, Grossman P, Sticová E, Hadravský L, Torday T, Kyclova J, Michal M, Kazakov DV. Spitz tumors with *ROS1* fusions: a clinicopathological study of 6 cases, including FISH for chromosomal copy number alterations and mutation analysis using next generation sequencing. Am J Dermatopathol., 2019 [Accepted for publication]

20. Donati M, **Kastnerova L,** Ptakova N, Michal M, Kazakov DV. Polypoid atypical Spitz tumor with a fibrosclerotic stroma, *CLIP2-BRAF* fusion and homozygous loss of 9p21. Am J Dermatopathol., 2019 [Accepted for publication]

CONCLUSIONS

Ph.D. thesis concludes postgraduate studies in pathology MD. Liubov Kastnerova (previous name Kyrpychova). During the studies, the required goals were reached. With the help of coauthors, we have documented the clinicopathological and molecular biologic characteristics of different cutaneous epithelial and nonepithelial tumors.

The result of the four-year study is eight first-author works; all of them are related to cutaneous neoplasms. The author also coauthored 12 publications. The results of all papers presented in the doctoral thesis were published in various American journals with impact factor.

ACKNOWLEDGMENTS

REFERENCES

1.   Elder DM, D; Scolyer, RA; Willemze, R. *WHO classification of skin tumours.* Lyon: IARC; 2018.
2.   Gerami P, Scolyer RA, Xu X, et al. Risk assessment for atypical spitzoid melanocytic neoplasms using FISH to identify chromosomal copy number aberrations. *Am J Surg Pathol.* 2013;37:676-684.
3.   Lee S, Barnhill RL, Dummer R, et al. TERT Promoter Mutations Are Predictive of Aggressive Clinical Behavior in Patients with Spitzoid Melanocytic Neoplasms. *Sci Rep.* 2015;5:11200.
4.   Wiesner T, He J, Yelensky R, et al. Kinase fusions are frequent in Spitz tumours and spitzoid melanomas. *Nat Commun.* 2014;5:3116.
5.   von Holstein SL, Fehr A, Persson M, et al. Adenoid cystic carcinoma of the lacrimal gland: MYB gene activation, genomic imbalances, and clinical characteristics. *Ophthalmology.* 2013;120:2130-2138.
6.   Persson M, Andren Y, Moskaluk CA, et al. Clinically significant copy number alterations and complex rearrangements of MYB and NFIB in head and neck adenoid cystic carcinoma. *Genes Chromosomes Cancer.* 2012;51:805-817.
7.   Ramakrishnan R, Chaudhry IH, Ramdial P, et al. Primary cutaneous adenoid cystic carcinoma: a clinicopathologic and immunohistochemical study of 27 cases. *Am J Surg Pathol.* 2013;37:1603-1611.
8.   Kazakov DV MM, Kacerovska D, et al. *Cutaneous adnexal tumors*. Philadelphia: LWW 2012.
9.   Martelotto LG, De Filippo MR, Ng CK, et al. Genomic landscape of adenoid cystic carcinoma of the breast. *J Pathol.* 2015;237:179-189.
10.   North JP, McCalmont TH, Fehr A, et al. Detection of MYB Alterations and Other Immunohistochemical Markers in Primary Cutaneous Adenoid Cystic Carcinoma. *Am J Surg Pathol.* 2015;39:1347-1356.
11.   Brill LB, 2nd, Kanner WA, Fehr A, et al. Analysis of MYB expression and MYB-NFIB gene fusions in adenoid cystic carcinoma and other salivary neoplasms. *Mod Pathol.* 2011;24:1169-1176.
12.   Chen TY, Keeney MG, Chintakuntlawar AV, et al. Adenoid cystic carcinoma of the lacrimal gland is frequently characterized by MYB rearrangement. *Eye (Lond).* 2017;31:720-725.
13.   Fujii K, Murase T, Beppu S, et al. MYB, MYBL1, MYBL2 and NFIB gene alterations and MYC overexpression in salivary gland adenoid cystic carcinoma. *Histopathology.* 2017;71:823-834.
14.   Mitani Y, Liu B, Rao PH, et al. Novel MYBL1 Gene Rearrangements with Recurrent MYBL1-NFIB Fusions in Salivary Adenoid Cystic Carcinomas Lacking t(6;9) Translocations. *Clin Cancer Res.* 2016;22:725-733.
15.   Steiner P, Andreasen S, Grossmann P, et al. Prognostic significance of 1p36 locus deletion in adenoid cystic carcinoma of the salivary glands. *Virchows Arch.* 2018;473:471-480.
16.   Roth MJ, Stern JB, Hijazi Y, et al. Oncocytic nodular hidradenoma. *Am J Dermatopathol.* 1996;18:314-316.
17.   Angulo J, Jaqueti G, Kutzner H, et al. Squamous cell apocrine hidradenoma. *J Cutan Pathol.* 2007;34:801-803.
18.   Behboudi A, Winnes M, Gorunova L, et al. Clear cell hidradenoma of the skin-a third tumor type with a t(11;19)--associated TORC1-MAML2 gene fusion. *Genes Chromosomes Cancer.* 2005;43:202-205.
19.   Nakayama T, Miyabe S, Okabe M, et al. Clinicopathological significance of the CRTC3-MAML2 fusion transcript in mucoepidermoid carcinoma. *Mod Pathol.* 2009;22:1575-1581.

20.   Mammino JJ, Vidmar DA. Syringocystadenoma papilliferum. *Int J Dermatol.* 1991;30:763-766.

21.   Kazakov DV, Requena L, Kutzner H, et al. Morphologic diversity of syringocystadenocarcinoma papilliferum based on a clinicopathologic study of 6 cases and review of the literature. *Am J Dermatopathol.* 2010;32:340-347.

22.   Skelton HG, 3rd, Smith KJ, Young D, et al. Condyloma acuminatum associated with syringocystadenoma papilliferum. *Am J Dermatopathol.* 1994;16:628-630.

23.   Shen AS, Peterhof E, Kind P, et al. Activating mutations in the RAS/mitogen-activated protein kinase signaling pathway in sporadic trichoblastoma and syringocystadenoma papilliferum. *Hum Pathol.* 2015;46:272-276.

24.   Llamas-Velasco M, Mentzel T, Rutten A. Primary cutaneous secretory carcinoma: A previously overlooked low-grade sweat gland carcinoma. *J Cutan Pathol.* 2018;45:240-245.

25.   Moore RF, Cuda JD. Secretory carcinoma of the skin: Case report and review of the literature. *JAAD Case Rep.* 2017;3:559-562.

26.   Bishop JA, Taube JM, Su A, et al. Secretory Carcinoma of the Skin Harboring ETV6 Gene Fusions: A Cutaneous Analogue to Secretory Carcinomas of the Breast and Salivary Glands. *Am J Surg Pathol.* 2017;41:62-66.

27.   Amin SM, Beattie A, Ling X, et al. Primary Cutaneous Mammary Analog Secretory Carcinoma With ETV6-NTRK3 Translocation. *Am J Dermatopathol.* 2016;38:842-845.

28.   Ambrojo P, Aguilar A, Simon P, et al. Basal cell carcinoma with matrical differentiation. *Am J Dermatopathol.* 1992;14:293-297.

29.   Aloi FG, Molinero A, Pippione M. Basal cell carcinoma with matrical differentiation. Matrical carcinoma. *Am J Dermatopathol.* 1988;10:509-513.

30.   Haskell HD, Haynes HA, McKee PH, et al. Basal cell carcinoma with matrical differentiation: a case study with analysis of beta-catenin. *J Cutan Pathol.* 2005;32:245-250.

31.   Kazakov DV, Sima R, Vanecek T, et al. Mutations in exon 3 of the CTNNB1 gene (beta-catenin gene) in cutaneous adnexal tumors. *Am J Dermatopathol.* 2009;31:248-255.

32.   Wiesner T, Obenauf AC, Murali R, et al. Germline mutations in BAP1 predispose to melanocytic tumors. *Nat Genet.* 2011;43:1018-1021.

33.   Mochel MC, Piris A, Nose V, et al. Loss of BAP1 Expression in Basal Cell Carcinomas in Patients With Germline BAP1 Mutations. *Am J Clin Pathol.* 2015;143:901-904.

34.   de la Fouchardiere A, Cabaret O, Savin L, et al. Germline BAP1 mutations predispose also to multiple basal cell carcinomas. *Clin Genet.* 2015;88:273-277.

35.   Troy JL, Ackerman AB. Sebaceoma. A distinctive benign neoplasm of adnexal epithelium differentiating toward sebaceous cells. *Am J Dermatopathol.* 1984;6:7-13.

36.   Rulon DB, Helwig EB. Cutaneous sebaceous neoplasms. *Cancer.* 1974;33:82-102.

37.   Misago N, Narisawa Y. Rippled-pattern sebaceoma. *Am J Dermatopathol.* 2001;23:437-443.

38.   Nielsen TA, Maia-Cohen S, Hessel AB, et al. Sebaceous neoplasm with reticulated and cribriform features: a rare variant of sebaceoma. *J Cutan Pathol.* 1998;25:233-235.

39.   Kazakov DV SD, Kacerovska D, et al. Unusual patterns of cutaneous sebaceous neoplasms. *Diagn Histopathol.* 2010:425-431.

40.   Misago N, Toda S. Sebaceous carcinoma within rippled/carcinoid pattern sebaceoma. *J Cutan Pathol.* 2016;43:64-70.

41.   Shields JA, Demirci H, Marr BP, et al. Sebaceous carcinoma of the ocular region: a review. *Surv Ophthalmol.* 2005;50:103-122.

42.   Shields JA, Demirci H, Marr BP, et al. Sebaceous carcinoma of the eyelids: personal experience with 60 cases. *Ophthalmology.* 2004;111:2151-2157.

43.   SC vdP. Anogenital "sweat" glands. Histology and pathology of

a gland that may mimic mammary glands. *Am J Dermatopathol.* 1991;13:557–567.

44.	Kazakov DV, Spagnolo DV, Kacerovska D, et al. Lesions of anogenital mammary-like glands: an update. *Adv Anat Pathol.* 2011;18:1-28.

45.	Belousova IE, Kazakov DV, Michal M, et al. Vulvar toker cells: the long-awaited missing link: a proposal for an origin-based histogenetic classification of extramammary paget disease. *Am J Dermatopathol.* 2006;28:84-86.

46.	Konstantinova AM, Shelekhova KV, Stewart CJ, et al. Depth and Patterns of Adnexal Involvement in Primary Extramammary (Anogenital) Paget Disease: A Study of 178 Lesions From 146 Patients. *Am J Dermatopathol.* 2016;38:802-808.

47.	Lam C, Funaro D. Extramammary Paget's disease: Summary of current knowledge. *Dermatol Clin.* 2010;28:807-826.

48.	Guarner J, Cohen C, DeRose PB. Histogenesis of extramammary and mammary Paget cells. An immunohistochemical study. *Am J Dermatopathol.* 1989;11:313-318.

49.	Delport ES. Extramammary Paget's disease of the vulva: An annotated review of the current literature. *Australas J Dermatol.* 2013;54:9-21.

50.	Smith JL, Jr., Butler JJ. Skin involvement in Hodgkin's disease. *Cancer.* 1980;45:354-361.

51.	Cerroni L, Beham-Schmid C, Kerl H. Cutaneous Hodgkin's disease: an immunohistochemical analysis. *J Cutan Pathol.* 1995;22:229-235.

52.	Lorenzen J, Thiele J, Fischer R. The mummified Hodgkin cell: cell death in Hodgkin's disease. *J Pathol.* 1997;182:288-298.

53.	Willemze R, Meyer CJ, Van Vloten WA, et al. The clinical and histological spectrum of lymphomatoid papulosis. *Br J Dermatol.* 1982;107:131-144.

54.	El Shabrawi-Caelen L, Kerl H, Cerroni L. Lymphomatoid papulosis: reappraisal of clinicopathologic presentation and classification into subtypes A, B, and C. *Arch Dermatol.* 2004;140:441-447.

55.	Kempf W, Kazakov DV, Scharer L, et al. Angioinvasive lymphomatoid papulosis: a new variant simulating aggressive lymphomas. *Am J Surg Pathol.* 2013;37:1-13.

56.	Singh Gomez C, Calonje E, Fletcher CD. Epithelioid benign fibrous histiocytoma of skin: clinico-pathological analysis of 20 cases of a poorly known variant. *Histopathology.* 1994;24:123-129.

57.	Doyle LA, Marino-Enriquez A, Fletcher CD, et al. ALK rearrangement and overexpression in epithelioid fibrous histiocytoma. *Mod Pathol.* 2015;28:904-912.

58.	Creytens D, Ferdinande L, Van Dorpe J. ALK Rearrangement and Overexpression in an Unusual Cutaneous Epithelioid Tumor With a Peculiar Whorled "Perineurioma-like" Growth Pattern: Epithelioid Fibrous Histiocytoma. *Appl Immunohistochem Mol Morphol.* 2017;25:e46-e48.

59.	Zedek DC, McCalmont TH. Spitz nevi, atypical spitzoid neoplasms, and spitzoid melanoma. *Clin Lab Med.* 2011;31:311-320.

60.	Barnhill RL. The Spitzoid lesion: rethinking Spitz tumors, atypical variants, 'Spitzoid melanoma' and risk assessment. *Mod Pathol.* 2006;19 Suppl 2:S21-33.

61.	Busam KJ, Kutzner H, Cerroni L, et al. Clinical and pathologic findings of Spitz nevi and atypical Spitz tumors with ALK fusions. *Am J Surg Pathol.* 2014;38:925-933.

62.	Amin SM, Haugh AM, Lee CY, et al. A Comparison of Morphologic and Molecular Features of BRAF, ALK, and NTRK1 Fusion Spitzoid Neoplasms. *Am J Surg Pathol.* 2017;41:491-498.

63.	Wiesner T, Kutzner H. [Morphological and genetic aspects of Spitz tumors]. *Pathologe.* 2015;36:37-43, 45.

64.	Perron E, Pissaloux D, Neub A, et al. Unclassified sclerosing malignant melanomas with AKAP9-BRAF gene fusion: a report of two cases and review of BRAF fusions in melanocytic tumors. *Virchows Arch.* 2018;472:469-476.